

The Medicinal Chemistry of Cyclo(Phe-4Cl-Pro) and Cyclo(D-Phe-4Cl-Pro)

Marnus Milne

Submitted in the fulfilment of the requirements for the degree of

MAGISTER SCIENTIAE

In the Faculty of Health Sciences at the

Nelson Mandela Metropolitan University

December 2011

Supervisor: Dr. G Dealtry

Co-Supervisor: Dr. G Kilian

DECLARATION

I, Marnus Milne, hereby declare that the work on which this dissertation is based is original (except where acknowledgements have been made) and that neither the whole work nor any part thereof has been, is being, or is to be submitted for another degree at this or any other university.

Marnus Milne

On this _____ day of _____ at the Nelson Mandela
Metropolitan University.

ACKNOWLEDGEMENTS

I extend my sincere appreciation and grateful thanks to the following people for their continuous invaluable support, guidance, time and dedication to this research undertaken:

Prof PJ Milne, for his constant encouragement, knowledge and guidance.

Dr G. Dealtry, to whom I owe much gratitude for all her assistance, time and knowledge.

Dr G Kilian for all his assistance and for being an inspiration.

Prof C Frost for all her assistance with the blood work.

Prof C McClelland for his assistance in the molecular modelling studies.

Prof M van de Venter, for her assistance in the cell and isotope labs.

Ms A Van Jaarsveld for all her assistance in the laboratory.

The department of Biochemistry and Microbiology, NMMU.

The department of Chemistry and Physics, NMMU.

Greenacres Hospital Dispensary, who made the completion of my internship possible.

My family and friends.

The *Almighty* for His faithfulness.

SUMMARY

Cyclic dipeptides have limited conformational freedom due to their diketopiperazine backbone and their small size. They are relatively simple to synthesise, making them ideal subjects for investigation into their biological effects. Cyclic dipeptides have also been known for their multitude of biological activities, including antimicrobial, anticancer and haematological properties.

In this study the cyclic dipeptides, cyclo(Phe-4Cl-Pro) and cyclo(D-Phe-4Cl-Pro), were synthesised from their corresponding linear precursors using a modified phenol-induced cyclisation procedure. The phenol induced cyclisation procedure resulted in good yields and purity of the cyclic dipeptides. Quantitative analysis and evaluation of the physicochemical properties of the cyclic dipeptides was achieved using high-performance liquid chromatography, scanning electron microscopy, thermal analysis and X-ray powder diffraction. Structural elucidation of the cyclic dipeptides was done by means of infrared spectroscopy, mass spectroscopy, nuclear magnetic resonance spectroscopy and molecular modelling.

The study's aim was to determine the biological activity of cyclo(Phe-4Cl-Pro) and cyclo(D-Phe-4Cl-Pro) with respect to their anticancer, antimicrobial, haematological and ant-diabetic studies. Anticancer studies revealed that cyclo(Phe-4Cl-Pro) and cyclo(D-Phe-4Cl-Pro) inhibited the growth of HeLa (cervical cancer), HT-29 (colon cancer) and MCF-7 (breast cancer) cancer cell lines. Both cyclic dipeptides also inhibited the growth of certain selected Gram-positive, Gram-negative and fungal microorganisms in the antimicrobial study. Although the inhibition of growth in the anticancer and antimicrobial studies was statistically significant, the clinical relevance is questionable, since the inhibition produced by both cyclic dipeptides was very limited compared to other pre-existing anticancer and antimicrobial agents. Both cyclic dipeptides caused a significant shortening of the APTT and PT clotting times and an increase in the fibrin and D-Dimer formation. Cyclo(D-Phe-4Cl-Pro) at a screening concentration of 12.5 mM and 3.125 mM, showed significant anti-platelet activity. Both cyclic dipeptides failed to produce any

inhibition of the α -Glucosidase enzyme and very limited inhibition of the α -Amylase enzyme.

Key words: Cyclic dipeptides, cyclo(Phe-4Cl-Pro), cyclo(D-Phe-4Cl-Pro), anticancer, antimicrobial, antifungal, anti-diabetic, haemostasis

TABLE OF CONTENTS

TITLE PAGE.....	i
DECLARATION.....	ii
ACKNOWLEDGEMENTS	iii
SUMMARY.....	iv
TABLE OF CONTENTS.....	vi
LIST OF ABBREVIATIONS.....	xix
LIST OF FIGURES.....	xxix
LIST OF TABLES.....	xxxviii
CHAPTER 1	1
INTRODUCTION.....	1
1.1 Background and problem definition	1
1.2 Aim	2
1.3 The objectives of this study.....	2
CHAPTER 2	3

LITERATURE REVIEW	3
2.1 Background	3
2.2 Amino acids, peptides and proteins	5
2.3 Cyclicdipeptides	17
2.3.1 General aspects of cyclic dipeptides.....	17
2.3.2 Conformational aspects of cyclic dipeptides	19
2.3.3 Physiochemical properties of cyclic dipeptides.....	22
2.3.3.1 Solubility of cyclic dipeptides	22
2.3.3.2 Physical stability of cyclic dipeptides	22
2.3.4 Absorption, transportation and metabolic stability of cyclic dipeptides	23
2.3.5 Biologically active cyclic dipeptides	25
2.4 Motivation for the research.....	34
CHAPTER 3	37
CYCLIC DIPEPTIDE SYNTHESIS	37
3.1 Introduction	37
3.2 Methodology.....	39
3.2.1 Synthesis of the linear dipeptides	40
3.2.2 Removal of the protective Boc group.....	42

3.2.3 Cyclisation	42
3.3 Results and Discussion	43
3.4 Thin layer chromatography	44
3.5 High-performance liquid chromatography	46
3.5.1 Introduction	46
3.5.2 Methodology	48
3.5.2.1 Preparation of solutions	48
3.5.2.2 HPLC analysis of the cyclic dipeptides	49
3.5.2.3 Results and discussion	50
CHAPTER 4	52
QUALITATIVE PHYSIOCHEMICAL ANALYSIS	52
4.1 Scanning electron microscopy	52
4.1.1 Introduction	52
4.1.2 Methodology	53
4.1.3 Results and discussion	53
4.2 Thermal analysis	57
4.2.1 Thermogravimetric analysis and derivative thermogravimetry	57
4.2.1.1 Introduction	57

4.2.2 Differential scanning calorimetry	58
4.2.2.1 Introduction	58
4.2.3 Methodology.....	59
4.2.4 Results and discussion	60
4.3 X-ray Powder Diffraction	62
4.3.1 Introduction	62
4.3.2 Methodology.....	64
4.3.3 Results and discussion	65
CHAPTER 5	68
STRUCTURAL AND CONFORMATIONAL ANALYSIS	68
5.1 Infrared spectroscopy.....	68
5.1.1 Introduction	68
5.1.2 Methodology.....	69
5.1.3 Results and discussion	70
5.2 Fast atom bombardment mass spectrometry	77
5.2.1 Introduction	77
5.2.2 Methodology.....	78
5.2.3 Results and discussion	78

5.3 Nuclear magnetic resonance spectroscopy	83
5.3.1 Introduction	83
5.3.2 Methodology.....	85
5.3.3 Results and discussion	85
5.4 Molecular modelling	101
5.4.1 Introduction	101
5.4.2 Methodology.....	102
5.4.3 Results and discussion	102
CHAPTER 6	125
ANTICANCER STUDIES	125
6.1 Introduction	125
6.1.1 Cell growth cycle	127
6.1.2 Carcinogenesis	131
6.1.3 Invasion and metastasis.....	133
6.1.4 Cancer therapy.....	134
6.1.4.1 Radiation therapy	134
6.1.4.2 Surgery.....	134
6.1.4.3 Chemotherapeutic agents	135

6.1.5 Agents utilised as controls for the assays	139
6.2 Methodology.....	140
6.2.1 Cell cultures	140
6.2.2 Cell line maintenance and routine culture	141
6.2.3 Preparation of solutions	142
6.2.3.1 Negative control	142
6.2.3.2 Polyethylene glycol (PEG)	143
6.2.3.3 Positive control.....	143
6.2.3.4 Cyclic dipeptide solutions.....	143
6.2.3.5 3-(4,5-dimethylthiazol-2-yl)-2,5-diphenyltetrazolium bromide (MTT) dye solution	143
6.3. Cytotoxicity assays utilizing MTT.....	144
6.4 Statistical analysis.....	145
6.5 Results and discussion	146
6.5.1 HeLa cell line.....	146
6.5.2 MCF-7 cell line	150
6.5.3 HT-29 cell line	153
6.6 Conclusion.....	157
CHAPTER 7	161

ANTIMICROBIAL STUDIES.....	161
7.1 Introduction	161
7.1.1 Current modes of antimicrobial therapy	165
7.1.2 Inhibitors of bacterial cell wall synthesis	166
7.1.3 Inhibitors of cell membrane functioning	171
7.1.4 Inhibitors of protein synthesis	172
7.1.5 Inhibitors of folate metabolism	173
7.1.6 Inhibitors of DNA and RNA synthesis	176
7.1.7 Bacterial resistance	176
7.1.8 Mechanisms of bacterial resistance	176
7.1.9 Implications	177
7.2 Experimental bacterial and fungal cultures	180
7.2.1 Gram-positive Bacteria.....	181
7.2.1.1 Bacillus subtilis	181
7.2.1.2 Staphylococcus aureus	181
7.2.2 Gram-negative Bacteria	181
7.2.2.1 Escherichia coli	181
7.2.2.2 Pseudomonas aeruginosa	182

7.2.3 Fungi	182
7.2.3 .1 Candida albicans.....	182
7.3 Control agents used to compare the antimicrobial activity of the cyclic dipeptides	182
7.3.1 Amoxicillin	182
7.3.2 Chloramphenicol	183
7.4 Methodology.....	183
7.4.1 Laboratory conditions.....	183
7.4.2 Preparations of solutions.....	184
7.4.2 .1 Negative controls	184
7.4.2.2 Positive controls	184
7.4.2.3 Cyclic dipeptide solutions.....	184
7.4.2 .4 MTT dye solution.....	185
7.5 Test organism cultures.....	185
7.6 Standardisation of the inoculum.....	186
7.7 MTT linearity assay	186
7.8 Antimicrobial assay	188
7.9 Statistical analysis	188
7.10 Results and discussion	190

7.10.1 MTT linearity assay	190
7.10.2 Cyclic dipeptide antimicrobial assay	192
7.11 Conclusion	204
CHAPTER 8	205
HEAMATOLOGICAL STUDIES	205
8.1 INTRODUCTION.....	205
8.1.1 Haemostasis	206
8.1.2 Vascular constriction	206
8.1.3 Platelet plug formation	207
8.1.4 Blood clotting via activation of the coagulation cascade.....	207
8.1.5 Fibrinolysis	209
8.1.6 Repair and regeneration of damaged blood vessels	210
8.1.7 Drugs affecting coagulation.....	210
8.1.8 Drugs used in the treatment of thrombotic and thromboembolic diseases.....	211
8.1.9 Antiplatelet drugs	211
8.1.10 Fibrinolytic drugs	212
8.2 Methodology.....	212
8.2.1 Collection and ethical approval of blood used in experiments.....	212

8.2.2	Coagulation assay.....	213
8.2.2.1	Prothrombin time test.....	214
8.2.2.2	Activated partial thromboplastin time (APTT)	214
8.2.2.3	Fibrinogen-C assay	215
8.2.2.4	D-Dimer	216
8.3	Platelet aggregation/adhesion studies	217
8.3.1	Isolation of platelets	217
8.3.2	Platelet count	218
8.3.3	Platelet aggregation (flow-cytometry method)	218
8.4	Statistical analysis.....	220
8.5	Results and discussion	220
8.5.1	Activated partial thromboplastin time assay (APTT).....	220
8.5.2	Prothrombin time assay (PT)	222
8.5.3	Fibrinogen-C assay (Fib-C).....	224
8.5.4	D-Dimer assay	227
8.5.5	Platelet aggregation studies.....	229
8.6	Summary.....	241
CHAPTER 9	242

ANTI-DIABETES	242
9.1 Introduction	242
9.2 Physiology of the Islet of Langerhans	242
9.3. Regulation of glucagon and insulin secretion	242
9.4. Diabetes Mellitus	244
9.4.1 Type 1 DM (T1DM)	244
9.4.2 Type 2 DM (T2DM)	244
9.4.3 Diagnosis of DM	245
9.4.4 Treatment of DM	245
9.5 Anti-diabetic drugs	245
9.5.1 Thiazolidinediones	245
9.5.2 Biguanides	246
9.5.3 α -Glucosidase inhibitors	247
9.5.4 Sulphonylurea derivatives	247
9.5.5 Meglitinides	248
9.5.6 Glucagon-like peptide 1	248
9.6 Methodology	248
9.6.1 Preparation of test solutions	248

9.6.1.1 Positive control	249
9.6.1.2 4-Nitrophenyl- α -D-glucopyranoside	249
9.6.1.3 Sodium carbonate	249
9.6.2 α -glucosidase assay.....	249
9.6.3 α -Amylase assay.....	250
9.7 Statistical analysis	251
9.8 Results and discussion	251
9.8.1 α -Glucosidase assay.....	251
9.8.2 α -Amylase activity	252
9.9 Summary.....	253
CHAPTER 10	254
CONCLUSIONS AND RECOMMENDATIONS.....	254
REFERENCES.....	258
APPENDIX A.....	281
LIST OF CHEMICALS.....	281
APPENDIX B.....	284
LIST OF SOLUTIONS.....	284
Buffer A	284

Mueller Hinton broth	284
Nutrient agar.....	284
MTT (determination of cell viability)	285
Phosphate-buffered saline (PBS).....	285
Tris buffer	285
APPENDIX C	286
LIST OF EQUIPMENT	286
APPENDIX D	289
HUMAN ETHICAL APPROVAL FORM.....	289
APPENDIX E.....	290
ARTICLE TO BE SUBMITTED FOR PUBLICATION	290

LIST OF ABBREVIATIONS

α	Alpha
β	Beta
δ	Chemical shift (ppm)
Θ	Theta
λ	lambda
ϵ	Molar extinction coefficient
%	Percentage
$^{\circ}\text{C}$	Degrees Celsius
μl	Microlitre
μm	Micrometer
^{13}C	Carbon-13
^{13}C DEPT	Distortionless enhancement by polarisation transfer
^1H	Proton
5-HT	Serotonin
\AA	Angstrom

A	Adenine
AcOH	Acetic acid
ADP	Adenosine diphosphate
AGW	Analytical grade water
AIDS	Autoimmune deficiency syndrome
Ala	Alanine
AMPK	5' adenosine monophosphate-activated protein kinase
API	Active pharmaceutical ingredient
APTT	Activated partial thromboplastin time
Ar	Aromatic
ARG	Arginine
Asp	Aspartic acid
ATP	Adenosine triphosphate
BSA	Bovine serum albumin
C	Cytosine
(C)	Untreated control
CCNS	Cell cycle non-specific

CCS	Cell cycle specific
CD	Circular dichroism
CDKs	Cyclin-dependant kinases
CID	Collision-induced dissociation
Cm	Centimeter
COSY	Correlation spectroscopy
COX	Cyclo-oxygenase
D	Right
DEPC	Diethylphosphoryl cyanide
DEPT	Distortionless enhancement by polarisation transfer
DIC	Disseminated intravascular coagulation
DKPs	Diketopiperazines
DM	Diabetes mellitus
DMSO	Dimethyl sulphoxide
DMSO-d ₆	Deuterated dimethyl sulphoxide
DNA	Deoxyribonucleic acid
DOPs	Dioxopiperazines

DSC	Differential scanning calorimetry
DTG	Derivative thermogravimetry
DVT	Deep vein thrombosis
E	Energy
EDTA	Ethylenediaminetetraacetic acid
F	Factor
FAB	Fast atom bombardment
FCS	Foetal calf serum
FTIR	Fourier-transform infrared
g	Gram
g	Gravity
G	Guanine
GC	Gas chromatography
GLP-1	Glucagon-like peptide 1
GLU	Glutamate
Gly	Glycine

GPRP	Peptide glycol-L-prolyl-L-arginyl-L-proline
GSA	Glutamic- γ -semialdehyde
GTT	Glucose tolerance test
HEPES	<i>N</i> -2-hydroxyethylpiperazine-2-ethanesulphonic acid
His	Histidine
HIV	Human immunodeficiency virus
HMBCGP	Heteronuclear multiple bond correlation experiment
HMQC	Heteronuclear Multiple Quantum Correlation experiment
HPLC	High performance liquid chromatography
HSQC	Heteronuclear Single Quantum Coherence
IC ₅₀	Inhibitory concentration (50%)
IDDM	Insulin-dependent diabetes mellitus
Ile	Isoleucine
IR	Infrared
KBr	Potassium bromide
Kcal	Kilocalorie
kg.cm ⁻²	Kilogram per centimeter squared

kJ/mol	Kilojoules per mole
L	Left
Leu	Leucine
levo	Left
LG	Liquid chromatography
Lys	Lysine
<i>m/e</i>	Mass per charge ratio
MAO	Mono-amine oxidase
mg/dL	Milligrams per decilitre
MHZ	Megahertz
ml	Millilitre
ml/min	Millilitre per minute
mM	Millimolar
mm	Millimetre
Mmol	Millimol
mmol/L	Millimol per litre
MS	Mass spectrometry

MSH	Melanocyte stimulating hormone
MTT	3-(4,5-dimethylthiazol-2-yl)-2,5-diphenyltetrazolium bromide
MW	Molecular weight
NIDDM	Non insulin dependent diabetes mellitus
nm	Nanometre
NMR	Nuclear magnetic resonance
ORD	Optical rotatory dispersion
ORN	Ornithine
<i>P</i>	Statistical significance value
P5C	Pyrroline-5-carboxylate
PBS	Phosphate buffer solution
PC	Positive control
PE	Pulmonary embolism
PEG	Polyethylene glycol
PEPT1	Peptide transporter 1
PEPT2	Peptide transporter 2
PF-4	Heparin-neutralising factor

PGI ₂	Prostaglandin I ₂
Phe	Phenylalanine
PKU	Phenylketonuria
PPAR	Proliferator-activated receptor
Ppm	Parts per million
pRB	Retinoblastoma protein
Pro	Proline
PRP	Platelet rich plasma
PT	Prothrombin time
Rel. E	Relative energy
Rf	Retardation factor
RMS	Root mean square
RNA	Ribonucleic acid
RPC	Reversed-phase chromatography
RPMI	Roswell Park Memorial Institute
SA	South Africa
SD	Standard deviation

SDT	Simultaneous DSC-TGA
SEM	Scanning electron microscopy
Ser	Serine
SUR1	Sulphonylurea receptor 1
SUR2	Sulphonylurea receptor 2
SUs	Sulphonylureas
TA	Thermal analysis
t-Boc	Tert- butyloxycarbonyl group
TF	Tissue factor
TG	Thermogravimetry
TGA	Thermogravimetric analysis
THF	Tetrahydrofuran
Thr	Threonine
TLC	Thin layer chromatography
TMS	Tetramethylsilane
t-PA	Tissue plasminogen activator
TRF	Thyroid-releasing factor

Trp	Tryptophan
TXA ₂	Thromboxane A ₂
Tyr	Tyrosine
TZDs	Thiazolidinediones
UK	United Kingdom
u-PA	Urinary plasminogen activator
USA	United States of America
UV	Ultraviolet rays
V/ V	Volume per Volume
Val	Valine
VWF	Von Willebrand factor
X-PRO	Imidodipeptide with proline as carboxyl terminus
XRPD	X-ray powder diffraction
Y-HyPro	Imidodipeptide with hydroxyproline as carboxyl terminus

LIST OF FIGURES

Figure 2.1	General structure of an amino acid (Campbell and Farrell, 2003).....	5
Figure 2.2	Illustrating the difference between α ; β and ϵ - amino acids. (Jakubke and Jeschkeit, 1977).	6
Figure 2.3	Schematic representation of the amino acid reservoir (Jakubke and Jeschkeit, 1977).	7
Figure 2.4	Conversion of tryptophan to serotonin, melatonin and niacin (Campbell and Farrell, 2003)...	8
Figure 2.5	Structure of Cyclo(Phe-4Cl-Pro)	9
Figure 2.6	Structure of Cyclo(D-Phe-4Cl-Pro)	9
Figure 2.7	Metabolic pathway of phenylalanine (Wang <i>et al.</i> , 2001)	11
Figure 2.8	Metabolic pathway of proline (Phanget <i>et al.</i> , 2008).....	12
Figure 2.9	Formation of a peptide bond (Campbell and Farrell, 2003)	13
Figure 2.10	General structures of a 2, 5-diketopiperazine, where R_1 and R_2 represent the substituting amino acid residues (Prasad, 1995).	17
Figure 2.11	Side chain conformations of cyclo(Phe-Pro) and cyclo(Phe-D-Pro). (Adapted from Young <i>et al.</i> , 1976).	21
Figure 3.1	Protective groups used in the synthesis of cyclo(Phe-4Cl-Pro) and cyclo(D-Phe-4Cl-Pro) (Method according to Milne <i>et al.</i> , 1992).....	40
Figure 3.2	Synthesis of the protected linear dipeptide ester (Adapted from Milne <i>et al.</i> , 1992).	42
Figure 3.3	Formate ester product (Adapted from Milne <i>et al.</i> , 1992).....	42

Figure 3.4 Mechanism of cyclisation of the linear dipeptide formate ester to cyclo(Phe-4Cl-Pro) (Adapted from Capasso <i>et al.</i> , 1998)	43
Figure 3.5 The HPLC chromatogram of cyclo(D-Phe-4Cl-Pro) ($t_R = 5.40$ minutes) at UV detection wavelength of 220 nm	51
Figure 3.6 The HPLC chromatogram of cyclo(Phe-4Cl-Pro) ($t_R = 5.39$ minutes) at UV detection wavelength of 220 nm	51
Figure 4.1 Electronmicrograph of cyclo(Phe-4Cl-Pro) with a magnification of 250x.....	54
Figure 4.2 Electronmicrograph of cyclo(Phe-4Cl-Pro) with a magnification of 2000x.....	55
Figure 4.3 Electronmicrograph of cyclo(D-Phe-4Cl-Pro) with a magnification of 250x.....	55
Figure 4.4 Electronmicrograph of cyclo(D-Phe-4Cl-Pro) with a magnification of 2000x.....	56
Figure 4.5 Simultaneous DSC-TGA thermogram of cyclo(Phe-4Cl-Pro)	61
Figure 4.6 Simultaneous DSC-TGA thermogram of cyclo(D-Phe-4Cl-Pro)	62
Figure 4.7 X-ray powder diffraction pattern of cyclo(Phe-4Cl-Pro)	66
Figure 4.8 X-ray powder diffraction pattern of cyclo(D-Phe-4Cl-Pro)	67
Figure 5.1 Infrared spectrum of cyclo(Phe-4Cl-Pro)	75
Figure 5.2 Infrared spectrum of cyclo(D-Phe-4Cl-Pro)	76
Figure 5.3 Possible fragmentation pathways of cyclo(Phe-4Cl-Pro) and cyclo(D-Phe-4Cl-Pro)	80
Figure 5.4 Mass spectrum of cyclo(Phe-4Cl-Pro)	81
Figure 5.5 Mass spectrum of cyclo(D-Phe-4Cl-Pro)	82
Figure 5.6 ^1H NMR spectrum of cyclo(Phe-4Cl-Pro)	89

Figure 5.7	^{13}C NMR spectrum of cyclo(Phe-4CL-Pro)	90
Figure 5.8	^{13}C COUPLED spectrum of cyclo(Phe-4CL-Pro).....	91
Figure 5.9	COSY spectrum of cyclo(Phe-4CL-Pro)	92
Figure 5.10	HMBCGP spectrum of cyclo(Phe-4CL-Pro).....	93
Figure 5.11	HSQC spectrum of cyclo(Phe-4CL-Pro)	94
Figure 5.12	^1H NMR spectrum of cyclo(D-Phe-4CL-Pro).....	95
Figure 5.13	^{13}C NMR spectrum of cyclo(D-Phe-4CL-Pro)	96
Figure 5.14	^{13}C GD spectrum of cyclo(D-Phe-4CL-Pro)	97
Figure 5.15	COSY spectrum of cyclo(D-Phe-4CL-Pro)	98
Figure 5.16	HMBCGP spectrum of cyclo(D-Phe-4CL-Pro).....	99
Figure 5.17	HSQC spectrum of cyclo(D-Phe-4CL-Pro)	100
Figure 5.18	Conformation 1 of cyclo(Phe-4Cl-Pro) in the gas phase	103
Figure 5.19	Conformation 2 of cyclo(Phe-4Cl-Pro) in the gas phase	103
Figure 5.20	Conformation 3 of cyclo(Phe-4Cl-Pro) in the gas phase	104
Figure 5.21	Overlay of conformation 1 and 2 of cyclo(Phe-4Cl-Pro) in the gas phase	104
Figure 5.22	Overlay of conformation 1 and 3 of cyclo(Phe-4Cl-Pro) in the gas phase	104
Figure 5.23	Overlay of conformation 2 and 3 of cyclo(Phe-4Cl-Pro) in the gas phase	105
Figure 5.24	Overlay of conformation 1, 2 and 3 of cyclo(Phe-4Cl-Pro) in the gas phase	105

Figure 5.25	Conformation 1 of cyclo(D-Phe-4Cl-Pro) in the gas phase	106
Figure 5.26	Conformation 2 of cyclo(D-Phe-4Cl-Pro) in the gas phase	106
Figure 5.27	Conformation 3 of cyclo(D-Phe-4Cl-Pro) in the gas phase	107
Figure 5.28	Overlay of conformation 1 and 2 of cyclo(D-Phe-4Cl-Pro) in the gas phase.....	107
Figure 5.29	Overlay of conformation 1 and 3 of cyclo(D-Phe-4Cl-Pro) in the gas phase.....	107
Figure 5.30	Overlay of Conformation 2 and 3 of cyclo(D-Phe-4Cl-Pro) in the gas phase.....	108
Figure 5.31	Overlay of conformation 1, 2 and 3 of cyclo(D-Phe-4Cl-Pro) in the gas phase.....	108
Figure 5.32	Conformation 1 of cyclo(Phe-4Cl-Pro) in the solvated (water) phase	109
Figure 5.33	Conformation 2 of cyclo(Phe-4Cl-Pro) in the solvated (water) phase	109
Figure 5.34	Conformation 3 of cyclo(Phe-4Cl-Pro) in the solvated (water) phase	110
Figure 5.35	Overlay of conformation 1 and 2 of cyclo(Phe-4Cl-Pro) in the solvated (water) phase.....	110
Figure 5.36	Overlay of conformation 1 and 3 of cyclo(Phe-4Cl-Pro) in the solvated (water) phase.....	111
Figure 5.37	Overlay of Conformation 2 and 3 of cyclo(Phe-4Cl-Pro) in the solvated (water) phase....	111
Figure 5.38	Overlay of Conformation 1, 2 and 3 of cyclo(Phe-4Cl-Pro) in the solvated (water) phase	112
Figure 5.39	Conformation 1 of cyclo(D-Phe-4Cl-Pro) in the solvated (water) phase	113
Figure 5.40	Conformation 2 of cyclo(D-Phe-4Cl-Pro) in the solvated (water) phase	113
Figure 5.41	Conformation 3 of cyclo(D-Phe-4Cl-Pro) in the solvated (water) phase	114
Figure 5.42	Overlay of conformation 1 and 2 of cyclo(D-Phe-4Cl-Pro) in the solvated (water) phase.	114

Figure 5.43	Overlay of Conformation 1 and 3 of cyclo(D-Phe-4Cl-Pro) in the solvated (water) phase	114
Figure 5.44	Overlay of Conformation 2 and 3 of cyclo(D-Phe-4Cl-Pro) in the solvated (water) phase	115
Figure 5.45	Overlay of Conformation 1, 2 and 3 of cyclo(D-Phe-4Cl-Pro) in the solvated (water) phase	115
Figure 5.46	Conformation 1 of cyclo(Phe-4Cl-Pro) in dimethyl sulphoxide (DMSO)	116
Figure 5.47	Conformation 2 of cyclo(Phe-4Cl-Pro) in dimethyl sulphoxide (DMSO)	117
Figure 5.48	Conformation 3 of cyclo(Phe-4Cl-Pro) in dimethyl sulphoxide (DMSO)	117
Figure 5.49	Overlay of conformation 1 and 2 of cyclo(Phe-4Cl-Pro) in dimethyl sulphoxide (DMSO) .	118
Figure 5.50	Overlay of conformation 1 and 3 of cyclo(Phe-4Cl-Pro) in dimethyl sulphoxide (DMSO) .	118
Figure 5.51	Overlay of conformation 2 and 3 of cyclo(Phe-4Cl-Pro) in dimethyl sulphoxide (DMSO) .	119
Figure 5.52	Overlay of conformation 1, 2 and 3 of cyclo(Phe-4Cl-Pro) in dimethyl sulphoxide (DMSO)	119
Figure 5.53	Conformation 1 of cyclo(D-Phe-4Cl-Pro) in dimethyl sulphoxide (DMSO)	121
Figure 5.54	Conformation 2 of cyclo(D-Phe-4Cl-Pro) in dimethyl sulphoxide (DMSO)	121
Figure 5.55	Conformation 3 of cyclo(D-Phe-4Cl-Pro) in dimethyl sulphoxide (DMSO)	122
Figure 5.56	Overlay of conformation 1 and 2 of cyclo(D-Phe-4Cl-Pro) in dimethyl sulphoxide (DMSO)	122
Figure 5.57	Overlay of conformation 1 and 3 of cyclo(D-Phe-4Cl-Pro) in dimethyl sulphoxide (DMSO)	123
Figure 5.58	Overlay of conformation 2 and 3 of cyclo(D-Phe-4Cl-Pro) in dimethyl sulphoxide (DMSO)	123

Figure 5.59 Overlay of conformation 1, 2 and 3 of cyclo(D-Phe-4Cl-Pro) in dimethyl sulphoxide (DMSO)	124
Figure 6.1 Diagram of the cell cycle specifying the four phases-G ₁ , G ₂ , M, S and G ₀ -and indicating the main sites of action of most anticancer agents (Koda-Kimble <i>et al.</i> , 2008).....	128
Figure 6.2 Percentage growth inhibition of HeLa cell line after 48 hour exposure to cyclo(Phe-4Cl-Pro) and cyclo(D-Phe-4Cl-Pro) and melphalan (n =4) (vehicle with PEG).....	147
Figure 6.3 Percentage growth inhibition of HeLa cell line after 48 hour exposure to cyclo(Phe-4Cl-Pro) and cyclo(D-Phe-4Cl-Pro) and melphalan (n =4) (vehicle without PEG).....	149
Figure 6.4 Percentage growth inhibition of MCF-7 cell line after 48 hour exposure to cyclo(Phe-4Cl-Pro) and cyclo(D-Phe-4Cl-Pro) and melphalan (n =4) (vehicle with PEG).....	151
Figure 6.5 Percentage growth inhibition of MCF-7 cell line after 48 hour exposure to cyclo(Phe-4Cl-Pro) and cyclo(D-Phe-4Cl-Pro) and Melphalan (n =4) (vehicle without PEG).....	152
Figure 6.6 Percentage growth inhibition of HT-29 cell line after 48 hour exposure to cyclo(Phe-4Cl-Pro) and cyclo(D-Phe-4Cl-Pro) and melphalan (n =4) (vehicle with PEG).....	155
Figure 6.7 Percentage growth inhibition of HT-29 cell line after 48 hour exposure to cyclo(Phe-4Cl-Pro) and cyclo(D-Phe-4Cl-Pro) and Melphalan (n =4) (vehicle without PEG).....	156
Figure 7.1 Sites of action of antimicrobial agents (Page <i>et al.</i> , 1997).	166
Figure 7.2 Peptidoglycan synthesis (Katzung, 2009).....	167
Figure 7.3 General structure of the penicillins (Katzung, 2009).....	168
Figure 7.4 General structure of cephalosporins (Katzung, 2009).	170
Figure 7.5 Inhibitors of protein synthesis (Page <i>et al.</i> , 1997).....	173
Figure 7.6 Structure of sulphonamides in comparison to <i>p</i> -aminobenzoic acid (PABA) (Katzung, 2009).	174
Figure 7.7 Folate metabolism (Katzung, 2009).....	175

Figure 7.8	<i>B. subtilis</i> linearity of MTT against bacteria count ($R^2 = 0.958$).....	190
Figure 7.9	<i>S. aureus</i> linearity of MTT against bacteria count ($R^2 = 0.976$).....	190
Figure 7.10	<i>E. coli</i> linearity of MTT against bacteria count ($R^2 = 0.974$)	191
Figure 7.11	<i>P. aeruginosa</i> linearity of MTT against bacteria count ($R^2 = 0.982$).....	191
Figure 7.12	<i>C. albicans</i> linearity of MTT against bacteria count ($R^2 = 0.969$)	191
Figure 7.13	Percentage growth inhibition of <i>B. subtilis</i> after 24 hour exposure to cyclo(D-Phe-4Cl-Pro), cyclo(Phe-4Cl-Pro), chloramphenicol and amoxicillin.....	193
Figure 7.14	Percentage growth inhibition of <i>S. aureus</i> after 24 hour exposure to cyclo(D-Phe-4Cl-Pro), cyclo(Phe-4Cl-Pro), chloramphenicol and amoxicillin.....	195
Figure 7.15	Percentage growth inhibition of <i>E. coli</i> after 24 hour exposure to cyclo(D-Phe-4Cl-Pro), cyclo(Phe-4Cl-Pro), chloramphenicol and amoxicillin.....	198
Figure 7.16	Percentage growth inhibition of <i>P. aeruginosa</i> after 24 hour exposure to cyclo(D-Phe-4Cl-Pro), cyclo(Phe-4Cl-Pro), chloramphenicol and amoxicillin.....	200
Figure 7.17	Percentage growth inhibition of <i>C. albicans</i> after 24 hour exposure to cyclo(D-Phe-4Cl-Pro), cyclo(Phe-4Cl-Pro), chloramphenicol and amoxicillin.....	203
Figure 8.1	A simplified line diagram of the plasma-coagulation cascade showing intersection of the intrinsic and extrinsic pathways (Vogler and Siedlecki, 2009).....	208
Figure 8.2	Standard curve illustrating the correlation between platelet count numbers and absorbance ($R^2 = 0.9976$).....	218
Figure 8.3	The effect of platelet activation on monoclonal antibody binding (Michelson <i>et al.</i> , 2000) .	219
Figure 8.4	Effects of heparin (positive control), cyclo(Phe-4Cl-Pro) and cyclo(D-Phe-4Cl-Pro) on APTT clotting time.....	222
Figure 8.5	Effects of heparin (positive control), cyclo(Phe-4Cl-Pro) and cyclo(D-Phe-4Cl-Pro) on PT clotting time.....	224

Figure 8.6 Effects of heparin (positive control), cyclo(Phe-4Cl-Pro) and cyclo(D-Phe-4Cl-Pro) on decreasing the formation of fibrin.....	227
Figure 8.7 Effects of heparin (positive control), cyclo(Phe-4Cl-Pro) and cyclo(D-Phe-4Cl-Pro) on D-Dimer formation.....	229
Figure 8.8 Fluorescence intensity and cell density plot representation of platelet aggregation caused by the untreated control (PRP)	231
Figure 8.9 Fluorescence intensity and cell density plot representation of platelet aggregation caused by the positive control (PRP with thrombin 50 U/ml)	232
Figure 8.10 Fluorescence intensity and cell density plot representation of platelet aggregation caused by 50 mM cyclo(Phe-4Cl-Pro).....	233
Figure 8.11 Fluorescence intensity and cell density plot representation of platelet aggregation caused by 25 mM cyclo(Phe-4Cl-Pro).....	234
Figure 8.12 Fluorescence intensity and cell density plot representation of platelet aggregation caused by 12.5 mM cyclo(Phe-4Cl-Pro).....	235
Figure 8.13 Fluorescence intensity and cell density plot representation of platelet aggregation caused by 3.125 mM cyclo(Phe-4Cl-Pro).....	236
Figure 8.14 Fluorescence intensity and cell density plot representation of platelet aggregation caused by 50 mM cyclo(D-Phe-4Cl-Pro).....	237
Figure 8.15 Fluorescence intensity and cell density plot representation of platelet aggregation caused by 25 mM cyclo(D-Phe-4Cl-Pro).....	238
Figure 8.16 Fluorescence intensity and cell density plot representation of platelet aggregation caused by 12.5 mM cyclo(D-Phe-4Cl-Pro).....	239
Figure 8.17 Fluorescence intensity and cell density plot representation of platelet aggregation caused by 3.125 mM cyclo(D-Phe-4Cl-Pro).....	240
Figure 9.1 α -Glucosidase enzyme inhibition caused by acarbose (positive control), cyclo(Phe-4Cl-Pro) and cyclo(D-Phe-4Cl-Pro).....	252

Figure 9.2 α -Amylase enzyme inhibition caused by acarbose, cyclo(Phe-4Cl-Pro) and cyclo(D-Phe-4Cl-Pro)..... 253

LIST OF TABLES

Table 2.1	Key groups of peptide- and protein-containing drugs (Bhattacharyya <i>et al.</i> , 2005).	14
Table 2.2	The difference between cyclic dipeptides and ordinary peptides	18
Table 2.3	Biological activity of some cyclic dipeptides	26
Table 2.4	Some biologically active Phenylalanine- and Proline-containing cyclic dipeptides	34
Table 3.1	Relative yields for (Phe-4Cl-Pro) and cyclo(D-Phe-4Cl-Pro)	44
Table 3.2	Mobile phase ratio compositions and the R_f values obtained for (Phe-4Cl-Pro) and cyclo(D-Phe-4Cl-Pro)	44
Table 3.3	Formulas for the preparation of the mobile phases	49
Table 5.1	Frequencies/absorption bands (cm^{-1}) of cyclo(Phe-4Cl-Pro) and cyclo(D-Phe-4Cl-Pro)	70
Table 5.2	NMR data of cyclo(Phe-4Cl-Pro) (DMSO-d_6)	85
Table 5.3	NMR data of cyclo(D-Phe-4Cl-Pro) (DMSO-d_6)	87
Table 5.4	Conformational search results calculated for cyclo(Phe-4Cl-Pro) in the gas phase	103
Table 5.5	Conformational search results calculated for cyclo(D-Phe-4Cl-Pro) in the gas phase	106
Table 5.6	Conformational search results calculated for cyclo(Phe-4Cl-Pro) in the solvated (water) phase	109
Table 5.7	Conformational search results calculated for cyclo(D-Phe-4Cl-Pro) in the solvated (water) phase	112
Table 5.8	Conformational search results calculated for cyclo(Phe-4Cl-Pro) in dimethyl sulphoxide (DMSO)	116

Table 5.9 Conformational search results calculated for cyclo(D-Phe-4Cl-Pro) in dimethyl sulphoxide (DMSO)	120
Table 6.1 Main types of cancers (Warshawsky and Landolph, 2006).....	125
Table 6.2 Currently available antineoplastic agents (Rang <i>et al.</i> , 2011).....	136
Table 6.3 Characteristics of cell cultures utilised for experiments.....	141
Table 6.4 Percentage growth inhibition of HeLa cell line after 48 hour exposure to cyclo(Phe-4Cl-Pro) and cyclo(D-Phe-4Cl-Pro) and melphalan (n =4) (vehicle with PEG).....	148
Table 6.5 Percentage growth inhibition of HeLa cell line after 48 hour exposure to cyclo(Phe-4Cl-Pro) and cyclo(D-Phe-4Cl-Pro) and melphalan (n =4) (vehicle without PEG).....	149
Table 6.6 Percentage growth inhibition of MCF-7 cell line after 48 hour exposure to cyclo(Phe-4Cl-Pro) and cyclo(D-Phe-4Cl-Pro) and Melphalan (n =4) (vehicle with PEG).....	151
Table 6.7 Percentage growth inhibition of MCF-7 cell line after 48 hour exposure to cyclo(Phe-4Cl-Pro) and cyclo(D-Phe-4Cl-Pro) and melphalan (n =4) (vehicle without PEG).....	153
Table 6.8 Percentage growth inhibition of HT-29 cell line after 48 hour exposure to cyclo(Phe-4Cl-Pro) and cyclo(D-Phe-4Cl-Pro) and melphalan (n =4) (vehicle with PEG).....	155
Table 6.9 Percentage growth inhibition of HT-29 cell line after 48 hour exposure to cyclo(Phe-4Cl-Pro) and cyclo(D-Phe-4Cl-Pro) and melphalan(n =4) (vehicle without PEG).....	156
Table 6.10 the percentage inhibition of the negative control, positive control, Cyclo(Phe-4Cl-Pro) and Cyclo(D-Phe-4Cl-Pro) on HeLa, HT-29 and MCF-7 cell lines (vehicle with 0.05% PEG 300)	158
Table 6.11 the percentage inhibition of the negative control, positive control, Cyclo(Phe-4Cl-Pro) and Cyclo(D-Phe-4Cl-Pro) on HeLa, HT-29 and MCF-7 cell lines (vehicle without 0.05% PEG 300)	159
Table 7.1 Normal colonising flora (Dipiro <i>et al.</i> , 2011).	162
Table 7.2 Commonly occurring pathogenic bacteria (Dipiro <i>et al.</i> , 2011).	163
Table 7.3 Classification of antimicrobial peptides according to Epanand and Vogel (1999)	178

Table 7.4	Percentage growth inhibition of <i>B. subtilis</i> after 24 hour exposure to cyclo(D-Phe-4Cl-Pro), cyclo(Phe-4Cl-Pro), chloramphenicol and amoxicillin.....	193
Table 7.5	Percentage growth inhibition of <i>S. aureus</i> after 24 hour exposure to cyclo(D-Phe-4Cl-Pro), cyclo(Phe-4Cl-Pro), chloramphenicol and amoxicillin.....	196
Table 7.6	Percentage growth inhibition of <i>E. coli</i> after 24 hour exposure to cyclo(Phe-4Cl-Pro), cyclo(D-Phe-4Cl-Pro), chloramphenicol and amoxicillin	198
Table 7.7	Percentage growth inhibition of <i>P. aeruginosa</i> after 24 hour exposure to cyclo(D-Phe-4Cl-Pro), cyclo(Phe-4Cl-Pro), chloramphenicol and amoxicillin	201
Table 7.8	Percentage growth inhibition of <i>C. albicans</i> after 24 hour exposure to cyclo(D-Phe-4Cl-Pro), cyclo(Phe-4Cl-Pro), chloramphenicol and amoxicillin.....	203
Table 8.1	Effects of heparin, cyclo(Phe-4Cl-Pro) and cyclo(D-Phe-4Cl-Pro) on APTT clotting times ..	221
Table 8.2	Effects of heparin, cyclo(Phe-4Cl-Pro) and cyclo(D-Phe-4Cl-Pro) on PT clotting times.....	223
Table 8.3	Effects of heparin, cyclo(Phe-4Cl-Pro) and cyclo(D-Phe-4Cl-Pro) on the formation of fibrin	225
Table 8.4	Effects of heparin, cyclo(Phe-4Cl-Pro) and cyclo(D-Phe-4Cl-Pro) on D-Dimer formation	228
Table 9.1	The metabolic effects of insulin and glucogan (Dipiro <i>et al.</i> , 2011).....	243

CHAPTER 1

INTRODUCTION

1.1 Background and problem definition

All living tissues consist of proteins. Proteins play a major role in regulating most signal transductions in eukaryotic cells and as hormones, neurotransmitters and neuromodulators (Nelson and Cox, 2005). Even though the use of peptides as novel drug compounds has been limited by their poor chemical and physical properties, structural similarities of cyclic dipeptides, also known as diketopiperazines (DKPs), cyclo dipeptides, 2,5-diketopiperazines (DKPs), 2,5-dioxopiperazines (DOPs), or dipeptide anhydrides to peptides, the abundance of their ring structure in several natural products coupled with the simplicity of their chemical structure has inspired new research (Witak and Wei, 1990).

2,5-Diketopiperazines (DKPs) are cyclic dipeptide derivatives, which show a multitude of interesting biological activities including efficient interactions with opioid receptors, potent cytotoxic effects and neuroprotective effects. Recently, they have also been associated with blockade of L-type calcium channels, tryptase inhibition, oxytocin receptor antagonism and plasminogen activator inhibition (Wyatt *et al.*, 2005).

No extensive research has yet been undertaken to determine the biological activity of cyclo(Phe-4Cl-Pro) and cyclo(D-Phe-4Cl-Pro). Chlorine was introduced on the side chain to increase the lipid solubility, optimise cell penetrability and the physiological response. In a study (Brauns *et al.*, 2004), selected cyclic dipeptides were evaluated for anti-cancer activity against a number of cell lines, namely MCF-7 (breast carcinoma), HeLa (cervical carcinoma) and HT-29 (colon carcinoma), indicating that one of the compounds tested, cyclo(phe-pro), showed inhibition of proliferation of some cell lines,

and in addition induced apoptosis in the HT-29 cell line. It thus indicates the potential for proline- and phenylalanine-containing cyclic dipeptides to inhibit the growth of tumours *in vivo*. Studies of cyclic dipeptides are therefore warranted.

1.2 Aim

The primary aim of this study is to synthesise, elucidate and determine the biological activity of cyclo(Phe-4Cl-Pro) and cyclo(D-Phe-4Cl-Pro), utilising qualitative and quantitative experimental approaches.

1.3 Objectives

Based on the aim, the objectives of the study can be outlined as follows:

- To successfully synthesise and purify cyclo(Phe-4Cl-Pro) and cyclo(D-Phe-4Cl-Pro) from their respective amino acid precursors.
- To elucidate the structures by means of fast atom bombardment mass spectrometry, nuclear magnetic resonance spectroscopy, and infrared spectroscopy.
- To determine the physicochemical characteristics of cyclo(Phe-4Cl-Pro) and cyclo(D-Phe-4Cl-Pro) using the following: Scanning electron microscopy, differential scanning calorimetry, thermogravimetric analysis and X-Ray powder diffraction.
- To determine the biological effects of the synthesised compounds with respect to their antimicrobial, anticancer, haematological and anti-diabetic activities.

CHAPTER 2

LITERATURE REVIEW

2.1 Background

The fundamental objectives of organic and medicinal chemistry involve the discovery, development, identification and interpretation of the mode of action of biologically active compounds at the molecular level. Even though the emphasis is put on drugs, medicinal chemistry also involves the study, identification and the synthesis of the metabolic by-products of drugs and related compounds (Wermuth, 2003).

The battle between scientific research and disease has been constant throughout human history and for all the success we have witnessed in the 20th century, only about one third of the 30,000 known diseases can be treated effectively (Rozek and Tully, 1999). Several diseases remain difficult to treat successfully such as cancer, auto-immune disorders, viral diseases (*e.g.*, influenza), and central nervous system disorders (*e.g.*, Alzheimers disease) (Kourounakis and Rekka, 1994). The emergence of multi-drug resistant microorganisms have added to the urgency in discovering new novel drugs or agents, a process that can take many years before a product is regarded as safe and efficient and reaches the market place (Shlaes *et al.*, 2004).

The costs associated with the development of new drugs (especially clinical evaluation) have increased dramatically in recent years, and therefore fewer ground-breaking drugs have made their way onto the market. There is a great need for the development of more active and selective drugs with minimal side effects, agents useful in prophylaxis and drugs that will cause less harmful contamination in an already polluted environment (Kourounakis and Rekka, 1994).

The demand for peptides and proteins as therapeutic agents is increasing rapidly with time. During the past 35 years the discovery of a vast range of naturally occurring

peptides with potent and specific biological activities has further increased their importance (Suresh Babu, 2001).

Peptide ligands can act as either agonists or antagonists at cell-surface receptors or acceptors that modulate cell function and animal behavior. This area encompasses approximately 50% of current drugs and will become even more important in the future. The biological and behavioral activities that are controlled or modulated by these interactions include response to stress, pain, inflammation, addiction, learning, memory, feeding behavior, sexual behavior, reproduction, the immune response, thermal control, cardiovascular function/regulation and kidney function. The development of peptide or peptidomimetic ligands that can target receptors or acceptors that modulate or control these biological activities thus remains a top priority of every pharmaceutical scientist (Hruby, 2002).

Biologically active peptides range in size from small molecules, containing only two or three amino acids, to large molecules containing many amino acids. Neuropeptides, hypothalamic hormones (releasing and releasing inhibiting hormones), proteohormones of the pituitary, thyroid hormones, gastrointestinal peptides, muramyl peptides, peptides of immunological significance, peptide vaccines, plasma kinins, atrial natriuretic peptides, peptide antibiotics, peptide toxins, peptide insecticides and herbicides are some of the important classes (Suresh Babu, 2001).

Cyclic dipeptides also known as 2,5-dioxopiperazines, 2,5-diketopiperazines, cyclo dipeptides or dipeptide anhydrides, are relatively simple dipeptides and are therefore commonly found in nature. Since their discovery at the start of the 20th century, a vast amount of peptides have been identified from natural origins (Anteunis,1978) and are currently attracting considerable attention due to certain biological activities (Prasad,1995). Some peptides are well known for their biological importance as antibiotics, hormones toxins and ion transport regulators (Ovchinnikov and Ivanov, 1975). The therapeutic potential of these compounds ranges from antibiotic, antiviral,

anti-tumour, tenso-active to muscle relaxant activity, to only name a few (Milne *et al.*, 1998).

2.2 Amino acids, peptides and proteins

Amino acids are classified as non-essential, essential and conditionally essential amino acids (Meier, 2005). Food and tissue proteins consist of twenty amino acids of nutritional importance. Nine of these amino acids (histidine, isoleucine, leucine, lysine, methionine, phenylalanine, threonine, tryptophan and valine) are known as essential or indispensable nutrients since they cannot be synthesized by the body and must therefore be obtained from the diet. The remaining eleven amino acids (alanine, arginine, aspartic acid, asparagine, cysteine, glutamic acid, glutamine, glycine, proline, serine and tyrosine) are known as nutritionally dispensable or non-essential nutrients since they can be synthesized by the body, but are also ordinarily obtained from the diet. They are equally as important as the indispensable amino acids for both nutrition and normal functioning of cells and organs (Campbell and Farrell, 2003). There are only a few diseases that may result in isolated amino acid deficiencies. In catabolic diseases, some of the amino acids (arginine, cysteine, glutamine, histidine, serine and tyrosine) become conditionally essential. The supplementation of these amino acids has been shown to have a positive effect on clinical outcome under specific conditions (Meier, 2005). The general structure of an amino acid (Figure 2.1) contains an amino group and a carboxyl group, both of which are bonded to the α -carbon (Campbell and Farrell, 2003).

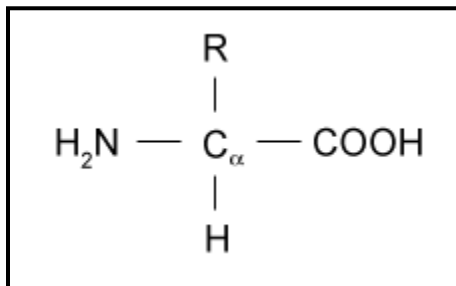


Figure 2.1 General structure of an amino acid (Campbell and Farrell, 2003).

Amino acids are a special kind of carboxylic acid consisting of a basic amine (NH₂) group and an acidic carbonyl (COOH) group. This dipolar ion can undergo intermolecular acid-base reactions and exist primarily in the form of zwitterions. Zwitterions show physical properties associated with salts, having large dipole moments, are soluble in water, insoluble in hydrocarbons and have very high melting points (McMurry, 2008). Amino acids can be distinguished on the basis that the amino and carboxylic functions are both linked to the same carbon. For example α-amino acids (shorter distance between functional groups) can be distinguished from β; γ; δ and ε-amino acids (greater distance between functional groups) as is illustrated in Figure 2.2 (Jakubke and Jeschkeit, 1977).

---CH ₂ CH ₂ (NH ₂)COOH	α-Amino acid
---CH ₂ CH ₂ (NH ₂)CH ₂ COOH	β-Amino acid
---CH ₂ (NH ₂)(CH ₂) ₄ COOH	ε- Amino acid

Figure 2.2 Illustrating the difference between α; β and ε- amino acids. (Jakubke and Jeschkeit, 1977).

Amino acids also form left (levo or L) and right (dextro or D) handed isomers. Only L-isomers of amino acids are found naturally in proteins (Campbell and Farrell, 2003).

The cellular tissue and fluid of living organisms contains a permanent reservoir of free amino acids. These free amino acids take part in numerous metabolic reactions illustrated in Figure 2.3 (Jakubke and Jeschkeit, 1977).

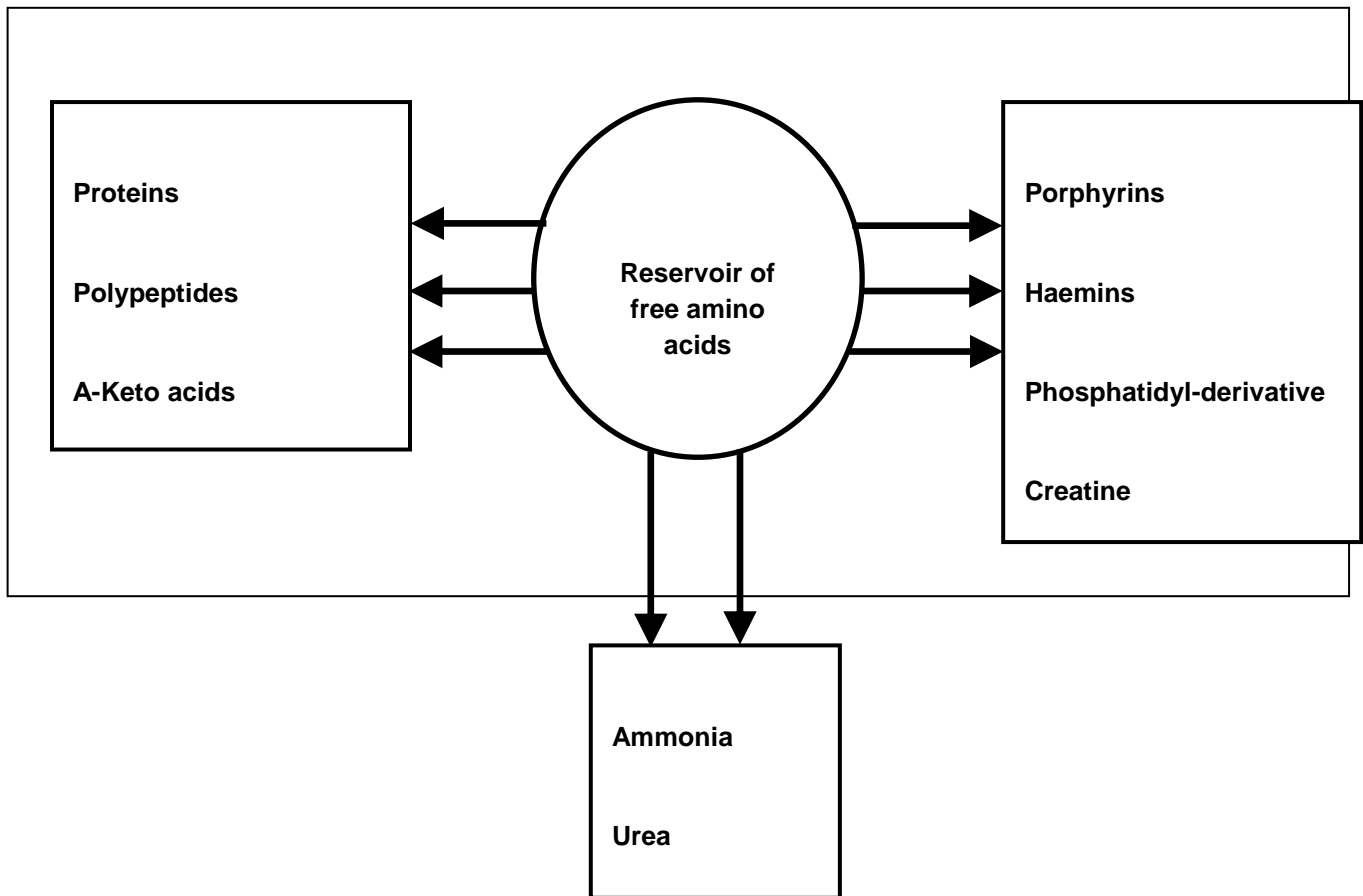


Figure 2.3 Schematic representation of the amino acid reservoir (Jakubke and Jeschkeit, 1977).

Apart from the metabolic roles they play, amino acids are also key precursors that can be converted to both hormones and neurotransmitters (Campbell and Farrell, 2003). Tryptophan is a key amino acid precursor that can be converted to both hormones and neurotransmitters.

Figure 2.4 Illustrates the conversion of tryptophan to serotonin (5-HT), melatonin and niacin, which is known to play a key role in several disease states, one being serotonin syndrome that is evoked by an interaction between serotonergic agents (5-HT re-uptake blockers and MAO (mono-amine oxidase)) inhibitors (Katzung, 2009).

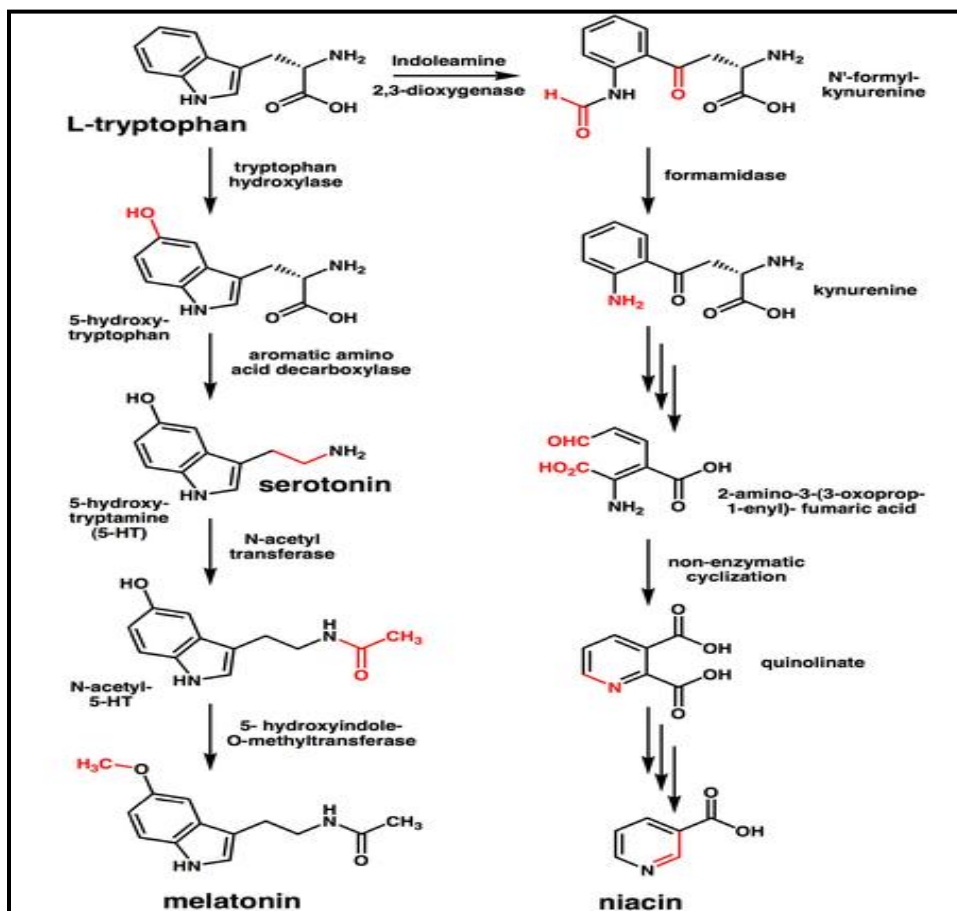


Figure 2.4 Conversion of tryptophan to serotonin, melatonin and niacin (Campbell and Farrell, 2003)

The compounds under investigation in this study are the phenylalanine-containing and proline-containing cyclic dipeptides, cyclo(Phe-4CI-Pro) and cyclo(D-Phe-4CI-Pro), as illustrated in Figures 2.5 and 2.6, respectively.

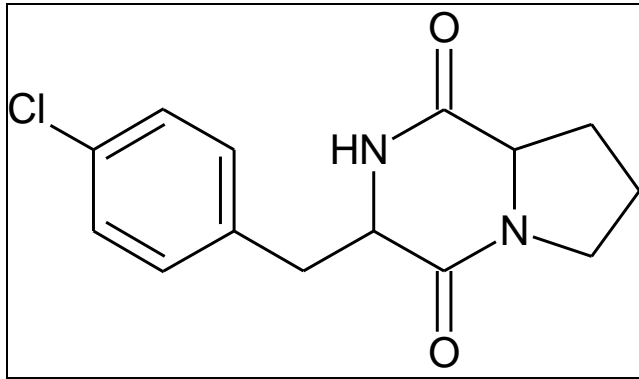


Figure 2.5 Structure of Cyclo(Phe-4Cl-Pro)

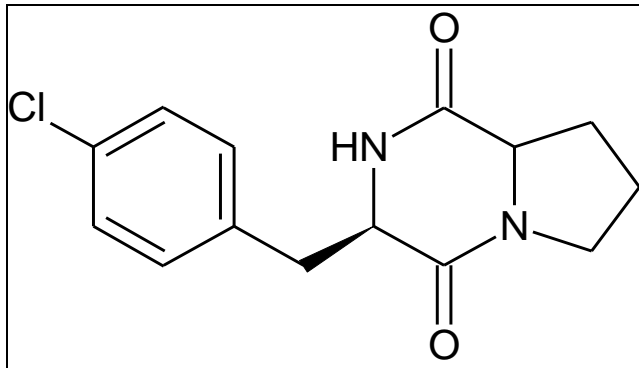


Figure 2.6 Structure of Cyclo(D-Phe-4Cl-Pro)

Phenylalanine (Phe or F); (2-amino-3-phenyl-propanoic acid); is a neutral, aromatic amino acid with the formula $\text{HOOCCH}(\text{NH}_2)\text{CH}_2\text{C}_6\text{H}_5$. It is classified as nonpolar because of the hydrophobic nature of the benzyl side chain (Katzung, 2009). Tyrosine and phenylalanine play a significant role not only in protein structure, but also as important precursors for thyroid and adrenocortical hormones as well as in the synthesis of neurotransmitters such as dopamine and noradrenaline (Katzung, 2009). The genetic disorder phenylketonuria (PKU) is the inability to metabolize phenylalanine. This is

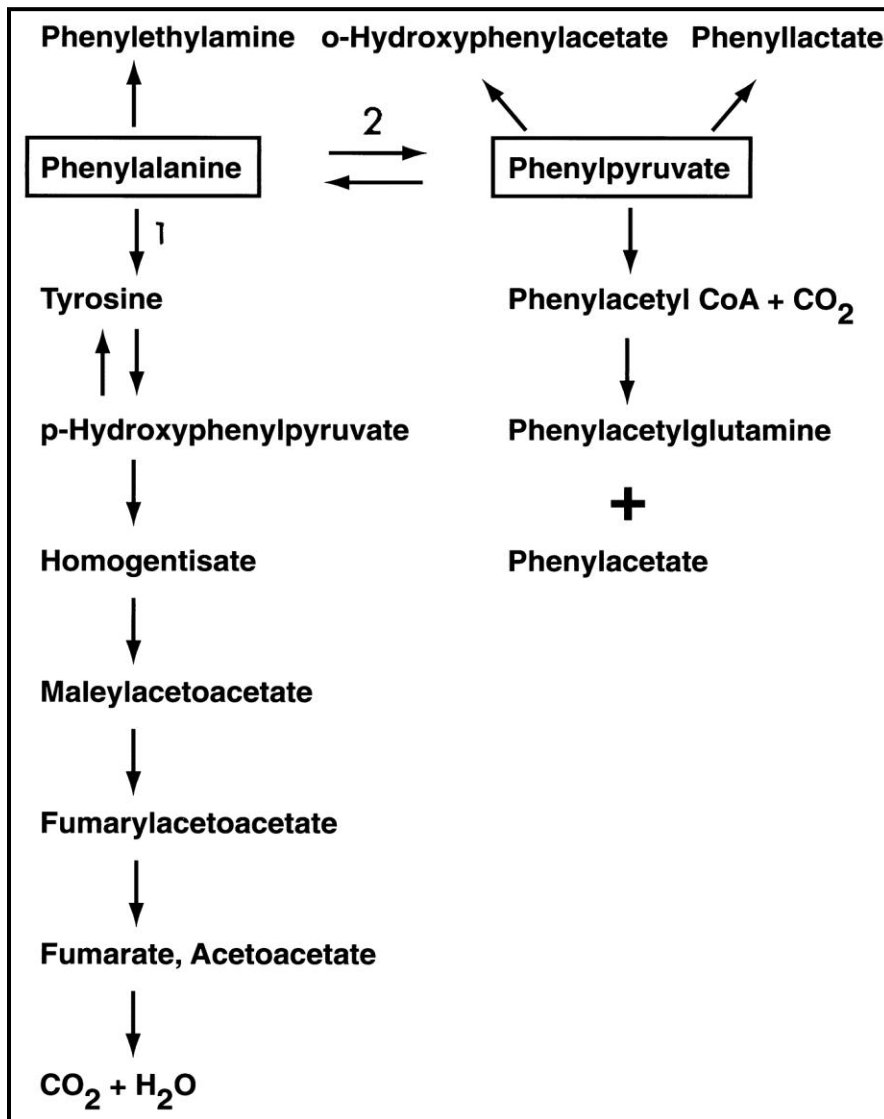
caused by a deficiency of the enzyme, phenylalanine hydroxylase with the result that there is an accumulation of phenylalanine in body fluids. Individuals with this disorder are known as "phenylketonurics" and must abstain from consumption of phenylalanine. A non food source of phenylalanine is the artificial sweetener aspartame (L-aspartyl-L-phenylalanine methyl ester) which is metabolized by the body into several by-products including phenylalanine. The side chain of phenylalanine does not undergo side reactions, but during catalytic hydrogenations the aromatic ring can be saturated and converted to a hexahydrophenylalanine residue (Campbell and Farrell, 2003).

Proline (Pro or P); ((S)-Pyrrolidine-2- carboxylic acid); is a nonpolar, neutral amino acid and is regarded as a helix breaker. The aliphatic side chain of proline differs from other amino acids in that its side chain is bonded to both to the α -carbon and nitrogen. Proline contains a secondary rather than a primary amino group, which makes it an *imino* acid (Campbell and Farrell, 2003). Proline can only act as a hydrogen bond acceptor, and not as a hydrogen bond donor, since it lacks hydrogen on the amide group. Proline is the only residue which leads to an N-Alkyl amide bond when incorporated into a peptide. Proline is therefore unique in having no amide proton to participate in hydrogen bonding and in having a cyclic side chain which establishes conformational restrictions (the pyrrolidine ring decreases the conformational mobility of the DKP moiety, so that the side-chain rotamers for the non-prolyl residue is well defined (Campbell and Farrell, 2003). Proline can cause reversal of direction of peptide chains in globular proteins (Campbell and Farrell, 2003) and acts as a conformational determinant in structural proteins *e.g.*, collagen. Inclusion of proline in DKPs increases the solubility of the compounds in chloroform. Furthermore, studies have shown that proline has the ability to isomerise and undergoes a transition from the all-*cis* form (polyproline I) to the all-*trans* form (polyproline II) (Campbell and Farrell, 2003).

Proline is found in naturally occurring biologically active peptides, including peptide hormones *e.g.*, angiotensin, bradykinin, oxytocin, vasopressin, MSH (melanocyte stimulating hormone), TRF (thyroid-releasing factor), gramicidin S, actinomycin, and

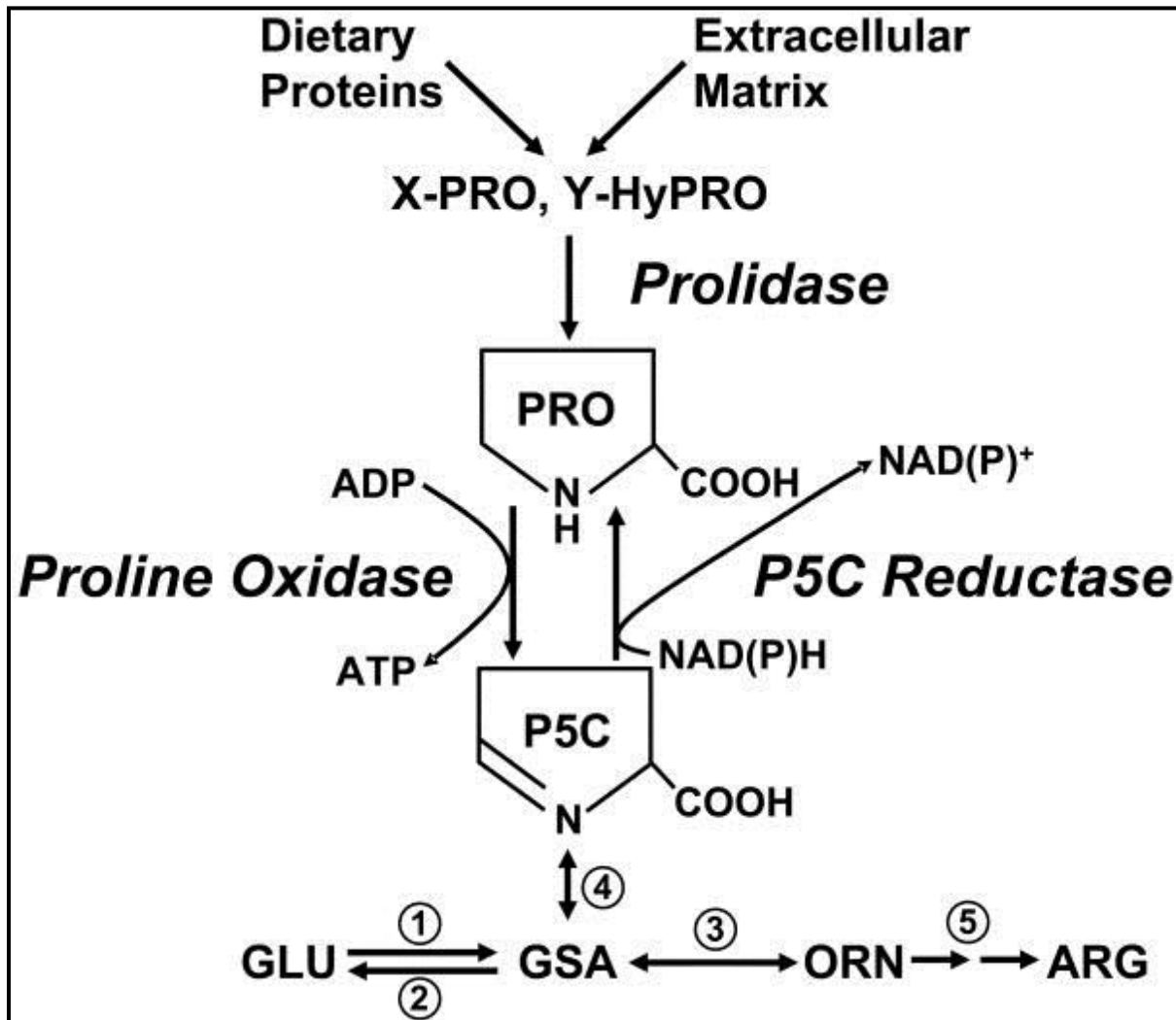
antamanide (Campbell and Farrell, 2003). Dipeptides containing a proline or a hydroxyproline residue, exhibit a marked propensity for intermolecular cyclization.

Figure 2.7 and Figure 2.8 illustrate the metabolic pathways of phenylalanine and proline respectively.



1, transaminase pathway with glutamate; 2, P5C dehydrogenase

Figure 2.7 Metabolic pathway of phenylalanine (Wang *et al.*, 2001)



1, P5C synthase; 2, P5C dehydrogenase; 3, ornithine aminotransferase; 4, spontaneous reaction; 5, urea cycle enzymes.

Figure 2.8 Metabolic pathway of proline (Phanget *et al.*, 2008)

Individual amino acids can be linked together by the formation of a covalent bond between them. Water is eliminated during the process and a bond is formed between the α -carboxyl group of one amino acid and the α -amino group of the next one (Figure 2.9). A bond formed this way is called a peptide bond. Peptides are compounds formed

by the linking of small numbers of amino acids, ranging from two to several dozen (Campbell and Farrell, 2003).

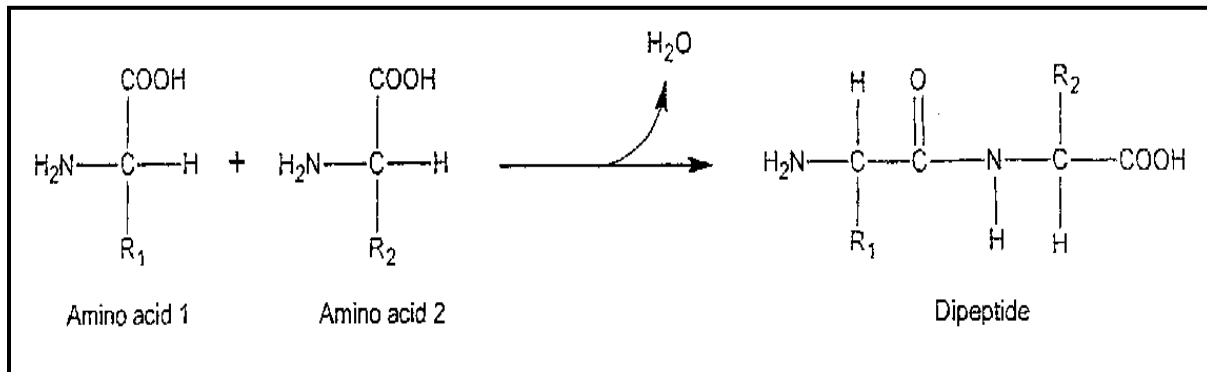


Figure 2.9 Formation of a peptide bond (Campbell and Farrell, 2003)

Proteins the fundamental building blocks of all life consist of polypeptide chains which are usually made up of more than 100 amino acids. The human body contains about 100 000 different proteins. Proteins are of variable length and structure, which fold upon themselves to generate a shape that is characteristic of each protein. The function and properties of different peptides and proteins are determined through the sequence of amino acids. This sequence is based on the genetic information contained in deoxyribonucleic acid (DNA) (Campbell and Farrell, 2003; Mohan, 2001).

Proteins and peptides control numerous biochemical reactions in the body and may represent an unexploited source of new drugs for treating a variety of diseases (Mohan, 2001).

Synthesised medicinal peptides represent a broad range of biological substances that will exert biological effects for related medicinal conditions. These substances represent a broad variety such as hormones, cytokines, enzymes, blood coagulation regulators, vaccines, poisons and antibiotics that are integral to the regulation and maintenance of biological processes (Frokjaer and Hovgaard, 2000). Table 2.1 illustrates the biological substances that are used clinically (Bhattyacharya *et al.*, 2005). Peptides in which

amino acids are key precursors include the vasodilators (bradykinin, natriuretic peptides, vasoactive intestinal peptides, substance P, neurotension, calcitonin gene related peptide) and vasoconstrictors (angiotension II, vasopression, endothelins and neuropeptide Y). These hormones and neurotransmitters control and maintain the function and integrity of all the body's major organ systems. Neurotransmitters function in the transmission of nerve impulses and the activation and inactivation of receptors and these vital functions will control normal body regulators such as metabolism, immune defences, digestion, respiration, reproduction and sensitivity to pain (Katzung, 2009). Peptides exhibit a very wide structural and functional variation and are therefore very important for the regulation and maintenance of biological processes (Frokjaer and Hovgaard, 2000). Table 2.1 illustrates the major peptide-and protein-containing drugs currently used (Bhattyacharyya *et al.*, 2005).

Table 2.1 Key groups of peptide- and protein-containing drugs (Bhattyacharyya *et al.*, 2005).

Peptides	
Antibiotics	Bacitracin, Bleomycin, Colitimetate sodium, Gramicidine
Hormones	Corticotropin, Glucagon, Gonadorelin hydrochloride, Lypressin, Oxytocin, Vasopressin, Calcitonin, Desmopressin, Leuprolide acetate, Demoferin acetate, Goserelin acetate, Teriparatide acetate, Sermorelin acetate, Cosyntropin, Corticorelin, Histrelin acetate, Protirelin, Secretin
Others	Polymyxin B, Cyclosporin, Eptifibatide
Non-glycosylated proteins	
Interleukins	Aldesleukin (IL-1), Anakinra (IL-2), Denileukindiftitox

Interferons	Interferon alfa-n1, Interferon alfa-n3, Interferon alfa-2a, Interferon alfa-2b Peginterferon alfa-2b, Interferon alfacon-1, Interferon beta-1b, Interferon gamma-1b
Enzyme /Inhibitors	Alpha-1 Proteinase Inhibitor, Anistreplase, Asparaginase, Pegaspargase, Rasburicase, Reteplase, Tenecteplase, Dornase alpha, Chymotrypsin, Hyaluronidase, Prancreatin, Pancrelipase, Papain, Trypsin, Urokinase, Alglucerase, Chymopapain, Deoxyribonuclease, Fibrinolysin, Imiglucerase, Pegademase, Streptokinase, Adenosine deaminase, Rasburicase, Lactase
Growth Factors/Hormones	Becaplermin, Filgrastim, Pegfilgrastim, menotropins
Antithrombotic Agents	Thrombin, fibrinogen, Fibrin, Hirudin, Hirulog
Others	Insulin, Insulin Lispro, Gelatin, Collagen, Prolactin, Digoxin, Immune Fab, Albumin Human, Haemoglobin
Glycosylated proteins	
Interferons	Interferon beta-1a
Antithrombotic Agents	Alteplase, Drotrecoginalfa, Antithrombin III

Antianaemic	Darbopoeitin alfa, Erythropoietin
Growth Hormones	Somatropin, Somatrem, Chorionic Gonadotropin Human, follitropin alpha, Follitropin beta, Urofollitropin, Thyrotropin
Immune globulins	Normal Immune Globulin, Hepatitis B Immune Globulin, Pertussis Immune Globulin, Rabies Immune Globulin, Tetanus Immune Globulin, Vaccinia Immune Globulin, CMV Immune Globulin, Varicella-Zoster Immune Globulin, Rho(D) Immune globulin, Intravenous Gamma Globulin, Lymphocyte Anti-Thymocyte Immune Globulin Equine, Lymphocyte Anti-Thymocyte Immune Globulin Rabbit
Coagulation Factors	Factor VII, Antihæmophilic factor, Cryoprecipitated AHF, Factor IX
(Factor VIII) Others	Etanercept (CSF), Sargramostim (TNF)
Monoclonal antibodies	
Abciximab, Alemtuzumab, Arcitumomab, Basiliximab, Capromab, Declizumab, Ibritumomab, Tiuxetan, Imciromab, Infliximab, Nofetumomab, Palivizumab, Rituximab, Trastuzumab, Daclizumab, Satumomab, Muromonab-CD ₃ , Gentuzumab	

2.3 Cyclidipeptides

2.3.1 General aspects of cyclic dipeptides

Cyclic dipeptides are heterocyclic compounds comprising of two amino acid residues linked to a central diketopiperazine (DKP) ring structure (Kilian, 2002). The general structure of cyclic dipeptides is illustrated in Figure 2.10 where R_1 and R_2 can be substituted with different amino acid side-chain residues, resulting in a number of chemical structures of varying chemical and biological properties.

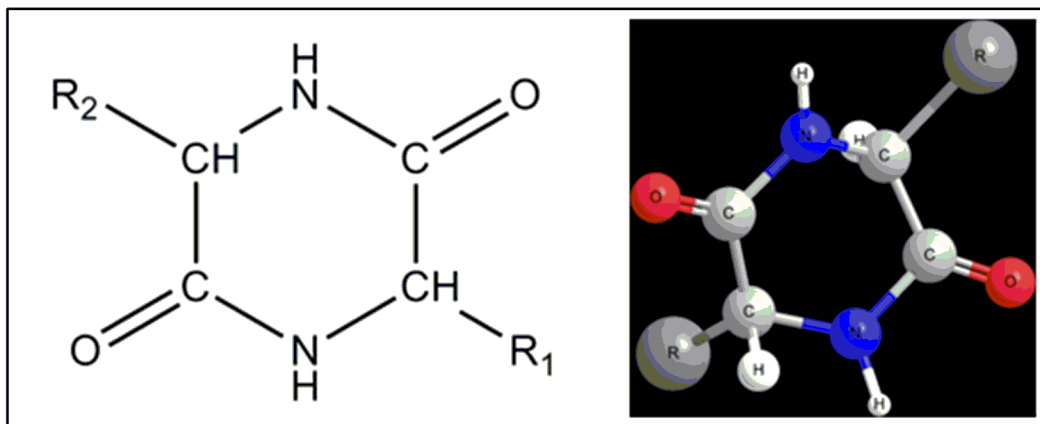


Figure 2.10 General structures of a 2,5-diketopiperazine, where R_1 and R_2 represent the substituting amino acid residues (Prasad, 1995).

In 1888 Curtius and Gloebel synthesised the first cyclic dipeptide, cyclo(Gly-Gly), for the sole purpose of examining their physiological properties, many simple diketopiperazines (DKPs) have been synthesised since then (Prasad, 1995).

Cyclic dipeptides are divided into two broad classes. Firstly cyclic dipeptides are termed homodetic if the linkage that contributes to the formation of the DKP ring is a peptide bond and secondly heterodetic if the cyclisation includes other bridges such as disulfide, ester (lactone), ether or thioether bridges. Several chemical strategies, including head-to-tail cyclisation reactions utilising solid- or solution-phase synthetic methods, have been developed to convert linear peptides to cyclic structures (Adessi and Soto, 2002).

Optimisation of potential drug candidates often precludes the use of peptides because of their poor physical and metabolic properties. As a result of the structural similarity of DKPs to peptides, their appearance in biologically active natural products has inspired medicinal chemists to use DKPs to circumvent the limitations of peptides. Constraining the nitrogen atoms of an α -amino amide into a DKP ring alters physical properties, reduces susceptibility to metabolic amide bond cleavage reactions and reduces conformational mobility. As a result of the change in structural and physical characteristics, DKPs can confer more drug-like properties to molecules and enhance favourable interactions with macromolecules (Dinsmore and Beshore, 2002). Table 2.2 lists some of the properties of cyclic dipeptides that make them different from ordinary peptides.

Table 2.2 The difference between cyclic dipeptides and ordinary peptides

The properties of cyclic dipeptides differ from those of ordinary peptides:
They do not exist as zwitterions and are often neutral compounds ¹
The simpler members of this group are water soluble ¹
They have the ability of forming hydrogen bonds with the solvent (via the two cis-amide groups in the cyclic dipeptide ring), and give rise to hydrophobic interactions ²
They are important metabolic intermediates and provoke the destruction of the secondary globular protein structure ^{3,4} , (especially non-ionic polar DKPs exhibit the potential to act as denaturing agents) ²
They are chirally enriched, easy accessible heterocycles and owing to their constrained nature, do not exhibit unwanted physical and metabolic properties ⁵

They are sensitive to oxidation, especially when *imino* acid residues are the building blocks⁵

They may act as powerful hydrolytic catalysts⁶

Their physico-chemical and biological properties are dependent on the spatial arrangement of their constituent atoms⁷

They do not have backbone terminal charged groups⁷

¹(Sammes, 1975), ²(Ramani *et al.*, 1977), ³(Krejcarek *et al.*, 1968), ⁴(Crescenzi *et al.*, 1973), ⁵(Haüsler *et al.*, 1978), ⁶(Imanishi *et al.*, 1975), ⁷(Ovchinnikov and Ivanov, 1975),

2.3.2 Conformational aspects of cyclic dipeptides

The DKP backbone is an important cornerstone in peptide research, drug discovery and design and for the development of peptidomimetics (Sammes, 1975). The DKP backbone is conformationally restrained by a six membered ring with side chains that are orientated in a spatially defined manner. The DKP ring contains two hydrogen bond accepting centres and two hydrogen bond donating sites which are important for potential interactions between the lead compound and receptor sites (Deslauriers *et al.*, 1975).

The conformations and molecular structures of cyclic dipeptides containing the DKP ring have been studied by a number of physical techniques, including X-ray crystallography,

infrared (IR) spectroscopy, nuclear magnetic resonance (NMR), optical rotatory dispersion (ORD) and circular dichroism (CD) spectroscopy (Deslauriers *et al.*, 1975).

A strong link between the physicochemical and biological properties of cyclic dipeptides and the spatial arrangements of their constituent atoms has been shown to exist (Ovchinnikov and Ivanov, 1975).

The two major considerations, with respect to conformational analysis of cyclic dipeptides, are the degree of planarity of the DKP ring and the degrees of folding or extension of the different side-chain substituents (Van der Merwe, 2005).

Structural models have shown that the six-membered DKP ring of cyclic dipeptides is slightly flexible and may thus adopt four main configurations (planar, boat, bowsprit-boat and twist-boat), which is strongly influenced by the substituents at the α -carbon atoms (Funasaki *et al.*, 1993). Three conformations of the DKP ring have been identified in the solid state *i.e.*, chairs, boat and twists (Jankowska and Ciarkowski, 1987).

The aromatic side chains of the two phenylalanine-containing rotamers [cyclo(Phe-Pro); cyclo(Phe-D-Pro)] can adopt one of three predominant conformations: a folded conformation; extended towards the nitrogen (E_N); or extended towards the oxygen (Young *et al.*, 1976).

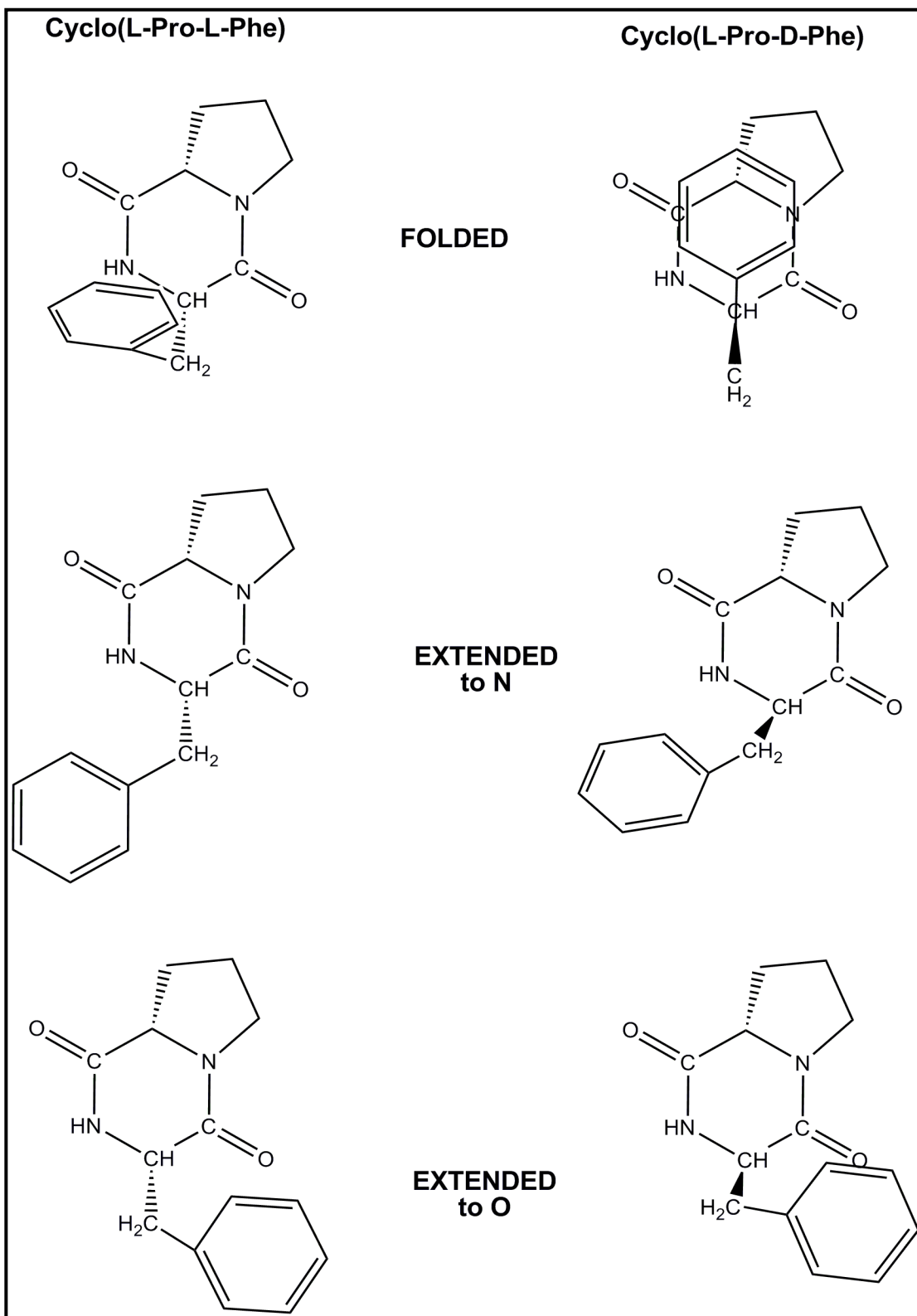


Figure 2.11 Side chain conformations of cyclo(Phe-Pro) and cyclo(Phe-D-Pro). (Adapted from Young *et al.*, 1976).

2.3.3 Physicochemical properties of cyclic dipeptides

2.3.3.1 Solubility of cyclic dipeptides

Interactions between water and the hydrophobic or hydrophilic parts of peptides, such as amino acid side chains and peptide groups, play a crucial role in their structure and stability (Della Gatta *et al.*, 2005).

As a result of the intramolecular aminolysis reaction, cyclic dipeptides are not capable of existing as zwitterions. Simpler members have been shown to exist exclusively as neutral compounds (Grant, 2002). Cyclic dipeptides share the capability of establishing hydrogen bonds with the solvents via the two *cis*-amide groups in the DKP ring, and of giving rise to hydrophobic interactions, the extent of which is determined by the R₁ and R₂ substituents. The solubility of non-ionic DKPs is limited, to DKPs containing short alkyl R substituents (Crescenzi *et al.*, 1973; Sammes, 1975).

2.3.3.2 Physical stability of cyclic dipeptides

Cyclic dipeptides exist as fairly stable entities. However, studies have shown that either of the two carbonyl groups of the DKP ring of cyclo(Phe-Pro) can undergo hydrolysis, thereby producing two different linear dipeptides, *i.e.*, Phe-Pro-OH and Pro-Phe-OH. This suggests their possible use as pro-drugs (Goolcharren and Borchardt, 1998).

Results from studies by Grant (2002) showed that aqueous solutions of some cyclic dipeptides, stored at high temperatures for a prolonged period of time, had a high degree of thermo stability. The *cis*-fused diketopiperazines are thermodynamically more stable, compared to their *trans*-fused counterparts, and constitute a predominant class of naturally occurring products. This seems logical considering their biosynthetic origin, usually from two proteinogenic L- α -amino acids. There are only a few reports on *trans*-configured diketopiperazines derived from natural sources (Siwicka *et al.*, 2005).

Cyclic dipeptides are also more stable between certain pH ranges. For example, cyclo(Phe-Pro) exist as a relatively stable entity between pH values 3 and 8,

but hydrolysis of the diketopiperazine nucleus occurs at pH values of less than 3 or greater than 8 (Goolcharren and Borchardt, 1998).

2.3.4 Absorption, transportation and metabolic stability of cyclic dipeptides

In order to exhibit or exert their pharmacological action, peptide and protein drugs must be transported without metabolic degradation to the systemic circulation. Although active transport of linear peptides and oligopeptides by intestinal oligopeptide transporters has been reported, overall intestinal absorption of peptides is very poor due to metabolic degradation by peptidases (Mizuma *et al.*, 2002).

Peptide transporters are integral plasma membrane proteins that mediate the cellular uptake of dipeptides and tripeptides in addition to a variety of peptidomimetics. Peptide transporters represent excellent targets for the delivery of pharmacologically active compounds, because their substrate binding site accommodates a wide range of molecules of differing size, hydrophobicity and charge (Rubio-Aliaga and Daniel, 2002).

Although intestinal and renal peptide transporters have similar features, such as substrate recognition and driving force, it has been suggested that the intestinal and renal transport systems are not identical. Molecular cloning studies revealed the existence of two homologous peptide transporters, PEPT1 (SLC15A1) and PEPT2 (SLC15A2) (Terada *et al.*, 1997).

PEPT1 and PEPT2 actively transport dipeptides and tripeptides, including peptidomimetics, across cell membranes in animals, microbes and plants (Rubio-Aliaga and Daniel, 2002). PEPT1 is a low-affinity/high-capacity transporter, which is found primarily on the brush-border membrane of the small intestine, and to a lesser extent in the proximal tubule of the kidney. In contrast, PEPT2 is a high-affinity/low-capacity transporter expressed predominantly in the apical membrane of the kidney (Shen *et al.*, 1999; Smith *et al.*, 1998). Both transporters function electrogenetically, as they are driven electrochemically *via* a gradient of proteins across the intestinal or renal brush-border membrane in the lumen-to-cytoplasm direction (Nussberger and Hediger, 1995).

In addition to amino acid transporters, peptide transporters contribute to the homeostasis of amino acids (Palacin *et al.*, 1998).

Mizuma *et al.* (2002) studied the uptake of cyclic dipeptides via the PEPT1 peptide transporters. They noted that the cellular uptake of cyclic dipeptides was pH dependent, and that the uptake was inhibited by the addition of PEPT1 substrates, which indicates PEPT1-mediated transport of the cyclic dipeptides. It was concluded that tyrosine had a high affinity for PEPT1 and that the phenolic hydroxyl group may enhance this affinity for PEPT1. According to Mizuma *et al.* (2002), cyclo(Ser-Tyr) and other cyclic dipeptides were stable enough to be transported in any region of the small intestine, while the linear dipeptides including seryltyrosine were too unstable to be transported and were degraded by peptidases.

Certain cyclic dipeptides have the ability to be transported by additional paracellular mechanisms, thereby effectively enhancing their transport beyond that of their corresponding linear dipeptides (Mizuma *et al.*, 1997). Not only absorptive transport, but also excretive transport is observed for certain cyclic dipeptides. That is, the intestinal absorption of certain cyclic dipeptides consists of carrier-mediated absorptive transport and carrier-mediated excretive transport in addition to passive transport. Absorptive transport is mediated by PEPT1, whereas excretive transport is mediated by a transporter that is closely linked to adenosine triphosphate (ATP). The concentration dependent preference of these absorptive and excretive transport cause atypical intestine absorption of certain cyclic dipeptides (Mizuma *et al.*, 2003).

As far as metabolism is concerned, possible recognition of peptide derivatives by hepatic cytochrome P450 3A has been suggested by binding and metabolism of numerous pseudopeptidic compounds such as ergot derivatives and cyclosporin. Natural linear or cyclic dipeptides containing hydrophobic amino acids produced by microorganisms and present in mammals are able to interact with the P450. Some cyclic dipeptides are rapidly transformed by cytochrome P450 3A to mono or

hydroxylated metabolites. This metabolism of cyclic dipeptides occurs in eight species including man (Delaforge *et al.*, 2001).

2.3.5 Biologically active cyclic dipeptides

Amongst the simplest and easiest to obtain peptide derivatives found in nature are cyclic dipeptides. They are common to synthetic, spontaneous and biological formation pathways. Since their discovery around the turn of the century, more than a hundred cyclic dipeptides have been identified from natural origins (Anteunis, 1978), and continue to be discovered. They are detected in sponges (Wegerski *et al.*, 2004; De Rosa *et al.*, 2003; Fu *et al.*, 1998; Prasad, 1995), microorganisms (Lautru *et al.*, 2002; Holden *et al.*, 1999; Kanoh *et al.*, 1997; Prasad, 1995; Park and Stroebel, 1994; Sammes, 1975) and mammals (Gudasheva *et al.*, 1997; Walter *et al.*, 1978).

Although cyclic dipeptides are commonly found in nature, very few of these molecules have been tested and only four are known to exhibit biological activity in mammals. These include cyclo(His-Pro), cyclo(Leu-Gly), cyclo(Tyr-Arg) and cyclo(Asp-Pro). Amongst these four compounds only cyclo(His-Pro) has been shown to be endogenous to mammals (Prasad, 1995).

Milne *et al.* (1998) studied the effects of cyclo(Phe-Pro), cyclo(Tyr-Pro), cyclo(Trp-Pro) and cyclo(Trp-Trp) on ion channel regulation in rat and guinea-pig myocytes, induction of differentiation in cultured cancer cell lines as well as the antimicrobial activity of these compounds. Results from the study suggest that the compounds could have potential as muscle relaxants, anticancer agents and antibiotics, if their solubilities can be increased. Evaluation of some cyclic dipeptides by Graz *et al.* (1999) further supported the potential of these compounds as antibacterial agents. Table 2.3 illustrates the biological activity of some cyclic dipeptides.

Table 2.3 Biological activity of some cyclic dipeptides

Cyclic Dipeptide	Biological activity
Cyclo(Phe-Pro), Cyclo(Tyr-Pro), Cyclo(Trp-Pro) and Cyclo(Trp-Trp) ^{1, 3, 29}	<ul style="list-style-type: none">• Calcium and sodium channel blocking activity• Antibacterial activity• Anticancer activity• Cyclo(Phe-Pro), cyclo(Tyr-Pro) and cyclo(Trp-Pro) play a role in the induction of differentiation in cancer cell lines
Cyclo(His-Pro) ^{2, 21, 22, 23, 24, 25, 26, 27, 29}	<ul style="list-style-type: none">• Played an important role in the perception of pain-induced by physical, mechanical, thermal and chemical stimuli• Inhibition of prolactin release from the pituitary gland• Decreased gastric mucosa blood flow• Production of hypothermia in mice• Suppression of stress induced eating, starvation induced eating and spontaneous eating over a ten hour period in mice• Antagonism of ethanol narcosis in mice• Modulation of glucose metabolism• Hormonal regulation

Cyclo(Leu-Gly) ²	<p>Caused the blockade of:</p> <ul style="list-style-type: none"> • The development of physical dependence on morphine • The development of tolerance to the pharmacological effects of β-endorphin • The development of tolerance to haloperidol-induced catalepsy and hypothermia • Dopaminergic supersensitivity after long-term morphine exposure • An increase in response latency measured in the rat yeast-paw test following oral administration of the peptide
-----------------------------	---

Cyclo(Pro-Phe) ²	<ul style="list-style-type: none"> • Blockade of the development of physical dependence on morphine
Cyclo(Tyr-Arg) ²	<ul style="list-style-type: none"> • Antinociceptive activity
Cyclo(Asp-Pro) ^{2, 29}	<ul style="list-style-type: none"> • Inhibition of caloric and dietary fat intake
Cyclo(Tyr-Pro) ²	<ul style="list-style-type: none"> • Phytotoxic action
Cyclo(Pro-Gly) ⁴	<ul style="list-style-type: none"> • Antiamnesia properties
Cyclo(Tyr-Tyr) ⁵	<ul style="list-style-type: none"> • Voltage dependent calcium channel blocking activity • Increased heart rate and coronary flow rate of isolated rat hearts • Mixed agonist and antagonist activity at μ-opioid receptors

Cyclo(Phe-Tyr) ⁵	<ul style="list-style-type: none"> • Inhibition of HT-29, HeLa and MCF-7 tumor cell lines • Calcium channel blocking activity • Decreased heart rate, coronary flow rate and ventricular pressure of isolated rat hearts • Agonist activity at μ-opioid receptors
Cyclo(Phe-Cys) and cyclo(Tyr-Cys) ⁶	<ul style="list-style-type: none"> • Decreased heart rate and coronary flow rate and, and increased ventricular pressure of isolated rat hearts • Inhibition of HT-29 and HeLa tumor cell lines • Cyclo(Tyr-Cys) also inhibited MCF-7 tumor cell lines • Deceleration of the rate of blood clot formation • Concentration dependent acceleration of thrombin substrate reaction • Concentration dependent change in rate of platelet aggregation • Deceleration of initial fibrin formation
Cyclo(Gly-Gly), Cyclo(Gly-Trp), Cyclo(Trp-Tyr), Cyclo(Trp-Trp), Cyclo(Phe-Trp), Cyclo(Phe-Phe), Cyclo(Pro-Gly), Cyclo(Pro-Pro), Cyclo(Phe-Pro), Cyclo(Pro-Trp), Cyclo(Ala-Pro), Cyclo(Glu-Phe),	<ul style="list-style-type: none"> • Antifungal activity

Cyclo(Tyr-Pro), Cyclo(Trp-Pro) ^{7, 29}	<ul style="list-style-type: none"> • Antifungal activity
---	---

<p>Cyclo(Gly-Gly), Cyclo(Trp-Tyr),</p> <p>Cyclo(Trp-Trp), Cyclo(Phe-Trp),</p> <p>Cyclo(Phe-Phe), Cyclo(Pro-Gly),</p> <p>Cyclo(Pro-Pro), Cyclo(Phe-Pro),</p> <p>Cyclo(Ser-Ser), Cyclo(Pro-Trp),</p> <p>Cyclo(Ala-Pro), Cyclo(Glu-Phe),</p> <p>Cyclo(Tyr-Pro), Cyclo(Phe-Leu),</p> <p>Cyclo(Trp-Pro)^{7, 20, 29}</p>	<ul style="list-style-type: none"> • Antibacterial activity • Cyclo(Pro-Pro) demonstrated anticancer activity
--	---

Cyclo(Met-Met) and cyclo(Met-Gly) ^{7, 8}	<ul style="list-style-type: none"> • Antifungal and antibacterial activity • Inhibition of adenosine diphosphate (ADP) and thrombin induced platelet aggregation • Calcium and sodium channel blocking activity
---	--

Cyclo(Gly-Tyr) and cyclo(Gly-Phe) ^{9, 29}	<ul style="list-style-type: none"> • Antibacterial activity • Inhibition of adenosine diphosphate (ADP) and thrombin induced platelet aggregation • Calcium and sodium channel blocking activity • Inhibition of HT-29, HeLa and MCF-7 tumor
--	--

	<p>cell lines</p> <ul style="list-style-type: none"> • Anticonvulsant activity
Cyclo(Trp-Tyr) and cyclo(D-Trp-L-Tyr) ¹⁰	<ul style="list-style-type: none"> • Inhibition of adenosine diphosphate (ADP) and thrombin induced platelet aggregation • Calcium channel agonistic activity • Increased coronary flow rate of isolated rat hearts
Cyclo(Met-Trp) and cyclo(Met-Tyr) ¹¹	<ul style="list-style-type: none"> • Inhibition of adenosine diphosphate (ADP) and thrombin induced platelet adhesion • Antifungal and antibacterial activity • Calcium and sodium channel blocking activity • Cyclo(Met-Trp) Inhibited HT-29, HeLa and MCF-7 tumour cell lines
Cyclo(His-Gly) and cyclo(His-Ala) ¹²	<ul style="list-style-type: none"> • Antifungal activity • Inhibition of MCF-7 tumour cell lines • Cyclo(His-Ala) also inhibited HT-29 and HeLa tumor cell lines • Decreased coronary flow rate of isolated rat hearts • Inhibition of adenosine diphosphate (ADP) and thrombin induced platelet aggregation • Inhibition of thrombin substrate binding

<p>Cyclo(His-Phe) and cyclo(His-Tyr)¹³</p>	<ul style="list-style-type: none"> • Inhibition of WHCO3, HeLa and MCF-7 tumor cell lines • Calcium and sodium channel blocking activity and opening of inward rectifying potassium ion channels • Cyclo(His-Phe) decreased heart rate and coronary flow rate while increasing ventricular pressure of isolated rat hearts • Cyclo(His-Tyr) increased heart rate and ventricular pressure of isolated rat hearts • Cyclo(His-Tyr) prolonged blood clotting time, slowed clot lysis and inhibited ADP-induced platelet adhesion and aggregation • Antifungal activity • Cyclo(His-Tyr) also demonstrated antibacterial activity
<p>Cyclo(Gly-Gly), Cyclo(Trp-Trp) and Cyclo(Gly-Trp)¹⁴</p>	<ul style="list-style-type: none"> • Inhibition of HT-29, HeLa and MCF-7 tumor cell lines • Inhibition of adenosine diphosphate (ADP) induced platelet adhesion and aggregation • Cyclo(Trp-Trp) also inhibited thrombin induced platelet aggregation • Cyclo(Gly-Gly) and cyclo(Gly-Trp) demonstrated calcium channel agonist activity while cyclo(Trp-Trp) showed calcium channel blocking activity • Cyclo(Trp-Trp) demonstrated antifungal activity
<p>Cyclo(L-Gly-L-Val) and cyclo(L-Gly-D-Val)</p>	<ul style="list-style-type: none"> • Antifungal and antibacterial activity • Inhibition of HT-29, HeLa and MCF-7 tumor cell lines • Decreased heart rate, coronary flow rate and ventricular pressure of isolated rat hearts • Increased the rate and extend of thrombin formation

Cyclo(Gly-Leu) and cyclo(Gly-Ile) ¹⁷	<ul style="list-style-type: none"> • Antifungal and antibacterial activity • Inhibition of HT-29, HeLa and MCF-7 tumor cell lines • Inhibition of ADP-induced platelet aggregation and fibrinolysis • Decreased heart rate, coronary flow rate and ventricular pressure of isolated rat hearts

Cyclo(L-Trp-L-Pro), Cyclo(L-Trp-D-Pro), Cyclo(D-Trp-L-Pro) and Cyclo(D-Trp-D-Pro) ¹⁵	<ul style="list-style-type: none"> • Cyclo(L-Trp-D-Pro) and cyclo(D-Trp-L-Pro) showed anticancer activity • Cyclo(L-Trp-L-Pro) and cyclo(D-Trp-L-Pro) inhibited Gram-positive bacteria, cyclo(L-Trp-D-Pro) inhibited Gram-negative bacteria and cyclo(D-Trp-D-Pro) inhibited fungi • Cyclo(D-Trp-L-Pro) showed calcium channel blocking activity; cyclo(L-Trp-L-Pro), cyclo(L-Trp-D-Pro) and cyclo(D-Trp-D-Pro) showed calcium channel agonistic activity • Cyclo(L-Trp-D-Pro) showed positive chronotropic activity, while cyclo(D-Trp-L-Pro) showed negative chronotropic activity of isolated rat hearts. Cyclo(L-Trp-D-Pro) and cyclo(D-Trp-L-Pro) also increased the coronary flow rate of isolated rat hearts • Cyclo(L-Trp-D-Pro) inhibited thrombin-induced platelet aggregation. All the cyclic dipeptides increased ADP induced platelet adhesion, yet caused reduced adhesion when the platelets
--	--

	were stimulated by thrombin
Cyclo(Gly-Thr) and cyclo(Gly-Ser) ¹⁸	<ul style="list-style-type: none"> • Gram-negative antibacterial activity • Inhibition of HT-29 and HeLa tumor cell lines • Cyclo(Gly-Ser) also showed cytotoxic activity against MCF-7 cell lines • Increased fibrin and thrombin formation • Enhanced ADP-induced platelet aggregation • Decreased heart rate and ventricular pressure of isolated rat hearts
Cyclo(Trp-Pro) and cyclo(Pro-Trp) ¹⁹	<ul style="list-style-type: none"> • Antifungal activity • Cyclo(Pro-Trp) also demonstrated antibacterial activity • Anticancer activity • Cyclo(Trp-Pro) modulated delayed-rectifier potassium and calcium channels

Cyclo(Leu-Ile) ²⁸	<ul style="list-style-type: none"> • Antibacterial activity
Cyclo(Arg-Lys) and Cyclo(Asp-Lys) ²⁹	<ul style="list-style-type: none"> • Immunomodulation
Cyclo(Ala-Phe) ²⁹	<ul style="list-style-type: none"> • Anticonvulsive activity
Cyclo(Phe-Phe) ²⁹	<ul style="list-style-type: none"> • Inhibition of cell division

¹(Milne *et al.*, 1998), ²(Prasad, 1995), ³(Graz *et al.*, 1999), ⁴(Gudasheva *et al.*, 1996), ⁵(Kilian, 2002), ⁶(Van der Merwe, 2005), ⁷(Graz, 2002), ⁸(Pitchen, 2002), ⁹(Olivier, 2002), ¹⁰(Versluis, 2002), ¹¹(Jones, 2002), ¹²(Lucietto, 2004), ¹³(McClelland, 2003), ¹⁴(Grant, 2002), ¹⁵(Jamie, 2002), ¹⁶(Peterson, 2006), ¹⁷(Huang, 2006), ¹⁸(Cunningham, 2006), ¹⁹(Haywood, 2000), ²⁰(Lautru *et al.*, 2002), ²¹(Prasad, 2001), ²²(Prasad, 1995), ²³(Jikihara *et al.*, 1993), ²⁴(Koskinen, 1986), ²⁵(Kukla *et al.*, 1985), ²⁶(Morley *et al.*, 1981), ²⁷(Prasad, 1987), ²⁸(Sammes, 1975), ²⁹(Brauns, 2004)

2.4 Motivation for the research

No investigations have yet been undertaken to determine the biological activity of the halogenated cyclic dipeptides, cyclo(Phe-4Cl-Pro) and cyclo(D-Phe-4Cl-Pro). Studies on these cyclic dipeptides are therefore warranted. Table 2.4 illustrates some other proline- and phenylalanine-containing cyclic dipeptides and their effects on some biological systems.

Table 2.4 Some biologically active Phenylalanine- and Proline-containing cyclic dipeptides

Cyclic dipeptide	Cyclo(Tyr-Pro)
Antimicrobial	Showed antimicrobial activity against: <i>Eschericia coli</i> ^{1, 5} , <i>Pseudomonas aerugenosa</i> ¹ , <i>Klebsiella pneumonia</i> ^{1, 5} , <i>Bacillus subtilis</i> ⁵ , <i>Staphylococcus areus</i> ⁵ , <i>Candida albicans</i> ⁵
Anticancer	Played a role in the induction of differentiation in HT-29 cancer cell lines ¹
Cyclic dipeptide	Cyclo(Phe-Pro)
Antimicrobial	Showed broad spectrum antibacterial properties ^{1, 2, 9}
Anticancer	Inhibit ed the growth of HT-29, HeLa and MCF-7. Induced apoptosis in HT-29 colon cancer cell lines ^{1, 2, 9}
Cyclic dipeptide	Cyclo(Phe-Phe)
Anticancer	Inhibit ed cell division ^{5, 9}
Antifungal	exhibited broad spectrum antifungal properties ^{5, 9}

Cyclic dipeptide	Cyclo(Phe-Tyr)
Anticancer	Inhibited HeLa , HT-29 and MCF-7 cells ³
Cyclic dipeptide	Cyclo(Phe-Cys)
Anticancer	Significantly reduced the growth of HeLa , HT-29 and MCF-7 cells ⁴
Cyclic dipeptide	Cyclo(His-Phe)
Anticancer	Inhibited WHCO3, HeLa and MCF-7 tumor cell lines ⁷
Antifungal	Antifungal activity ⁷
Cyclic dipeptide	Cyclo(D-Trp-L-Pro)
Anticancer	Showed anticancer properties against Hepatocyte cell lines ⁸
Antimicrobial	Showed activity against <i>Streptococcus</i> ⁸
Cyclic dipeptide	Cyclo(L-Trp-L-Pro)
Antibacterial	Showed activity against Gram-positive bacteria: <i>S. aureus</i> and <i>Streptococcus</i> ⁸
Cyclic dipeptide	Cyclo(L-Trp-D-Pro)

Antibacterial	Showed activity against <i>E. Coli</i> ⁸
Cyclic dipeptide	Cyclo(L-Trp-D-Pro)
Antibacterial	Showed activity against <i>C.albicans</i> ⁸
Anticancer	Caused the inhibition of HeLa cell lines ⁸
Cyclic dipeptide	Cyclo(Gly-Phe)
Haematological	Caused the inhibition of endogenous agonists (ADP and thrombin) induced aggregation of isolated platelets ^{6,9}
Antibacterial	Showed the activity against <i>B.Subtilis</i> , <i>E.coli</i> , <i>Klebsiella sp.</i> , <i>S.aureus</i> , <i>P.aeruginosa</i> ^{6,9}
Cyclic dipeptide	Cyclo(Phe-Cys)
Haematological	Slowed the rate of clot formation ⁴
Antibacterial	Showed activity against <i>B.Subtilis</i> ⁴

¹(Milne *et al.*, 1998), ²(Graz *et al.*, 1999), ³(Kilian, 2002), ⁴(Van der Merwe, 2005), ⁵(Graz, 2002), ⁶(Olivier, 2002), ⁷(Mcleland, 2003), ⁸(Jamie, 2002), ⁹(Brauns, 2004)

As indicated in Table 2.4 phenylalanine- and proline-containing cyclic dipeptides have shown potentially promising biological activity, and the biological investigation of cyclo(Phe-4Cl-Pro) and cyclo(D-Phe-4Cl-Pro) are therefore warranted.

CHAPTER 3

CYCLIC DIPEPTIDE SYNTHESIS

3.1 Introduction

Diketopiperazines (DKPs), the smallest cyclic dipeptides, represent an important class of biologically active natural products and research into their characteristics has been fundamental to many aspects of peptide chemistry. The advent of combinatorial chemistry has revived interest in DKPs for two reasons: firstly, they are simple heterocyclic scaffolds in which diversity can be introduced and stereochemically controlled at up to four positions; secondly, they can be prepared from readily available α -amino acids using robust synthetic procedures (Fischer, 2002).

Peptides are formed by the condensation of two amino acids under the formation of an amide group with the release of water. However, when a carboxylic acid and an amine are mixed, an acid-base reaction takes place instead of a covalent bond formation. Thus the formation of an amide bond has to overcome unfavourable thermodynamics. Therefore the carboxylic acid has to be activated, in order for the amino to attack. A range of methods and reagents are used to facilitate the formation of amino bonds (Montalbetti and Falque, 2005). Some of the most common methods involve the use of carbodiimides, pentafluorophenyl or succinimide esters, uronium or phosphonium reagents, symmetrical or asymmetrical anhydrides and acyl chlorides as coupling reagents (Montalbetti and Falque, 2005).

Several methods have been reported for the synthesis of cyclic dipeptides. These include (i) heating linear dipeptides in β -naphthol (Lichtenstein, 1938), (ii) solid phase synthesis (Gisin and Merrifield, 1972), (iii) acetic acid catalysed synthesis (Suzuki *et al.*, 1998), (iv) boiling the formate salts of dipeptide methyl esters in a neutral solvent for 3 hours (Nitecki *et al.*, 1968) and (v) heating linear dipeptides in phenol (Kopple and Ghazarian, 1968).

The formation of the DKP rings, like any other cyclisation procedure, requires the generation of mutually reactive chain-ends and the reaction of these ends under conditions favouring intramolecular processes. The mutually reactive ends are commonly free amino acid groups that are not reduced in nucleophilicity by protonation or substitution, and carboxyl groups that are activated to be susceptible to nucleophilic attack (Bodanszky, 1993; Bodanszky, 1988).

Although many novel approaches have been developed to accomplish the head-to-tail synthesis of peptides, one of the most commonly used methods is still the solution-phase synthesis using peptide-coupling reagents. A rational selection of coupling reagents can effectively improve the results of peptide cyclisation (Peng and Roller, 2002; Loughlin *et al.*, 2000). Solution-phase cyclisation of dipeptides can be achieved by utilising unprotected linear dipeptides or protected linear dipeptide esters (Lambert *et al.*, 2001).

DKP rings may be produced without great difficulty and may also form without particular activation of the carboxyl groups of linear dipeptide precursors (Bodanszky, 1993). Kopple and Ghazarian (1968) reported an efficient method for the cyclisation of linear dipeptides without particular activation of their carbonyl groups. They described the formation of cyclic dipeptides by heating the unprotected linear dipeptide in phenol. This relatively fast three hour procedure produced high yields of cyclic dipeptides, with little racemisation. It is however necessary for at least one of the amino acid residues of the free linear dipeptide to be sensitive to phenol for the cyclisation procedure to occur (Kopple and Ghazarian, 1968).

Cyclisation of some linear dipeptides may be an inherently improbable and slow process, and the exposure to reagents necessary for the cyclisation may lead to extensive racemisation when optically pure linear dipeptide precursors are utilised (Nitecki *et al.*, 1968). This racemisation can be avoided by protecting the amino and carboxyl terminals of the dipeptide precursors with blocking groups, which are capable of being selectively removed when necessary (Kopple, 1972). Among other blocking

groups (Han and Kim, 2004), *tert*-butyloxycarbonyl (t-Boc) has been used to protect the amino groups of linear dipeptide precursors (Nitecki *et al.*, 1968). Nitecki *et al.* (1968) reported a method for the cyclisation of the formate salts of dipeptide methyl esters. The formate salts were formed as a result of successful deblocking t-Boc dipeptides with formic acid (98%) at room temperature for three hours. Subsequent heating of the deblocked dipeptides in a neutral medium resulted in the formation of sterically pure cyclic dipeptides. The procedure decreased racemisation and improved the yields of acetic sensitive amino acids (Nitecki *et al.*, 1968).

3.2 Methodology

The cyclic dipeptides were synthesised according to a modified method as developed by Milne *et al.* (1992). The *tert*-butyloxycarbonyl group (t-Boc) is the most common amino protecting group and is distinguished from the other amino protecting groups (e.g., Trityl) in its ability to show selectivity of the removal by trifluoroacetic acid (Jakubke and Jeschkeit, 1997). According to Milne *et al.* (1992), the t-Boc group of the ester can be removed by dissolving the compound in formic acid (20 ml) and anisole (0.2 ml) which is then stirred for three hours at room temperature and dried *in vacuo* leading to the formation of a formate ester. Both cyclo(Phe-4Cl-Pro) and cyclo(D-Phe-4Cl-Pro) will be synthesised using phenylalanine as the primary amino acid component (amino component protected by N-*tert*-butyloxycarbonyl (t-Boc)) and proline as the secondary amino acid component (carbonyl component protected by methyl ester), resulting in the protected linear dipeptides. The t-Boc group was then removed followed by boiling in a neutral medium (Sec-butanol and toluene 4:1) giving rise to cyclo(Phe-4Cl-Pro) and cyclo(D-Phe-4Cl-Pro).

High performance liquid chromatography (HPLC) (Shimadzu, Japan) and thin layer chromatography (TLC) (R_f values for each compound was calculated) was performed to confirm the purity of the compounds. HPLC, like other forms of chromatography, is essentially a technique for the separation of chemical compounds in mixtures by a continuous distribution of the components between two phases: a mobile phase and a stationary phase. The simplicity and rapidity of TLC makes it a useful tool to monitor the

progress of organic reactions and to check the purity of the products (Skoog *et al.*, 2001).

3.2.1 Synthesis of the linear dipeptides

All reagents used were of reagent grade. Starting amino acids (Indicated in Figure 3.1) (FLUKA (PTY) LTD, SA) were *tert*-butyloxycarbonyl phenylalanine (N-t-boc-L-Phe-4Cl or N-t-boc-D-Phe-4Cl) (Molecular weight = 299.75) and proline methyl ester (L-Pro-OMe) (Molecular weight = 165.62).

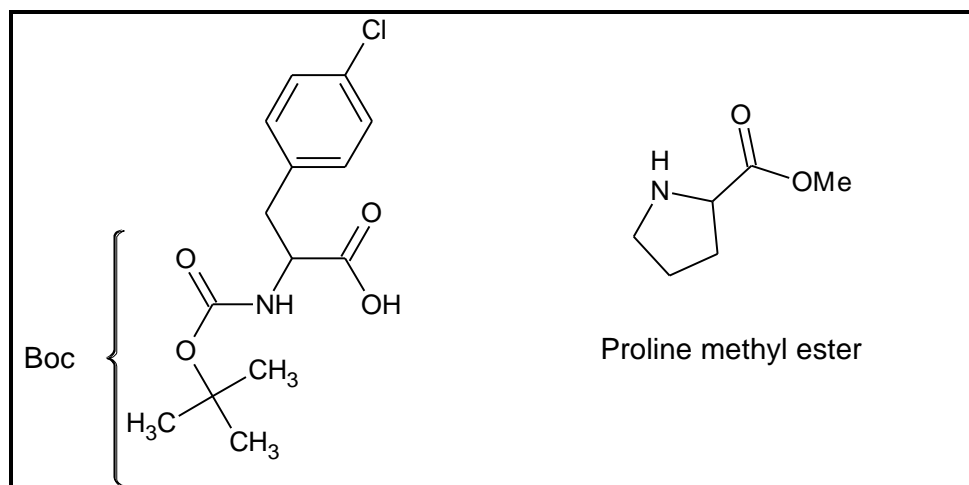


Figure 3.1 Protective groups used in the synthesis of cyclo(Phe-4Cl-Pro) and cyclo(D-Phe-4Cl-Pro) (Method according to Milne *et al.*, 1992).

According to the method of Milne *et al.* (1992):

N-t-Boc-L-Phe/ N-t-Boc-D-Phe (2 g, 6.57 mmol) and 1.10 g of L-Pro-OMe (6.67 mmol) were dissolved in 40 ml of 1,2-dimethoxyethane at 0 °C.

DEPC (diethylphosphoryl cyanide) (1.11 ml, 7.60 mmol) and triethylamine (1.91 ml, 13.71 mmol) were added drop wise to the above mixture and stirred for 1 hour at 0 °C, after which it was allowed to reach room temperature.

The entire reaction was carried out in a positive inert atmosphere (N_2) and complete dipeptide formation was observed after a further 4 hours stirring at room temperature. The reaction mixture was then diluted to 250 ml with chloroform and successively washed with 50 ml of a 5% hydrochloric acid solution, 50 ml of aqueous sodium hydrogen carbonate and 50 ml of saturated brine solution.

Removal of the solvent phase with the aid of vacuum yielded the protected dipeptide as a colourless viscous liquid of a syrup consistency. Figure 3.2 illustrates the mechanism of the reaction.

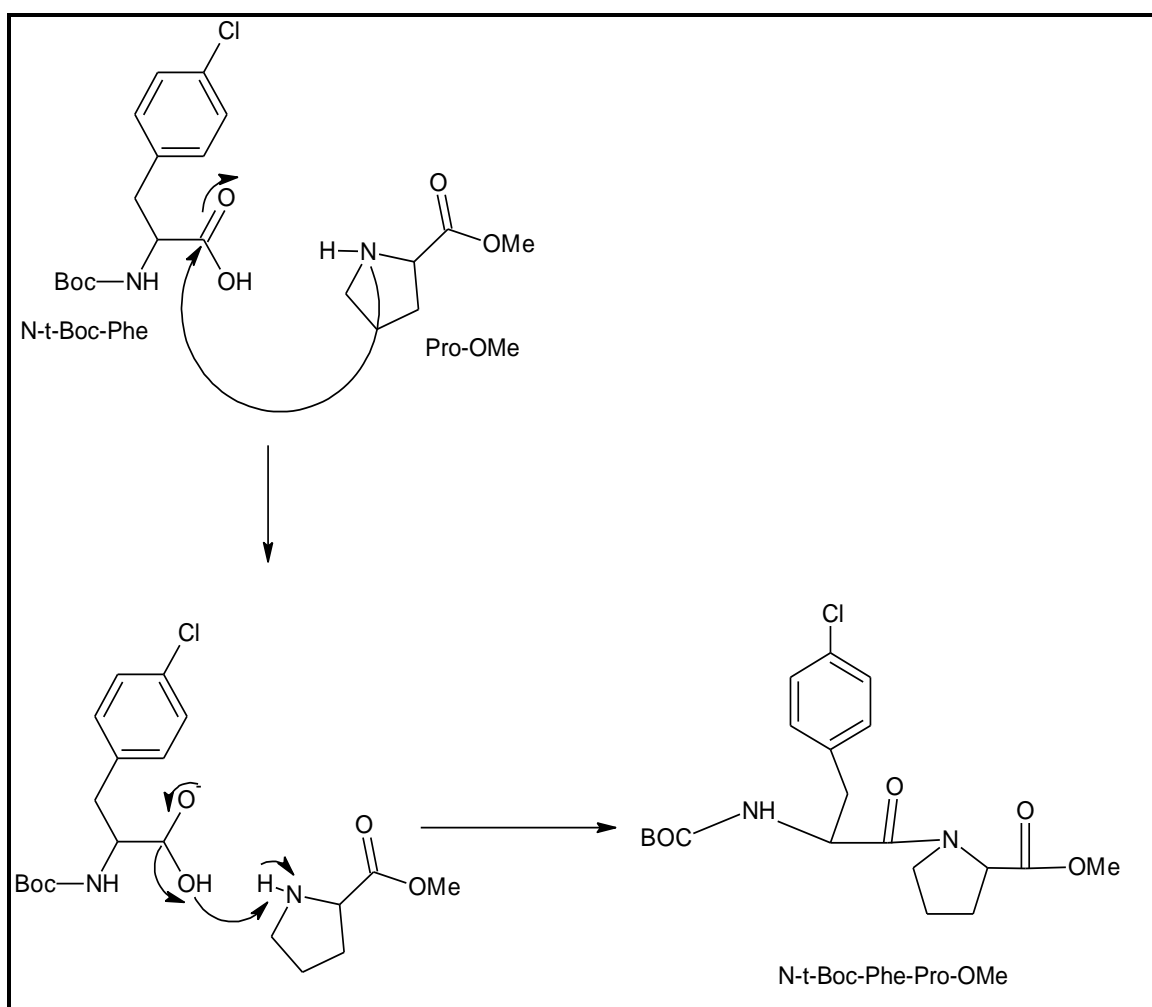


Figure 3.2 Synthesis of the protected linear dipeptide ester (Adapted from Milne *et al.*, 1992).

3.2.2 Removal of the protective Boc group

The N-t-Boc dipeptide ester was dissolved in formic acid (20 ml) containing anisole (0.2 ml) and stirred for 3 hours at room temperature. The reaction mixture was then dried *in vacuo*. The removal of the Boc group led to the formation of a formate ester product (Figure 3.3).

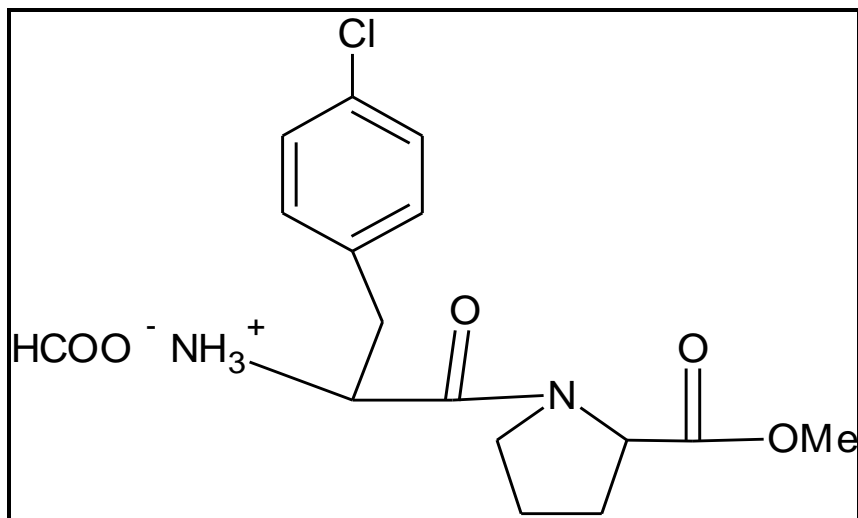


Figure 3.3 Formate ester product (Adapted from Milne *et al.*, 1992).

3.2.3 Cyclisation

A volume of 40 ml *sec*-butanol and toluene mixture (4:1, V/ V) was added to the residue containing the crude dipeptide formate ester and the solution was refluxed in a oil bath for 3 hours at 120 °C. After 3 hours the solvent was evaporated off until about 8 ml were left. This concentrated solution was then cooled to 0 °C. This resulted in the precipitation of the cyclic dipeptide which was then filtered out and washed with ether. Recrystallisation from MeOH/ether gave rise to crystals for both cyclo(Phe-4Cl-Pro) and cyclo(D-Phe-4Cl-Pro). Figure 3.4 mechanistically illustrates the cyclization of the linear L- or D-Phe-4Cl-Pro formate esters to the respective cyclic compounds.

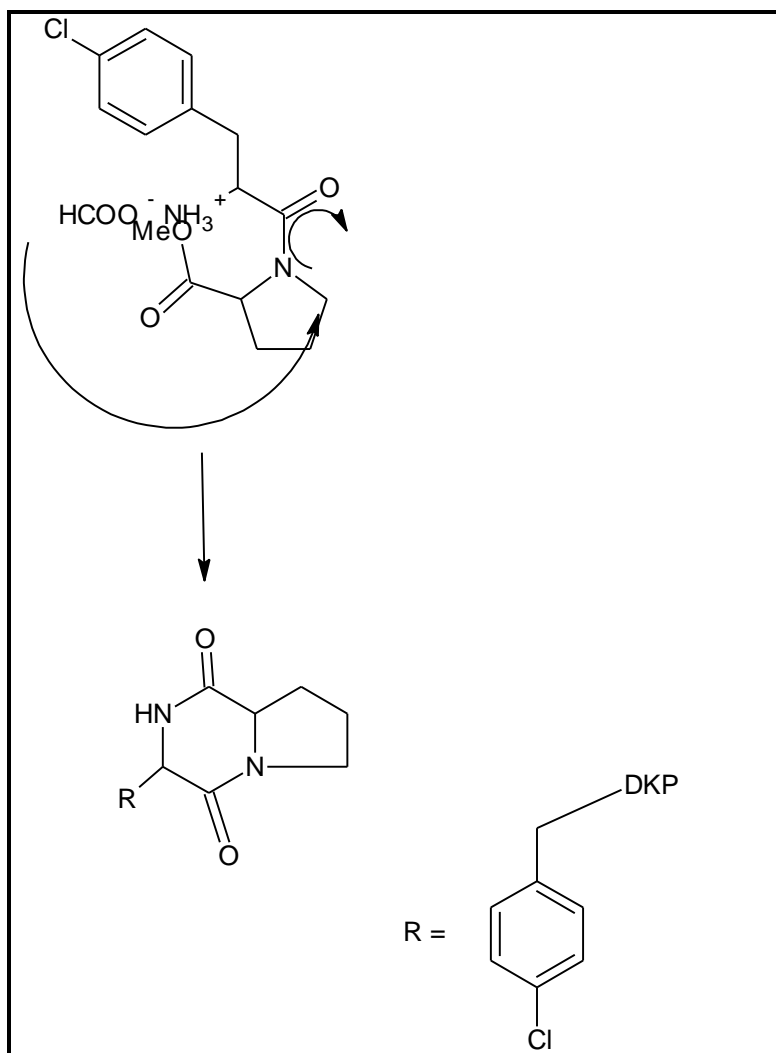


Figure 3.4 Mechanism of cyclisation of the linear dipeptide formate ester to cyclo(Phe-4Cl-Pro) (Adapted from Capasso *et al.*, 1998).

3.3 Results and Discussion

The yields obtained after the cyclisation of cyclo(Phe-4Cl-Pro) and cyclo(D-Phe-4Cl-Pro) are summarised in Table 3.1

Table 3.1 Relative yields for (Phe-4Cl-Pro) and cyclo(D-Phe-4Cl-Pro)

Compound	Percentage yield (neutral medium cyclisation)
Cyclo(Phe-4Cl-Pro)	54%
Cyclo(D-Phe-4Cl-Pro).	62%

3.4 Thin layer chromatography

Purity of the compounds was assessed by thin layer chromatography (TLC) in two different solvent systems. Table 3.2 lists the mobile phase ratio compositions and the R_f values obtained.

Table 3.2 Mobile phase ratio compositions and the R_f values obtained for (Phe-4Cl-Pro) and cyclo(D-Phe-4Cl-Pro)

Compound	Mobile phase	Ratios	R_f
cyclo(Phe-4Cl-Pro)	Chloroform/MeOH	7/3	0.81
	Chloroform/MeOH/AcOH 32%	14/2/1	0.91
cyclo(D-Phe-4Cl-Pro).	Chloroform/MeOH	7/3	0.75
	Chloroform/MeOH/AcOH 32%	14/2/1	0.76

No signs of unwanted by-products were visualised by way of TLC, with only a single spot being recorded consistently. The cyclisation method produced high yields of both cyclic dipeptides.

3.5 High-performance liquid chromatography

3.5.1 Introduction

Today high-performance liquid chromatography (HPLC) is the most versatile and widely used type of elution chromatography. It is a broadly applicable and valuable analytical tool for scientist in a number of diverse fields. This can mainly be attributed to its sensitivity, its high resolution and speed of analysis, its ready adaptability to accurate quantitative determinations, its ease of automation, its suitability for separating nonvolatile species or thermally fragile ones, HPLC columns can also be reused without repacking or regeneration and reproducibility is greatly improved as the parameters affecting the efficiency of the separation can be closely controlled. HPLC is ideally suited for the separation and identification of amino acids, carbohydrates, lipids, nucleic acids, proteins, pigments, steroids, pharmaceuticals, and many other biological active molecules (Skoog *et al.*, 2004).

HPLC is used in analytical development to quantify the active pharmaceutical ingredient (API) and to evaluate impurity and degradation products profile of drug substances and drug products. Additional uses of HPLC include the determination of content uniformity of dosage forms, monitoring of dissolution profiles, determination of antioxidant and microbial preservative content, and to support cleaning evaluations (Ahuja and Dong, 2005).

Column chromatography methods can generally be classified into Gas chromatography (GC) and Liquid chromatography (LG). In liquid chromatography, the mobile phase is a liquid solvent containing the sample as a mixture of solutes. HPLC can be classified by the separation mechanism or by the type of stationary phase. These include: partition or liquid-liquid chromatography, adsorption or liquid-solid chromatography, ion-exchange or ion chromatography, size-exclusion chromatography, affinity chromatography and chiral chromatography (Skoog *et al.*, 2004).

The rapid advancement in peptide research over the past 25 years must be attributed, in part, to the effectiveness of HPLC, particularly reversed-phase chromatography (RPC) (Gazes, 2001). Normal phase separations (adsorption) are performed on a adsorbent (silica Gel; Alumina) column and a non-polar mobile phase, whereas reversed phase separations are done on a non-polar column with a polar mobile phase. If the components to be separated are soluble in relatively polar solvents say H₂O/MeOH systems RPC method can be utilised by selecting a polar mobile phase e.g., H₂O/MeOH and a non-polar stationary phase e.g., μ BONDPAK C₁₈. Conversely, if the solutes are insoluble in polar solvents, a non-polar mobile phase with a polar column packing is selected e.g., n-Hexane/THF/CHCl₃ and μ Porasil. RPC has found both analytical and preparative applications in the area of biochemical separation and purification. Molecules that possess some degree of hydrophobic character, such as proteins, peptides and nucleic acids, can be separated by RPC with excellent recovery and resolution (Ahuja and Dong, 2005).

In normal-phase chromatography the least polar component is eluted first, thus increasing the polarity of the mobile phase and decreasing the elution time. Conversely in reversed-phase chromatography the most polar component elutes first, increasing the mobile-phase polarity and elution time. Other advantages of reverse-phase chromatography are that water, an inexpensive, nontoxic, UV-transparent solvent compatible with many biological solutes, can be used as the mobile phase, the ability to change the composition of the mobile phase to accommodate a wide variety of solutes. Increased mass transfer speed and solvent equilibration is also reached more rapidly (Skoog *et al.*, 2004).

In order to fully understand the fundamentals of HPLC we must first look at what chromatography entails. Chromatography can be defined as a separation process in which the sample mixture is distributed between two phases in the chromatographic bed (column or plane). One phase is stationary whilst the other passes through the chromatographic bed. The stationary phase is either a solid, porous, surface-active material in small-particle form or a thin film of liquid coated on a solid support or column

wall. The mobile phase is a gas or liquid. If a gas is used, the process is known as gas chromatography (GC); the mobile phase is always liquid in all types of liquid chromatography (LC) (Meyer, 2004).

Martin and Synge, The inventors of modern chromatography, were aware as far back as 1941 that, in theory, the stationary phase requires very small particles and hence a high pressure is essential for forcing the mobile phase through the column. As a result, HPLC is sometimes referred to as high-pressure liquid chromatography (Meyer, 2004).

HPLC differs from the classical LC in that many aspects of the separation system have been optimised to provide increased speed, resolution and sensitivity (Pieper and Rutledge, 1989). These advantages of HPLC are the result of two major advances. Firstly, the development of stationary supports with very small particle sizes and large surface areas, and secondly, the improvement of elution rate by applying high pressure to solvent flow. A combination of the application of high pressure and adsorbents of small particle size leads to high resolving power and a short period of time is needed for analysis. Pumping pressures of several hundred atmospheres are required to achieve reasonable flow rates with packaging, of adsorbents, in the 3 to 10 μm size range.

HPLC is thus a separation technique conducted in the liquid phase in which a sample is separated into its constituent components (or analytes) by distributing between the mobile phase (*i.e.*, a flowing liquid) and a stationary phase (*i.e.*, adsorbents packed inside a column). An online detector monitors the concentration of each separated component (or contaminant) in the column effluent and generates a chromatogram (Ahuja and Dong, 2005).

3.5.2 Methodology

3.5.2.1 Preparation of solutions

Stock solutions containing 2 mM of cyclo(Phe-4Cl-Pro) and cyclo(D-Phe-4Cl-Pro) were prepared. All chemicals used were either of analytical or HPLC grade. All water

containing solutions required for analysis were prepared by utilising analytical grade water (AGW) obtained from an ultra clear TWF UF TM Reverse Osmotic water purification system SG[®]. Acetonitrile, for the preparation of the mobile phase, were obtained from Sigma Chemicals Co., USA. The mobile phases for the respective cyclic dipeptides were prepared according to the formulae indicated in Table 3.3. The mobile phase and cyclic dipeptide solutions were filtered through 0.45 µm (Millipore[™], USA) and 0.22 µm Millipore[™], USA), filters respectively, prior to use.

Table 3.3 Formulas for the preparation of the mobile phases

Cyclic dipeptide	% Acetonitrile	% Water
Cyclo(Phe-4Cl-Pro)	31%	69%
Cyclo(D-Phe-4Cl-Pro)	28%	72%

The Mobile phases were prepared with boiled, carbondioxide-free, AGW water

3.5.2.2 HPLC analysis of the cyclic dipeptides

HPLC analysis of cyclo(Phe-4Cl-Pro) and cyclo(D-Phe-4Cl-Pro) were carried out on a Shimadzu LC2020 analytical liquid chromatography system fitted with a photodiode array (PDA) detector (Shimadzu, Tokyo, Japan). As this analysis was performed using a PDA detector, purity of the peak could also have been determined using the peak purity curve, which the software generated automatically. The analyses were performed using a 4.6 x 150 mm, 5 µm reverse phase Atlantis[®] dC18 column (Waters[®], Ireland). To standardise sample delivery, analyses were performed by initial injection of a 20 µl sample solution and using a constant flow rate of 1.0 ml/min for optimal resolution.

UV detection was at 220 nm (Gazes, 2001) for cyclo(Phe-4Cl-Pro) and cyclo(D-Phe-4Cl-Pro).

3.5.2.3 Results and discussion

The detectability of peptides varies greatly, depending on their amino acid composition. The aromatic amino acids (eg., tyrosine, tryptophan, and phenylalanine) offer selective detection by UV light at 280 nm and 254 nm. In the absence of these amino acids, low wavelength (< 220 nm), which also detected many other substances, including components of the mobile phase, must be used (Gazes, 2001). UV detection of cyclo(Phe-4Cl-Pro) and cyclo(D-Phe-4Cl-Pro) was at 220 nm.

The observed HPLC chromatograms, indicating the retention times (t_R), for cyclo(Phe-4Cl-Pro) and cyclo(D-Phe-4Cl-Pro) are illustrated in Figures 3.5 and 3.6, respectively. The HPLC chromatograms for both cyclic dipeptides show single peaks with high resolution, indicating that the cyclic dipeptides were free from impurities. Further structural elucidation studies, including infrared spectroscopy, mass spectrometry, molecular modeling and nuclear magnetic resonance spectroscopy are, however, necessary to ultimately confirm the structure and presence of the cyclic dipeptides. The peaks observed at ± 2.1 are the void volume.

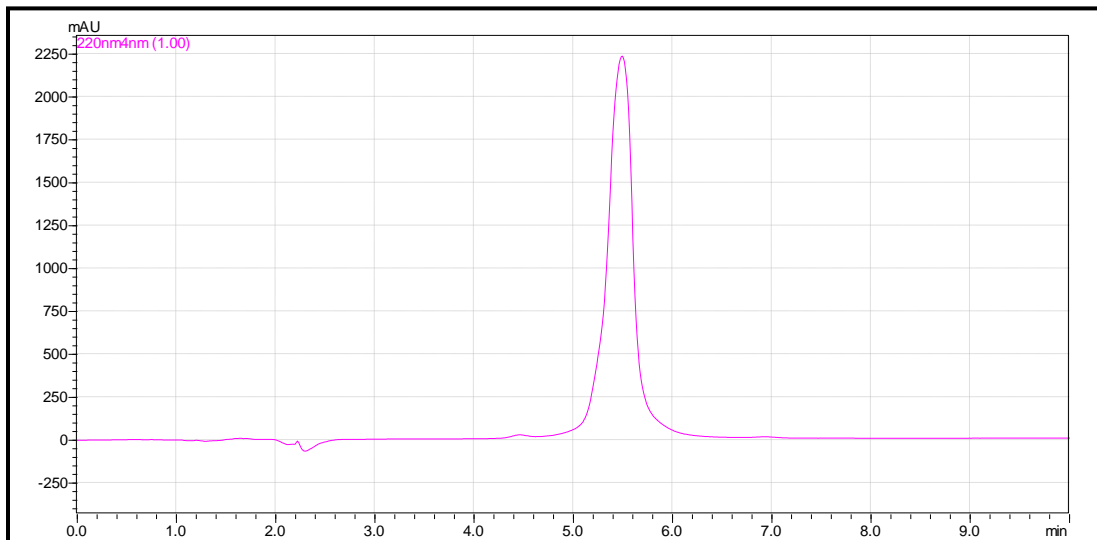


Figure 3.5 The HPLC chromatogram of cyclo(D-Phe-4Cl-Pro) ($t_R = 5.40$ minutes) at UV detection wavelength of 220 nm

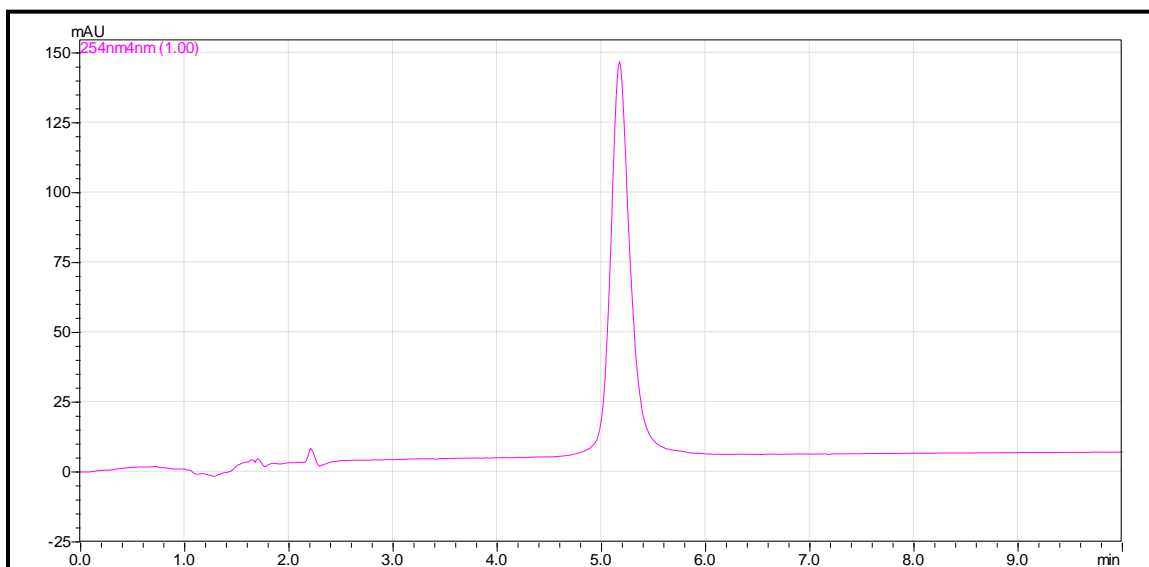


Figure 3.6 The HPLC chromatogram of cyclo(Phe-4Cl-Pro) ($t_R = 5.39$ minutes) at UV detection wavelength of 220 nm

CHAPTER 4

QUALITATIVE PHYSIOCHEMICAL ANALYSIS

Qualitative analysis and evaluation of cyclo(Phe-4Cl-Pro) and cyclo(D-Phe-4Cl-Pro) was performed using scanning electron microscopy, thermal analysis and X-ray powder diffraction.

4.1 Scanning electron microscopy

4.1.1 Introduction

Physical characterisation of pharmaceutical solids is fundamental in the drug development process. Surface topography of drugs is of significant interest to science, technology and industry (Castle and Zhdan, 1997; Laitinen, 2003).

Optical microscopy used to be the conventional method for obtaining detailed information about the physical nature of surfaces, it is still an important technique. However the resolution of optical microscopy is limited by diffraction effects to about the wavelength of light. Much higher resolution information is obtainable by using one of the electron microscopic methods (scanning electron microscopy (SEM) or transmission electron microscopy). SEM provides images of external morphology, similar to those accessed by the human eye (Skoog *et al.*, 2004).

SEM can reveal topographical details of a surface with clarity and detail, which cannot be obtained by any other means. It can also detect surface potential distributions, subsurface conductivity, surface luminescence, surface composition and crystallography (Hayat, 1974).

In obtaining an SEM image, the interaction of the primary electron beam with the sample surface is accompanied by the formation of a flux of secondary and back-scattered electrons that are collected by detectors. Secondary electrons formed near the impact area of the primary electron beam are used to produce images with a spatial

resolution closely related to the cross-sectional area of the scanning beam of electrons. The intensity of the emitted electrons in a material of a given homogeneous composition depends on the local angle of the surface to the scanning beam moderated by the probability of them reaching the detector. The three dimensionality of a typical scanning electron micrograph is subjective, but can be used for obtaining topographic information of surfaces (Skoog *et al.*, 2004).

The major advantages of scanning electron microscopy (SEM) characterisation of materials are the presence of several modes that can provide important complimentary information on various properties of materials, and in most cases its ability to examine macroscopic specimens with no special sample preparation steps (Yacobi *et al.*, 1994).

4.1.2 Methodology

The scanning electronmicrographs of cyclo(Phe-4Cl-Pro) and cyclo(D-Phe-4Cl-Pro) were recorded on a Philips[®] XL30 Scanning Electron Microscope (Philips[®], UK). A portion of each respective cyclic dipeptide was mounted on carbon tags on a sample stub using conductive adhesive glue. The mounted specimens were then sputter coated with a thin layer of gold using a Novotech[®] SEM prep 2-sputter coater (Novotech[®], Germany). Electronmicrographs were then recorded, showing the typical shape and the surface topography of the crystals (Skoog *et al.*, 2004; Van der Merwe, 2005).

4.1.3 Results and discussion

The electronmicrographs for cyclo(Phe-4Cl-Pro) and cyclo(D-Phe-4Cl-Pro) are illustrated in Figures 4.1 to 4.4. The electronmicrographs show the shape and surface topography of the cyclic dipeptides. Six crystal systems are known, which are commonly referred to as cubic, tetragonal, orthorhombic, monoclinic, triclinic, and hexagonal. Crystal morphology occurs as a result of molecular arrangement. The molecular arrangements are predetermined for a specific polymorphic form, and cannot be changed provided that there are no changes in the polymorphic form. Five types of crystal habits are recognized, which can occur in any crystal system. The crystal habits are referred to as tubular (moderate expansion of two parallel faces), platy (plates),

prismatic (columns), acicular (needle-like) and bladed (flat acicular) (Aulton, 2002). The crystal habit is the macromolecular appearance of a crystal. It depends on conditions of crystallisation and can change without change in physical characteristics. The crystals of both cyclo(Phe-4Cl-Pro) and cyclo(D-Phe-4Cl-Pro) were obtained *via* identical synthetic pathways. Cyclo(Phe-4Cl-Pro) (Figures 4.1 and 4.2) appears to form a platy (plates) crystal habit predominantly, whereas cyclo(D-Phe-4Cl-Pro) (Figures 4.3 and 4.4) form an prismatic (columns) crystal habit. The surface area of undissolved solid particles is influenced by the size of the solid particles. The surface area is universally proportional to particle size. The particle shape may influence pharmaceutical processes such as powder flow and compressability. Fine particles with with very high surface to mass ratios are more cohesive compared to coarser particles, which are influenced more by gravitational forces. Particles larger than 250 μm are relatively free flowing, but sizes below 100 μm powders become cohesive and flow problems tend to occur. Powders with similar particle sizes, but dissimilar shapes can have slightly different flow properties, due to differences in interparticle contact areas (Skoog *et al.*, 2004).

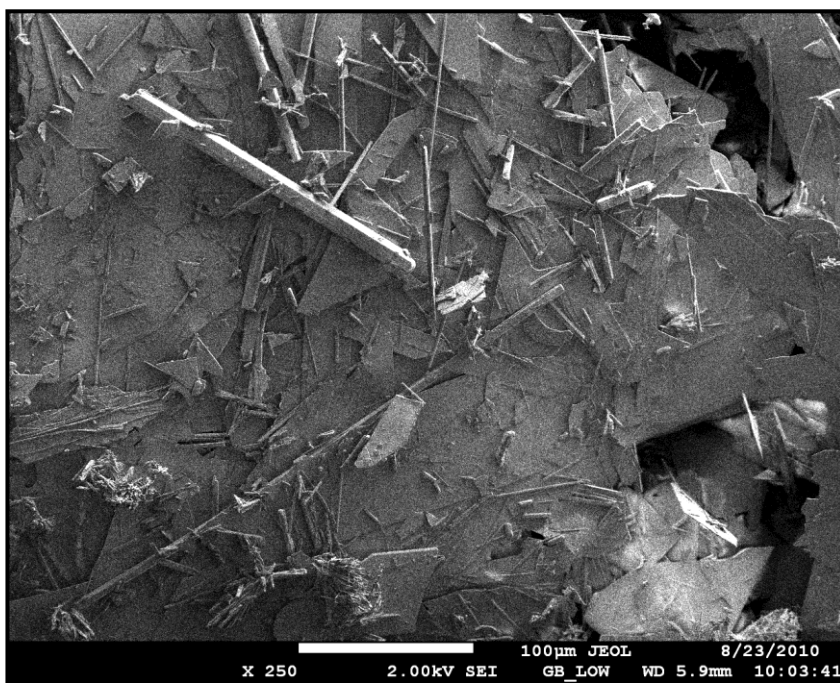


Figure 4.1 Electronmicrograph of cyclo(Phe-4Cl-Pro) with a magnification of 250x

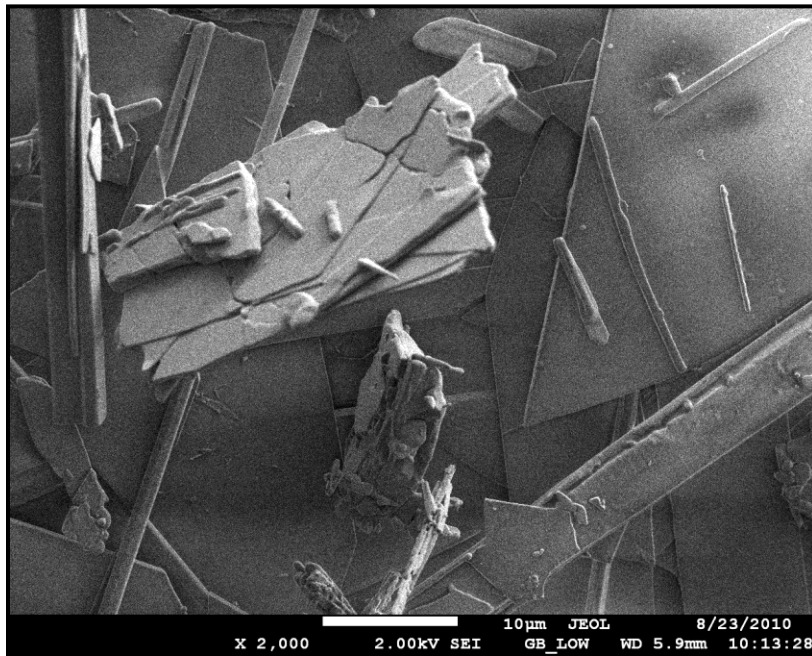


Figure 4.2 Electronmicrograph of cyclo(Phe-4Cl-Pro) with a magnification of 2000x

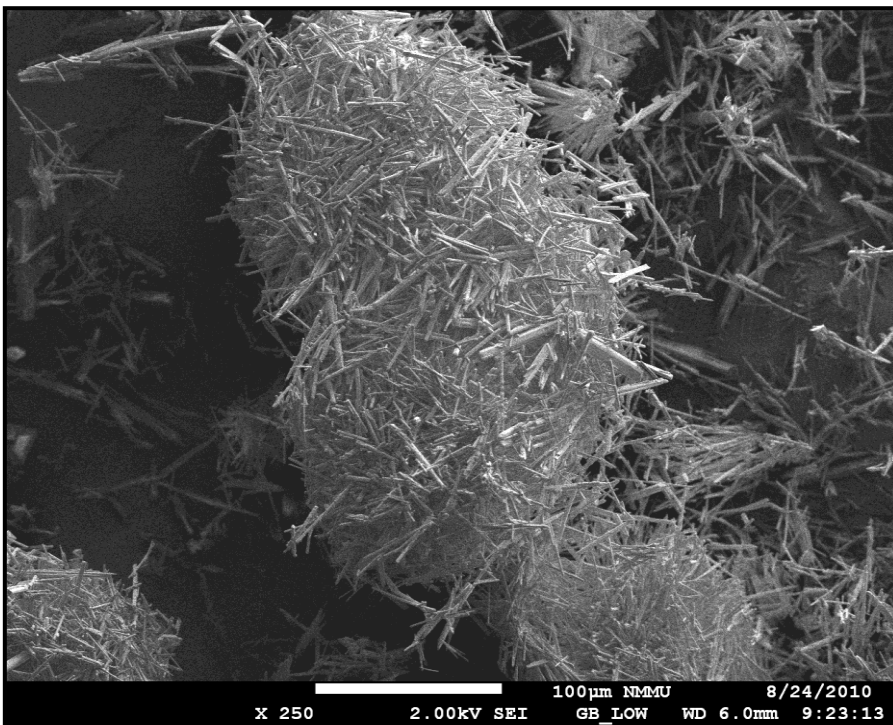


Figure 4.3 Electronmicrograph of cyclo(D-Phe-4Cl-Pro) with a magnification of 250x

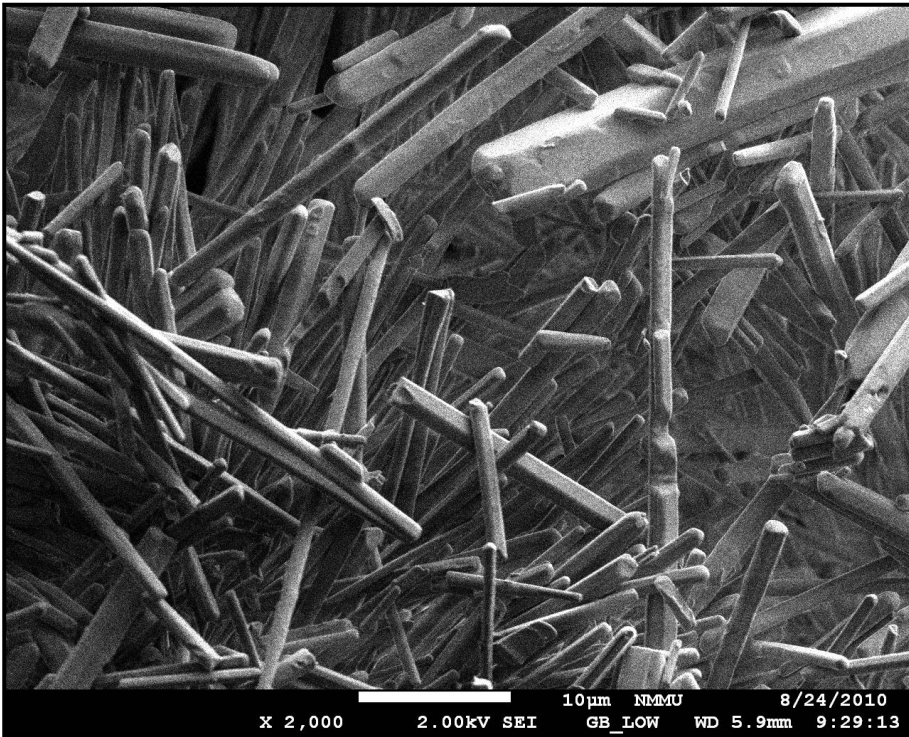


Figure 4.4 Electronmicrograph of cyclo(D-Phe-4Cl-Pro) with a magnification of 2000x

4.2 Thermal analysis

Thermal analyses comprise a family of techniques whereby a physical property (*i.e.* heat flow, weight loss) is measured as a function of temperature or time. It is a general term covering a group of related techniques whereby the dependence of the parameters of any physical property of a substance on temperature is measured. The physical parameter is determined as a dynamic function of temperature. Measurements made at fixed or isothermal temperatures are normally not included. Using the definition, the principal thermal analysis techniques are thermogravimetry and differential thermal analysis (Sichina, 2001).

The development and manufacturing of drugs requires that close attention to be paid to purity, quality, stability and safety in order to assure that the drug performs as intended. Pharmaceuticals or organic compounds have a propensity to exist in different structural or morphological forms and this gives rise to concerns over processing, long-term stability, aging and biodelivery. Due to the complexity of the formulation of pharmaceutical material, it becomes important to have a complete understanding of the properties of pharmaceutical materials. One of the best analytical techniques for characterisation of pharmaceutical material is thermal analysis. Two most widely used thermal analytical techniques for the characterisation of pharmaceuticals are differential scanning calorimetry and thermogravimetric analysis (Sichina, 2001).

4.2.1 Thermogravimetric analysis and derivative thermogravimetry

4.2.1.1 Introduction

The thermal analysis technique of thermogravimetry (TG) is one where the change in sample mass (loss or gain) in a controlled atmosphere, is determined as a function of temperature or time (Skoog *et al.*, 2004). Derivative thermogravimetry (DTG) is a method of expressing the results of TG by giving the first derivative curve as a function of temperature or time (Dodd and Tonge, 1987). This provides quantitative information on weight change processes, and enables the stereochemistry of a reaction to be followed directly, *e.g.*, reactant (solid) → product (solid) + gas (Leung and Grant, 1997;

Dodd and Tonge, 1987). It is also easier to compare the shape or overlap of DTG curves with other differential measurements such as DSC. The use of DTG improves the resolution of complex or overlapping TG curves, thus providing additional information about decomposition or mass loss phenomena of compounds (Sichina, 2001).

In Thermogravimetric analysis (TGA) a sample is placed into a tared TGA sample pan which is attached to a sensitive microbalance assembly. The sample holder portion of the TGA balance is subsequently placed into a high temperature furnace. The balance assembly measures the initial sample weight at room temperature and then continuously monitors changes in sample weight as heat is applied to the sample. TGA tests may be run in a heating mode at a controlled heating rate, or isothermally. Dynamic TG, in which the sample is heated in an environment whose temperature, is changing in a predetermined manner, preferably linear, is a common mode of TG (Brown, 1998; Wendlandt, 1986).

The resulting mass change versus temperature curve, also known as a thermogram, provide information concerning the thermal stability and composition of the initial sample, the thermal stability and composition of any intermediate compounds that may be formed, and the composition of the residue, if any (Wendlandt, 1986). Typical weight loss profiles could therefore be analysed to determine the amount or percent of weight loss at any given temperature, the amount or percent of non-combusted residue at some final temperatures, and the temperatures of various sample degradation processes (Brown, 1998).

4.2.2 Differential scanning calorimetry

4.2.2.1 Introduction

DSC is a thermal analysis technique which has been used for more than two decades to measure the temperatures and heat flows associated with transitions in materials as a function of time and temperature. Such measurements provide quantitative and

qualitative information about physical and chemical changes that involve endothermic or exothermic processes, or changes in heat capacity (TA211, 2002).

DSC is one of the most widely used thermal analysis techniques for the characterisation of pharmaceutical solids. Thermal events such as melting, recrystallisation, decomposition, and glass transitions can be measured with it. Additionally, quantitative mixture analysis (e.g., to establish the presence of different polymorphs) can be performed utilising DSC. The use of modulated DSC expands the capabilities of DSC and allows one to measure heat capacities and characterise reversible and non-reversible thermal transitions (Sichina, 2001).

DSC records the energy necessary to establish a zero temperature difference between a substance and a reference material against either time or temperature, as the two specimens are subject to identical temperature regimes in an environment heated or cooled at a controlled rate (Pope and Judd, 1977).

When a thermal transition occurs in a sample, thermal energy is added to either the sample or the reference containers in order to maintain both the sample and reference at the same temperature. The balancing of energy yields a calorimetric measurement of the transition energy, because the energy transferred is exactly equivalent to the energy absorbed or evolved in the transition (Dodd and Tonge, 1987).

Thermal transition events in the sample thus appear as deviations from the DSC baseline, in either an endothermic or exothermic direction, depending upon whether more or less energy has to be supplied to the sample relative to the reference material (Brown, 1998).

4.2.3 Methodology

The TGA and DSC thermograms for cyclo(Phe-4Cl-Pro) and cyclo(D-Phe-4Cl-Pro) were obtained by heating the samples in a TA Instruments Q600 SDT (simultaneous DSC-

TGA) V8.3 (TA Instruments, USA). The TA Instruments Q600 SDT was calibrated for temperature using the melting points of indium and tin. Cyclo(Phe-4Cl-Pro) (2.710 mg) and cyclo(D-Phe-4Cl-Pro) (2.472 mg) were heated in open aluminium crucibles at a heating rate of 5 °C per minute, over a temperature range of 50 to 400 °C, with nitrogen as the purging gas (flow rate of 50 ml per minute).

4.2.4 Results and discussion

In all TGA thermograms the region x (as shown in the thermograms below) indicates a loss of weight. This could be free water, waters of hydration, or loss of solvent. This is followed by a weight loss portion (region y), indicating a melt. The inflection (region Z) indicates a change in the rate of decomposition.

In the TGA thermogram (Figure 4.5) the plateau of constant weight (region x) indicated free water or waters of hydration, coming off above 100 °C. A small decrease in the TGA curve is seen at 100 °C. The corresponding DSC peak relates to this enthalpy of hydration. The onset of the narrow endotherm starts at 172.71 °C, corresponding to the melting point of cyclo(Phe-4Cl-Pro) . The dipeptide started to decompose soon after the melting point.

A loss of mass in the TGA thermogram (Figure 4.6) at around 50 °C is observed. This can be associated to the presence of acetone, an indication that the compound was not dried properly. The onset point of the narrow endotherm starts at 174.06 °C, corresponding to the melting point of cyclo(D-Phe-4Cl-Pro) . From the spectrum it is very clear that the dipeptide started to decompose soon after the melting point.

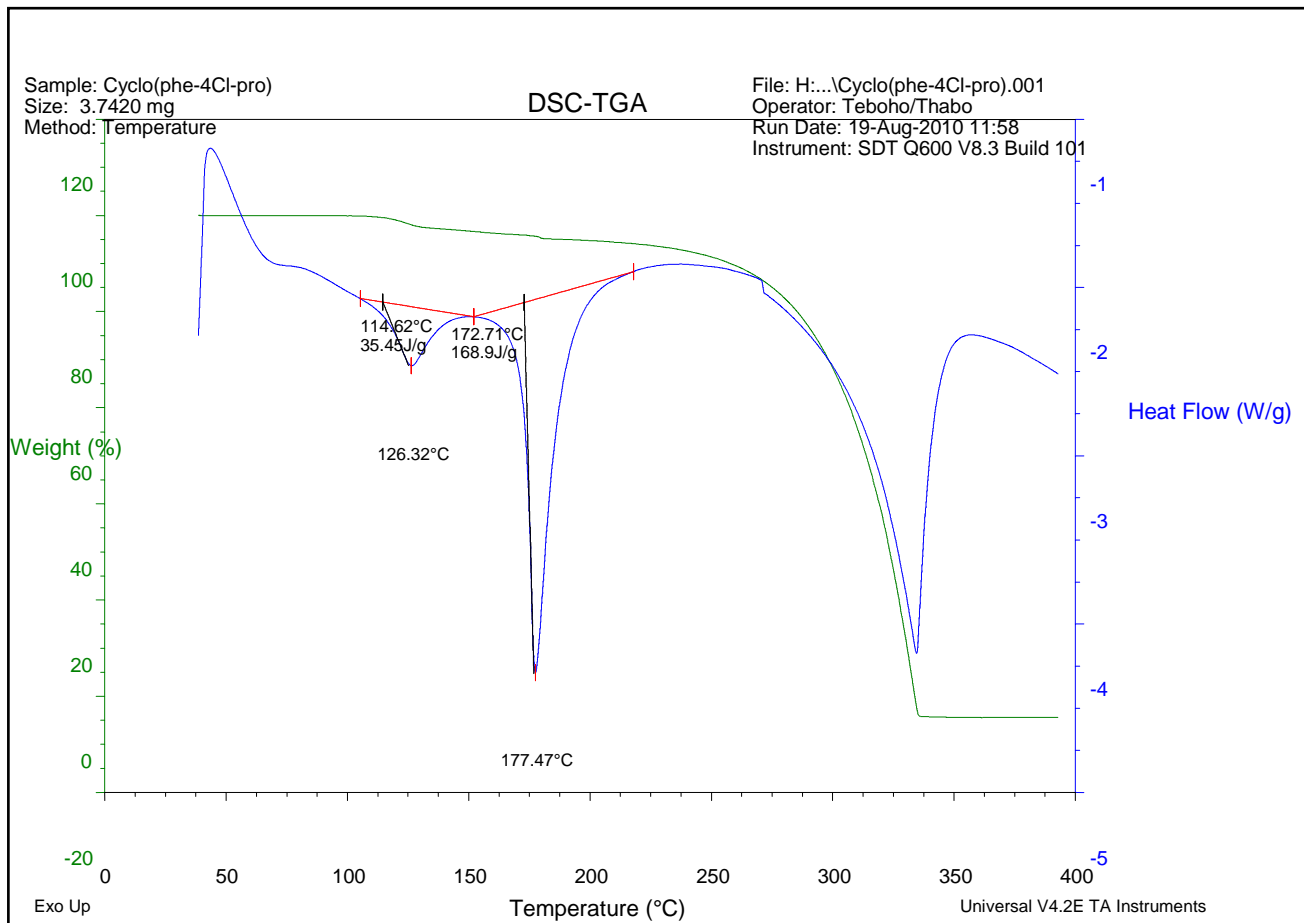


Figure 4.5 Simultaneous DSC-TGA thermogram of cyclo(Phe-4Cl-Pro)

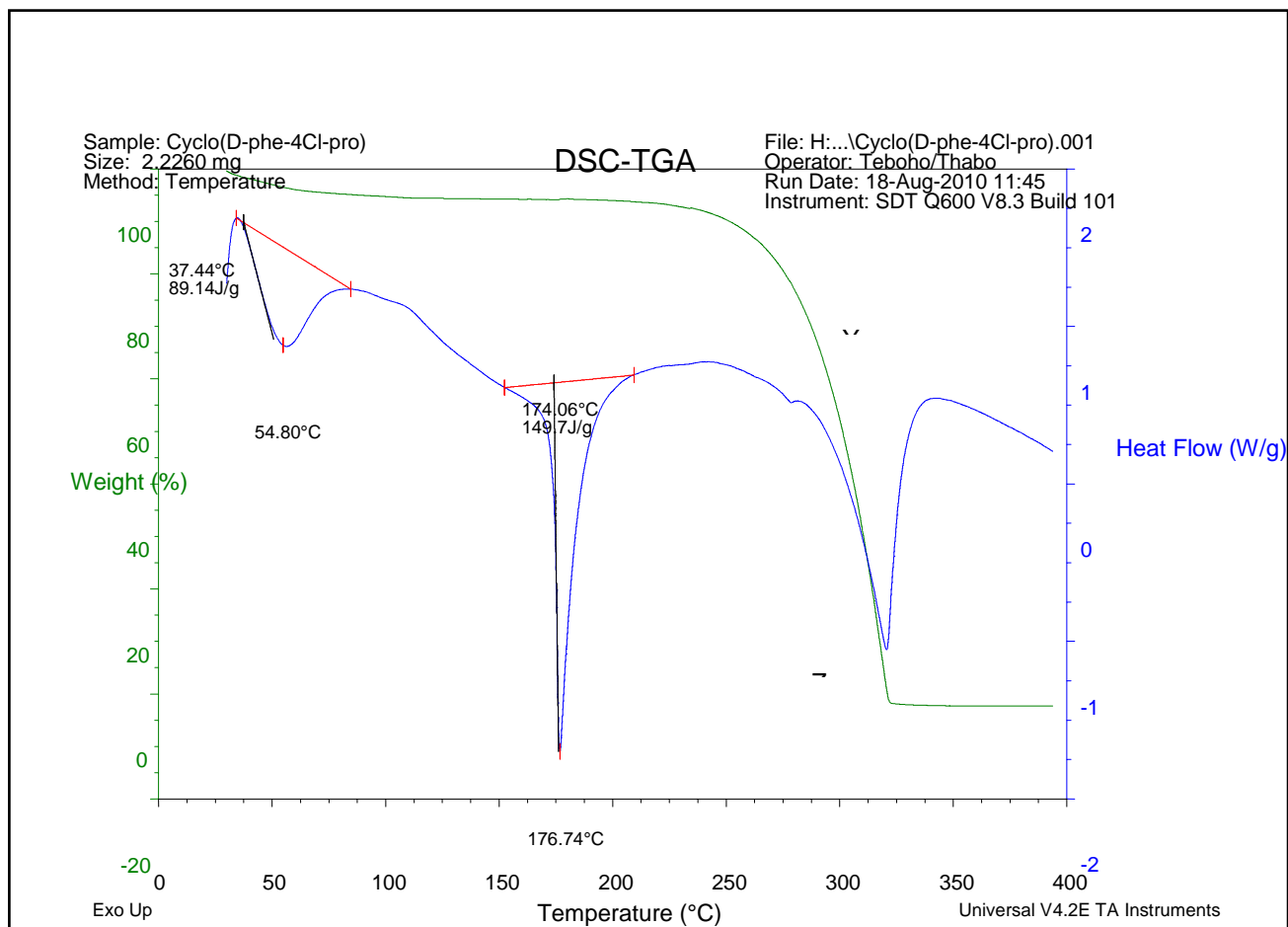


Figure 4.6 Simultaneous DSC-TGA thermogram of cyclo(D-Phe-4Cl-Pro)

4.3 X-ray Powder Diffraction

4.3.1 Introduction

The X-ray powder diffraction (XRPD) experiment is the foundation of a truly basic material characterisation technique called diffraction analysis, and has been used for many decades with exceptional success to provide accurate information about the structure of materials (Pecharsky and Zavalij, 2005).

Much of what is known about the arrangement and the spacing of atoms in crystalline materials has been determined directly from diffraction studies. XRPD provides a convenient and practical means for the qualitative identification of crystalline

compounds. It is the only analytical method that is capable of providing qualitative and quantitative information about the compounds present in a solid sample (Skoog *et al.*, 2004).

XRPD materials analysis involves characterisation of the sample by means of atomic arrangements in the crystal lattice. XRPD uses single or multiphase specimens, comprising of a random orientation of small crystallites, each of the order of 1-50 μm in diameter. Each crystallite, in turn, is made up of a regular, ordered array of atoms. An ordered arrangement of atoms (the crystal lattice) contains planes of high atomic density which in turn means planes of high electron density. A monochromatic beam of X-ray photons will be scattered by these atomic electrons and if the scattered photons interfere with each other, diffraction maxima may occur. A diffraction pattern is typically in the form of a graph of diffraction angle (or inter planar spacing) against diffracted line intensity. The pattern is made up of a series of super-imposed diffractograms, one for each unique phase in the specimen. Each of the unique patterns can act as an empirical “fingerprint” for the identification of various phases (Meyers, 2000).

Although powder data usually lack the three dimensionality of a diffraction image, the fundamental nature of the method is easily appreciated from the fact that each powder diffraction pattern represents a one-dimensional snapshot of the three-dimensional reciprocal lattice. The quality of the powder diffraction pattern is usually limited by the nature and the energy of the available radiation, by the resolution of the instrument and by the physical and chemical conditions of the specimen (Pecharsky and Zavalij, 2005).

Of all the methods available to the analytical chemist, only X-ray diffraction is capable of providing general purpose qualitative and quantitative information on the presence of phases in an unknown mixture. A diffraction pattern contains a good deal of information of which three parameters are of special interest:

- The position of the diffraction maxima.
- The peak intensities.

- The intensity distribution as a function of diffraction angle.

These three species of information can, in principle, be used to identify and quantify the contents of the sample, as well as to calculate the material's crystallite size and distribution, crystallinity, stress and strain (Meyers, 2000).

The role of XRPD for identification of unknown chemicals is limited in the pharmaceutical industry, since there are numerous techniques available for determining molecular structure of organic molecules. The techniques of mass spectrometry and nuclear magnetic resonance are predominant in this role. On the other hand, due to its speed of data acquisition and sensitivity XRPD exists as the primarily tool for phase identification (Stephenson, 2005; Beckers, 2004). While it does serve as a means for identification of primarily inorganic unknowns, by non-destructively determining the crystallographic constitution of samples, XRPD is used to:

- Determine crystal structures.
- Screen for polymorphs or hydrates.
- Detect changes in morphology or crystalline state of active ingredients (e.g., during processing or at non-ambient conditions).
- Detect and quantify crystalline impurities (in some cases down to 0.05%).
- Determine the crystallinity or the crystallite size of a compound.
- Analyse and optimise final dosage forms.

XRPD data on a compound or drug is also required for new product registration and patent application/protection (Litterer and Beckers, 2005).

4.3.2 Methodology

XRPD patterns for cyclo(Phe-4Cl-Pro) and cyclo(D-Phe-4Cl-Pro) were obtained by using an Bruker Advanced Solutions XRD Commander (Diffrac^{plus} Version 2.3) diffractometer (Bruker Advanced Solutions, Germany), and the resultant diffraction

patterns were interpreted using Bruker Advanced X-ray Solutions Eva Software (Diffrac^{plus} Version 10.0 Rev.1). n-Hexane (BD Laboratory Supplies, England) was used as a wetting agent, which enabled small samples of the cyclic dipeptide to adhere to silicon plates, without causing dissolution of the compounds. The silicon plates were then placed within the X-ray powder diffractometer and scanned for 1 hour.

4.3.3 Results and discussion

The diffraction patterns obtained from powdered samples can only be identified when compared alongside the diagrams of known substances until a match is obtained (Willard *et al.*, 1998).

The XRPD patterns of cyclo(Phe-4Cl-Pro) and cyclo(D-Phe-4Cl-Pro) are illustrated in Figures 4.7 and Figures 4.8, respectively. Determining the phase composition of the cyclic dipeptides was not possible, since none of the powder diffraction databases available included experimental diffraction patterns to which the compounds could be compared. Since the obtained Bragg angles and intensities of the cyclo(Phe-4Cl-Pro) and cyclo(D-Phe-4Cl-Pro) have no known match, the collected data can potentially be used as a “fingerprint” to identify new crystalline substances. The identity of the cyclic dipeptides should, however, firstly be confirmed through structural elucidation to ensure that it is not a mixture of compounds.

From the diffraction patterns of both cyclic dipeptides it can be seen that they are crystalline solids, since the curve of scattered intensity versus 2θ for crystalline solids is zero everywhere except at certain angles where sharp maxima occur.

Both amorphous solids and liquids have structures characterised by an almost complete lack of periodicity and tendency to order. The atoms in amorphous structures also show preference for a particular interatomic distance, resulting in x-ray diffractograms exhibiting only one or two broad maxima.

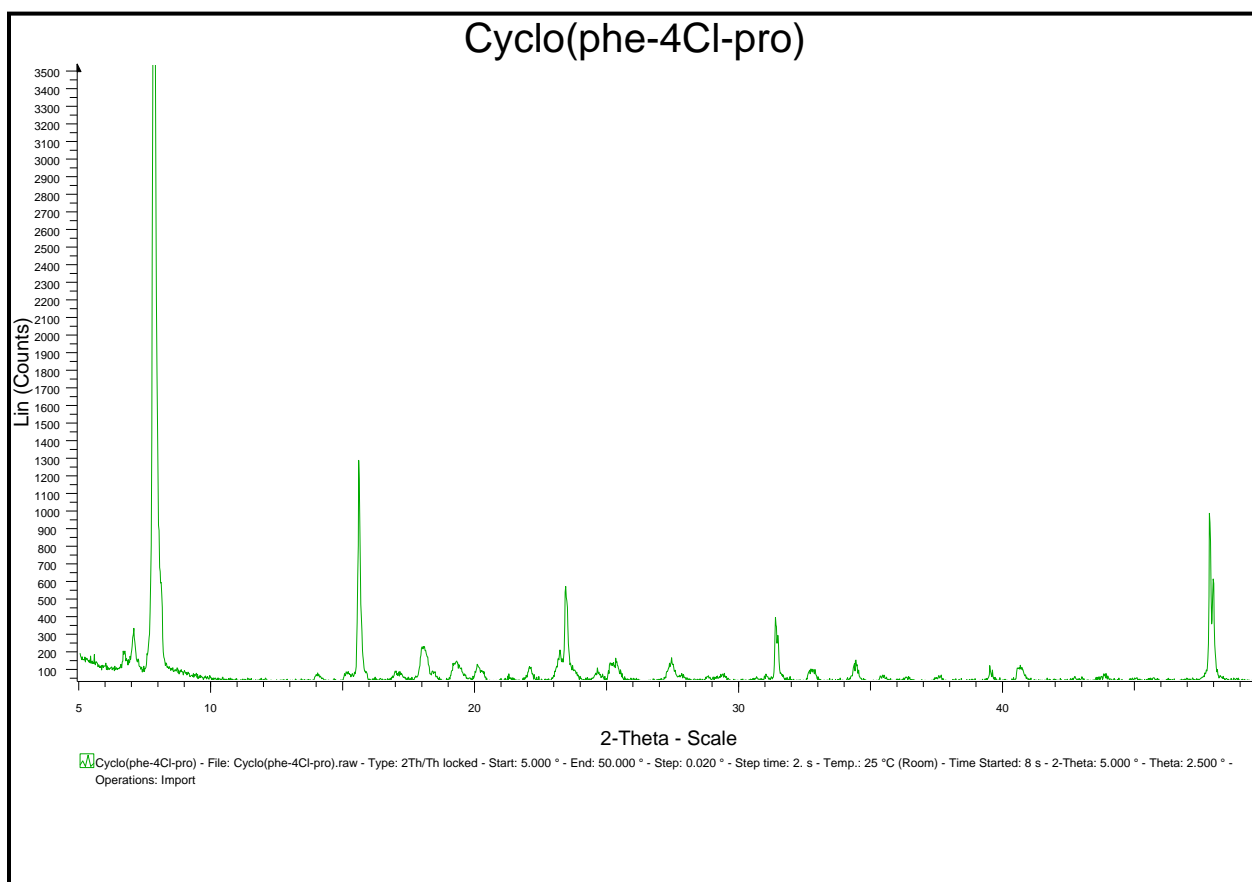


Figure 4.7 X-ray powder diffraction pattern of cyclo(Phe-4Cl-Pro)

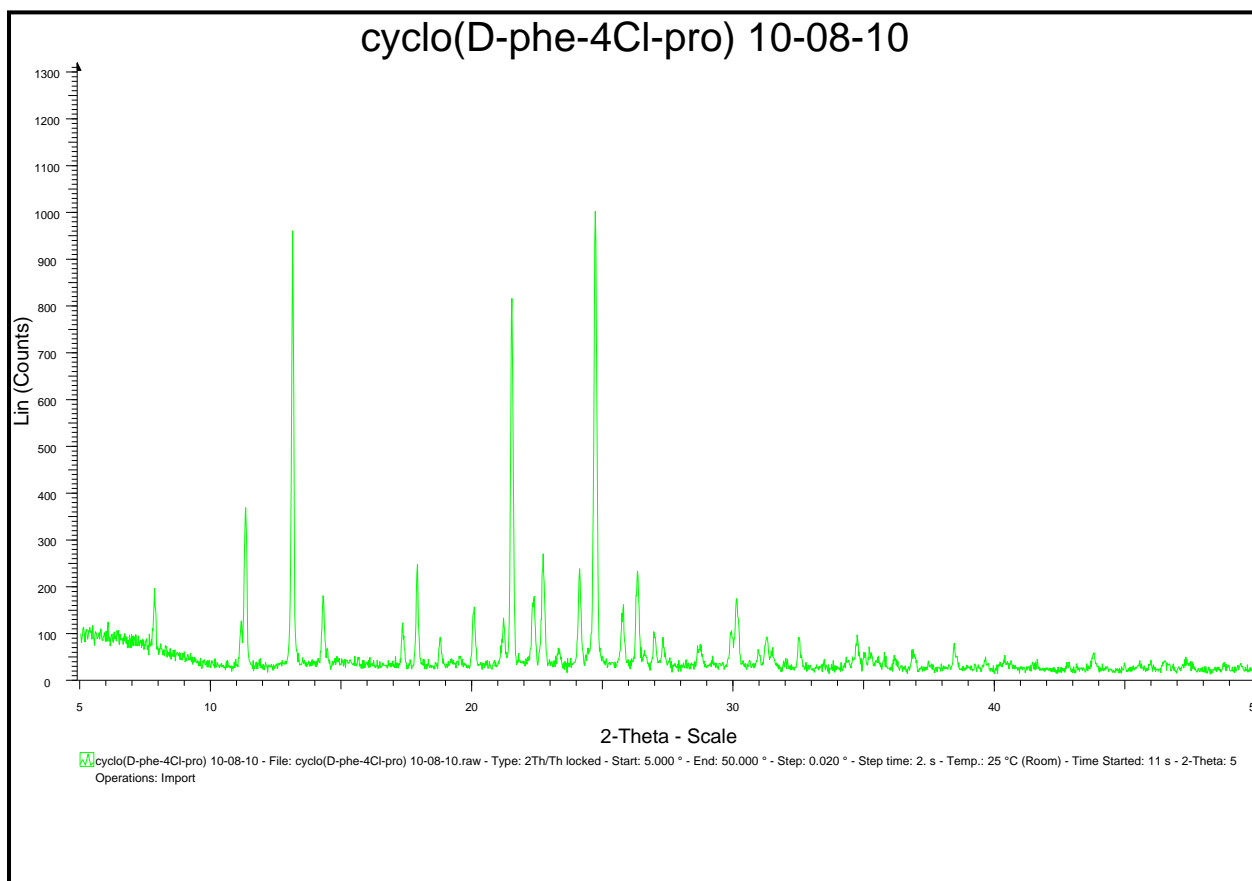


Figure 4.8 X-ray powder diffraction pattern of cyclo(D-Phe-4Cl-Pro)

CHAPTER 5

STRUCTURAL AND CONFORMATIONAL ANALYSIS

Structural and conformational analysis of cyclo(Phe-4Cl-Pro) and cyclo(D-Phe-4Cl-Pro) was performed using infrared spectroscopy, mass spectrometry, molecular modelling and nuclear magnetic resonance spectroscopy.

5.1 Infrared spectroscopy

5.1.1 Introduction

Infrared spectroscopy (IR) is a technique based on the vibrations of the atoms of a molecule. It involves the examination of the twisting, bending, rotating and irrational motions of atoms in a molecule. IR spectroscopy has been extensively used in both qualitative and quantitative pharmaceutical analysis. All molecular species, with the exception of O₂, N₂, CL₂ and H₂ absorb infrared radiation (Skoog *et al.*, 2004). Many functional groups in organic molecules show characteristic molecular vibrations and rotations, which correspond to absorption bands in defined regions of the infrared spectrum. These molecular vibrations are localised within the functional groups and do not extend over the rest of the molecule. Thus such functional groups can be identified by their absorption bands (Stuart, 2004).

An IR spectrum is commonly obtained by passing IR radiation through a sample and determining what fraction of the incidence radiation is absorbed at a particular energy. The energy at which any peak in an absorption spectrum appears corresponds to the frequency of a vibration of a part of a sample molecule (Stuart, 2004). The wave number, expressed in centimeter units (cm⁻¹), is the reciprocal of the wavelength in centimeters, *i.e.*, Wave number = 1/λ (cm) (McMurry, 2008). Polar bonds are associated with strong IR absorption while symmetrical bonds may not absorb at all. The vibrational frequency, *i.e.*, the position of the IR bands in the spectrum, depends on the nature of the bond. Shorter and stronger bonds have their stretching vibrations at the higher energy end (shorter wavelength) of the IR spectrum than the longer and weaker bonds.

Similarly, bonds to lighter atoms, e.g., hydrogen, vibrate at higher energy than bonds to heavier atoms (Field *et al.*, 2001).

Fourier-transform infrared (FTIR) spectroscopy is based on the interference of radiation between two beams to yield an interferogram. The latter is a signal produced as a function of the change of pathlength between the two beams. The two domains of distance and frequency are interconvertible by the mathematical method of Fourier-transformation. The radiation emerging from a source is passed through an interferometer to the sample before reaching a detector. Upon amplification of the signal, in which high-frequency contributions have been eliminated by a filter, the data are converted to digital form by an analogue-to-digital converter and transferred to the computer for Fourier-transformation (Stuart, 2004).

The infrared spectrum can be divided into three main regions: the far-infrared ($< 400 \text{ cm}^{-1}$), the mid-infrared ($400 - 4000 \text{ cm}^{-1}$) and the near-infrared ($4000 - 13000 \text{ cm}^{-1}$). Many infrared applications employ the mid-infrared region, but the near- and far-infrared regions also provide important information about certain materials. Generally there are less infrared bands in the $1800 - 4000 \text{ cm}^{-1}$ region with many bands between 400 cm^{-1} and 1800 cm^{-1} (Stuart, 2004).

5.1.2 Methodology

The infrared spectra of cyclo(Phe-4Cl-Pro) and cyclo(D-Phe-4Cl-Pro) were recorded on a Shimadzu 1600 spectrophotometer (Shimadzu, Tokyo, Japan). Approximately 1 mg of each cyclic dipeptide, dried in a dessicator, was mixed with approximately 100 mg of dry, powdered, spectral grade potassium bromide (KBr) (Merck, SA). Potassium bromide is suitable for use since it is transparent over the whole IR range, *i.e.*, it has no IR bands of its own (Field *et al.*, 2001). Potassium bromide is however hygroscopic, so that traces of water can rarely be totally excluded during the grinding and pressing of the KBr disc. Therefore a weak band is usually observed at 3450 cm^{-1} (Field *et al.*, 2001). The mixture was then ground using an agate mortar and pestle. A Perkin Elmer[®] Bench Press set at a pressure of $1 \times 10^4 \text{ kg. cm}^{-2}$, was then used to press the powdered

mixture into a thin transparent disc. The disc was transferred to the KBr sample cell of the IR spectrophotometer and the spectra recorded after 16 scans. The infrared spectra of the two cyclic dipeptides were then recorded within the frequency range of 4000 cm^{-1} to 400 cm^{-1} .

5.1.3 Results and discussion

The IR spectra for cyclo(Phe-4Cl-Pro) and cyclo(D-Phe-4Cl-Pro) are illustrated in Figures 5.1 and 5.2, respectively. The main functional groups found in cyclo(Phe-4Cl-Pro) and cyclo(D-Phe-4Cl-Pro) were identified by comparing the peaks obtained from the IR spectra with the observed reference values from literature, shown in Table 5.1.

Table 5.1 Frequencies/absorption bands (cm^{-1}) of cyclo(Phe-4Cl-Pro) and cyclo(D-Phe-4Cl-Pro)

Description of band	<i>Cis</i> -amide absorption bands	<i>Trans</i> -amide absorption bands	Cyclo(Phe-4Cl-Pro)	Cyclo(D-Phe-4Cl-Pro)
Amide I band (CO stretch)	1670-1690 ¹	1650	1658.84	1647.26
Amide II band (NH-in plane vibration)	1440-1450 1420-1460 ²	1550	1454.38 1425.44	1491.02
Amide III (<i>cis</i> CONH)	1300-1350 ³	Not present	1294.28	-
NH bending	1450 ¹	1450	1454.38	1458.23

CN stretching	1350 ¹	1350	1365.65	1332.86
NH stretching	3180-3195 ⁴	3350	3149.86	3344.68
Combination band of CO stretching and NH bending vibrations of the <i>cis</i> CONH group	3100, 3200 ¹	3100, 3300	3101.64, 3267.52	3119.00, 3344.68
CH ₂ twisting	1249 ¹		1234.48	1251.84
CH ₂ bending	1468 ¹		1454.38	1458.23
CH ₂ wagging	1340 ¹		1365.65	1332.86
CH ₂ rocking	998 ¹		1045.45	1003.02
CO in-plane bending	806 ¹		810.13	813.99
Skeletal stretching (NMe stretching)	1075 ¹		1078.24	1070.53
C-Me stretching	910 ¹		1045.45	920.08
Free NH groups	3420-3480 ⁴		-	-
Hydrogen bonded	3300-3380 ⁴		3340.00	3344.68

NH groups				
-----------	--	--	--	--

¹(Miyazawa, 1960), ²(Ovchinnikov and Ivanov, 1975), ³(Bláhaet *al.*, 1966), ⁴(Sammes, 1975), ⁵(Stuart, 2004)

The presence of secondary amide and carbonyl groups together with the absence of carboxylic acid groups was necessary to confirm that the diketopiperazine (DKP) rings were present in the structure of the cyclic dipeptides.

According to literature, secondary amide functional groups will show N-H stretching absorption bands between 3180 – 3195 cm⁻¹ (*cis*) and 3350 cm⁻¹ (*trans*), with carbonyl stretching (Amide I) absorption bands being observed between 1650 cm⁻¹ (*trans*) and 1670 – 1690 cm⁻¹ (*cis*) (Stuart, 2004; Sammes, 1975; Miyazawa, 1960). The amide II for secondary amide groups is due to the coupling of N-H bending and C-N stretching and appears between 1420 – 1460 cm⁻¹ (*cis*) (Ovchinnikov and Ivanov, 1975). A weak band which is an overtone of the amide II band also appears at 650 cm⁻¹ (Stuart, 2004).

For cyclo(Phe-4Cl-Pro) and cyclo(D-Phe-4Cl-Pro) the presence of secondary amide groups were confirmed by the presence of N-H stretching absorption bands at 3149.86 cm⁻¹ for cyclo(Phe-4Cl-Pro) and 3344.60 cm⁻¹ for cyclo(D-Phe-4Cl-Pro), carbonyl stretching was observed at 1658.84 cm⁻¹ for cyclo(Phe-4Cl-Pro) and at 1647.26 cm⁻¹ for cyclo(D-Phe-4Cl-Pro), the amide II bands occurring at 1467.6 cm⁻¹ for cyclo(Phe-4Cl-Pro) and 1467.6 cm⁻¹ for cyclo(D-Phe-4Cl-Pro) and weak bands representing the overtones of the amide II occurring at 751.8 cm⁻¹ and 732.0 cm⁻¹ for cyclo(Phe-4Cl-Pro) and cyclo(D-Phe-4Cl-Pro), respectively.

The absence of carboxylic acid groups is also necessary to confirm that the cyclisation of the linear dipeptides had occurred. Carboxylic acid groups show a strong broad O-H stretching band in the 2500 cm⁻¹ to 3300 cm⁻¹ range. The C=O stretching band of the free acid band is observed at 1760 cm⁻¹. Carboxylic acids also show characteristic C-O stretching and in-plane and out-plane O-H bending at 930 cm⁻¹ and 1430 cm⁻¹,

respectively (Stuart, 2004). The absence of these characteristic bands, for both cyclic dipeptides, indicated the absence of carboxyl (COOH) end groups.

The presence of secondary amide functional groups, together with the absence of any carboxylic acid functional groups for cyclo(Phe-4Cl-Pro) and cyclo(D-Phe-4Cl-Pro) therefore suggested that a DKP ring is present in the structures of the cyclic dipeptides and that cyclisation therefore had occurred during the synthesis of these compounds.

Infrared spectroscopy also reliably discriminates between *cis* and *trans* secondary amides (Ovchinnikov and Ivanov, 1975; Miyazawa, 1960). As a consequence of their biosynthetic origin from the two L- α -amino acids, most naturally occurring DKPs are *cis*-configured (Bull *et al.*, 1998).

The *cis*-amide bond nature of cyclo(Phe-4Cl-Pro) and cyclo(D-Phe-4Cl-Pro) was revealed through the values of the C=O stretching mode (amide I), which produced a peak at approximately 1670 cm^{-1} to 1690 cm^{-1} (Miyazawa, 1960). Strong peaks appeared at 1680.3 cm^{-1} for cyclo(Phe-4Cl-Pro) and at 1666.0 cm^{-1} for cyclo (D-Phe-4Cl-Pro), confirming the presence of *cis*-amide configuration. Further evidence for *cis*-amide configuration was given by the absence of *trans*-peaks at 1650 cm^{-1} for the cyclic dipeptides (Miyazawa, 1960).

Amide II vibrations are present due to interactions of the N-H bending and C-N stretching modes. The difference in frequencies between these two modes is approximately 100 cm^{-1} , which is due to negligible interactions between them. A difference of approximately 100 cm^{-1} exists between the N-H bending and the C-N stretching modes of cyclo(Phe-4Cl-Pro) and cyclo(D-Phe-4Cl-Pro) , and according to (Miyazawa, 1960), this is only apparent in the *cis*-CONH configuration which further confirmed the *cis*-amide configuration of the cyclic dipeptides.

The amide type II mode is represented by a single absorption band within the 1420 cm^{-1} to 1460 cm^{-1} region (Ovchinnikov and Ivanov, 1975). N-H bonding contributes the most

to amide II vibrations, whereas the C-N stretching vibration contributed more to the amide III band. The amide II vibrations occurred at 1467.6 cm^{-1} for cyclo(Phe-4Cl-Pro) and at 1467.1 cm^{-1} for cyclo(D-Phe-4Cl-Pro), confirming *cis*-amide configuration. Once again the absence of the trans-peaks between 1480 cm^{-1} and 1575 cm^{-1} (Ovchinnikov and Ivanov, 1975), provided further evidence of the *cis*-amide configuration of the cyclic dipeptides.

The *cis*-amide type III mode is represented by absorption bands within the 1300 cm^{-1} to 1350 cm^{-1} region (Bláha *et al.*, 1966). Amide III vibrations occurred at 1327.6 cm^{-1} for cyclo(Phe-4Cl-Pro) and at 1345.0 cm^{-1} for cyclo(D-Phe-4Cl-Pro), which confirmed the *cis*-amide configuration.

The N-H stretching mode of the *cis*-bond is represented by absorption band within the 3180 cm^{-1} to 3195 cm^{-1} region (Sammes, 1975). N-H stretching vibrations occurred at 3240.3 cm^{-1} for cyclo(Phe-4Cl-Pro) and at 3185.6 cm^{-1} for cyclo(D-Phe-4Cl-Pro), confirming the *cis*-amide configuration. The absence of trans-peaks at 3350 cm^{-1} provided further evidence of the *cis*-amide configuration.

The CH_2 bending vibration is also present within the amide II mode, and since only a single absorption band appears in this range, it is difficult to determine the presence of each mode. Similarly the CH_2 wagging vibration is overlapped by the C-N stretching mode, and is therefore not clearly defined. CH_2 twisting and rocking was observed at 1234.2 cm^{-1} and 976.8 cm^{-1} for cyclo(Phe-4Cl-Pro) and at 1223.6 cm^{-1} for cyclo(D-Phe-4Cl-Pro).

Figure 5.1 and figure 5.2 illustrates the overlay of cyclo(Phe-4Cl-Pro) and cyclo(D-Phe-4Cl-Pro) respectively. The spectrum of cyclo(Phe-4Cl-Pro), however, shows absorption bands at 1520.6 cm^{-1} and at 1620.1 cm^{-1} . These absorption bands, which are not seen in the spectrum of cyclo(D-Phe-4Cl-Pro), are due to aromatic C=C stretching caused by the aromatic tyrosine side-chain.

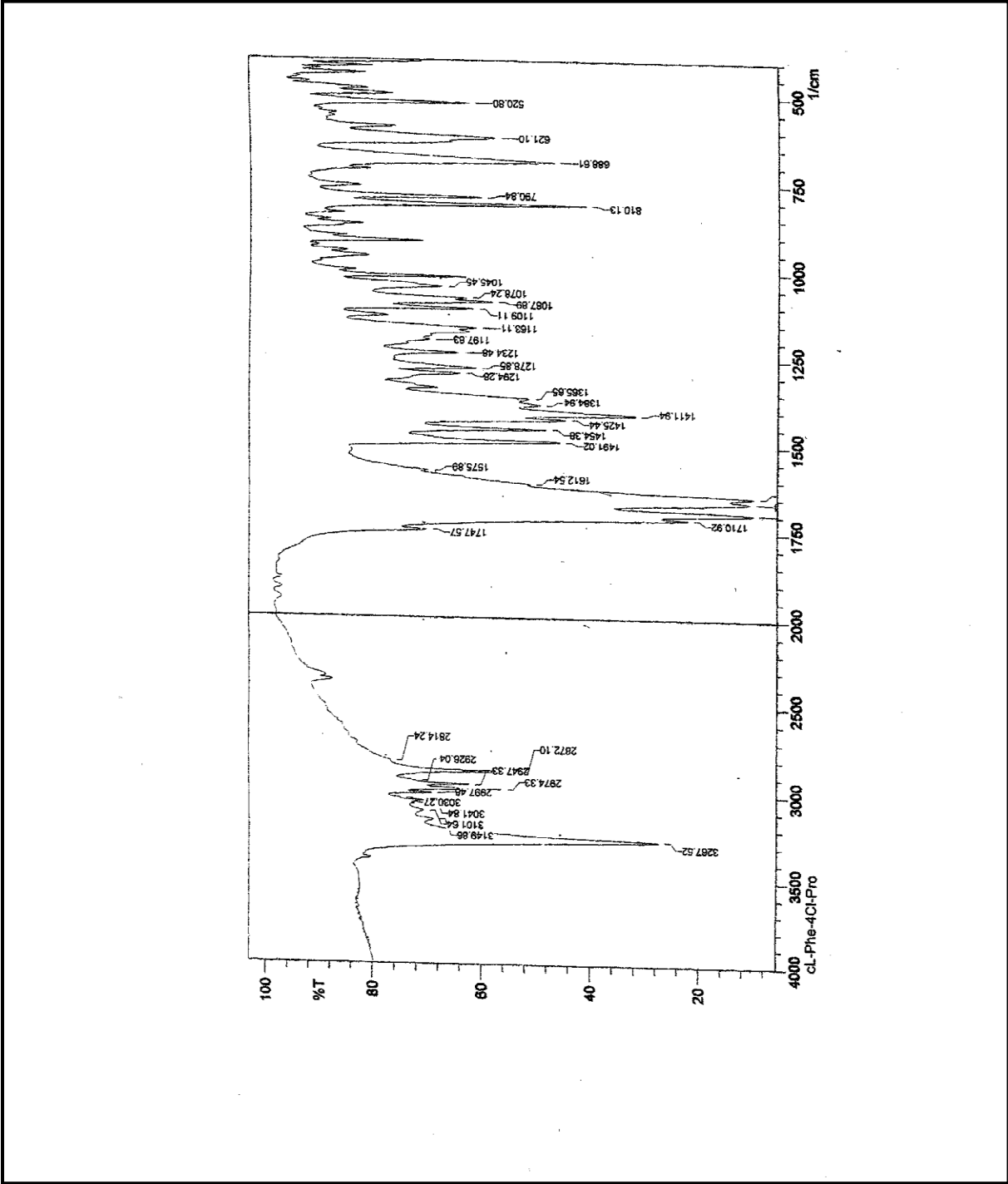


Figure 5.1 Infrared spectrum of cyclo(Phe-4Cl-Pro)

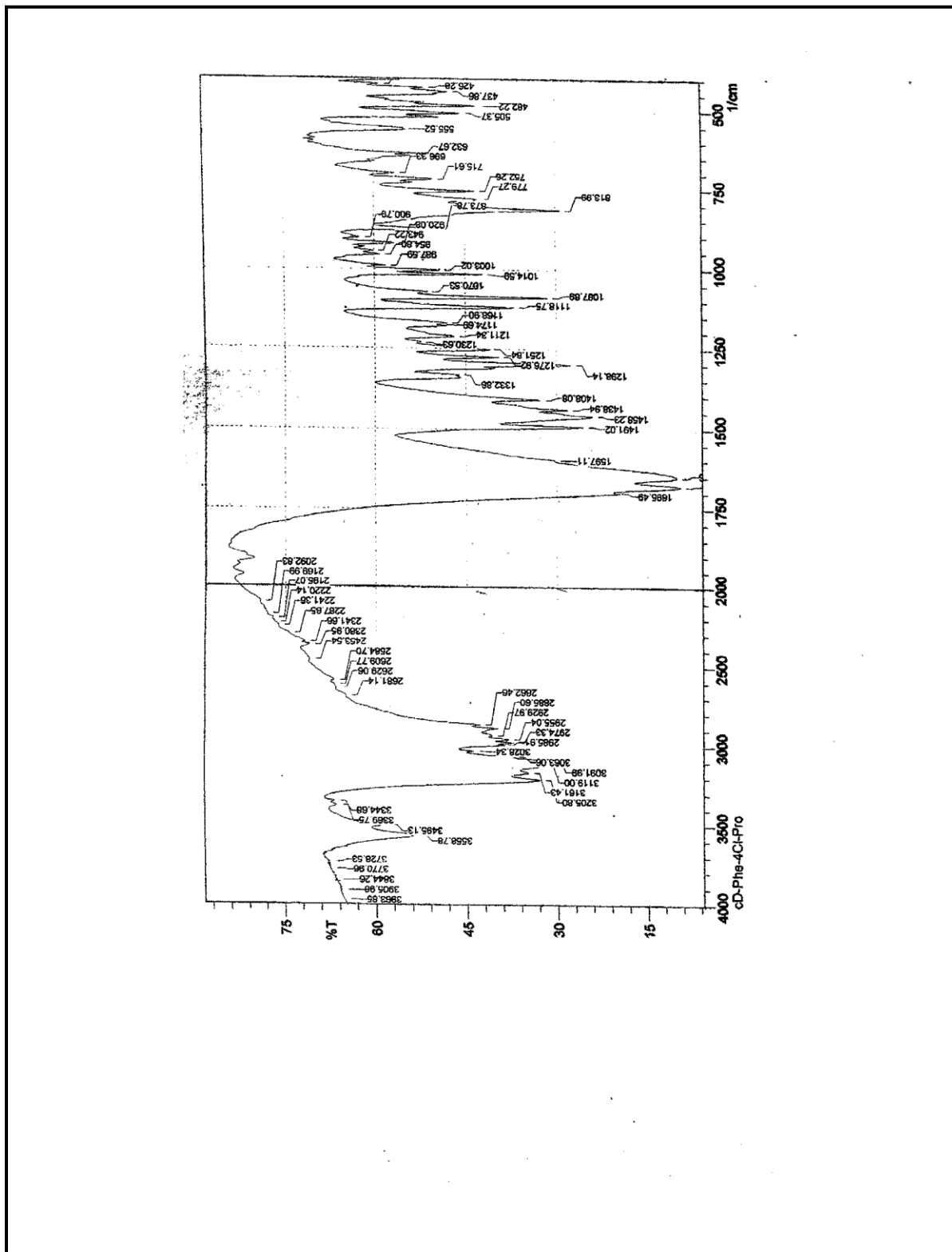


Figure 5.2 Infrared spectrum of cyclo(D-Phe-4Cl-Pro)

5.2 Fast atom bombardment mass spectrometry

5.2.1 Introduction

The objective of drug screening is to detect and quantify active molecules, metabolites and toxic compounds. Fast atom bombardment (FAB) mass spectrometry is the preferred ionization technique for the collision-induced dissociation (CID) spectra of $[M+H]^+$ ions of simple cyclic dipeptides generated by FAB ionization with a tandem mass spectrometer (Siuzdak, 2005).

Mass spectrometry (MS) is a technique for measuring the mass, and therefore the molecular weight (MW), of a molecule. In addition it is often possible to gain structural information about a molecule by measuring the masses of the fragments produced when molecules are broken apart (McMurry, 2008). MS can also provide a method for characterising impurities in drugs and formulation excipients (Watson, 2005). FAB is an ionisation source that uses a matrix and a highly energetic beam of particles to desorb ions from a surface. FAB is a soft ionisation source that requires the use of a direct insertion probe for sample introduction and a beam of xenon neutral atoms or cesium ions to sputter the sample and matrix from the direct insertion probe surface. It is common to detect matrix ions in the FAB spectrum as well as the protonated or cationised molecular ion of the analyte of interest. The FAB matrix is typically a non-volatile liquid material that serves to constantly replenish the surface with new sample as it is bombarded by the continuous incident ion beam. By absorbing most of the incident energy the matrix also minimises sample degradation from the high-energy particle beam. Two of the most common matrices used with FAB are *m*-nitrobenzyl alcohol and glycerol. The fast atoms or ions impinge on or collide with the matrix causing the matrix and analyte to be desorbed into the gas phase. The sample may already be charged and get transferred into the gas phase by FAB, or it may become charged during FAB desorption through reactions with surrounding molecules or ions. Once in the gas phase, the charged molecules can be propelled electrostatically to the mass analyzer (Siuzdak, 2005).

5.2.2 Methodology

The FAB mass spectra for cyclo(Phe-4Cl-Pro) and cyclo(D-Phe-4Cl-Pro) were recorded on a VG-7070E spectrometer (Biotech, UK) equipped with a VG2035 data system. All samples were run under positive ion operating conditions. 3 Nitro-benzylalcohol was used as the sample matrix and the solvent was deuterated dimethyl sulphoxide (DMSO- d_6). A small amount of each cyclic dipeptide was mixed on the probe tip with the sample. The spectra obtained were subsequently analysed in order to determine the molecular mass and possible fragments of the cyclic dipeptides.

5.2.3 Results and discussion

Possible fragmentation pathways of cyclo(Phe-4Cl-Pro) and cyclo(D-Phe-4Cl-Pro) are illustrated in Figure 5.3

The mass spectra of cyclo(Phe-4Cl-Pro) and cyclo(D-Phe-4Cl-Pro) are illustrated in Figures 5.4 and 5.5, respectively.

The mass spectra of both cyclo(Phe-4Cl-Pro) and cyclo(D-Phe-4Cl-Pro) indicated a peak at m/e 154, which corresponds to the base peak for DKPs. The mass spectra of the cyclic dipeptides also had other important similarities. The common peaks found at 105, 107, 115, 120, 136, 152 and 165 are all characteristic of DKPs.

The mass spectrum of cyclo(Phe-4Cl-Pro) indicated a parent peak at m/e 279, which corresponds to the molecular mass of the protonated form of the cyclic dipeptide *i.e.*, $[C_{14}H_{16}O_2N_2]^+$. This ion has a saturation index of 8, which confirms it to be the parent peak. The saturation index, which is an indicator of the number of rings and/or double bonds present in a molecule, is calculated from the formula $C_xH_yN_zO_n$, where the total number of rings and/or bonds = $X - \frac{1}{2} Y + \frac{1}{2} Z + 1$, where x represents the number of carbons, y the number of hydrogens and z the number of nitrogens. The saturation index will therefore equal $14 - \frac{1}{2} (16) + \frac{1}{2} (2) + 1$, which equals 8 and corresponds to the total number of rings and double bonds in the structure. The number of oxygens

does not play a role in the calculation (Lee, 1998). The mass spectra of cyclo(Phe-4Cl-Pro) also indicates the principle fragmentations of the cyclic dipeptide. A positive ion peak at m/e 115, indicates the fragmentation of the cyclic dipeptide to form the DKP ring $[C_4H_4O_2N_2]^+$. In analysing mass spectra of simple cyclic dipeptides, certain fragmentation patterns are evident.

The parent ion dominates the following fragmentations:

- a) loss of CO or CHO;
- b) amine fragmentation ($R_2CH=^+NH_2$); and
- c) elimination of cyanuric acid (HNCO) (Sammes, 1975).

When proline is present, in some cyclic dipeptides, there is a two mass shift to the left of some characteristic peaks (Svec and Junk, 1964). The following ions usually indicate the existence of a cyclic dipeptide ring: m/e 114; m/e 113; and m/e 85 (Szafranek et al., 1976).

With reference to the molecular mass of the cyclic dipeptides, the following m/e ratios corresponding to the positive ion of the following fragmentations were of importance:

- a) the positive ion, relating to the cleavage of the aromatic side chain (m/e 155)
- b) cyclic dipeptide pyrrolidine fragment (m/e 154)
- c) loss of the CO group (m/e 251)
- d) amine fragmentation (m/e 125)

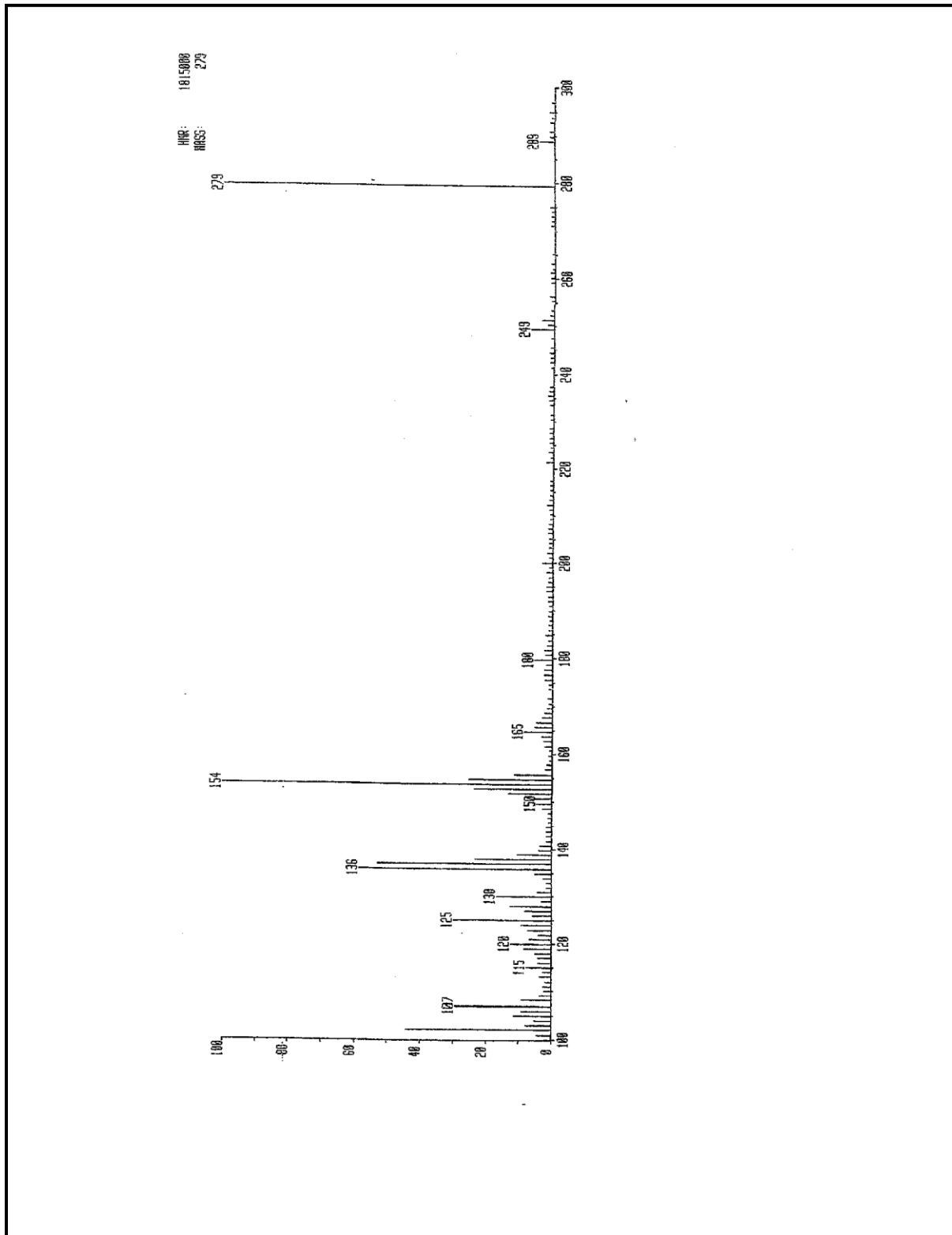


Figure 5.4 Mass spectrum of cyclo(Phe-4Cl-Pro)

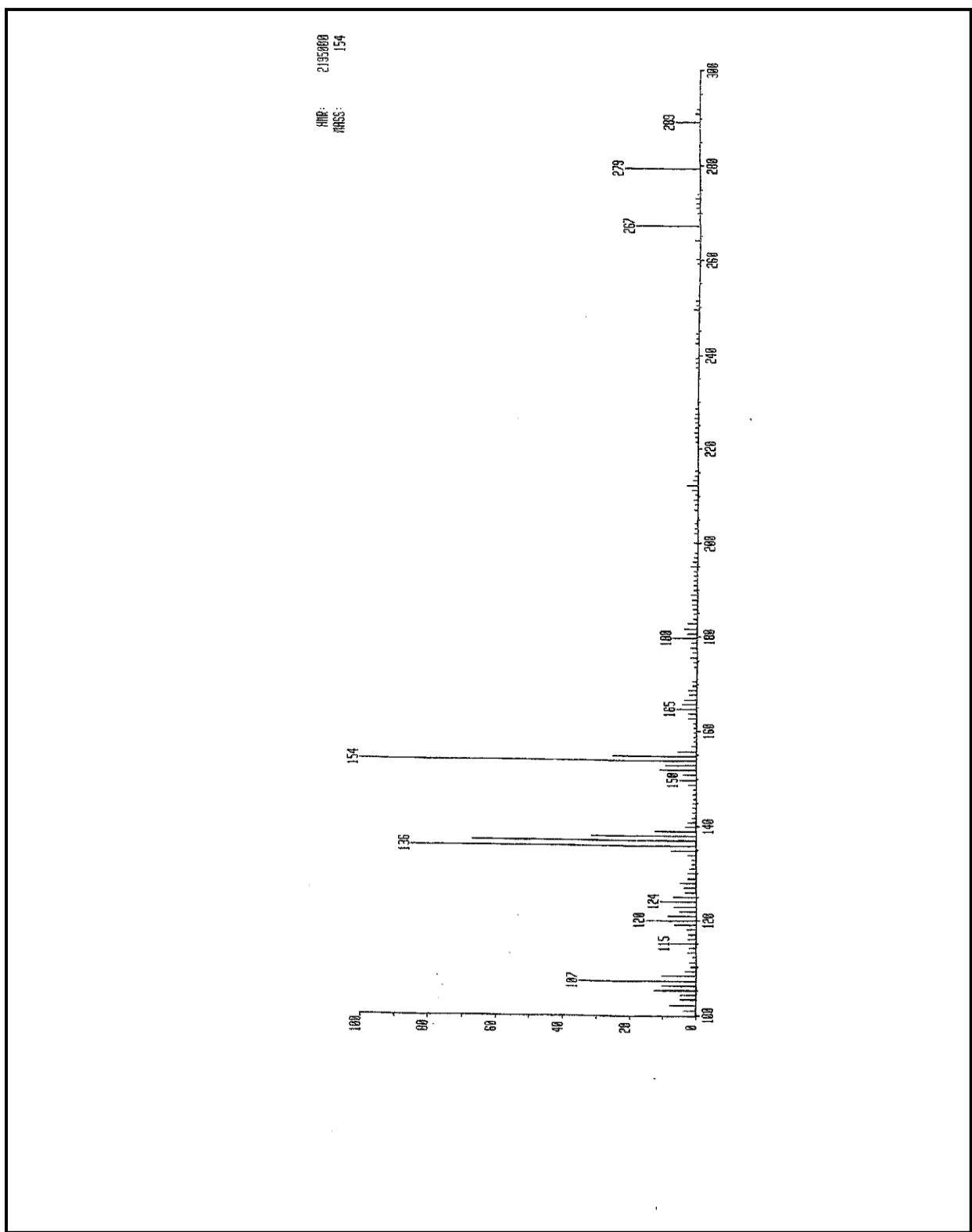


Figure 5.5 Mass spectrum of cyclo(D-Phe-4Cl-Pro)

5.3 Nuclear magnetic resonance spectroscopy

5.3.1 Introduction

Nuclear magnetic resonance (NMR) spectroscopy has for many decades been an important tool in the pharmaceutical sciences. Its initial role was to identify and characterise chemically synthesised drugs, or biologically active compounds derived from a variety of natural sources. Today, NMR remains a premier method for the structural characterisation of pharmaceutical compounds. The development for methodology for assigning and determining the structures of peptides and proteins by two-dimensional NMR has made possible, a variety of new applications in the field of drug design (Abraham and Mobli, 2004).

Nuclear magnetic resonance spectroscopy (NMR) provides a “map” of the carbon-hydrogen framework of an organic molecule. NMR, infrared spectroscopy and mass spectrometry are used together to determine the complete structure of a molecule (McMurry, 2008).

The nuclei of certain isotopes e.g., ^1H and ^{13}C (^{12}C has no nuclear spin and cannot be observed by NMR) have an intrinsic spinning motion around their axes. The spinning of the positive charged particles will generate magnetic moment around and along their axes of spin. When the nuclei (^1H and ^{13}C) are placed in an external magnetic field, the magnetic field of the isotopes can either align with (parallel to) or against (antiparallel to) the external magnetic field (Willard *et al.*, 1998). The parallel orientation is lower in energy than the antiparallel orientation. If the nuclei (parallel or antiparallel orientation) are irradiated with electromagnetic radiation energy absorption will occur and the lower energy states will “spin-flip” to a higher energy state (McMurry, 2008). NMR has various applications in pharmaceutical analysis:

- It is used as a powerful technique for the characterisation of the exact structure of raw materials and finished products.
- It can determine impurities, including enantiomeric impurities.

- It can potentially be used for finger printing mixtures.
- It is also a good agent for quantitative analysis of drugs in formulations without prior separation (Watson, 2005).

^1H NMR spectra offer three important parameters which can be extracted, the ^1H chemical shift (δ), the ^1H , ^1H coupling constants ($^n\text{J}_{\text{HH}}$; n = number of intervening bonds, generally 2-4), and the signal intensity (integral) (Bechmann *et al.*, 2004).

The COSY (Correlation spectroscopy) spectrum is a symmetrical spectrum which has the ^1H NMR spectrum of the substance at both of the two chemical shift axes. The COSY shows which pairs of nuclei in a molecule are coupled (Ozaki *et al.*, 1999).

^{13}C DEPT (distortionless enhancement by polarization transfer) contains only signals arising from protonated carbons and gives information about the number of protons bonded to each carbon (McMurry, 2008).

HMBCGP (Heteronuclear multiple bond correlation experiment) gives information about weak proton-carbon J-couplings. A weak proton-carbon J-coupling indicates that the proton is two, three or four bonds away from the carbon. HMBCGP also gives information about which protons are near to (but not directly bonded to) different carbons. HMBCGP together with HMQC (Heteronuclear Multiple Quantum Correlation experiment) provides an enormous amount of information about the molecular structure, since the long range proton-carbon correlations can include quaternary carbons, in addition to protonated carbons (Würtzet *et al.*, 2008).

HSQC (Heteronuclear Single Quantum Coherence) is a two-dimensional spectrum with one axis for the ^1H protons and the other for a heteronucleus (atomic nucleus other than a proton *i.e.* ^{13}C). The spectrum contains a peak for each unique proton attached to the heteronucleus being considered. If the chemical shift of a specific proton is known, the chemical shift of the coupled heteronucleus can be determined (Samuel *et al.*, 2011).

5.3.2 Methodology

The ^1H (300.13 MHz) and ^{13}C (75.48 MHz) spectra for cyclo(Phe-4Cl-Pro) and cyclo(D-Phe-4Cl-Pro) were recorded on a Bruker AMS 300 (Bruker, Germany). COSY, HSQC, HMBCGP, was also recorded for the assignment of the proton to proton, and proton to carbon couplings within the respective cyclic dipeptides. Cyclic dipeptide solutions were prepared using DMSO- d_6 (Merck, Germany) as the solvent. TMS was used as the internal standard, specified at 0 parts per million (ppm), for the determination of the chemical shifts.

5.3.3 Results and discussion

All recorded NMR spectra are shown in Figures 5.6 to 5.16 with NMR results recorded as shifts in parts per million (ppm). The ^1H and ^{13}C assignments of cyclo(Phe-4Cl-Pro) and cyclo(D-Phe-4Cl-Pro) are given in Tables 5.2 and 5.3.

Table 5.2 NMR data of cyclo(Phe-4Cl-Pro) (DMSO- d_6)

^1H -NMR δ -values (ppm)	^{13}C -NMR δ -values (ppm)
1.481 (1H; m) Pro- β	22.34 (t) Pro- γ
1.752 (2H; m) Pro- γ	28.31 (t) Pro- β
2.045 (1H; m) Pro- β	34.90 (t) Phe- β
3.040 (2H; m) Phe- β (distorted triplet)	45.07 (t) Pro- δ
3.287 (1H; m) Pro- δ	55.95 (d) Phe- α
3.313 (1H; m) Pro- δ	58.86 (d) Pro- α

4.092 (1H; distorted t) Pro- α	128.31 (d) Phe-Ar
4.376 (1H; t) Phe- α	131.53 (m) Phe-Ar
7.314 (4H; m) Phe-Ar	132.20 (q) Phe-Ar
8.150 (1H; s) Phe-NH)	136.74 (q) Phe-Ar
	165.39 (s) Phe-C=O
	169.67 (s) Pro-C=O

s = singlet, d = doublet, t = triplet, q = quartet, m = multiplet

The Pro- β and Pro- δ protons of cyclo(Phe-4Cl-Pro) are non-equivalent as they resonated at 1.481 ppm and 2.045 ppm , 3.287 ppm and 3.313 ppm respectively indicating that the one β -proton and one δ -proton are more shielded. The Pro- γ and Phe- β protons resonated at 1.752 ppm and 3.040 ppm respectively. The Pro- α proton resonated upfield (4.092 ppm) compared with the Phe- α proton which resonated at 4.376 ppm, indicating greater deshielding of the Phe- α proton. The aromatic protons and Phe-NH resonated far downfield at 7.314 ppm and 8.150 ppm respectively.

From the ^{13}C -NMR spectrum it can be seen that the Pro- α carbon resonated downfield at 58.86 ppm compared with the Phe- α carbon which resonated at 55.95 ppm. The Pro- γ , Pro- β , Phe- β and Pro- δ carbons resonated at 22.34 ppm, 28.31 ppm, 34.90 ppm and 45.07 ppm respectively.

The carboxyl groups resonated far downfield at 165.39 ppm and 169.67 ppm respectively, while the aromatic carbons resonated downfield between 128.31 ppm and 136.74 ppm

Table 5.3 NMR data of cyclo(D-Phe-4Cl-Pro) (DMSO-_{d6})

¹ H-NMR δ-values (ppm)	¹³ C-NMR δ-values (ppm)
1.639 (2H; m) Pro-β, Pro-γ	21.87 (t) Pro-γ
1.806 (1H; m) Pro-γ	29.01 (t) Pro-β
2.020 (1H; m) Pro-β	38.94 (t) Phe-β
2.907 (1H; dd) Phe-β	45.29 (t) Pro-δ
2.994 (1H, dd) Phe-β	57.80 (d) Phe-α
3.236 (1H; m) Pro-δ	58.26 (d) Pro-α
3.775 (1H; m) Pro-δ	128.69 (d) Phe-Ar
3.954 (2H; q) Pro-α, Phe-α	132.05 (m) Phe-Ar
7.165 (2H; d) Phe-Ar	135.71 (m) Phe-Ar
7.353 (2H; d) Phe-Ar	165.22 (s) Phe-C=O
8.183 (1H; d) Phe-NH)	168.89 (s) Pro-C=O

s = singlet, d = doublet, t = triplet, q = quartet, m = multiplet, dd = doublet of doublets

The Pro-β and Pro-γ protons of cyclo(D-Phe-4Cl-Pro) are non-equivalent as they resonated at 1.639 ppm, 1.806 ppm and 2.020 ppm indicating that the one β-proton and

one γ -proton are more shielded. The Pro- δ protons are also non-equivalent as they resonated at 3.236 ppm and 3.775 ppm indicating that the one δ -proton is more shielded. The Phe- β protons resonated at 2.907 ppm and 2.994 ppm. The Pro- α proton and Phe- α proton resonated at 3.954 ppm. The aromatic protons and Phe-NH resonated far downfield at 7.165 ppm, 7.353 ppm and 8.183 ppm respectively.

From the ^{13}C -NMR spectrum it can be seen that the Pro- α carbon resonated down field at 58.26 ppm compared with the Phe- α carbon which resonated at 57.80 ppm. The Pro- γ , Pro- β , Phe- β and Pro- δ carbons resonated at 21.87 ppm, 29.01 ppm, 38.94 ppm and 45.29 ppm respectively.

The carboxyl groups resonated far downfield at 165.22 ppm and 168.89 ppm respectively, while the aromatic carbons resonated downfield between 128.69 ppm and 135.71 ppm

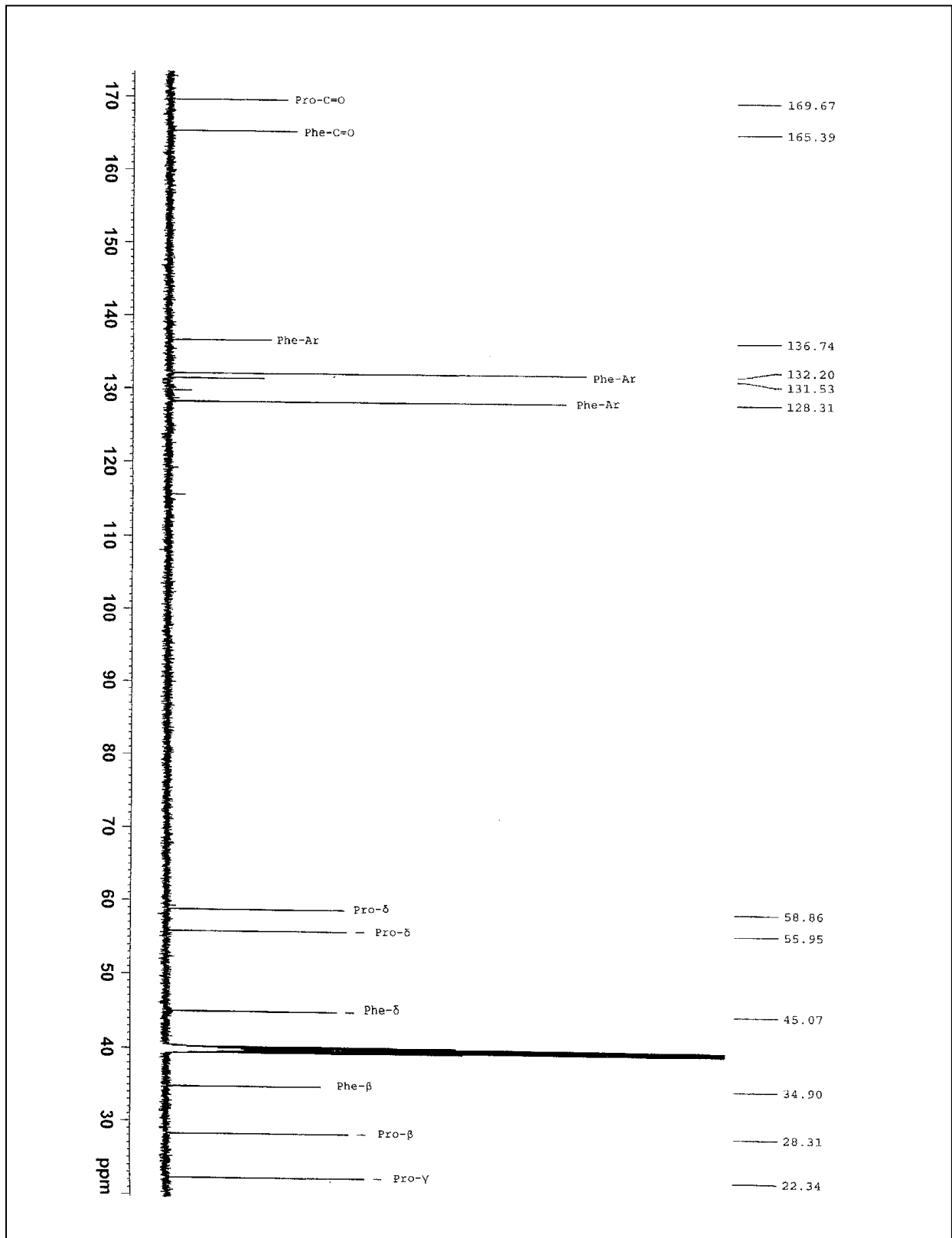


Figure 5.7 ^{13}C NMR spectrum of cyclo(Phe-4CL-Pro)

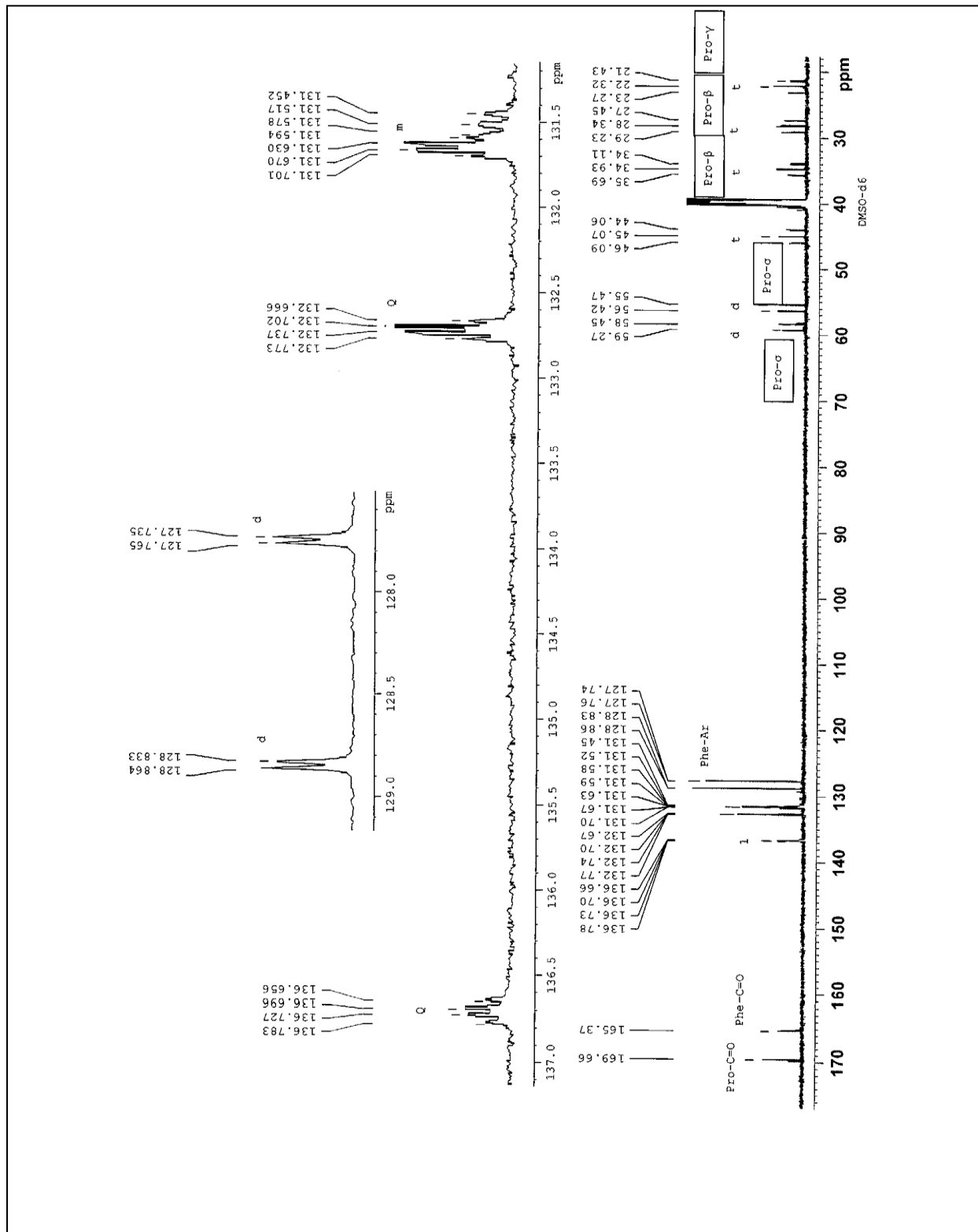


Figure 5.8 ^{13}C COUPLED spectrum of cyclo(Phe-4CL-Pro)

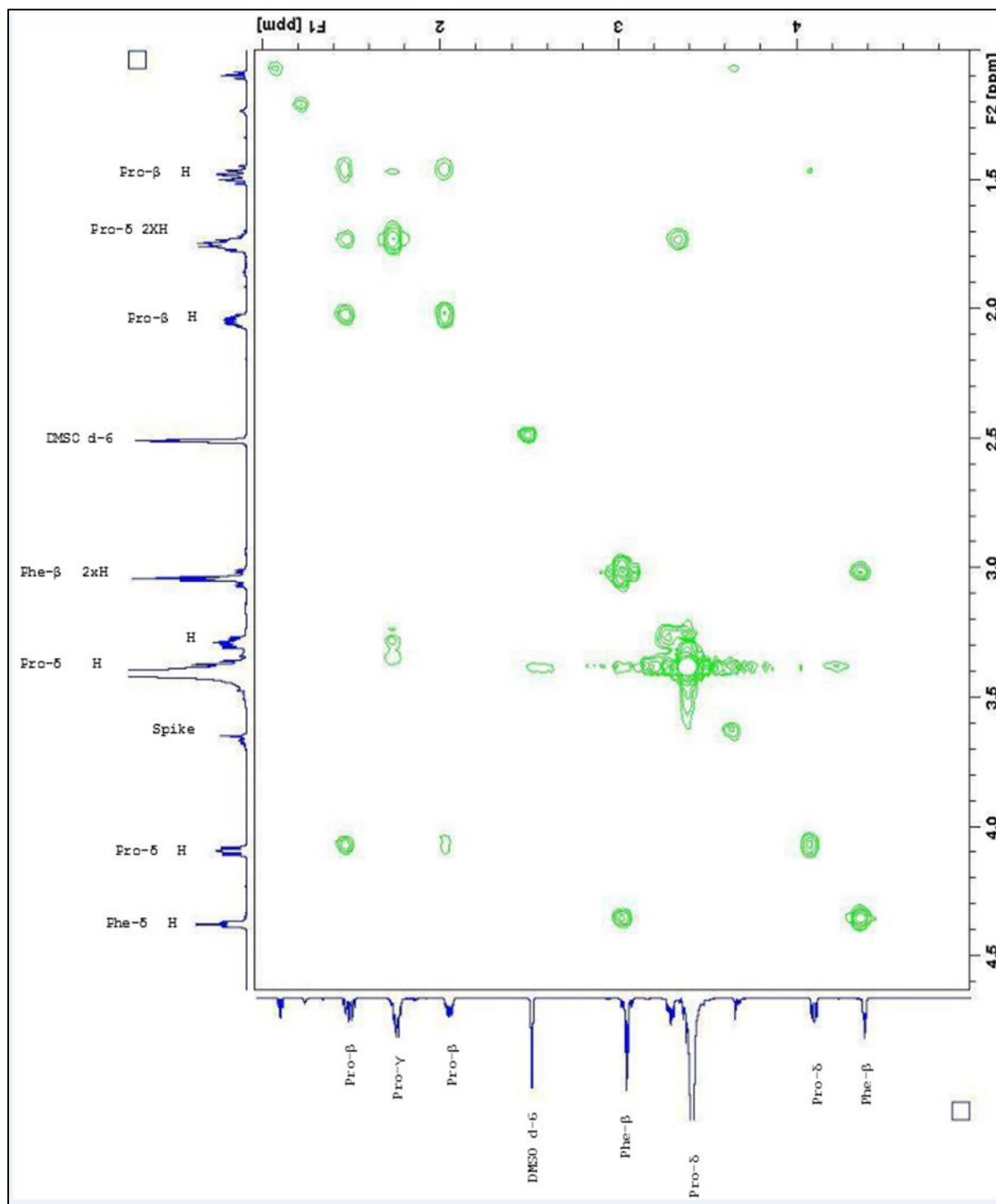


Figure 5.9 COSY spectrum of cyclo(Phe-4CL-Pro)

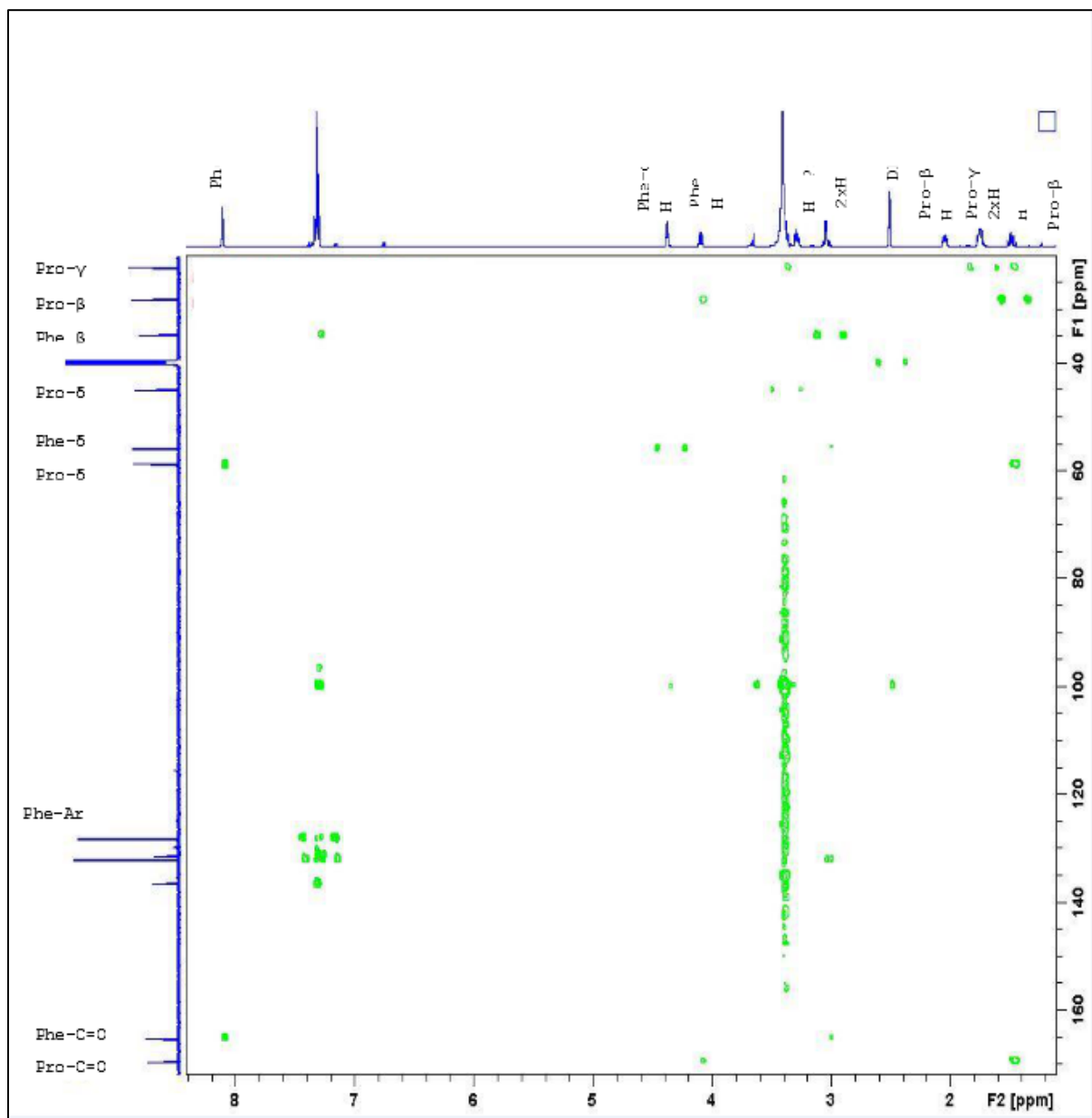


Figure 5.10 HMBCGP spectrum of cyclo(Phe-4CL-Pro)

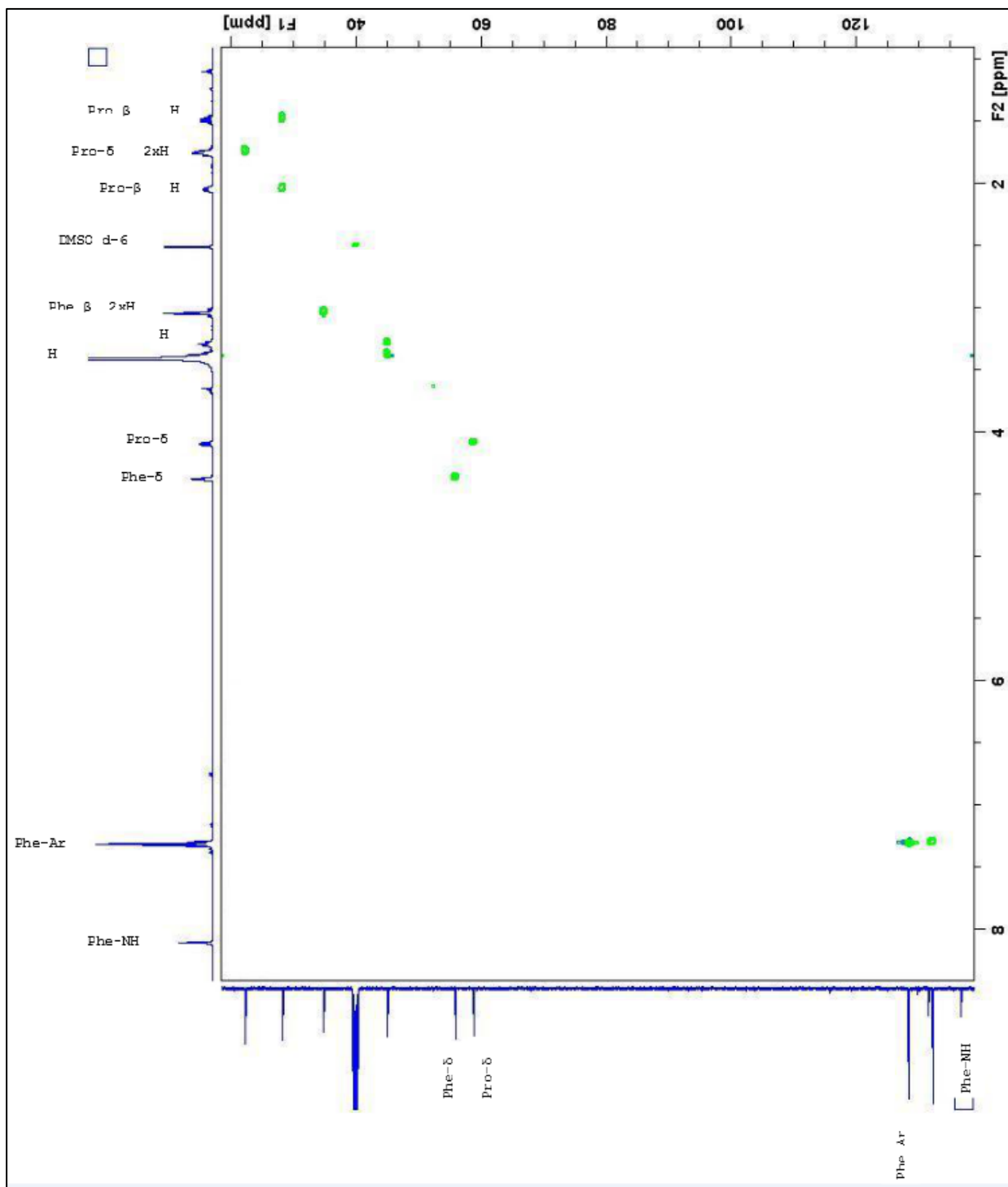


Figure 5.11 HSQC spectrum of cyclo(Phe-4CL-Pro)

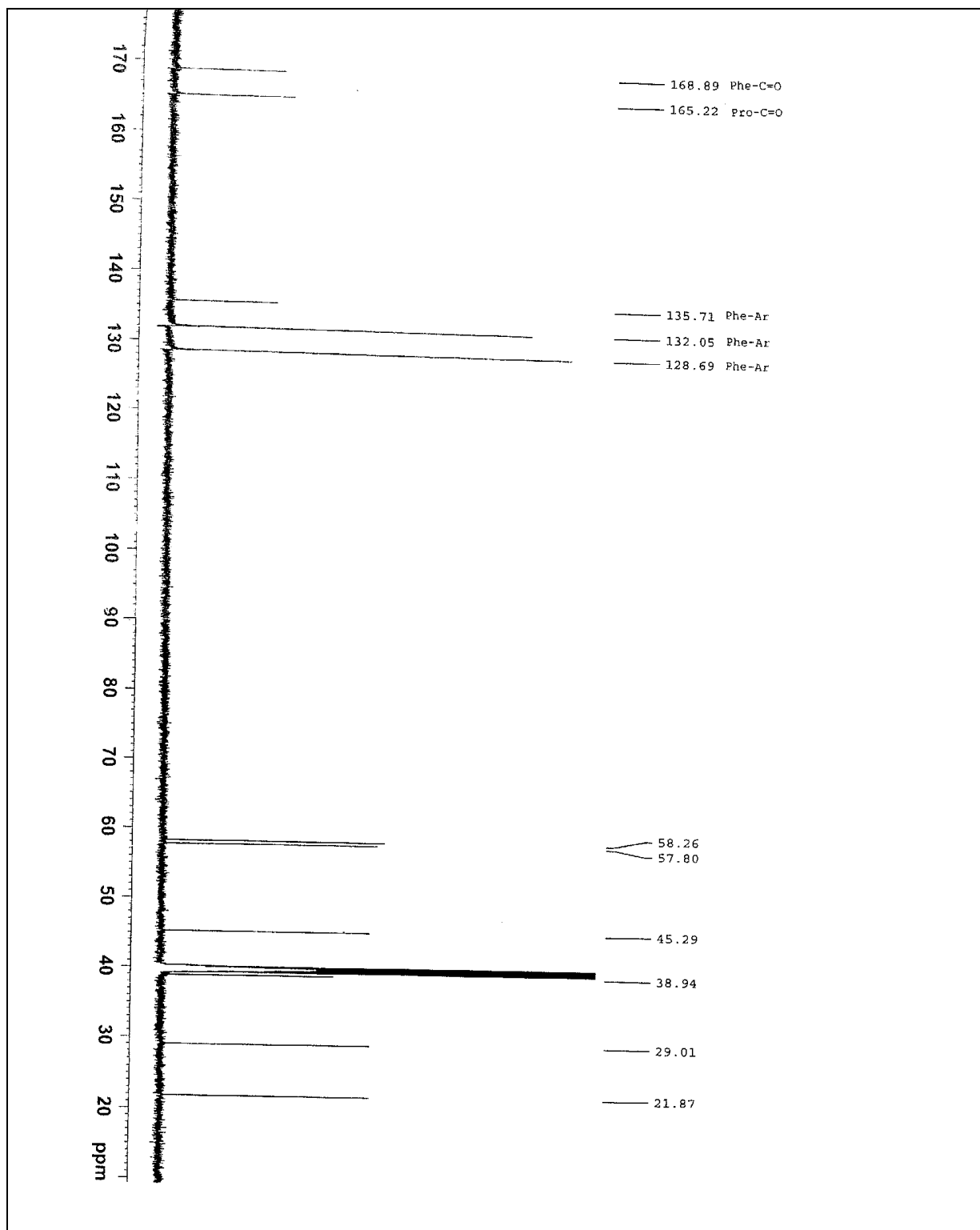


Figure 5.12 ¹³C NMR spectrum of cyclo(D-Phe-4CL-Pro)

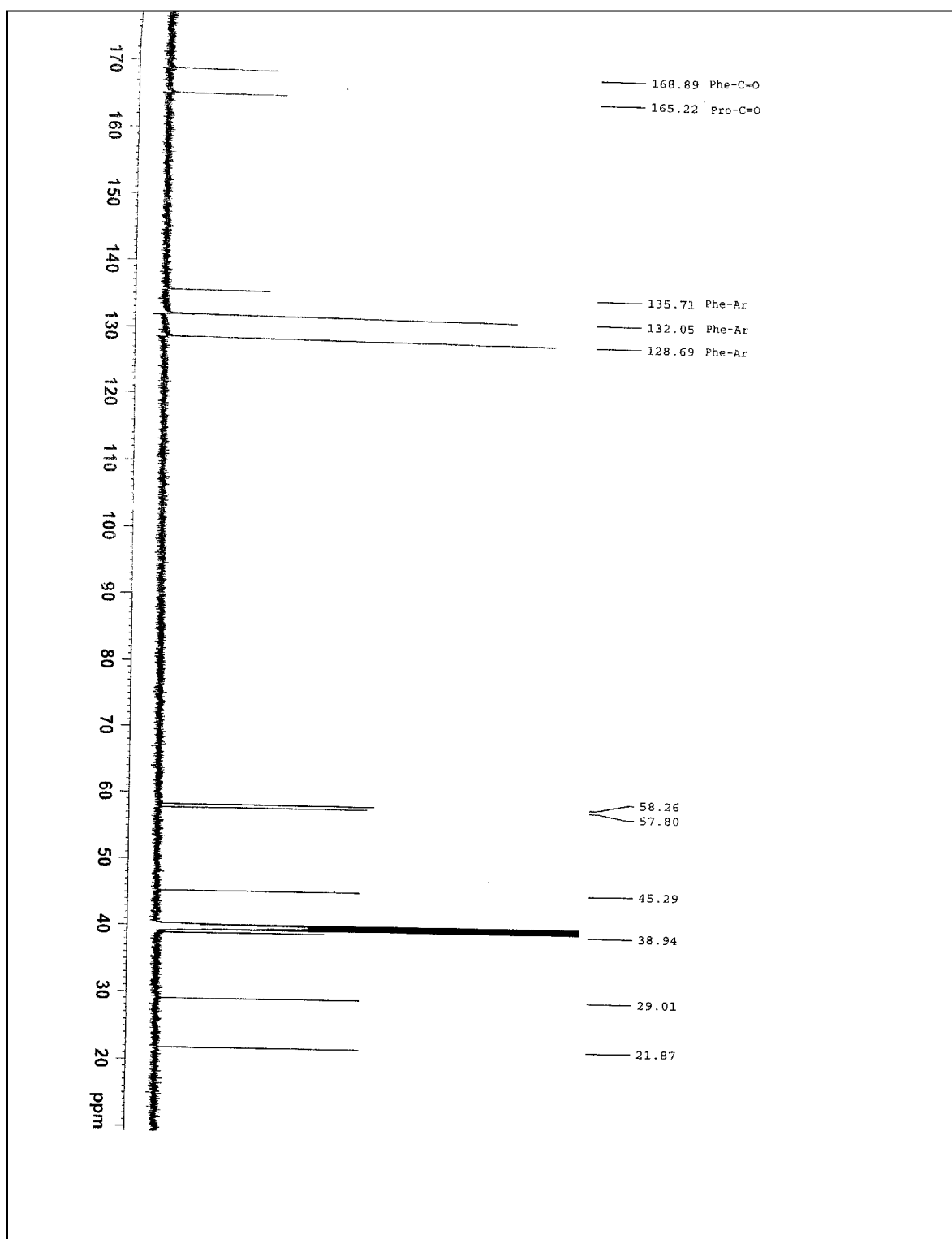


Figure 5.13 ^{13}C NMR spectrum of cyclo(D-Phe-4CL-Pro)

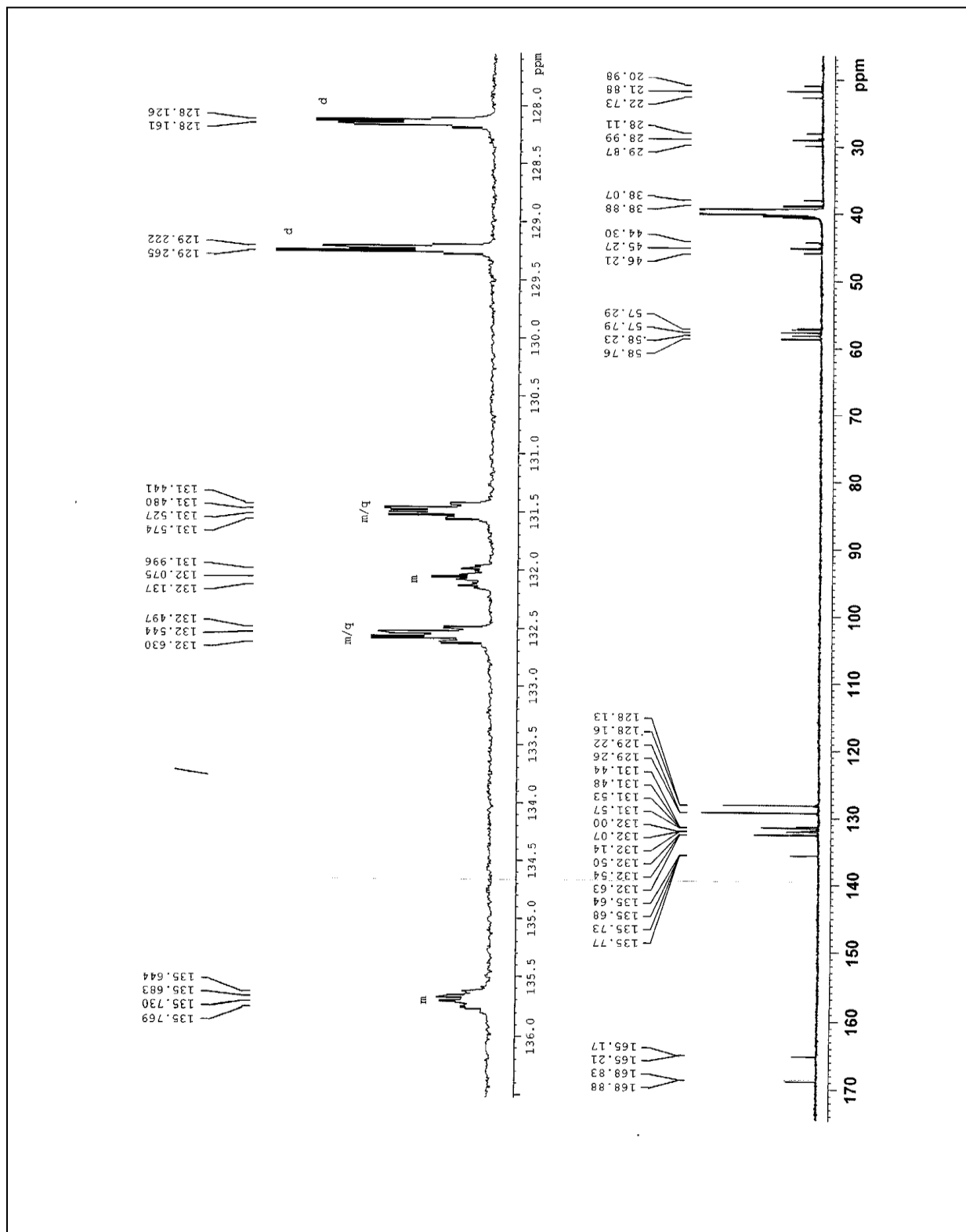


Figure 5.14 ^{13}C GD spectrum of cyclo(D-Phe-4CL-Pro)

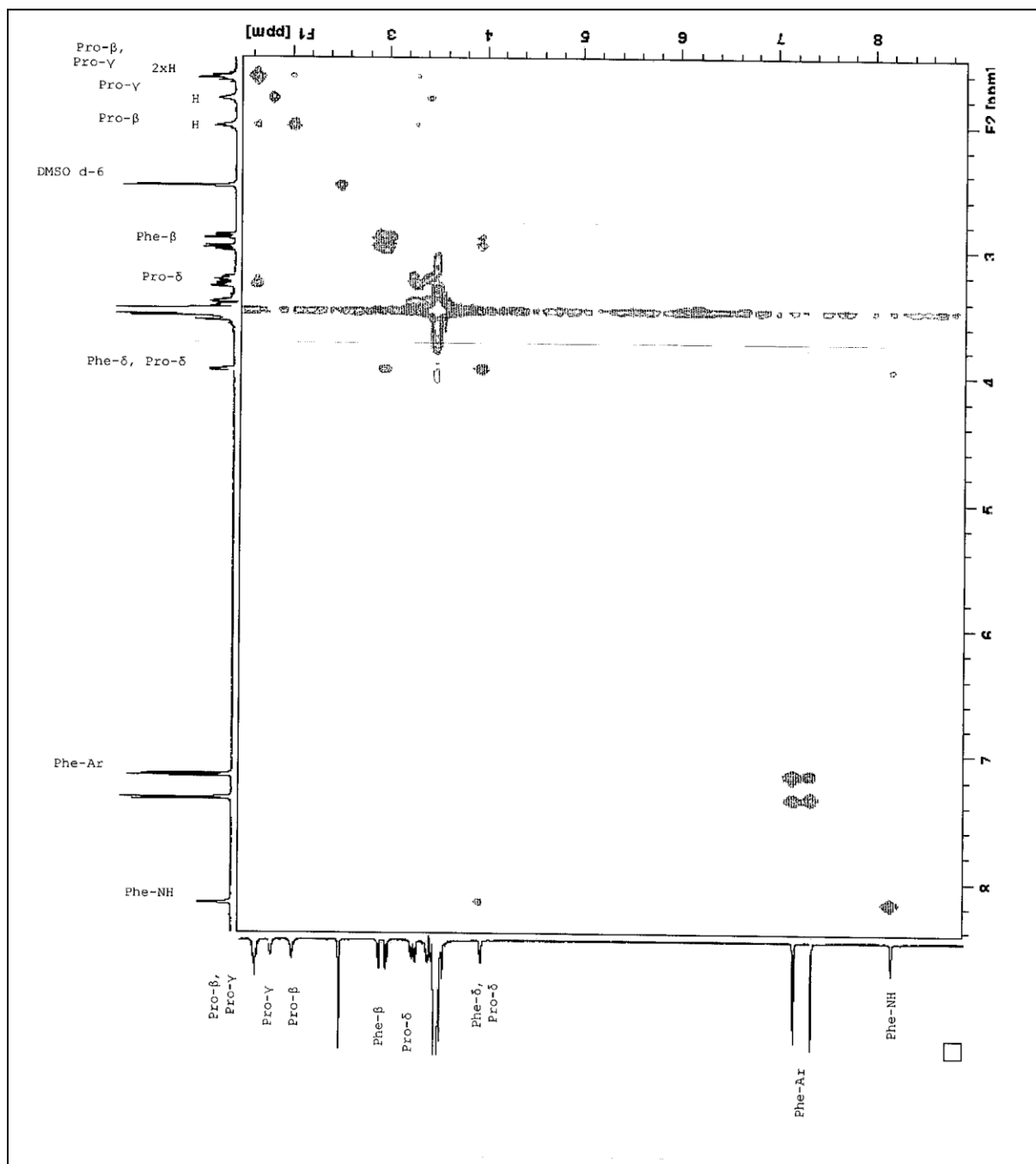


Figure 5.15 COSY spectrum of cyclo(D-Phe-4CL-Pro)

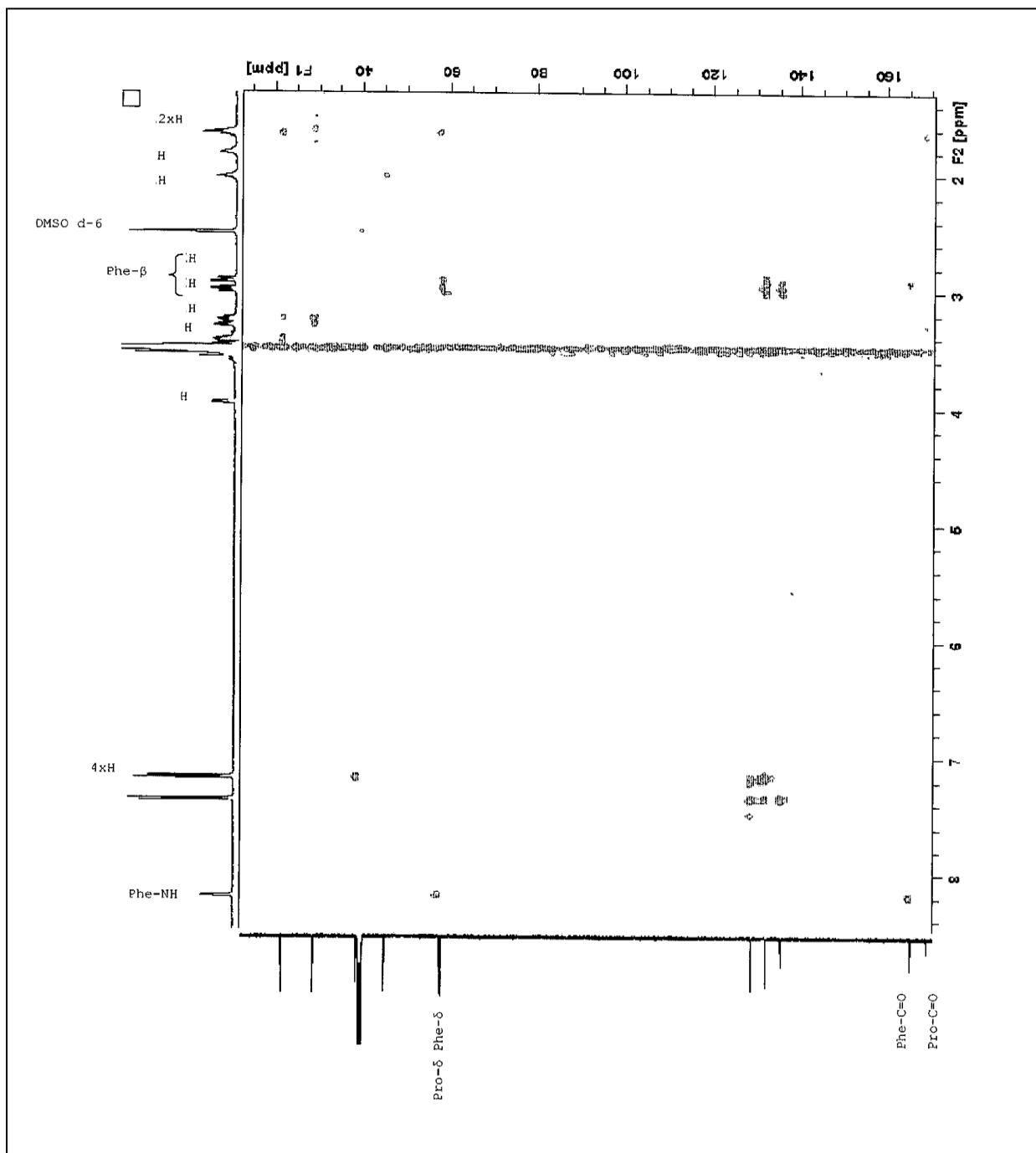


Figure 5.16 HMBCGP spectrum of cyclo(D-Phe-4CL-Pro)

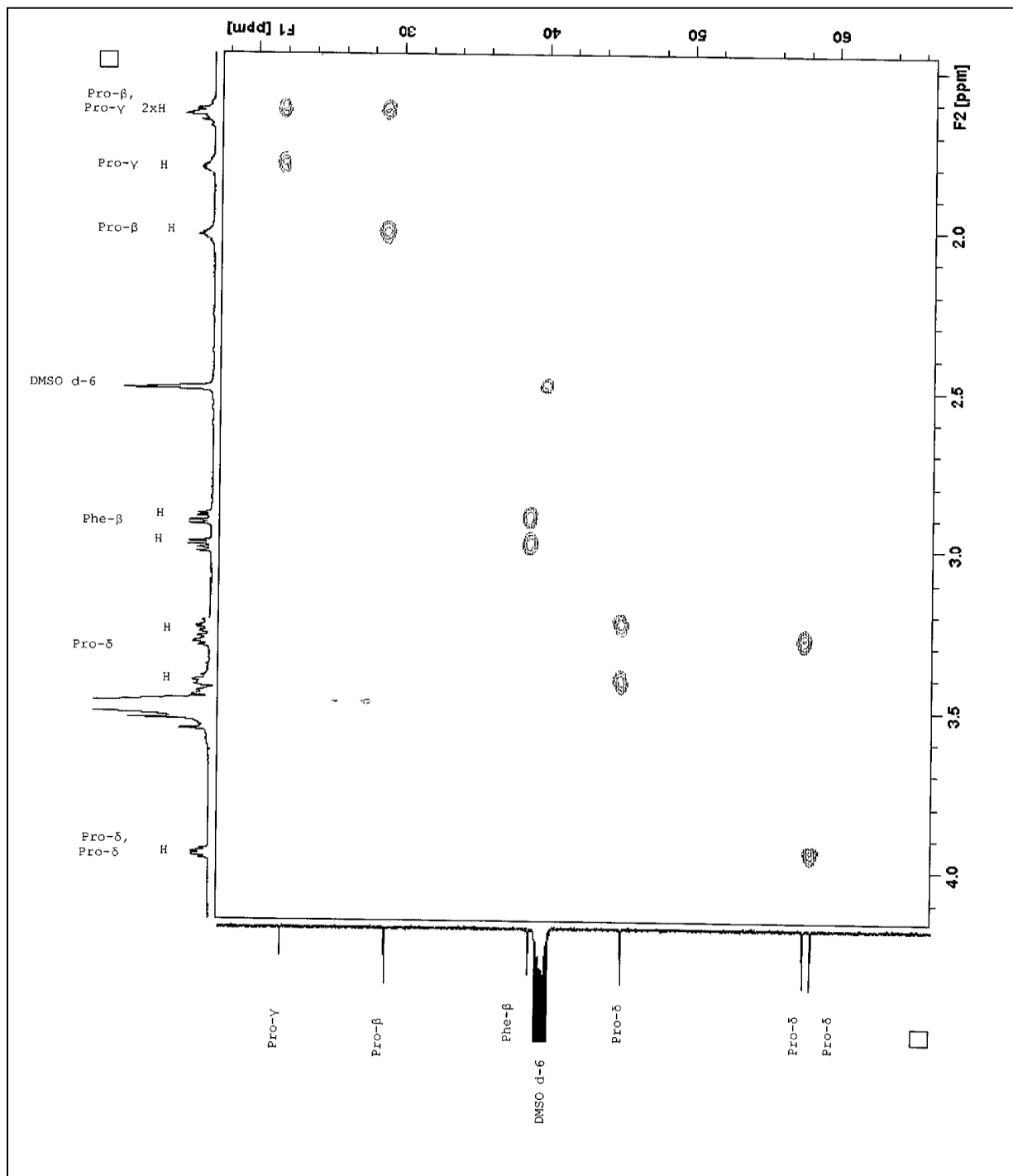


Figure 5.17 HSQC spectrum of cyclo(D-Phe-4CL-Pro)

5.4 Molecular modelling

5.4.1 Introduction

Pharmaceutical chemists today are facing numerous intricate challenges. The most demanding and rewarding one is the rational design of new therapeutic agents for treating human diseases (Cohen, 2007).

Recent scientific developments have changed the way pharmaceutical research produces new bio-active molecules. The traditional “trial and error” drug discovery processes are now slowly being replaced by structure based rational drug design. This includes the use of X-ray crystallography and NMR for the determination of the 3-dimensional structure of a target protein followed by various modelling techniques for the design of ligands that could interact with the target structure (Zsoldos *et al.*, 2003). Active conformation can be defined as the conformation, which a drug molecule adopts when bonding to either an enzyme or a receptor. This conformation is not necessarily the most energetically preferred one, but rather contains the correct spatial arrangement of all essential binding groups. Knowledge of the preferred conformation is nevertheless valuable as a means of explaining activity profiles and for the design of new analogues (Lucietto, 2004). The main challenge of structure based rational drug design is finding small molecular structures that bind strongly to a given protein due to steric and electrostatic complementarity and is readily available or easy to synthesise (Zsoldos *et al.*, 2003).

The difficulty lies in keeping equal focus on both the above-mentioned criteria. Two main approaches are used to overcome this problem, each prioritising one of the criteria over the other:

- Flexible docking of potential ligands from a database of 3-D structures of known compounds. Here the availability criterion is a given, since the considered structures are all available (or synthesisable).

- Build up complimentary structures from scratch-de novo design focused on generating the best possible fit to the constraints (Zsoldos *et al.*, 2003).

5.4.2 Methodology

The energetically favourable conformation distributions of cyclo(Phe-4Cl-Pro) and cyclo(D-Phe-4Cl-Pro) were elucidated by using Spartan'10[®] (Professional Version 1.10) computer molecular modelling software. Local minima conformations were obtained for each cyclic dipeptide by the use of molecular mechanics (AMBER force field) optimisation methods, due to the fact that it does not consider hydrogens explicitly (Wishart and Case, 2001).

The cyclic dipeptides cyclo(Phe-4Cl-Pro) and cyclo(D-Phe-4Cl-Pro) were initially built by using the amino acid database included in the Spartan'10[®] software. A step-wise approach to energy minimisation was then followed. Geometrical optimisation was achieved by an initial steepest-descent run, which was run for at least 200 cycles or until the root mean square (RMS) of $0.1 \text{ kcal.mol}^{-1}\text{\AA}^{-1}$ was achieved. Geometrical optimisation of the cyclic dipeptides was then followed by a PolakRibiere (Conjugated gradient) minimisation, which was done in repeated runs of 32560 cycles, until suitable low energy conformations with RMS of less than $0.001 \text{ kcal.mol}^{-1}\text{\AA}^{-1}$ was obtained. The conformational search was executed in order to identify the three lowest energy conformations, which could then be analysed to produce conclusions on the conformations of the cyclic dipeptides.

5.4.3 Results and discussion

The data for the three lowest energy conformers for each cyclic dipeptide are reported in Tables 5.4, 5.5, 5.6 and 5.7 respectively. The lower the heat of formation, or energy of the conformer, E (kJ/mol), the greater the stability of the conformer and thus the most likely to be found in nature, under standard conditions. The relative energy, Rel. E (kJ/mol), is calculated relative to the lowest energy conformer which is assigned a energy of 0 kJ/mol.

Table 5.4 Conformational search results calculated for cyclo(Phe-4Cl-Pro) in the gas phase

Conformer	Energy (kJ/mol)	Rel. E (kJ/mol)	Boltzmann Distribution
1	360.77	0	0.924
2	368.03	7.26	0.049
3	369.53	8.76	0.027

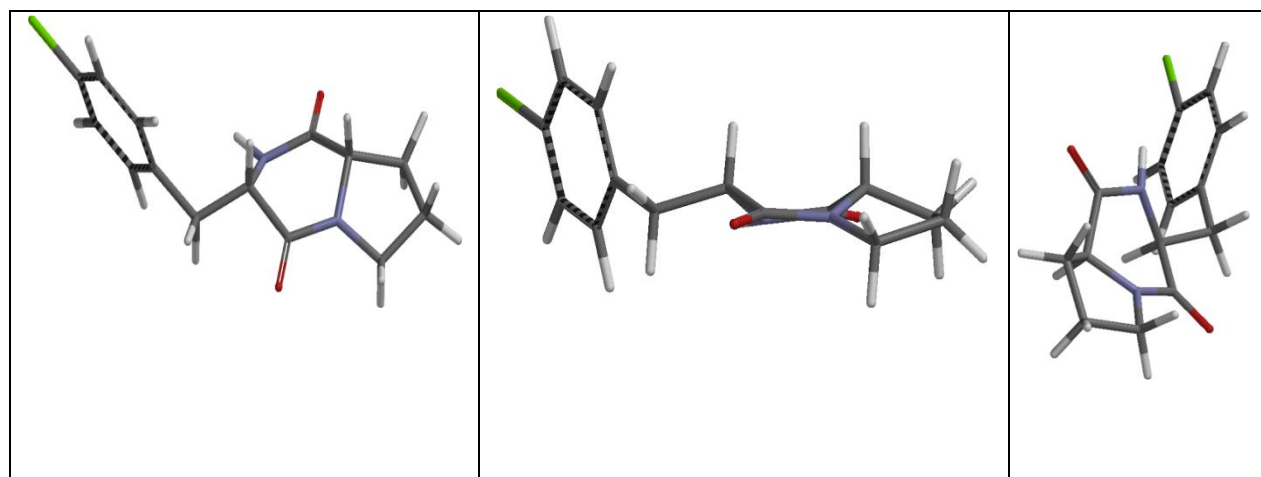


Figure 5.18 Conformation 1 of cyclo(Phe-4Cl-Pro) in the gas phase

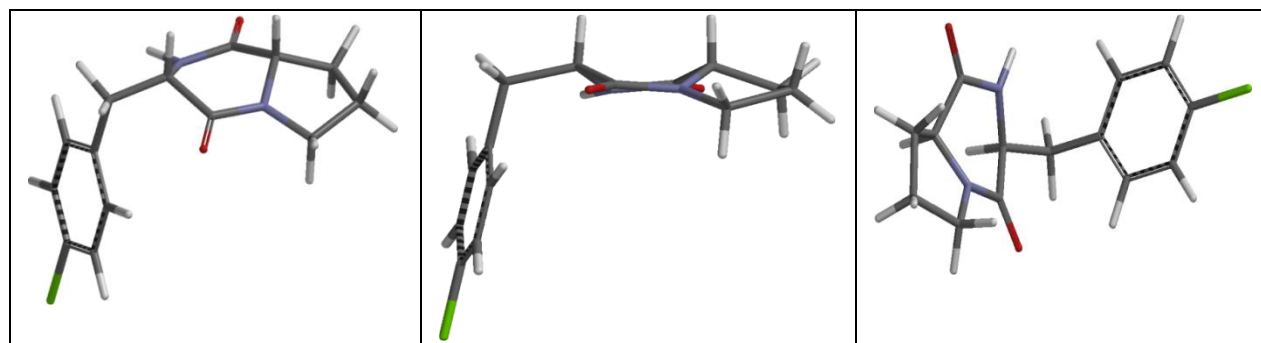


Figure 5.19 Conformation 2 of cyclo(Phe-4Cl-Pro) in the gas phase

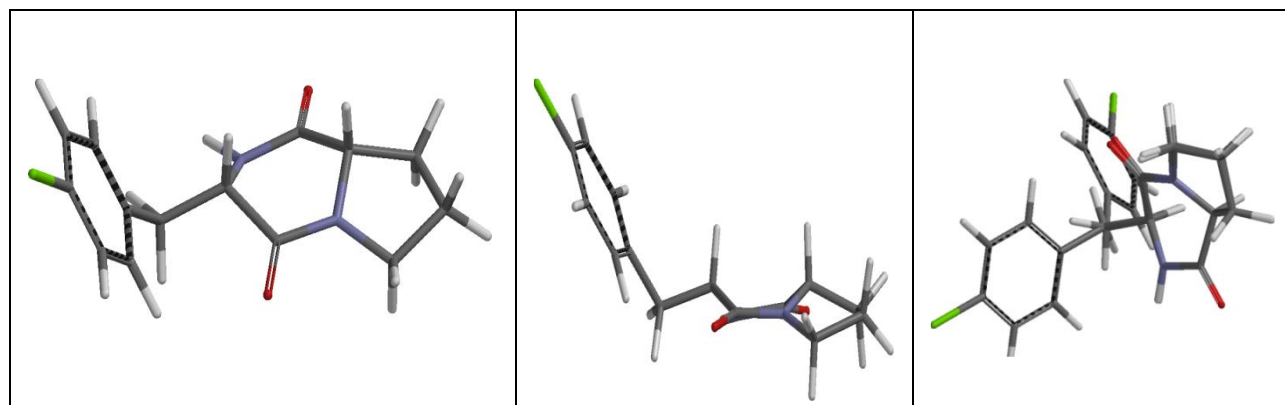


Figure 5.20 Conformation 3 of cyclo(Phe-4Cl-Pro) in the gas phase

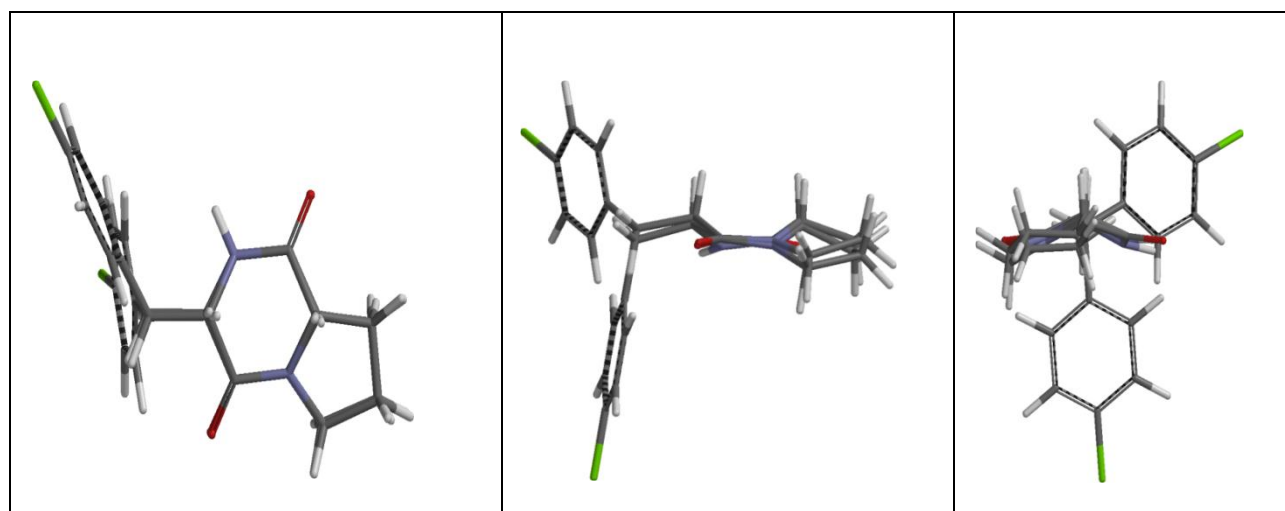


Figure 5.21 Overlay of conformation 1 and 2 of cyclo(Phe-4Cl-Pro) in the gas phase

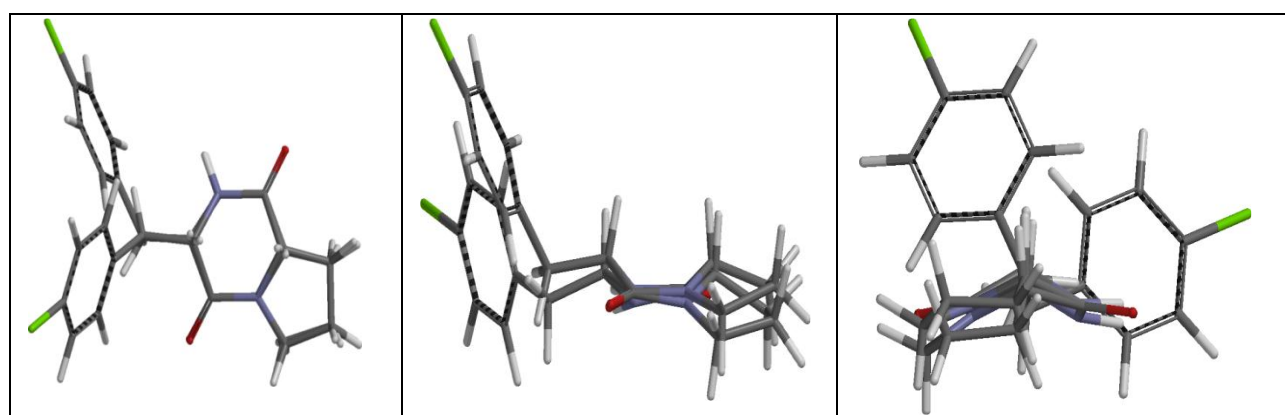


Figure 5.22 Overlay of conformation 1 and 3 of cyclo(Phe-4Cl-Pro) in the gas phase

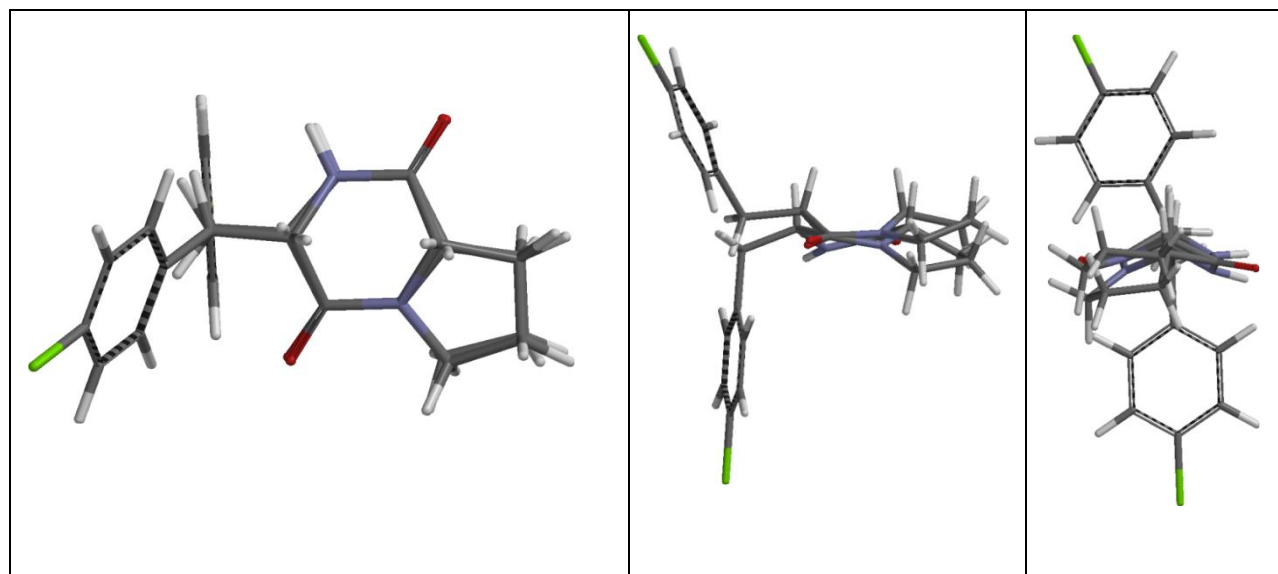


Figure 5.23 Overlay of conformation 2 and 3 of cyclo(Phe-4Cl-Pro) in the gas phase

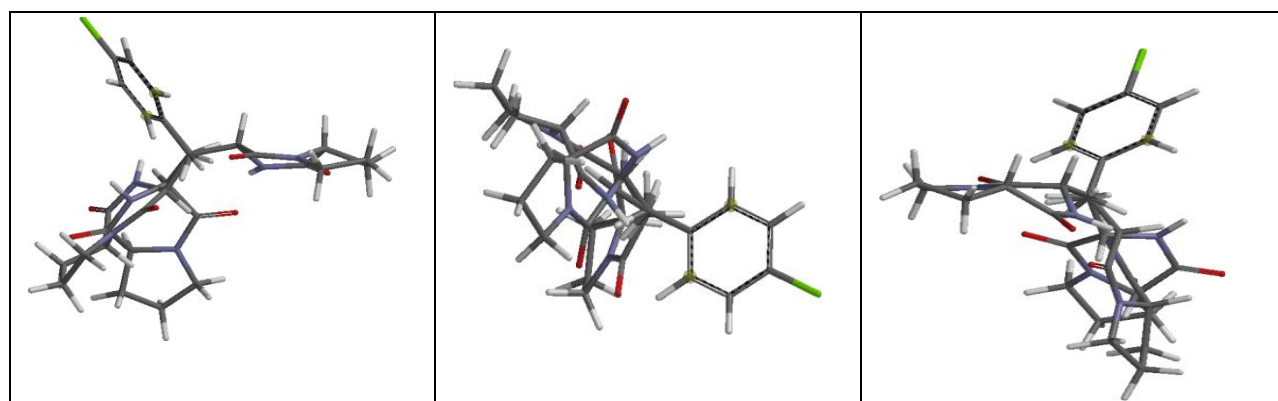


Figure 5.24 Overlay of conformation 1, 2 and 3 of cyclo(Phe-4Cl-Pro) in the gas phase

Table 5.5 Conformational search results calculated for cyclo(D-Phe-4Cl-Pro) in the gas phase

Conformer	Energy (kJ/mol)	Rel. E (kJ/mol)	Boltzmann Distribution
1	0	365.03	0.814
2	3.88	368.91	0.17
3	9.76	374.8	0.016

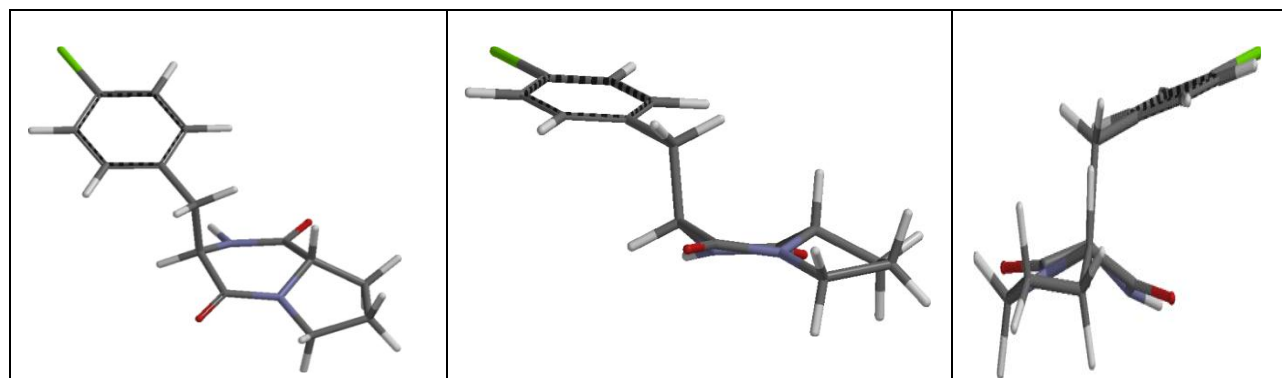


Figure 5.25 Conformation 1 of cyclo(D-Phe-4Cl-Pro) in the gas phase

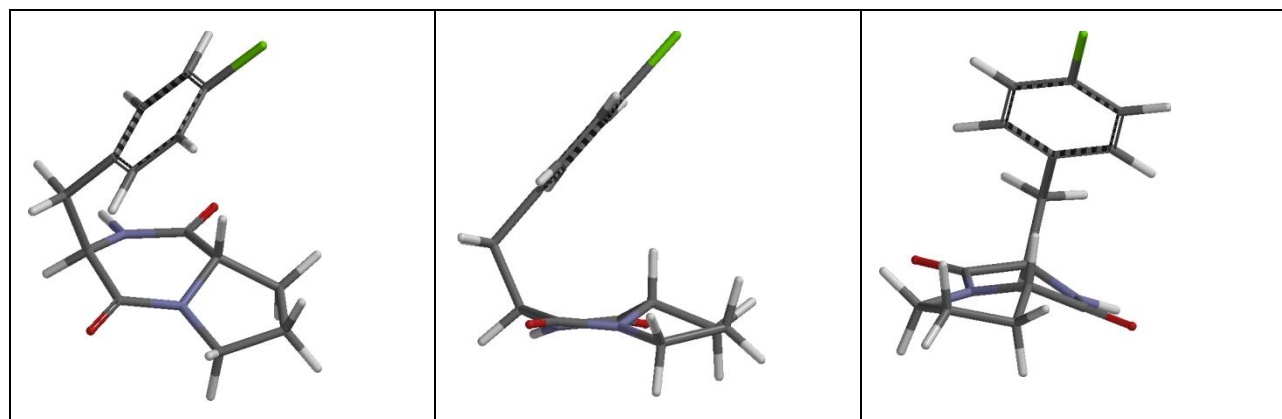


Figure 5.26 Conformation 2 of cyclo(D-Phe-4Cl-Pro) in the gas phase

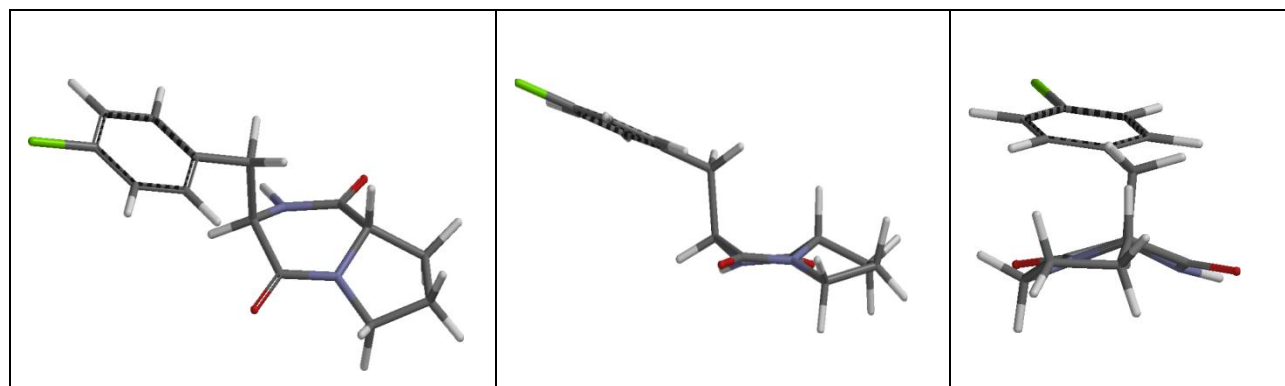


Figure 5.27 Conformation 3 of cyclo(D-Phe-4Cl-Pro) in the gas phase

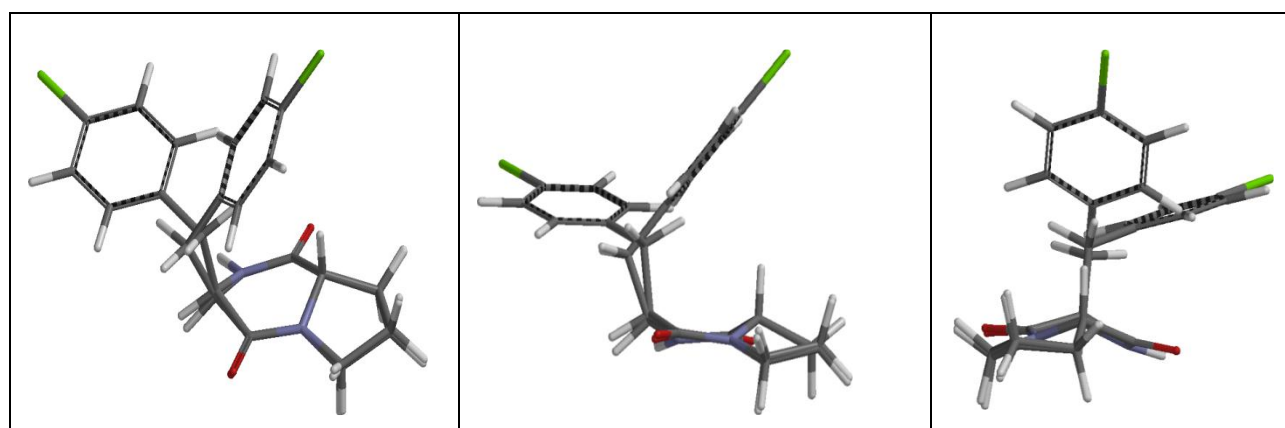


Figure 5.28 Overlay of conformation 1 and 2 of cyclo(D-Phe-4Cl-Pro) in the gas phase

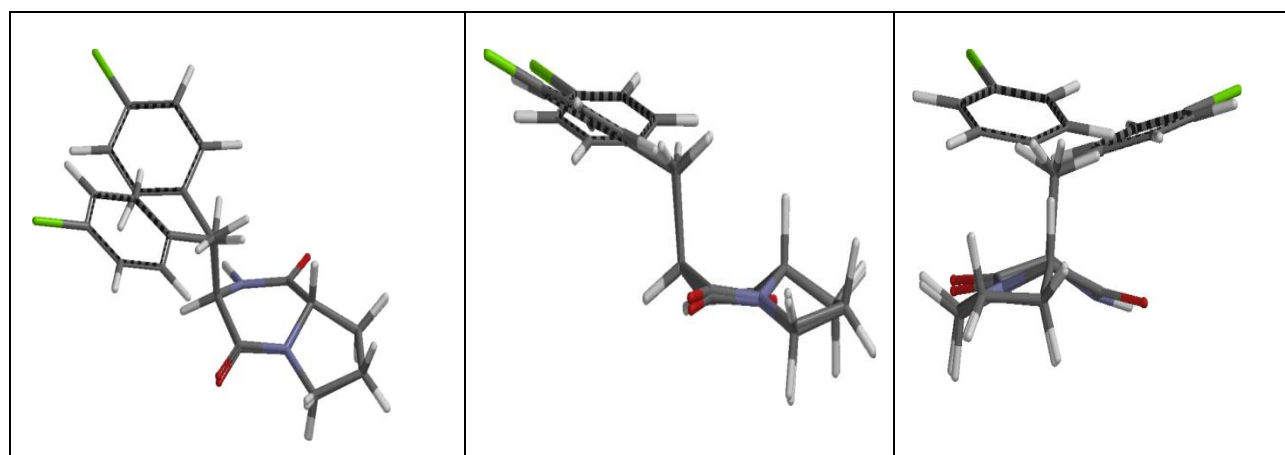


Figure 5.29 Overlay of conformation 1 and 3 of cyclo(D-Phe-4Cl-Pro) in the gas phase



Figure 5.30 Overlay of Conformation 2 and 3 of cyclo(D-Phe-4Cl-Pro) in the gas phase

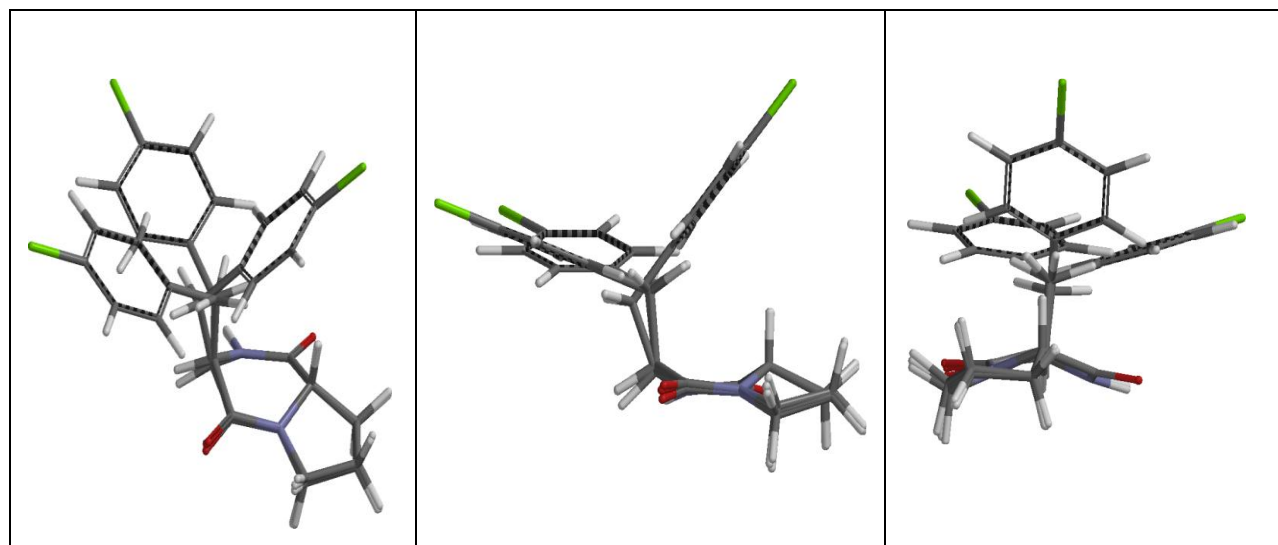


Figure 5.31 Overlay of conformation 1, 2 and 3 of cyclo(D-Phe-4Cl-Pro) in the gas phase

Table 5.6 Conformational search results calculated for cyclo(Phe-4Cl-Pro) in the solvated (water) phase

Conformer	Energy (kJ/mol)	Rel. E (kJ/mol)	Boltzmann Distribution
1	287.86	0	0.942
2	296.19	8.33	0.033
3	296.84	8.98	0.025

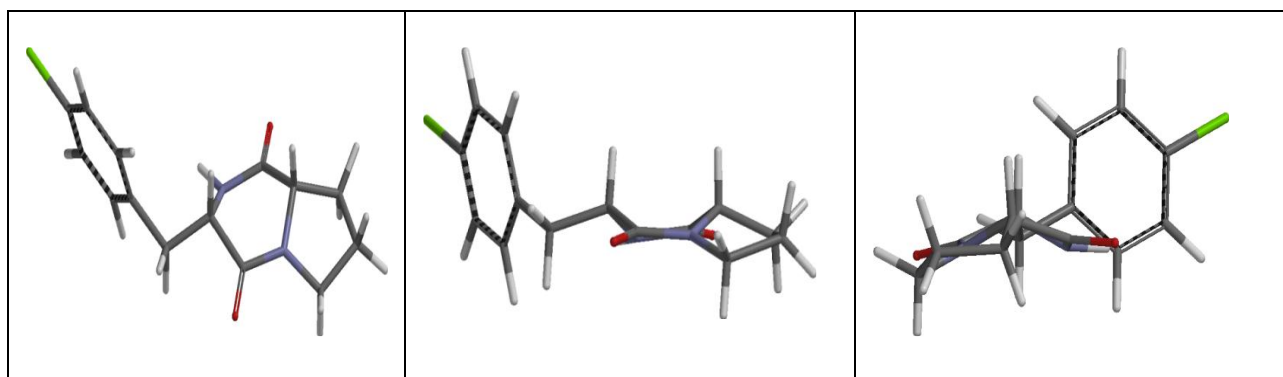


Figure 5.32 Conformation 1 of cyclo(Phe-4Cl-Pro) in the solvated (water) phase

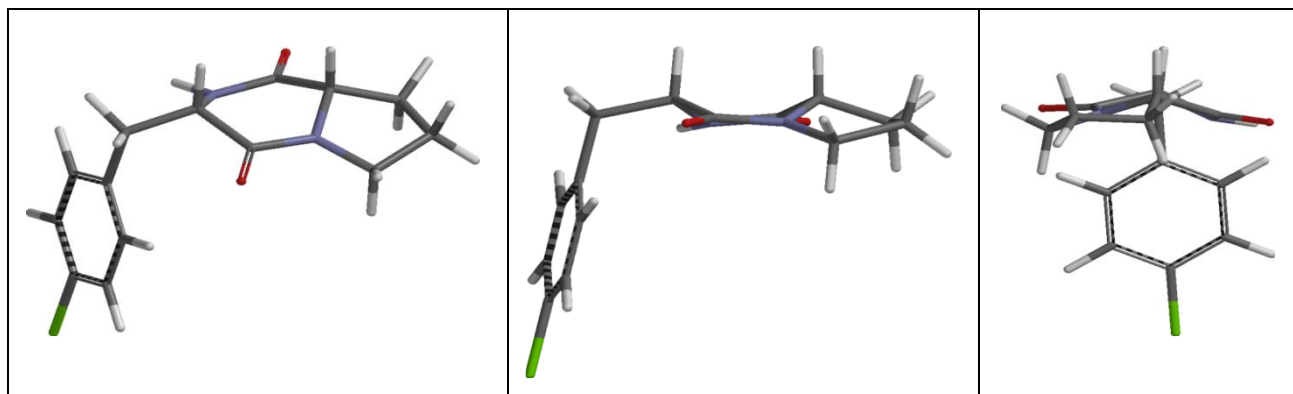


Figure 5.33 Conformation 2 of cyclo(Phe-4Cl-Pro) in the solvated (water) phase

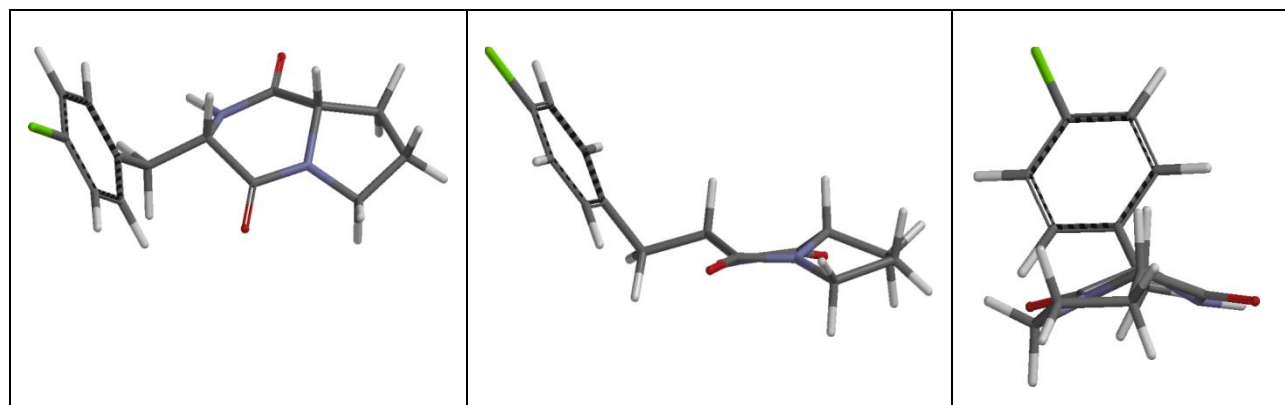


Figure 5.34 Conformation 3 of cyclo(Phe-4Cl-Pro) in the solvated (water) phase

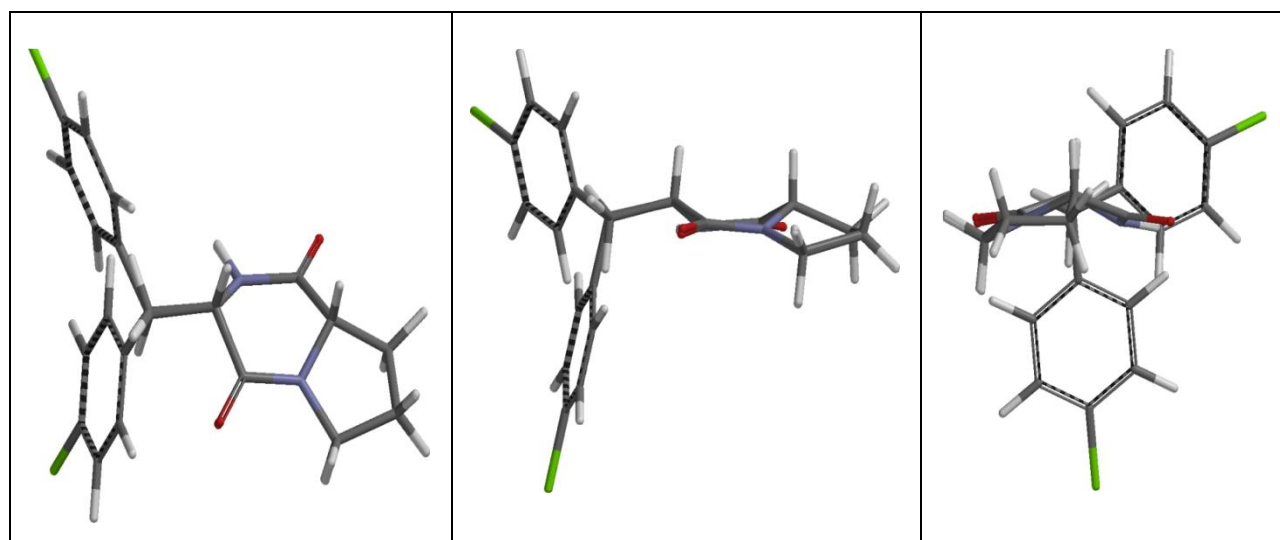


Figure 5.35 Overlay of conformation 1 and 2 of cyclo(Phe-4Cl-Pro) in the solvated (water) phase

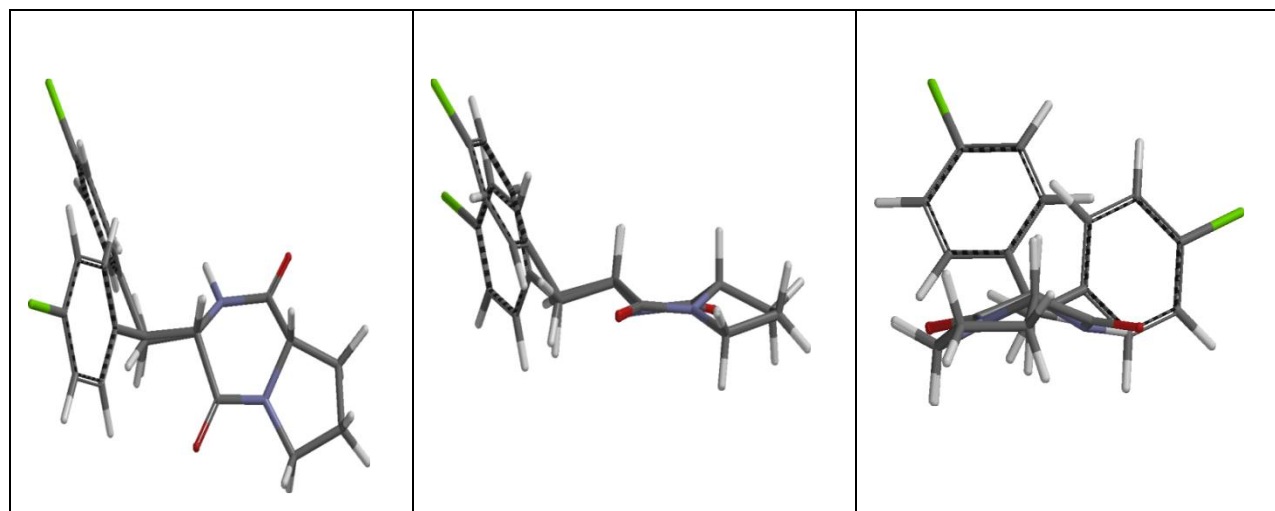


Figure 5.36 Overlay of conformation 1 and 3 of cyclo(Phe-4Cl-Pro) in the solvated (water) phase

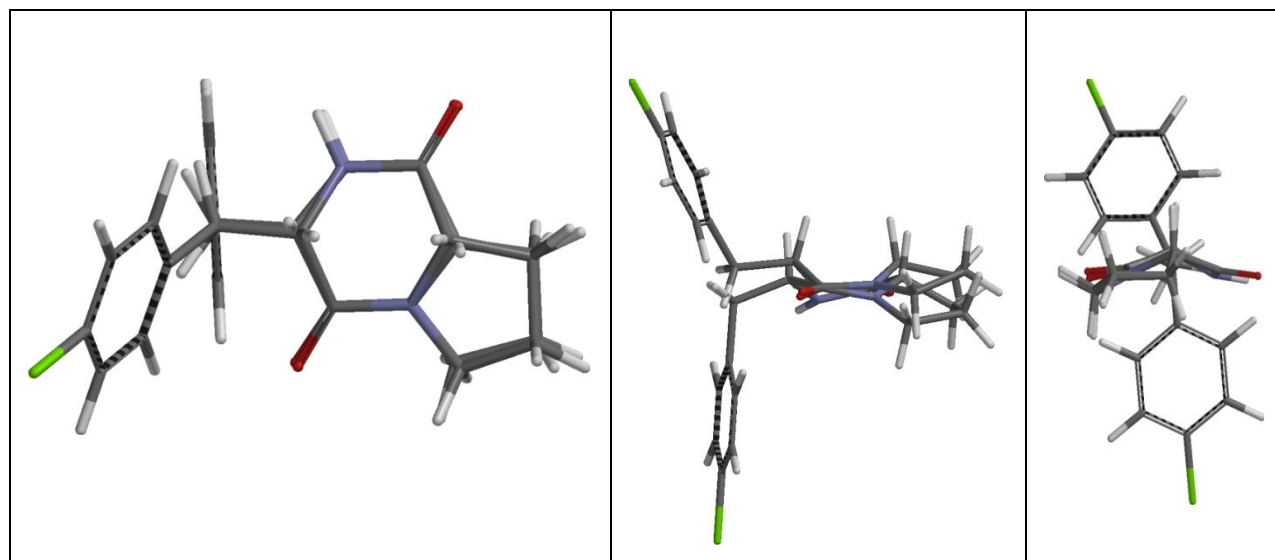


Figure 5.37 Overlay of Conformation 2 and 3 of cyclo(Phe-4Cl-Pro) in the solvated (water) phase

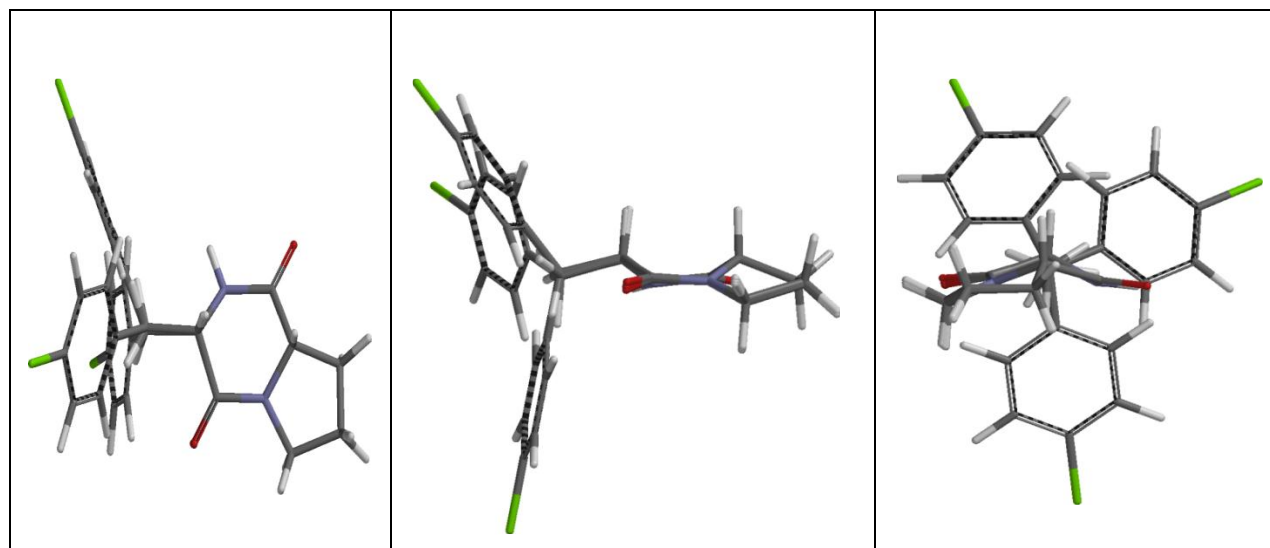


Figure 5.38 Overlay of Conformation 1, 2 and 3 of cyclo(Phe-4Cl-Pro) in the solvated (water) phase

Table 5.7 Conformational search results calculated for cyclo(D-Phe-4Cl-Pro) in the solvated (water) phase

Conformer	Energy (kJ/mol)	Rel. E (kJ/mol)	Boltzmann Distribution
1	291.37	0	0.791
2	294.83	3.46	0.916
3	301.54	10.16	0.013

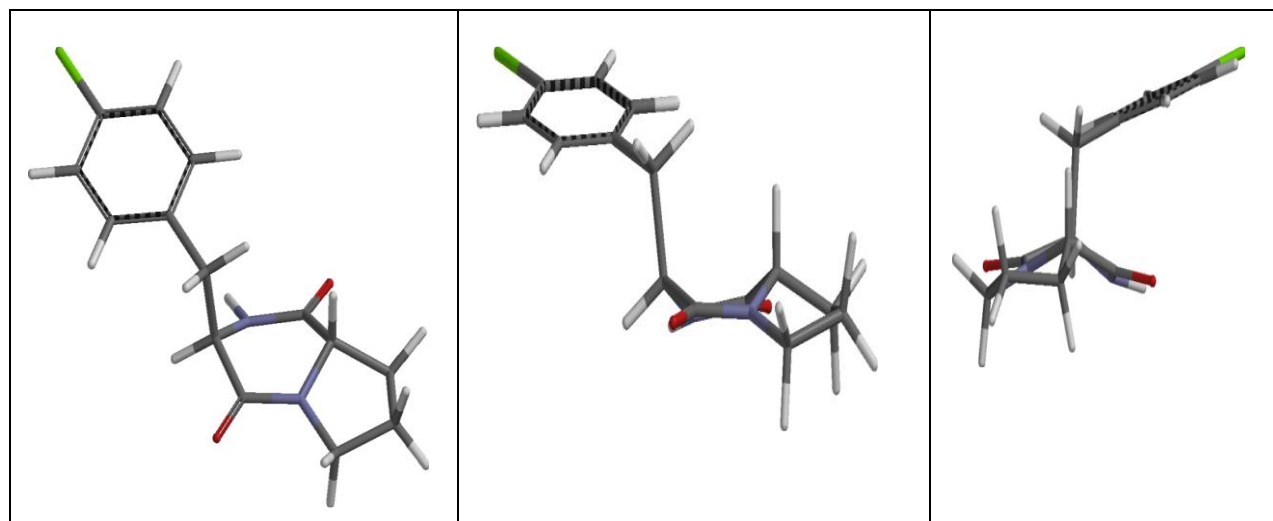


Figure 5.39 Conformation 1 of cyclo(D-Phe-4Cl-Pro) in the solvated (water) phase

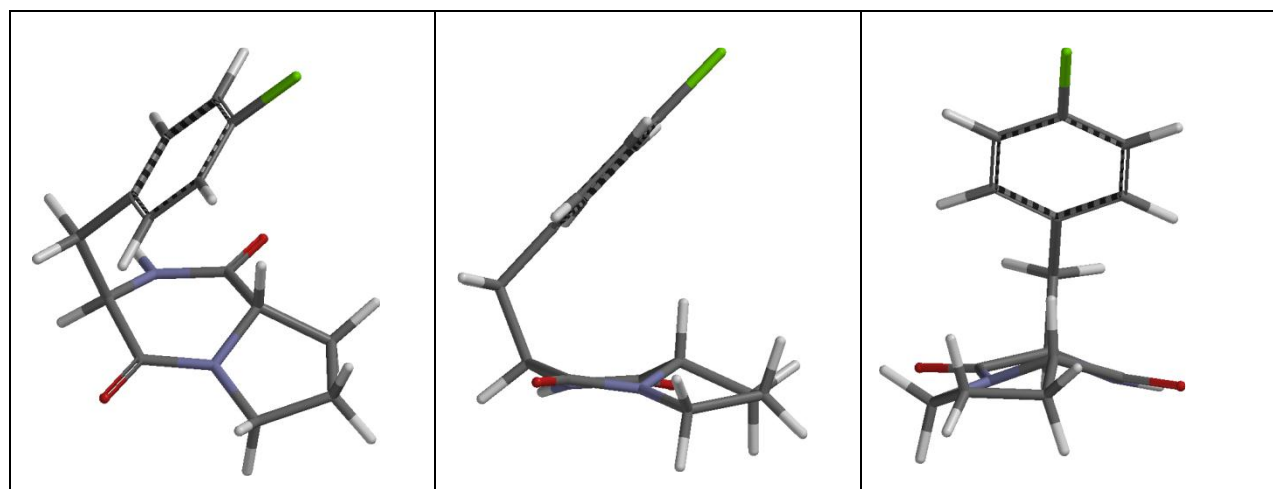


Figure 5.40 Conformation 2 of cyclo(D-Phe-4Cl-Pro) in the solvated (water) phase

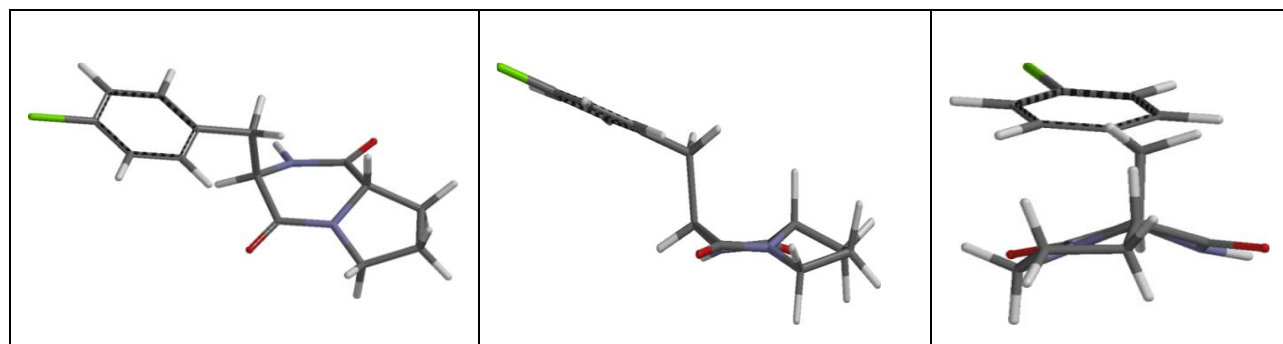


Figure 5.41 Conformation 3 of cyclo(D-Phe-4Cl-Pro) in the solvated (water) phase

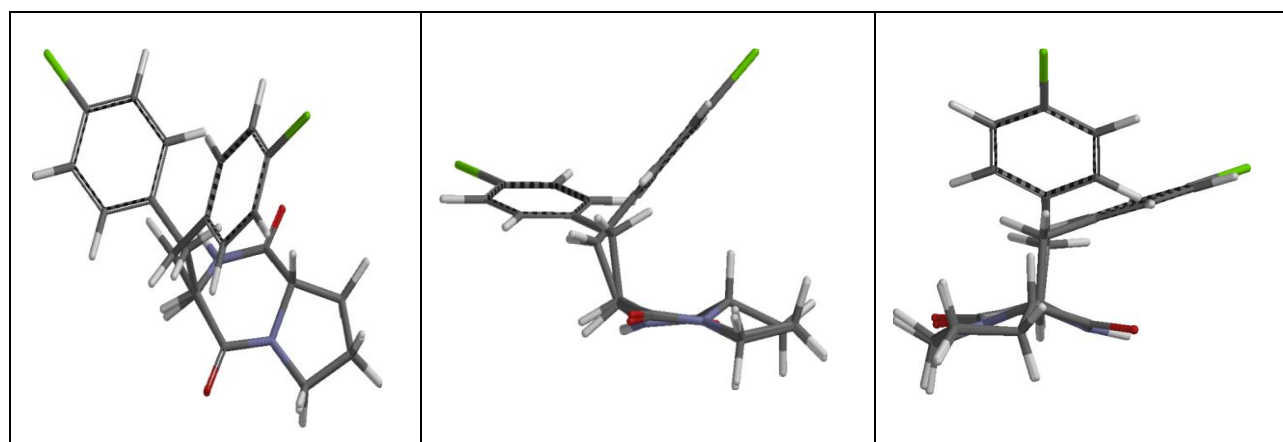


Figure 5.42 Overlay of conformation 1 and 2 of cyclo(D-Phe-4Cl-Pro) in the solvated (water) phase

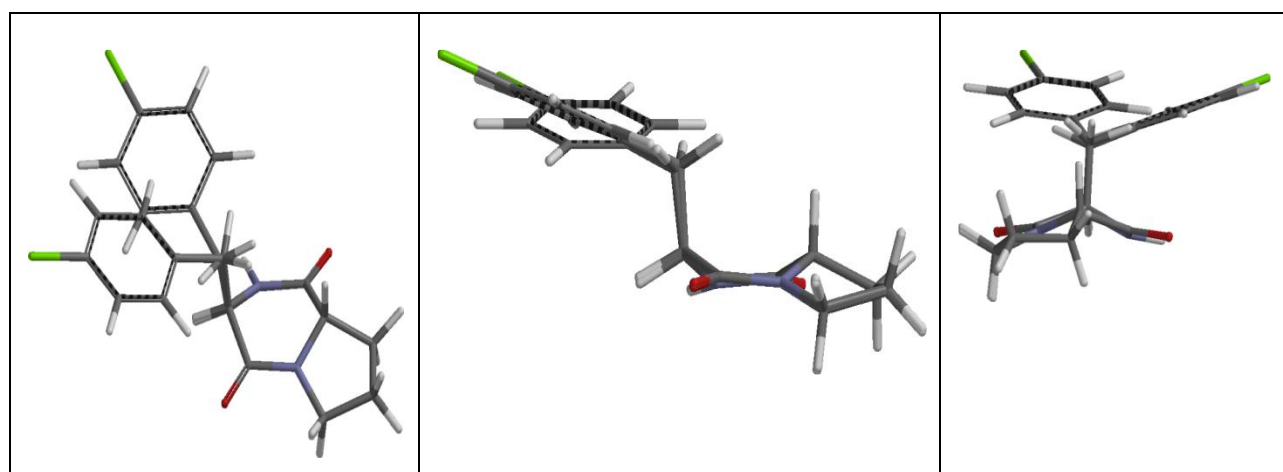


Figure 5.43 Overlay of Conformation 1 and 3 of cyclo(D-Phe-4Cl-Pro) in the solvated (water) phase

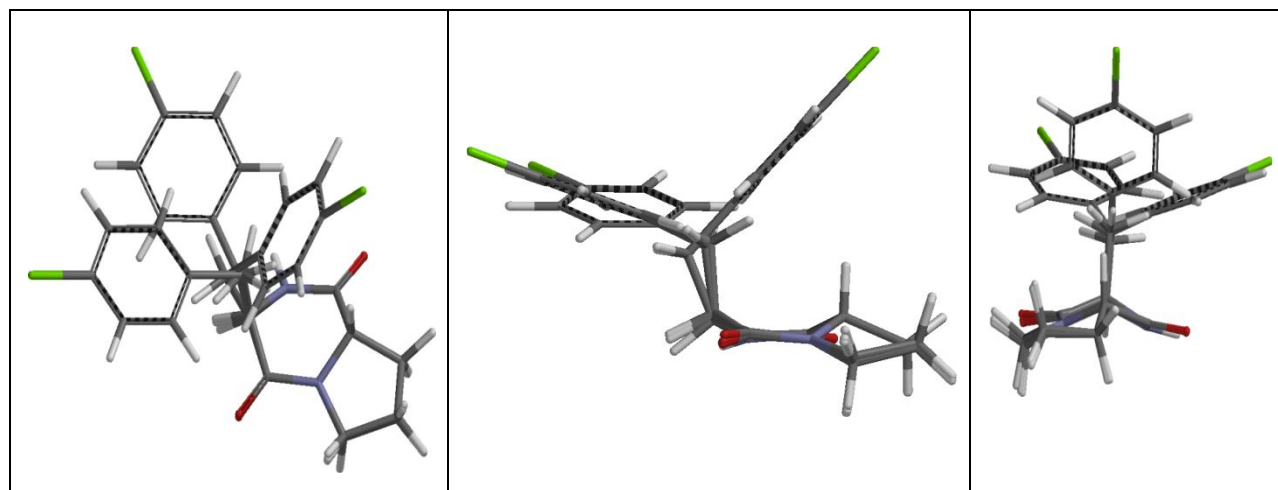


Figure 5.44 Overlay of Conformation 2 and 3 of cyclo(D-Phe-4Cl-Pro) in the solvated (water) phase

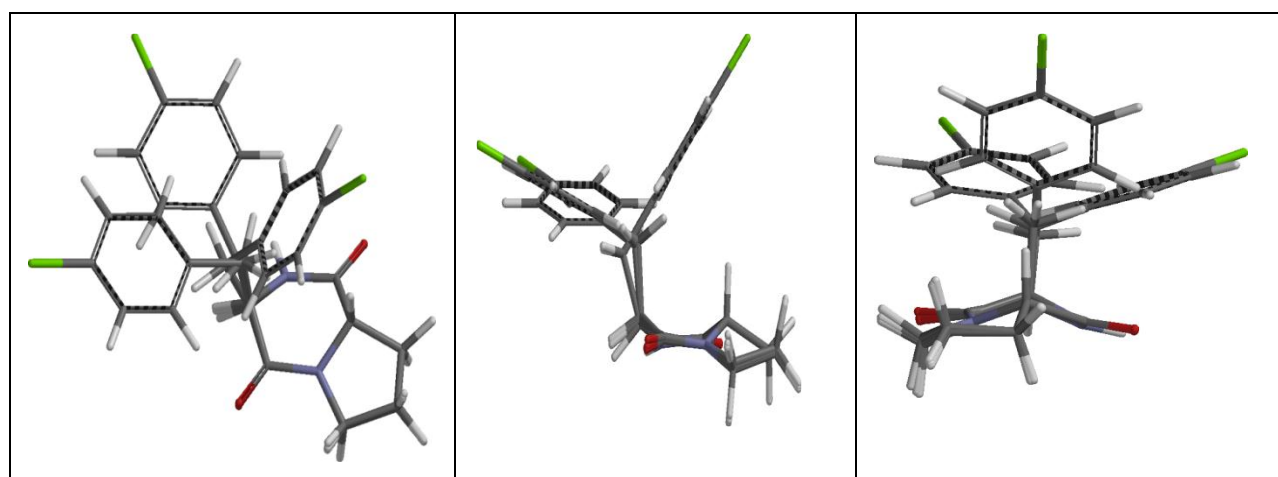


Figure 5.45 Overlay of Conformation 1, 2 and 3 of cyclo(D-Phe-4Cl-Pro) in the solvated (water) phase

Table 5.8 Conformational search results calculated for cyclo(Phe-4Cl-Pro) in dimethyl sulphoxide (DMSO)

Conformer	Energy (kJ/mol)	Rel. E (kJ/mol)	Boltzmann Distribution
1	-3315302.5	0	0.648
2	-3315300.02	2.49	0.238
3	-3315298.2	4.3	0.114

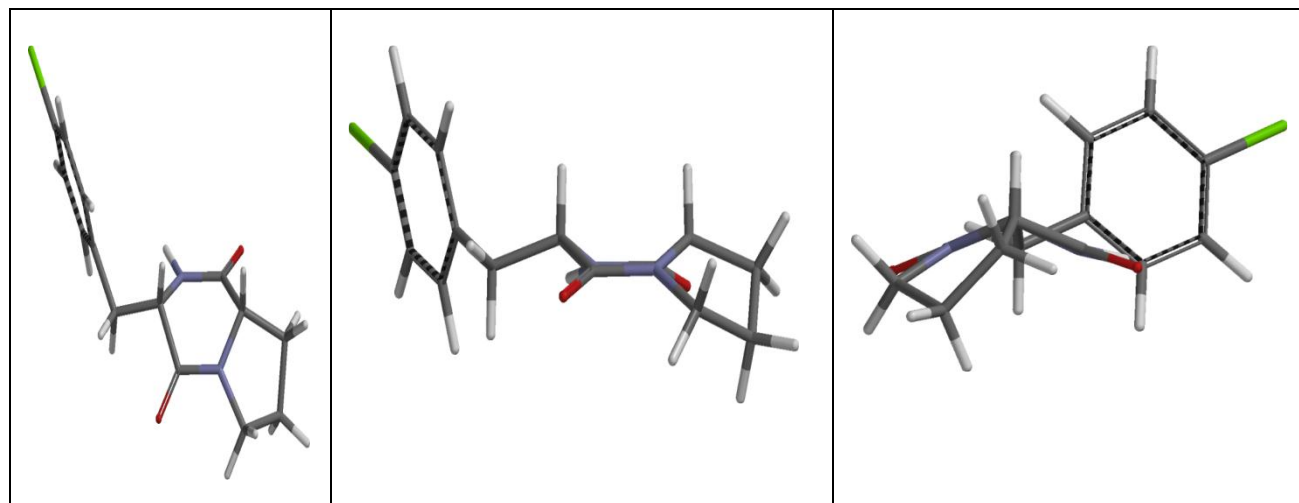


Figure 5.46 Conformation 1 of cyclo(Phe-4Cl-Pro) in DMSO

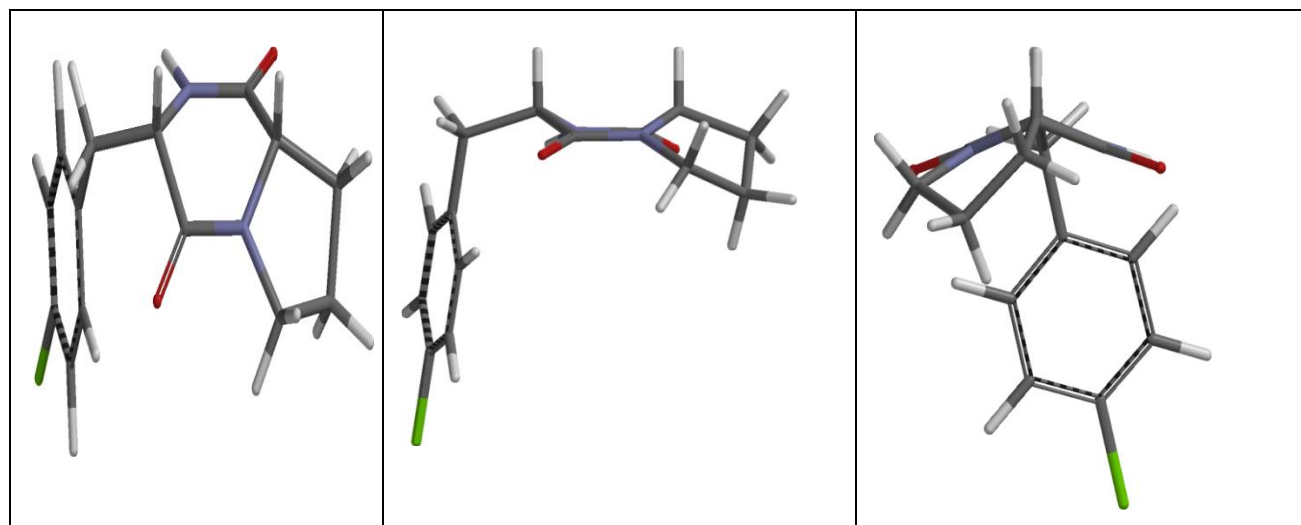


Figure 5.47 Conformation 2 of cyclo(Phe-4Cl-Pro) in DMSO

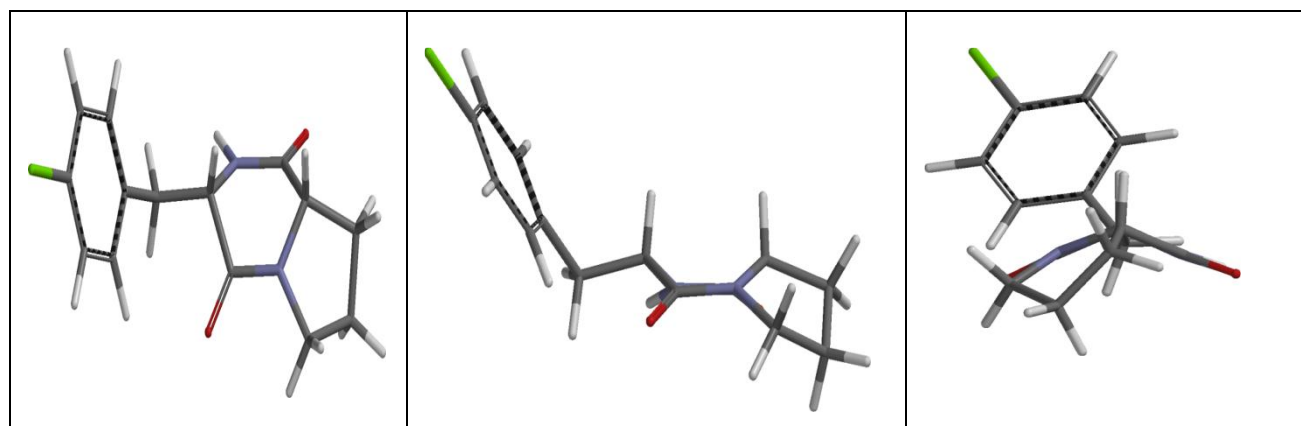


Figure 5.48 Conformation 3 of cyclo(Phe-4Cl-Pro) in DMSO

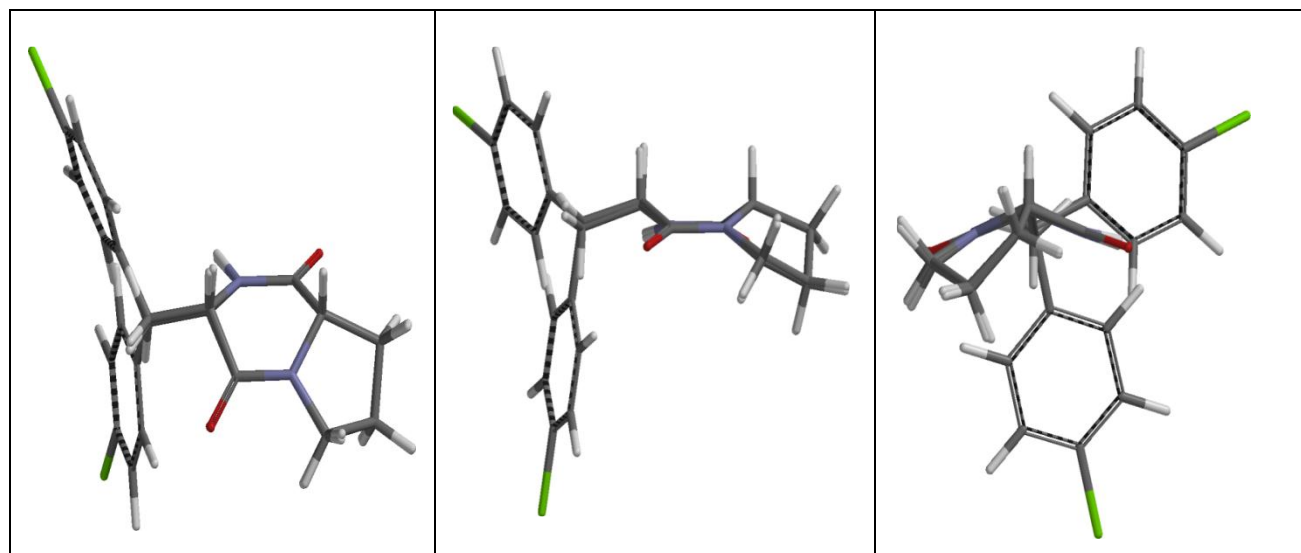


Figure 5.49 Overlay of conformation 1 and 2 of cyclo(Phe-4Cl-Pro) in DMSO

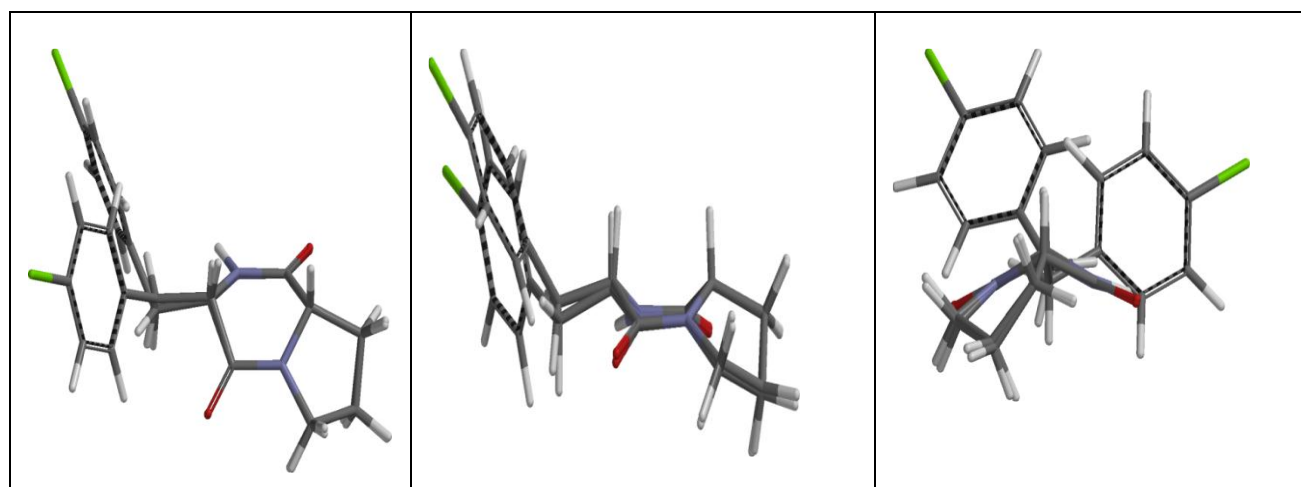


Figure 5.50 Overlay of conformation 1 and 3 of cyclo(Phe-4Cl-Pro) in DMSO

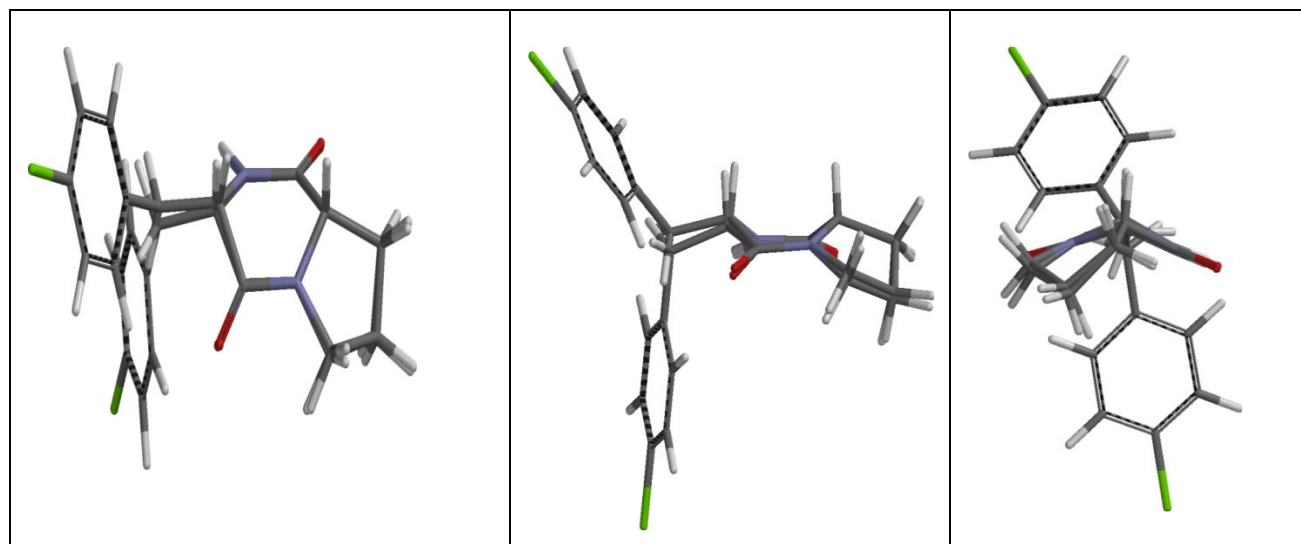


Figure 5.51 Overlay of conformation 2 and 3 of cyclo(Phe-4Cl-Pro) in DMSO

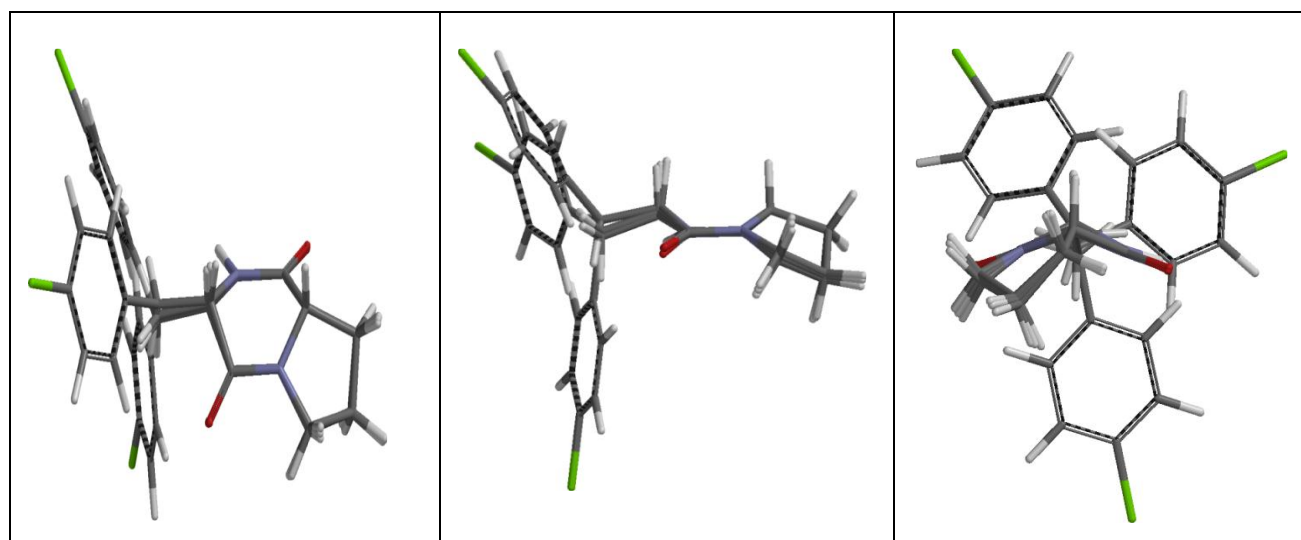


Figure 5.52 Overlay of conformation 1, 2 and 3 of cyclo(Phe-4Cl-Pro) in DMSO

Table 5.9 Conformational search results calculated for cyclo(D-Phe-4Cl-Pro) in DMSO

Conformer	Energy (kJ/mol)	Rel. E (kJ/mol)	Boltzmann Distribution
1	-3315307	0	0.673
2	-3315304	2.05	0.295
3	-3315299	7.54	0.032

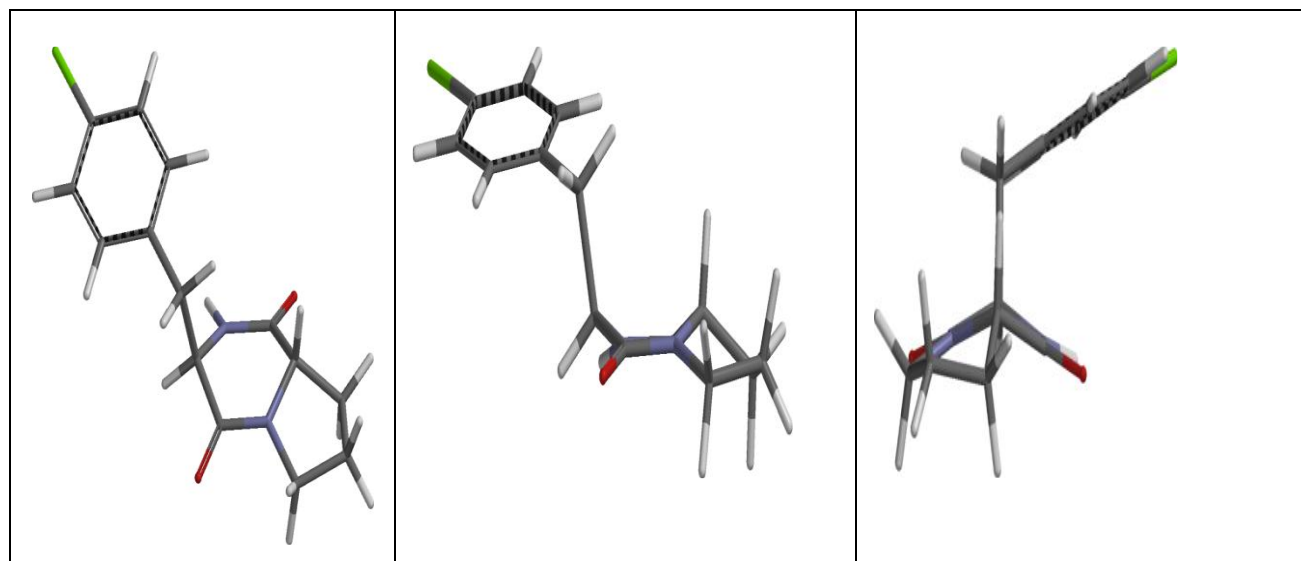


Figure 5.53 Conformation 1 of cyclo(D-Phe-4Cl-Pro) in DMSO

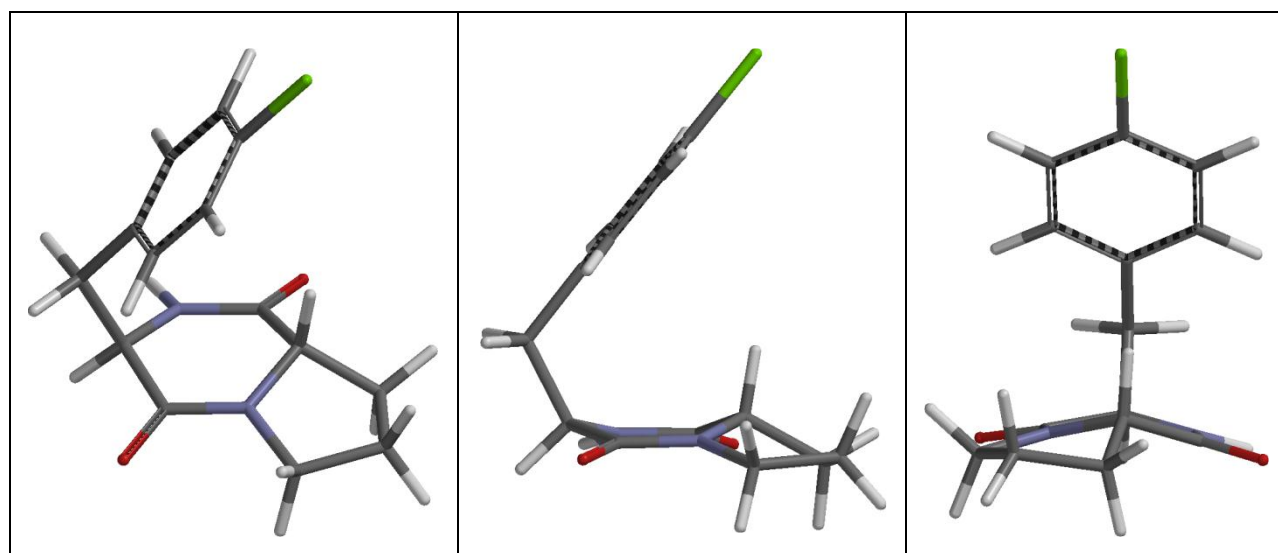


Figure 5.54 Conformation 2 of cyclo(D-Phe-4Cl-Pro) in DMSO

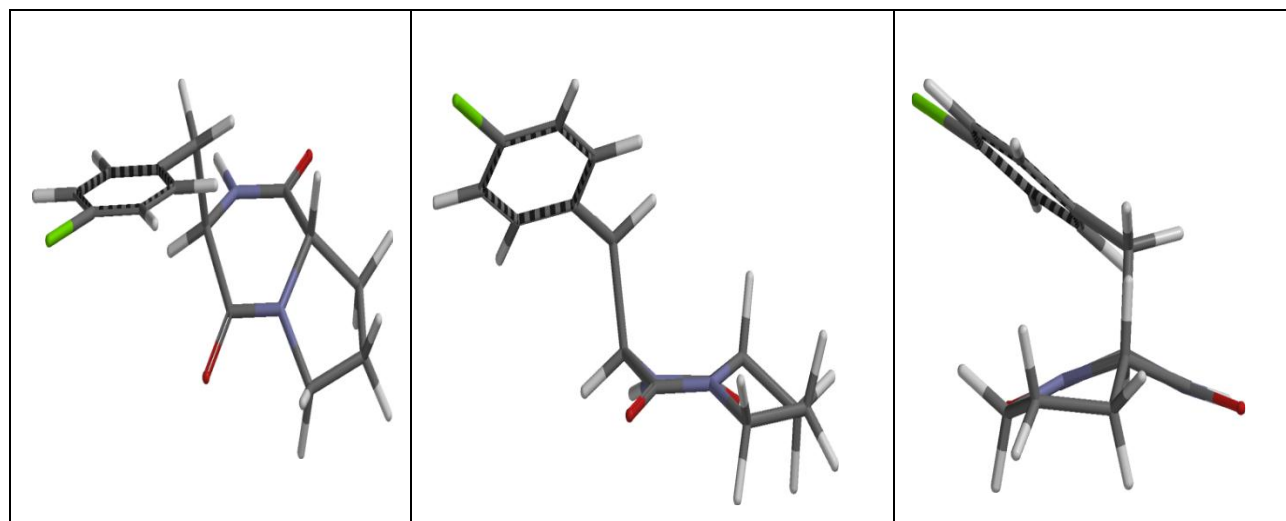


Figure 5.55 Conformation 3 of cyclo(D-Phe-4Cl-Pro) in DMSO

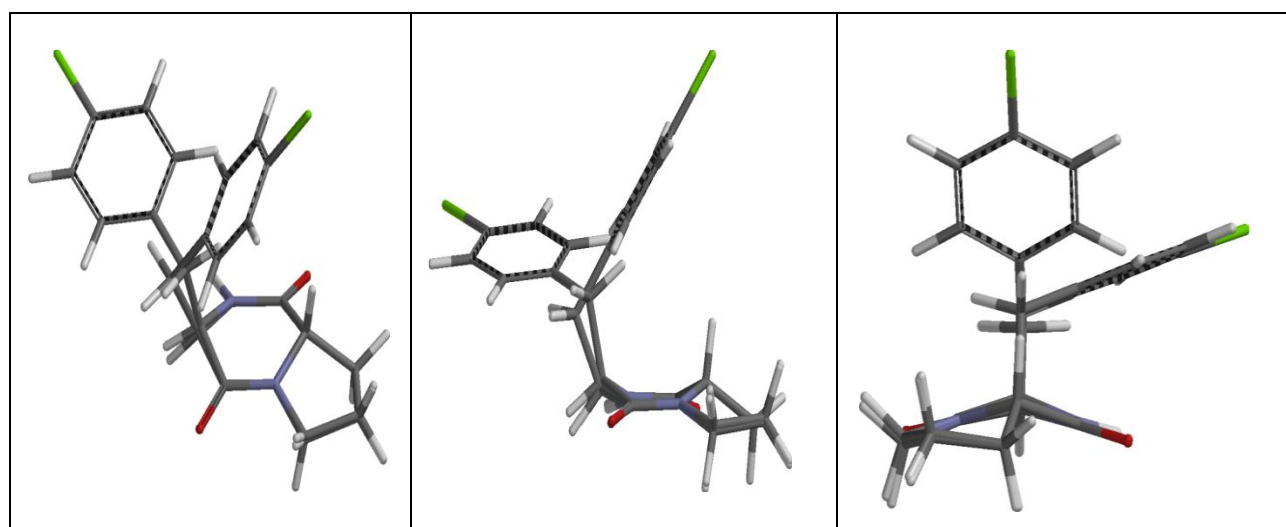


Figure 5.56 Overlay of conformation 1 and 2 of cyclo(D-Phe-4Cl-Pro) in DMSO

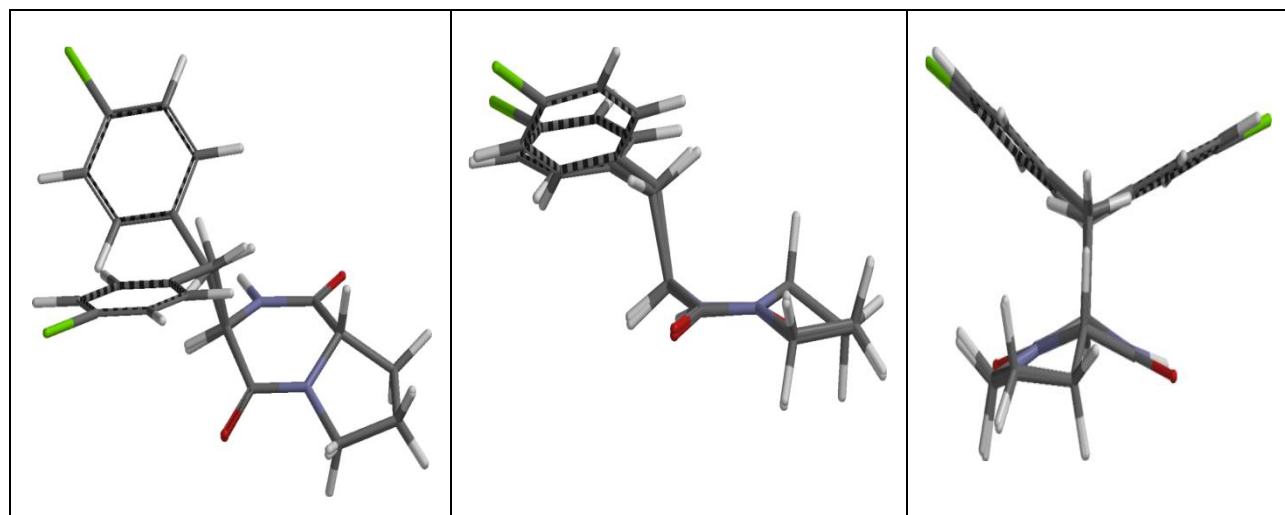


Figure 5.57 Overlay of conformation 1 and 3 of cyclo(D-Phe-4Cl-Pro) in DMSO

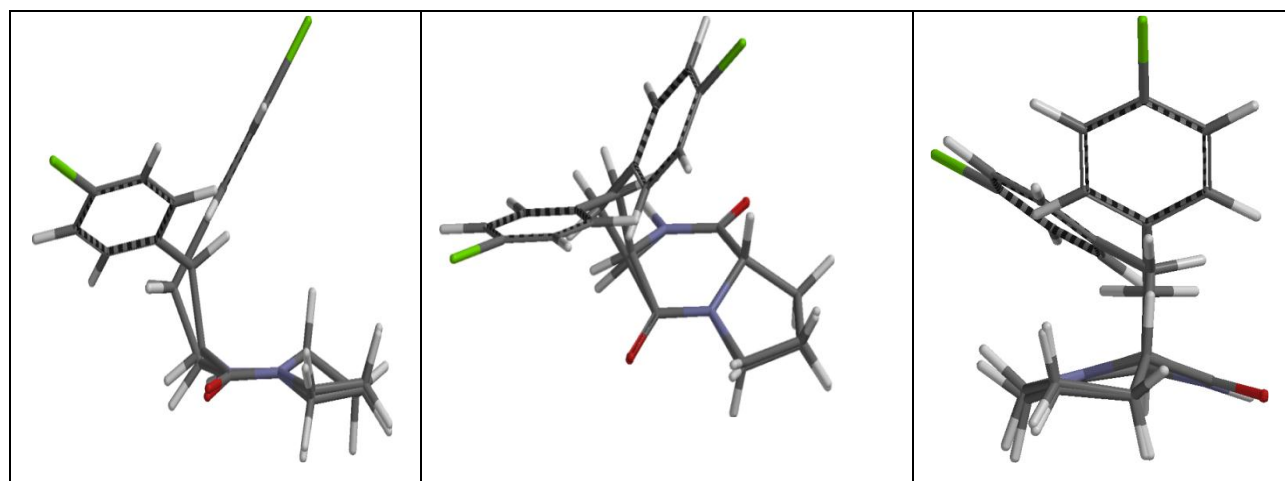


Figure 5.58 Overlay of conformation 2 and 3 of cyclo(D-Phe-4Cl-Pro) in DMSO

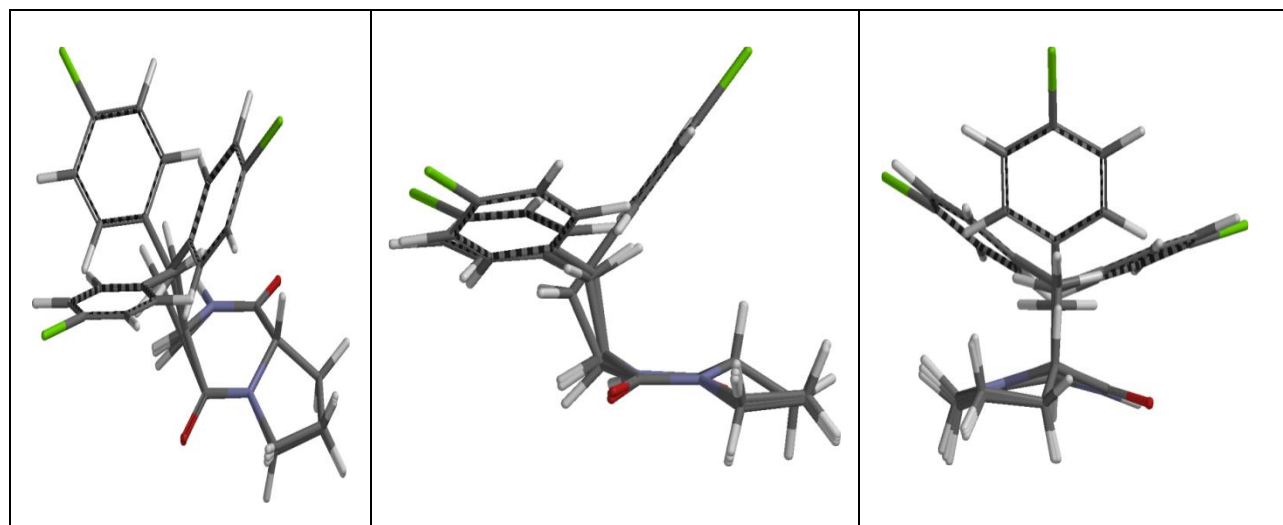


Figure 5.59 Overlay of conformation1, 2 and 3 of cyclo(D-Phe-4Cl-Pro) in DMSO

The aromatic cyclic side chain is extended and not folded onto the cyclic dipeptide ring due to steric hindrance caused by the halogen atom. This is a possible indication that the keto-groups are free to bind to a complimentary receptor.

CHAPTER 6

ANTICANCER STUDIES

6.1 Introduction

The term cancer can be defined as an unregulated growth of cells arising from one abnormal cell. The clinical term malignant neoplasm, is defined as a relatively autonomous growth of tissue not subject to the rules and regulations of normal growing cells. Tumour is a general term indicating any abnormal mass or growth of tissue. The main characteristics of benign tumours can be summarised as encapsulation, slow growth, and non-invasive growth into surrounding tissue, in other words lack of the ability to metastasise. Malignant tumours grow rapidly, are not encapsulated and incomplete if present, invade surrounding tissues and metastasise. Benign growths generally have a normal complement of chromosomes, exhibit good differentiation, and have limited cell division whereas the opposite is characteristic of malignant neoplasms (Warshawsky and Landolph, 2006). Table 6.1 illustrates the main type of cancers.

Table 6.1 Main types of cancers (Warshawsky and Landolph, 2006).

Tissue	Benign	Malignant
Epithelial		
Glands or ducts (e.g., gut, breast, lung, uterus)	Adenoma Carcinoma-in-situ	Adenocarcinoma
Stratified squamous tissue (e.g., skin, lung)	Squamous cell papilloma	Squamous cell or epidermoid carcinoma
Basal cells (skin)	-	Basal cell carcinoma

Melanocytes (skin)	Nevus	Malignant melanoma
Renal epithelium	Renal tubular adenoma	Renal cell carcinoma
Liver cells	Liver cell carcinoma	Hepatocellular carcinoma
Connective tissue and derivatives		
Fibroblast	Fibroma	Fibrosarcoma
Cartilage	Chondroma	Chondrosarcoma
Bone	Osteoma	Osteogenic sarcoma
Striated muscle	Rhabdomyoma	Rhabdomyosarcoma
Blood vessels	Haemangioma	Angiosarcoma
Bone marrow, spleen		
Haematopoietic (blood-forming) cells	-	Leukemias, erythroleukemia, myeloma, lymphomas
Nerves		
Peripheral nervous system	-	Neuroblastomas
Central nervous system	-	Gliomas, Astrocytomas, Medullablastomas

Cancer is either inherited or results from mutations caused by an accumulation of environmental factors. About 5 to 10 percent of cancers are hereditary. The remaining cancers result from damage to genes that occur throughout our lifetime either due to internal (e.g., inherited mutations, hormones, immune conditions and mutations that occur from metabolism) or external (e.g., tobacco, infectious organisms, chemicals and radiation) factors. Statistics reveal that about 80 percent of all human cancers deaths are related to external factors that can be controlled or prevented (Warshawsky and Landolph, 2006).

6.1.1 Cell growth cycle

Figure 6.1 illustrates the cell growth cycle. A cell cycle is the period from formation of a new somatic cell to the time at which that new cell divides. It is an orderly sequence of events by which the somatic cell duplicates its contents and divides into two. Cancer cells, like normal cells, proceed through a specific and orderly set of events during cellular replication referred to as the cell cycle (Koda-Kimble *et al.*, 2008). The rate of cellular proliferation within any population of cells depends on three parameters: the rate of cell division, the fraction of cells within the population undergoing cell division (growth fraction), and the rate of cell loss from the population due to terminal differentiation or cell death (Tortora and Grabowski, 2009).

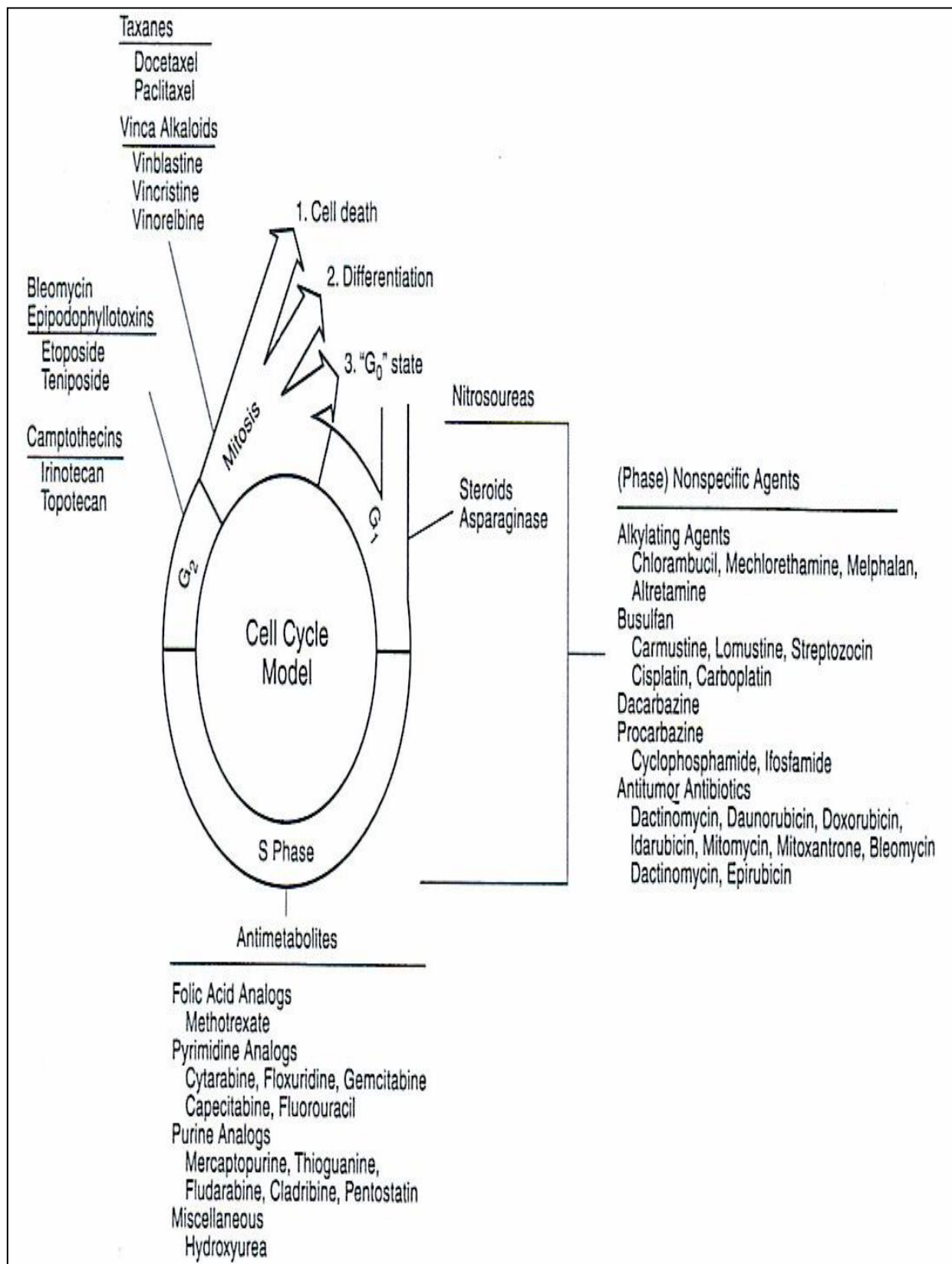


Figure 6.1 Diagram of the cell cycle specifying the four phases-G₁, G₂, M, S and G₀-and indicating the main sites of action of most anticancer agents (Koda-Kimble *et al.*, 2008).

The cell division cycle can be divided into the interphase period, in which a cell is not dividing and the mitotic period, in which the cell is actively dividing. Two functional phases, the S and M, and two preparatory phases, the G_1 and G_2 can be distinguished. During the interphase the cell replicates its deoxyribonucleic acid (DNA). It also produces additional organelles and cytosolic components. The interphase is the state of high metabolic activity, and during this time the cell does most of its growing and performs its metabolic and physiological functions. The interphase consists of three phases: G_1 , S and G_2 . The S phase occurs between G_1 and G_2 and is defined as the phase in which DNA is replicated. Under normal circumstances, the time it takes a typical human cell to complete the S phase is about eight hours and is invariant. The M phase consists of nuclear division, or mitosis and cytoplasmic division, or cytokinesis. The M phase can be divided into four stages; prophase, metaphase, anaphase and telophase (Tortora and Grabowski, 2009). Fully replicated chromosomes are segregated to each of the two daughter nuclei by the process of mitosis during the M phase (Koda-kimble *et al.*, 2008; Andreeff *et al.*, 2000; Prosser *et al.*, 2006). The length of the M phase is about 1 hour and is also normally invariant. The cells that complete mitosis may either continue to proceed through the cell cycle to divide again, differentiate or mature into specialised cells and eventually die or enter a third resting phase called the G_0 phase (Koda-Kimble *et al.*, 2008). The G_1 and G_2 phases have key regulating functions and are required for the synthesis of cellular constituents needed to support further phases, which is ultimately necessary to complete cell division (Koda-Kimble *et al.*, 2008). The G_1 phase precedes the S phase, whereas the G_2 phase precedes the M phase. In mammalian cells, the length of the G_2 phase is about 2 hours. The length of the G_1 phase is highly variable and can range from about 6 hours to several days or longer. The varying length of the G_1 phase accounts for most of the differences seen in the rate of cell division, between different cell types or between cells growing under different conditions (Andreeff *et al.*, 2000; Prosser *et al.*, 2006). The G_0 phase is a period within the G_1 phase of the cell cycle in which cells exist in a stable resting state.

Proliferation of normal cells (or cell renewal) is under fine control to balance the loss of mature functional cells with the production of new cells. Proto-oncogenes and tumour-suppressor genes provide the stimulatory and inhibitory signals respectively, which regulate the cell cycle (Koda-Kimble *et al.*, 2008). The messages are conveyed to the cell by the cell cycle “clock” (Dipiro *et al.*, 2011). In a normal cell, the clock collects the inhibitory signals to determine whether the cell should undergo division. The clock consists of interacting proteins found in the nucleus, including cyclins and cyclin-dependant kinases (CDKs). The cyclins combine with the CDKs to form complexes that act as a molecular switch. The molecular switch allows the cell to move through the restriction point that occurs late in the G₁ phase to the S phase. If insufficient amounts of cyclins and CDKs are present during the G₁ phase, the cell will not enter the S phase to start cell division. The complexes release phosphate groups from molecules of adenosine triphosphate (ATP) and transfer them to a protein called a retinoblastoma protein (pRB). If the pRB acquires enough phosphate groups, the protein will release the transcription factors needed by the cell to make proteins, which are essential for cell division. New evidence suggests that the function of cyclins, CDKs and inhibitory proteins may be disrupted by a malignant transformation, or these proteins could undergo changes that cause a malignant transformation (Koda-Kimble *et al.*, 2008).

The cell cycle clock further regulates cell division by interpreting the inhibitory and stimulatory signals it receives from surrounding cells (Rang *et al.*, 2011). Stimulatory growth factors interact with complementary receptors on the cell surface and modify the signalling pathways that affect the cell cycle clock. Inhibitory growth factors can also interact with complementary receptors and modify signalling pathways. The presence of excess stimulatory (*i.e.*, cyclins and CKDs) or the absence of inhibitory proteins can cause excessive proliferation. Stimulatory growth factors trigger the molecular switch, whereas inhibitory growth factors turn the switch off. Two inhibitory proteins, lost or muted in 50% of human cancers, include pRB and p53. Altered inhibitory signals can lead to a malignant transformation (Koda-Kimble *et al.*, 2008; Rang *et al.*, 2011).

If the stimulatory and inhibitory signals do not program the cell to stop dividing, other mechanisms, including apoptosis (a normal mechanism of cell death required for tissue homeostasis) and senescence (aging), can help control excessive cell division (Rang *et al.*, 2011). Unfortunately, proto-oncogenes and tumour-suppressor genes regulate these processes. Any gene mutation or deletion can disrupt normal cellular turnover. New research is under way to target these genes, proteins, and receptors in an attempt to discover new cancer treatments and the prevention of cancer (Dipiro *et al.*, 2011; Koda-Kimble *et al.*, 2008).

In cancer cells, cell cycle control is disrupted by (1) abnormal growth factor function and/or (2) abnormal cyclin /CKDs function and/or (3) abnormal DNA synthesis as a result of oncogene activity and/or (4) abnormal decrease in negative regulatory forces owing to mutation of tumour-suppressor genes. Carcinogenesis can activate tumour-suppressor genes, resulting in the initiation and promotion of carcinogenesis (Rang *et al.*, 2011; Heath, 2001).

Anticancer agents fall into two specific groups: cell cycle specific groups (CCS), which exert their action on cells passing through the cell cycle (phases G₁ to M); and cell cycle non-specific drugs (CCNS), which acts on cells irrespective of whether they are resting in the G₀ phase or passing through the cell cycle (Dipiro *et al.*, 2011).

6.1.2 Carcinogenesis

A cancer, or neoplasm, is thought to develop from a cell in which the normal mechanisms for control of growth and proliferation are altered (Heath, 2001). Current evidence supports the concept of carcinogenesis as a multistage process consisting of initiation, promotion and progression (Dipiro *et al.*, 2011).

The first process of carcinogenesis is initiation, which involves the exposure of normal cells to carcinogenic substances. The general classes include: physical agents (radiation), viruses, chemicals (Warshawsky and Landolph, 2006). Ionising and ultraviolet radiation have been shown to cause cancers in humans and experimental

animals. The possible role of viruses in the etiology of human cancers is not yet clear. There have however, been positive correlations between human cancers and viruses. These viruses include the: Hepatitis B virus, Epstein-Barr virus, Humanpapilloma virus, human immunodeficiency virus (HIV), and the Human T-Cell lymphotropic virus type 1 (Warshawsky and Landolph, 2006). Chemical carcinogens are classified into two groups, according to their mode of action: firstly, direct-acting alkylation agents and secondly chemicals requiring activation. Direct-acting carcinogens are chemically and biologically reactive by virtue of their structure and are electrophilic in character. The majorities of chemical carcinogens, however, are chemically and biologically inert and are termed procarcinogens. Specific, spontaneous or biochemical activation reactions convert procarcinogens to either proximal or intermediate carcinogens and to ultimate electrophilic carcinogens. The exposure to carcinogens may cause a change in DNA, ribonucleic acid (RNA), or protein that, if not repaired, results in irreversible cellular mutations (Warshawsky and Landolph, 2006).

The second phase of carcinogenesis, termed the promotion phase, results in the formation of latent tumour cells, which leads to a neoplastic growth and eventually tumour formation. This phase is considered to be reversible up to a certain point (Warshawsky and Landolph, 2006; Coussens and Werb, 2002). During the promotion phase carcinogens and the other factors (such as species, strain, age, sex, diet, intestinal flora condition, health status, chronic irritation and inflammation) alter the environment to favour growth of the mutated cell population over normal cells. Depending on the type of cancer, months to years may elapse between the two carcinogenic phases and the development of clinically detectable cancer, a process which is called conversion (Dipiro *et al.*, 2011).

The final stage of neoplastic growth, called progression, involves further genetic changes leading to increased cell proliferation. The critical elements of this phase include tumour invasion into local tissues and the development of metastasis, in which malignant cells detach from the primary tumour and invade a body cavity or enter the blood or lymphatic system. If these cells survive secondary tumours may be

established, becoming vascularised to provide nutrients for further growth (Dipiro *et al.*, 2011).

6.1.3 Invasion and metastasis

Invasion and metastasis are the most dangerous and life-threatening aspects of cancer. The capacity for invasion may not initially be expressed or occur in all tumours. However, most cancers develop invasive potential, thus progressing to malignancy from pre-existing carcinoma *in situ*, adenomas, or disorders of epithelial proliferation. Once the neoplasm becomes invasive, it can disseminate readily through whatever means available to it: *via* the lymphatic and/or vascular channels (Liotta and Kohn, 2000; Prosser *et al.*, 2006). Invasion and metastasis kill host cells through two processes: firstly local invasion and secondly distant organ injury. Local invasion can compromise the function of involved tissue by local compression, local destruction, or prevention of normal organ functioning. The most significant turning point in the disease, however, is the establishment of metastasis. At this stage, the patient can no longer be cured by local therapy alone. The patient with metastatic disease most commonly succumbs to injury caused by cancer dissemination or less often to complications associated with cytotoxic therapies (Liotta and Kohn, 2000; Prosser *et al.*, 2006).

Tumours of comparable size and histology can have widely divergent metastatic potential, depending on their genotype and local environmental influences. Metastatic potential is influenced by the local microenvironment, angiogenesis, stroma-tumour interactions, and elaboration of cytokines by the local tissue, and more significantly by its molecular phenotype. The malignant phenotype is the culmination of a series of genetic changes in the primary tumour and its metastasis, through which the investigation of activation, regulation, and the manipulation of regulatory elements can be exploited as a new frontier for metastasis research (Liotta and Kohn, 2000; Prosser *et al.*, 2006).

6.1.4 Cancer therapy

Treatment of cancer involves three main treatment modalities, namely (1) radiation therapy, (2) surgical removal of the tumour, and (3) chemotherapy (Katzung, 2009). Successful therapy must be focused on the primary tumour and its metastasis, whether clinically apparent or microscopic. Thus local and regional therapy, surgery, or radiation must be integrated with systemic therapy, *i.e.*, drugs. The ideal antineoplastic drug would destroy cancer cells, without adverse effects or toxicities on normal cells (Sartoreli, 2001).

6.1.4.1 Radiation therapy

Radiation therapy, or radiotherapy, involves the use of ionising radiation to eradicate localised tumour masses (Koda-Kimble *et al.*, 2008). Ionising radiation may be delivered by X-ray beams, beams of ionising particles *e.g.*, electrons or by beta or gamma irradiation produced in the decay of radioactive isotopes (Koda-Kimble *et al.*, 2008). Not all cancers are sensitive to the lethal effects of radiation, so this modality has limited application in the treatment of only some cancers (Koda-Kimble *et al.*, 2008). Unfortunately, the usefulness of radiation therapy can be limited by its toxic effects on normal tissues surrounding the tumour, or heat damage to the skin that develops as radiation passes through it to reach an underlying tumour (Koda-Kimble *et al.*, 2008). Many complex and sophisticated techniques, however, have been developed and used to maximise the dose reaching the tumour while minimising the destructive effects on normal tissues (Dipiro *et al.*, 2011).

6.1.4.2 Surgery

Surgery is the oldest modality of cancer therapy and still forms the mainstay of treatment in solid tumours (Pollock and Morton, 2000). The surgical approach to therapy is simple and direct. It seeks to physically remove the tumour mass and thus eliminate the problem. However, the nature of tumour growth and metastasis presents certain and often major, difficulties (Nowak and Handford, 2004). The type of surgery required is

normally determined by the type of tumour and the anatomical site, and may thus include any of the following:

- Wide local excision of the tumour mass, *e.g.*, local excision of a breast lump.
- Removal of part of an organ and surrounding tissue, *e.g.*, partial glossectomy and neck dissection for a carcinoma of the tongue.
- Removal of an entire organ, *e.g.*, laryngectomy, cystectomy, or hysterectomy (Nowak and Handford, 2004).

6.1.4.3 Chemotherapeutic agents

Almost all chemotherapeutic agents currently available kill cancer cells by affecting DNA synthesis or function, a process that occurs during each cell cycle. Each drug varies in the way this occurs within the cycle. Drugs used in cancer chemotherapy can be divided into three different groups: cytotoxic (antineoplastic) agents, hormones and miscellaneous agents (Rang *et al.*, 2011). Table 6.2 summarises the currently available chemotherapeutic agents, their mechanism of action, main indication and side effects.

Table 6.2 Currently available antineoplastic agents (Rang *et al.*, 2011).

Class	Mechanism of action	Tumours commonly responsive	Adverse effects
<p><u>Alkylating agents</u></p> <p>Mechlorethamine</p> <p>Chlorambucil</p> <p>Cyclophosphamide</p> <p>Melphalan</p> <p>Ifosfamide</p>	<p>Alkylation of DNA with restriction of strands uncoiling and replication</p>	<p>Hodgkin's, malignant lymphoma, small cell lung carcinoma, carcinoma of the breast and testis</p>	<p>Alopecia, nausea and vomiting, myelosuppression, permanent sterility</p>
<p><u>Antimetabolites</u></p> <p>Folate antagonist <i>e.g.</i>, Methotrexate</p> <p>Purine antagonist <i>e.g.</i>, 6-Mercaptopurine</p> <p>Pyrimidine antagonist</p>	<p>Binds to dehydrofolate reductase, interfering with pyrimidine synthesis</p> <p>Blocks de novo purine synthesis</p> <p>Interferes with</p>	<p>Carcinoma of the head, neck, ovary, malignant lymphoma, Osteogenic sarcoma</p> <p>Acute leukaemia</p>	<p>Mucosal ulceration, bone marrow suppression, myelosuppression, alopecia, mucositis, diarrhoea and vomiting, hyperpigmentation, skin rash</p>

<p>e.g., 5-Fluorouracil</p> <p>Cytarabine</p>	<p>thymidylatesynthetase to reduce thymidine production</p> <p>DNA polymerase inhibition</p>	<p>Gastrointestinal neoplasms, carcinoma of the breast</p> <p>Acute leukaemia, malignant lymphoma</p>	
<p><u>Plant alkaloids</u></p> <p>Vincas e.g., Vincristine</p> <p>Podophyllotoxins e.g., Etoposide</p>	<p>Mitotic arrest by alterations of microtubular proteins</p> <p>Inhibition of mitosis</p>	<p>Lymphomas, leukaemias, carcinoma of the breast and testis</p> <p>Lymphoma, Hodgkin's, carcinoma of the testis and lung, acute leukaemia</p>	<p>Peripheral neuropathy, alopecia, nausea and vomiting, myelosuppression</p>
<p><u>Antibiotics</u></p> <p>Doxorubicin</p> <p>Bleomycin</p>	<p>Inhibit DNA uncoiling</p> <p>Incision of DNA strands</p>	<p>Acute leukaemia, Hodgkin's, carcinoma of the breast and lung</p> <p>Squamous cell carcinoma, lymphoma, carcinoma of testis and lung</p> <p>Carcinoma of colon breast and lung</p>	<p>Nausea and vomiting, myelosuppression, alopecia, cardiac toxicity, anaphylaxis, chills and fever, skin rash, leucopaenia, alopecia, thrombocytopenia</p>

Mitomycin	Inhibit DNA synthesis		
<u>Nitrosoureas</u> Carmustine	Alkylating of DNA restricting uncoiling and replication	Brain tumours, lymphoma	Myelosuppression, pulmonary and renal toxicity
Lomustine	Carbamylation of amino acids in proteins	Brain tumours, lymphoma	Pulmonary and renal toxicity
<u>Inorganic ions</u> Cisplatin	Inhibits DNA uncoiling	Carcinoma of the lung, testis, breast and stomach	Anaemia, Ototoxicity, Peripheral neuropathy

<u>Biological response modification</u> Interferon	Antiproliferative effect	Lymphomas, renal cell carcinoma, melanoma	Fatigue, fever, myalgias, arthralgias, Myelosuppression
<u>Enzymes</u> Asparaginase	Depletion of asparagine	Acute lymphocytic leukaemia	Acute anaphylaxis, hyperthermia, hyperglycaemia
<u>Hormones</u> Tamoxifen Flutamide	Anti-oestrogen Anti-androgen	Carcinoma of the breast Carcinoma of the prostate	Hot flashes, deep vein thrombosis Hot flashes, gynaecomastia

(Beers and Berkow, 2004; McClelland, 2003; Dipro *et al.*, 2011)

6.1.5 Agents utilised as controls for the assays

Melphalan is currently one of the most widely used anticancer drugs in the world (Katzung, 2009).

Melphalan was first synthesized in 1953 by Bergel and Stock, and was found to have significant antitumor activity against multiple myeloma, melanoma, ovarian and breast cancer (Katzung, 2009).

Melphalan is classified as a bifunctional alkylating agent. It is thus able to react with two groups, causing intra- or interchain cross-linking. Melphalan is thus able to interfere with both transcription and replication. Other effects of alkylation at guanine N₇ includes excision of the guanine base with main chain scission, or pairing of the alkylated guanine with thymine instead of cytosine and ultimately substitution of the guanine (G)

cytosine (C) (GC) pair by adenine (A) thymine (T)(AT) pair. The main action occurs during replication, when some parts of the DNA are unpaired and more susceptible to alkylation. In other words the effects take place during the S phase of the cell cycle, resulting in a block at G₂ and ultimately apoptotic cell death. Alkylating agents are most active in the resting phase of the cell. These drugs are cell cycle non-specific. Melphalan is a phenylalanine derivative of nitrogen mustard. Nitrogen mustards are related to sulphur mustard, the “mustard gas” used during the First World War, with a basic formula RN-bis-(2-chloroethyl). In the body the 2-chloroethyl side-chain undergoes an intermolecular cyclisation with the release of a Cl⁻ ion. The highly reactive ethylene immonium derivative can thus interact with the DNA and other molecules (Rang *et al.*, 2011).

6.2 Methodology

Methods employed by Huq *et al.* (2004) and Cunningham (2006) were adapted to develop a method to test the anticancer activity of cyclo(Phe-4Cl-Pro) and cyclo(D-Phe-4Cl-Pro).

6.2.1 Cell cultures

Three human cancerous cell lines, namely HeLa, HT-29 and MCF-7, were used in the experiments. Primary cell cultures were obtained from Highveld Biological, South Africa (SA), and were stored in liquid nitrogen until needed. Table 6.3 illustrates the characteristics of the respective cancerous cell cultures.

Table 6.3 Characteristics of cell cultures utilised for experiments

Characteristic	HeLa	HT-29	MCF-7
Morphology	Epithelial	Epithelial	Epithelial
Origin	Cervix	Colon	Pleural effusion from breast tissue
Species	Human	Human	Human
Age	Adult	Adult	Adult
Ploidy	Aneuploid	Aneuploid	Aneuploid
Characteristics	Continuous cell line from neoplastic tissue	Continuous cell line from neoplastic tissue	Continuous cell line from neoplastic tissue; oestrogen receptor positive
Adherent/Suspension culture	Adherent	Adherent	Adherent

(Jones, 2002; Pitchen 2002)

6.2.2 Cell line maintenance and routine culture

All procedures for experiments were carried out using sterile culture techniques. The cells were sub-cultured and maintained using standard procedures (Freshney, 2001). HeLa, HT-29 and MCF-7 cell cultures were routinely maintained in 25 cm³ culture flasks (Corningware, Cambridge, USA) in RPMI 1640 growth medium (pH 7.4) (Highveld Biological, SA), containing 10% heat-inactivated foetal calf serum (FCS) (Adcock Ingram, SA). Conventional culture conditions were maintained, namely 37 °C with 5% CO₂ humidification in a Labtec® humidified carbon dioxide incubator (Labtec®

ThermoForma®, SA). Growth medium was replaced every 48 hours. Cell lines were sub-cultured at a seeding density of 2.5×10^4 cells/ml in 10 ml. For sub-culturing, the respective cell line was rinsed with phosphate buffered saline (PBS). This was followed by removing the cells from the culture substrate. The cells were dissociated by the addition of 1 ml of 0.25% trypsin in ethylenediaminetetraacetic acid (EDTA), pre-warmed at 37 °C (Roche Diagnostics GmbH, Mannheim). This initial wash with trypsin/EDTA was removed immediately, and 1 ml trypsin/EDTA were added to the cells for approximately 5 minutes at 37°C. This was removed along with disaggregation by pipetting of the detaching cells into growth medium (final density of 1/10 in the medium). The dish and any residual cells were washed with more medium and added to the first cell suspension. The cells were incubated in a Labtec® humidified carbon dioxide incubator (Labcon®, SA) for 10 minutes, before being resuspended in 9 ml of growth medium. Sub-culturing allows for the expansion of the culture, providing large amounts of consistent material suitable for prolonged use (Freshney, 2001).

6.2.3 Preparation of solutions

6.2.3.1 Negative control

The negative control was utilised to indicate 100% viability of cell line growth and consisted of untreated cells. The positive control anti-cancer agent Melphalan was dissolved in 1% ethanol. Therefore vehicle controls consisting of 0.5% or 0.25% DMSO or 1% ethanol made up to a final volume in RPMI medium containing 10% FCS pre-warmed to 37 °C to control for any effect the DMSO or ethanol might have on the cell growth. Vehicle controls consisted of dimethyl sulphoxide (DMSO), made up to a final volume of 0.5% or 0.25% with RPMI medium containing 10% FCS pre-warmed to 37 °C. to control for any effect the DMSO might have upon the cell growth. DMSO was used to aid the solubilisation of the relevant cyclic dipeptides to be tested. Labrofil, was also tested as a potential agent, but was found to be too toxic to the cells, so this was not used. All test and control solutions were filter-sterilised through a sterile 0.22 µm acrodisc and added using a Falcon® serological pipette (Falcon®, USA).

6.2.3.2 Polyethylene glycol (PEG)

Polyethylene glycol (PEG) is a polyether compound. PEG 300 was added at a concentration of 0.05% to increase the effectiveness of uptake of the cyclic dipeptides. Concentrations of PEG higher than 0.05% was found to be toxic to the cells. This was added to the DMSO or ethanol as a vehicle in one set of experiments.

6.2.3.3 Positive control

The positive control, consisting of melphalan (Adcock Ingram, SA) at a concentration of 100 μM , was utilised to test the susceptibility of the cancerous cell cultures. Melphalan was dissolved in 1% ethanol (final concentration) together with vortex agitation (Vortex Mixer BM300, Laboratory supplies (Pty) Ltd, SA) to aid in the solubilisation of melphalan. The positive control was then made up to concentration with RPMI medium containing 10% FCS, which was pre-warmed to 37°C. The positive control was filter-sterilised through a 0.22 μm acrodisc (separations) and added to all cell cultures using a sterile Falcon[®] serological pipette (Falcon[®], USA).

6.2.3.4 Cyclic dipeptide solutions

Cyclo(Phe-4Cl-Pro) (A) and cyclo(D-Phe-4Cl-Pro) (B) were aseptically prepared in 0.25%, or 0.5% DMSO (final concentration) which together with vortex agitation initially aided in the solubilisation of the cyclic dipeptides. The cyclic dipeptides were then made up to concentration with RPMI medium containing 10% FCS, which was pre-warmed to 37°C. The cyclic dipeptides were filter-sterilised through a 0.22 μm sterile acrodisc (separations) and added to all cell cultures using a Falcon[®] serological pipette (Falcon[®], USA).

6.2.3.5 3-(4,5-dimethylthiazol-2-yl)-2,5-diphenyltetrazolium bromide (MTT) dye solution

Tetrazolium salts have been used extensively to demonstrate the reductive capacity of tissues. Tetrazolium salts are a large group of heterocyclic organic compounds that form highly coloured and often insoluble formazans after reduction. First prepared in 1894, these compounds have been used widely as indicators of both biological redox

systems and viability. MTT is a monotetrazolium salt, the reduction of which is one of the most frequently used methods for measuring cell proliferation and cytotoxicity. MTT is water soluble yielding a yellowish solution when prepared in media or salt solutions lacking phenol red. Dissolved MTT is converted to an insoluble purple formazan by cleavage of the tetrazolium ring by dehydrogenase enzymes. Only active mitochondrial dehydrogenases of living cells, and not dead cells, will cause this conversion. The water insoluble formazan can then be dissolved using DMSO or other solvents and the dissolved material is measured spectrophotometrically yielding absorbance as a function of concentration of the converted dye. Absorbance of the converted dye is measured at a wavelength of 540 nm (Liu *et al.*, 1997; Mosmann, 1983).

MTT (Sigma Chemicals Co., USA) was dissolved in 0.1 M PBS (pH 7.4) to give a stock concentration of 1 mg/ml. The solution was then filter-sterilised through a 0.22 µm acetate filter and stored, for not more than two weeks, in a sterile Schott bottle at 4 °C and away from light until needed.

6.3. Cytotoxicity assays utilizing MTT

HeLa, HT-29 and MCF-7 cell lines (Section 6.2.1) in exponential growth, showing 70-80% confluence, were trypsinised with 0.25% trypsin to enable the detachment of cells (Section 6.2.2). Cell numbers were then determined by haemocytometer counts using an improved Neubauer chamber (Bright-line Superior, Germany), and diluted with growth medium (Section 6.2.2) to a concentration of 6000 cells/200 µl prior to use. Each cell line was tested in separate 96-well flat-bottom microtitre plates (Costar, Corning). 200 µl of each cell suspension was transferred to the wells of 96-well flat-bottom microtitre plates leaving a control set of 4 replicate wells that contained the medium alone (blanks for MTT) assay. This was incubated at 37 °C with 5% CO₂ humidification for 24 hours. After incubation the cells had attached to the bottom of the wells, which enabled the growth medium to be aspirated off. The negative controls (Section 6.2.3.1), positive control (Section 6.2.3.3) and cyclic dipeptide solutions (Section 6.2.3.4) were then added to the wells in aliquots of 200 µl at appropriate final concentration in culture medium, such that each treatment yielded results in quadruplicate. The microtitre plates

were subsequently incubated at 37 °C with 5% CO₂ humidification for a further 48 hours. Incubation allowed for the drug compounds to interact with the respective cell lines. After 48 hours of incubation the growth medium was aspirated off and discarded from each well. 200 µl aliquots of MTT solution (Section 6.2.3.4) were then added to each well of the microtitre plates. The MTT containing microtitre plates were then incubated at 37 °C with 5% CO₂ humidification for three hours to allow for the metabolic reduction of the MTT. This resulted in the formation of insoluble formazan precipitates. The MTT supernatant was aspirated off and discarded, and replaced with 200 µl aliquots of DMSO, which were required to dissolve the formazan precipitate. Each microtitre plate was then placed on a plate shaker for 5 minutes and the absorbance read immediately at 540 nm on a multiscan MS[®] (version 4.0) Labsystem[®] type 352 microtitre plate spectrophotometer (Multiscan MS[®], England) (Huq *et al.*, 2004; Cunningham, 2006). Experiments were conducted in quadruplicate. Results were reported as the percentage inhibition of growth for each cell culture, after 48 hours of exposure to the cyclic dipeptides or the positive control, relative to the appropriate negative vehicle control culture.

6.4 Statistical analysis

Results were obtained as quadruplicate values and the blank (no cell) subtracted from each of the values. Data was represented as a mean ± standard deviation (SD). Percentage growth inhibition, after 48 hours of exposure to the cyclic dipeptides, was calculated with reference to the appropriate vehicle and compared to the positive controls.

Percentage growth inhibition was calculated as follows:

$$\% \text{ inhibition} = 100 - \left[\frac{\text{Absorbance of treatment}}{\text{Absorbance of appropriate vehicle}} \right] \times 100$$

0.25% DMSO was the vehicle for the 1 mM concentrations, 0.5% DMSO was the vehicle for the 2 mM concentrations and 1% ethanol was the vehicle for Melphalan.

Data were represented graphically with the aid of statistical software packages, Microsoft Excel[®] (Version 2007) and Graph Pad Prism[®] (Version 5). In order to determine whether the cyclic dipeptides under investigation caused statistically significant reduction in cell viability relative to the negative control, Student's *t*-tests were performed on the raw data for each concentration of cyclic dipeptide. Calculated *p*-values of less than 0.05 were defined as an indication of statistical significance.

6.5 Results and discussion

The inhibitory effects produced by the different concentrations of cyclo(Phe-4Cl-Pro) and cyclo(D-Phe-4Cl-Pro) and melphalan on HeLa, MCF-7 and HT-29 cell growth after 48 hours of exposure to the compounds are illustrated in Figures 6.2, 6.3, 6.4, 6.5, 6.6 and 6.7 respectively. The inhibitory effects produced by all concentrations of cyclic dipeptides were compared to that of melphalan (Tables 6.4, 6.5, 6.6, 6.7, 6.8, and 6.9). The effects of PEG to aid entry/uptake of the compounds were tested by omitting PEG from the treatments.

6.5.1 HeLa cell line

The percentage growth inhibition produced by all screening concentrations of cyclo(Phe-4Cl-Pro) and cyclo(D-Phe-4Cl-Pro) was found to be notably less than that produced by melphalan. Melphalan at a concentration (in 1% ethanol and with 0.05% PEG 300) of 100 μ M exhibited a percentage growth inhibition of $86.88\% \pm 5.869$ ($P < 0.0001$). Cyclo(Phe-4Cl-Pro) (in 0.5% or 0.25% DMSO with 0.05% PEG 300) at concentrations of 2000 μ M and 1000 μ M exhibited percentage growth inhibitions of only $55.28\% \pm 0.4332$ ($P < 0.0001$) and $-1.747\% \pm 2.355$ ($P < 0.0001$), respectively. Similarly, cyclo(D-Phe-4Cl-Pro) (in 0.5% or 0.25% DMSO with 0.05% PEG 300) at concentrations of 2000 μ M and 1000 μ M exhibited percentage growth inhibitions of $32.86\% \pm 2.144$ ($P < 0.0001$) and $11.75\% \pm 2.697$ ($P = 0.0460$), respectively.

Melphalan (in 1% ethanol without PEG 300) at a concentration of 100 μ M exhibited a growth inhibition of $14.47\% \pm 6.606$ ($P < 0.0001$). Cyclo(Phe-4Cl-Pro) (in 0.5% or 0.25%

DMSO without 0.05% PEG 300) at concentrations of 2000 μM and 1000 μM exhibited growth inhibitions of only $34.61\% \pm 1.14519$ ($P = 0.0402$) and $26.29\% \pm 1.4287$ ($P < 0.0001$), respectively. Cyclo(D-Phe-4Cl-Pro) (in 0.5% or 0.25% DMSO without 0.05% PEG 300) at concentrations of 2000 μM and 1000 μM exhibited growth inhibitions of $45.86\% \pm 7.706$ ($P < 0.0001$) and $32.13\% \pm 19.779$ ($P < 0.0001$), respectively. Percentage growth inhibition of HeLa cells produced by cyclo(Phe-4Cl-Pro) and cyclo(D-Phe-4Cl-Pro) was found to be concentration-dependant, with increasing concentrations causing enhanced inhibition. Although cyclo(Phe-4Cl-Pro) and cyclo(D-Phe-4Cl-Pro) produced statistically significant inhibition of growth relative to the negative control, it is evident that their clinical cytotoxic potential against HeLa cell growth is fairly limited, since melphalan at 100 μM concentration is more than twice as effective in inhibiting the cell growth. The effects produced by cyclo(Phe-4Cl-Pro), cyclo(D-Phe-4Cl-Pro) and melphalan compared to the negative control, are represented in Table 6.4.

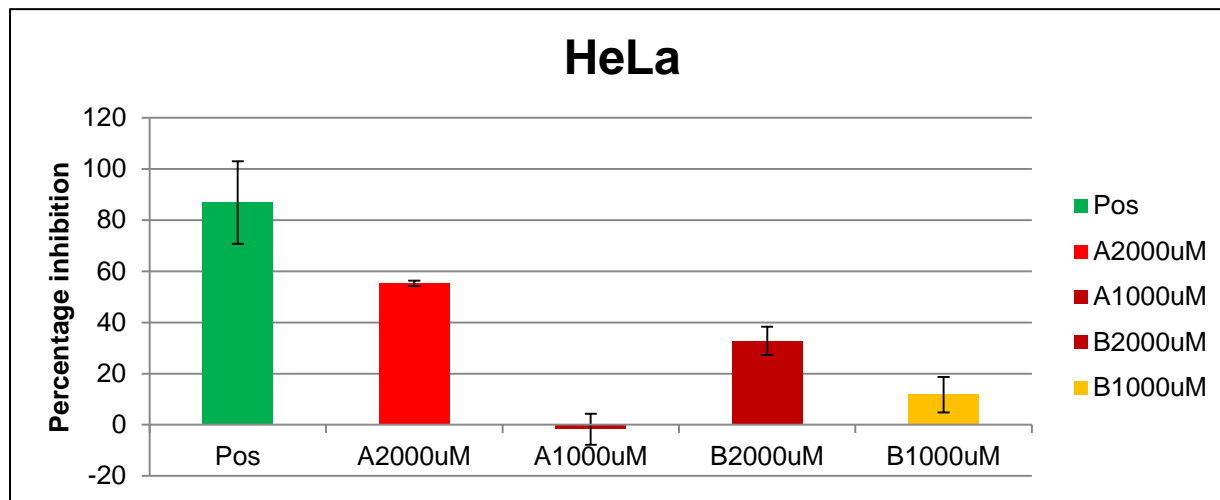


Figure 6.2 Percentage growth inhibition of HeLa cell line after 48 hour exposure to cyclo(Phe-4Cl-Pro) (A) and cyclo(D-Phe-4Cl-Pro) (B) and melphalan (n =4) (vehicle with PEG)

Table 6.4 Percentage growth inhibition of HeLa cell line after 48 hour exposure to cyclo(Phe-4Cl-Pro) and cyclo(D-Phe-4Cl-Pro) and melphalan (n =4) (vehicle with PEG)

Agent	Concentration	% Inhibition	P-value
Melphalan	100 μ M	86.88 \pm 5.869	< 0.0001
Cyclo(Phe-4Cl-Pro)	2000 μ M	55.28 \pm 0.4332	<0.0001
	1000 μ M	-1.747 \pm 2.355	< 0.0001
Cyclo(D-Phe-4Cl-Pro)	2000 μ M	32.86 \pm 2.144	< 0.0001
	1000 μ M	11.75 \pm 2.697	< 0.0001

Results are reported as percentage inhibition relative to the negative control cell lines

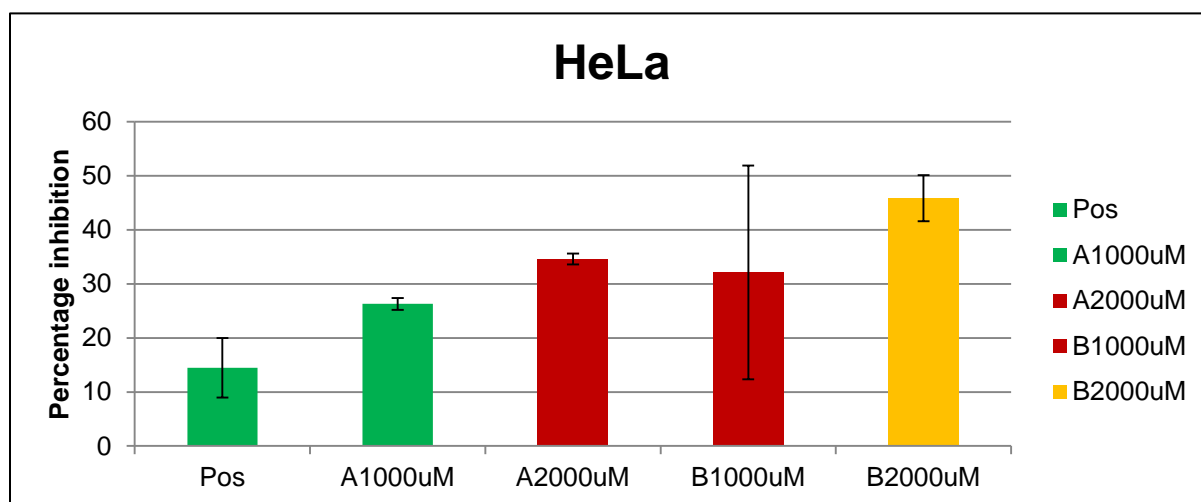


Figure 6.3 Percentage growth inhibition of HeLa cell line after 48 hour exposure to cyclo(Phe-4Cl-Pro) (A) and cyclo(D-Phe-4Cl-Pro) (B) and melphalan (n =4) (vehicle without PEG)

Table 6.5 Percentage growth inhibition of HeLa cell line after 48 hour exposure to cyclo(Phe-4Cl-Pro) and cyclo(D-Phe-4Cl-Pro) and melphalan (n =4) (vehicle without PEG)

Agent	Concentration	% Inhibition	P-value
Melphalan	100 μ M	14.47 \pm 6.606	< 0.0001
Cyclo(Phe-4Cl-Pro)	2000 μ M	34.61 \pm 1.4519	0.0402
	1000 μ M	26.29 \pm 1.4287	< 0.0001

Cyclo(D-Phe-4Cl-Pro)	2000 μ M	45.86 \pm 7.706	< 0.0001
	1000 μ M	32.13 \pm 19.779	< 0.0001

Results are reported as percentage inhibition relative to the negative control cell lines

6.5.2 MCF-7 cell line

The inhibitory effects produced by the different screening concentrations of cyclo(Phe-4Cl-Pro), cyclo(D-Phe-4Cl-Pro) and melphalan on MCF-7 cell growth after 48 hours of exposure to the compounds are illustrated in Figure 6.4. Percentage growth inhibition produced by all screening concentrations of cyclo(Phe-4Cl-Pro) and cyclo(D-Phe-4Cl-Pro) was found to be notably less than that produced at a 100 μ M concentration for melphalan. Melphalan (in 1% ethanol with 0.05% PEG 300) at a concentration of 100 μ M exhibited percentage growth inhibition of 82.39% \pm 2.058 ($P < 0.0001$). Cyclo(Phe-4Cl-Pro) (in 0.5% or 0.25% DMSO with 0.05% PEG 300) at concentrations of 2000 μ M and 1000 μ M exhibited percentage growth inhibitions of 71.62% \pm 0.1252 ($P < 0.0001$) and 31.66% \pm 1.127 ($P < 0.0001$), respectively. Cyclo(D-Phe-4Cl-Pro) (in 0.5% or 0.25% DMSO with 0.05% PEG 300) at concentrations of 2000 μ M and 1000 μ M exhibited percentage growth inhibitions of 50.84% \pm 0.5489 ($P < 0.0001$) and 29.79% \pm 0.9773 ($P < 0.0001$), respectively.

Melphalan (in 1% ethanol without 0.05% PEG 300) at a concentration of 100 μ M exhibited a growth inhibition of 86.06% \pm 1.632 ($P < 0.0001$). Cyclo(Phe-4-Cl-Pro) (in 0.5% or 0.25% DMSO without 0.05% PEG 300) at concentrations of 2000 μ M and 1000 μ M exhibited percentage growth inhibitions of 18.56% \pm 1.972 ($P < 0.0001$) and -5.499% \pm 0.5015 ($P < 0.0001$). Cyclo(D-Phe-4Cl-Pro) (in 0.5% or 0.25% DMSO without PEG) at concentrations of 2000 μ M and 1000 μ M exhibited percentage growth inhibitions of 21.98091% \pm 4.750 ($P = 0.0340$) and 19.77% \pm 2.382 ($P < 0.0001$).

Although cyclo(Phe-4Cl-Pro) and cyclo(D-Phe-4Cl-Pro) at concentrations of 2000 μM and 1000 μM produced statistically significant inhibition of growth relative to the negative control, their clinical relevance against MCF-7 cell growth is questionable, since melphalan at 100 μM is more than three times as effective in inhibiting the cell growth. The effects produced by cyclo(Phe-4Cl-Pro) and cyclo(D-Phe-4Cl-Pro) and melphalan compared to the negative control, are represented in Table 6.6.

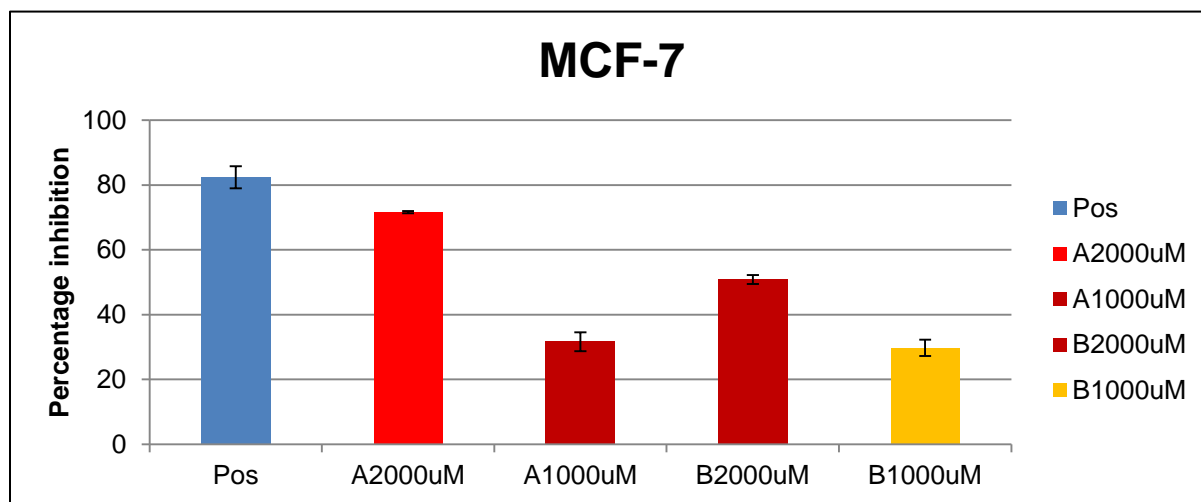


Figure 6.4 Percentage growth inhibition of MCF-7 cell line after 48 hour exposure to cyclo(Phe-4Cl-Pro) (A) and cyclo(D-Phe-4Cl-Pro) (B) and melphalan (n =4) (vehicle with PEG)

Table 6.6 Percentage growth inhibition of MCF-7 cell line after 48 hour exposure to cyclo(Phe-4Cl-Pro) and cyclo(D-Phe-4Cl-Pro) and Melphalan (n =4) (vehicle with PEG)

Agent	Concentration	% Inhibition	P-value
Melphalan	100 μM	82.39 \pm 2.058	< 0.0001

Cyclo(Phe-4Cl-Pro)	2000 μ M	71.62 \pm 0.1252	<0.0001
	1000 μ M	31.66 \pm 1.127	<0.0001
Cyclo(D-Phe-4Cl-Pro)	2000 μ M	50.84 \pm 0.5489	< 0.0001
	1000 μ M	29.79 \pm 0.9773	<0.0001

Results are reported as percentage inhibition relative to the negative control cell lines

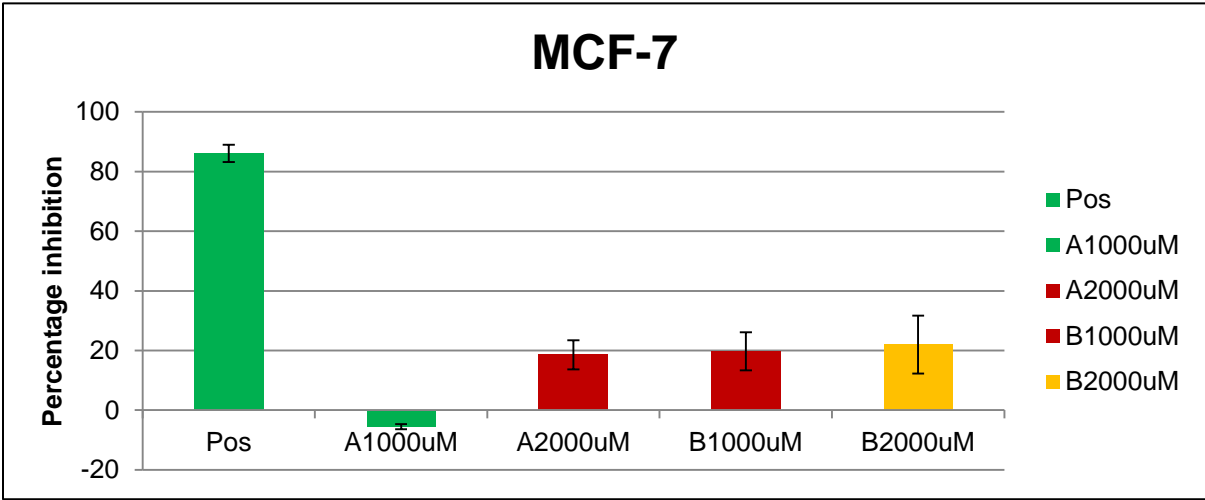


Figure 6.5 Percentage growth inhibition of MCF-7 cell line after 48 hour exposure to cyclo(Phe-4Cl-Pro) (A) and cyclo(D-Phe-4Cl-Pro) (B) and Melphalan (n =4) (vehicle without PEG)

Table 6.7 Percentage growth inhibition of MCF-7 cell line after 48 hour exposure to cyclo(Phe-4Cl-Pro) and cyclo(D-Phe-4Cl-Pro) and melphalan (n =4) (vehicle without PEG)

Agent	Concentration	% Inhibition	P-value
Melphalan	100 μ M	86.06 \pm 1.632	< 0.0001
Cyclo(Phe-4Cl-Pro)	2000 μ M	18.56 \pm 0.5015	< 0.0001
	1000 μ M	-5.499 \pm 1.972	< 0.0001
Cyclo(D-Phe-4Cl-Pro)	2000 μ M	21.98091 \pm 2.382	0.0340
	1000 μ M	19.77 \pm 4.750	< 0.0001

Results are reported as percentage inhibition relative to the negative control cell lines

6.5.3 HT-29 cell line

The inhibitory effects produced by the different screening concentrations cyclo(Phe-4Cl-Pro), cyclo(D-Phe-4Cl-Pro) and melphalan on HT-29 cell growth after 48 hours of exposure to the compounds are illustrated in Figure 6.6. Again percentage growth inhibition produced by all screening concentrations of cyclo(Phe-4Cl-Pro) and cyclo(D-Phe-4Cl-Pro) was found to be notably less than that produced for melphalan. Melphalan at a concentration (in 1% ethanol with 0.05% PEG 300) of 100 μ M exhibited percentage

growth inhibition of $71.30\% \pm 1.035$ ($P = 0.0006$). Cyclo(Phe-4Cl-Pro) (in 0.5% or 0.25% DMSO with 0.05% PEG 300) at a concentration of 2000 μM exhibited a percentage growth inhibition of $56.65\% \pm 0.3647$ ($P = 0.0006$) and at 1000 μM $35.73\% \pm 2.645$ ($P < 0.0001$). Cyclo(D-Phe-4Cl-Pro) (in 0.5% or 0.25% DMSO with 0.05% PEG 300) at a concentration of 2000 μM exhibited percentage growth inhibition of $47.63\% \pm 1.583$ ($P < 0.0001$), and at 1000 μM $32.54\% \pm 3.261$ ($p < 0.0001$).

Melphalan (in 1% ethanol without 0.05% PEG 300) at a concentration of 100 μM exhibited a growth inhibition of $44.45\% \pm 3.370$ ($P < 0.0001$). Cyclo(Phe-4Cl-Pro) (in 0.5% or 0.25% DMSO without 0.05% PEG 300) at a concentration of 2000 μM exhibited a percentage growth inhibition of $25.66\% \pm 1.525$ ($P = 0.0007$) and at 1000 μM $19.77\% \pm 4.750$ ($P < 0.0001$). Cyclo(D-Phe-4Cl-Pro) (0.5% or 0.25% DMSO without PEG 300) at a concentration of 2000 μM exhibited a percentage growth inhibition of $24.60\% \pm 2.4200$ ($P = 0.0002$) and at a 1000 μM $21.61\% \pm 2.3300$ ($P < 0.0001$). Percentage inhibition of HT-29 cell growth produced by cyclo(Phe-4Cl-Pro), cyclo(D-Phe-4Cl-Pro) and melphalan was found to also be concentration-dependant. Although cyclo(Phe-4Cl-Pro) and cyclo(D-Phe-4Cl-Pro) produced statistically significant inhibition of growth relative to the negative control, it is evident that both cyclic dipeptides' cytotoxic potential against HT-29 cell growth is very limited, since melphalan at 100 μM is more than ten times as effective in inhibiting the cell growth. The effects produced by cyclo(Phe-4Cl-Pro), cyclo(D-Phe-4Cl-Pro) and melphalan compared to the negative control, are represented in Table 6.8.

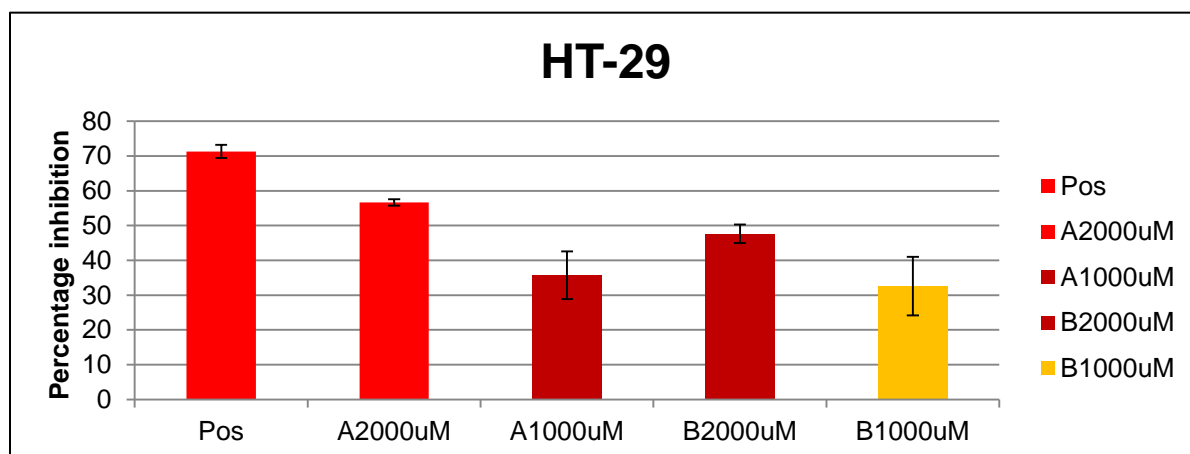


Figure 6.6 Percentage growth inhibition of HT-29 cell line after 48 hour exposure to cyclo(Phe-4Cl-Pro) (A) and cyclo(D-Phe-4Cl-Pro) (B) and melphalan (n =4) (vehicle with PEG)

Table 6.8 Percentage growth inhibition of HT-29 cell line after 48 hour exposure to cyclo(Phe-4Cl-Pro) and cyclo(D-Phe-4Cl-Pro) and melphalan (n =4) (vehicle with PEG)

Agent	Concentration	% Inhibition	P-value
Melphalan	100 μ M	71.30 \pm 1.035	0.0006
Cyclo(Phe-4Cl-Pro)	2000 μ M	56.65 \pm 0.3647	0.0006
	1000 μ M	35.73 \pm 2.645	< 0.0001
Cyclo(D-Phe-4Cl-Pro)	2000 μ M	47.63 \pm 1.583	< 0.0001

	1000 μ M	32.54 ± 3.261	< 0.0001
--	--------------	-------------------	------------

Results are reported as percentage inhibition relative to the negative control cell lines

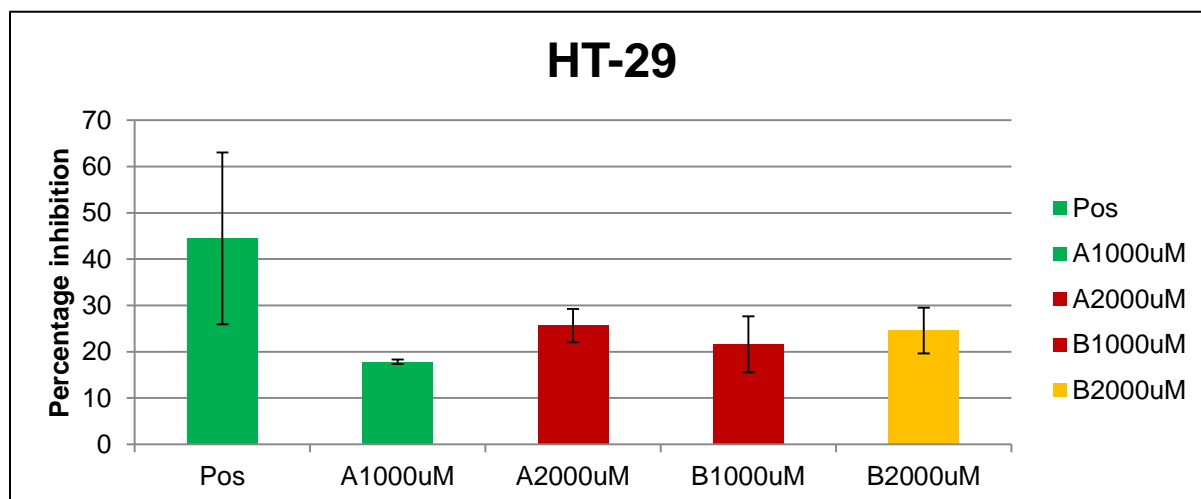


Figure 6.7 Percentage growth inhibition of HT-29 cell line after 48 hour exposure to cyclo(Phe-4Cl-Pro) (A) and cyclo(D-Phe-4Cl-Pro) (B) and Melphalan (n =4) (vehicle without PEG)

Table 6.9 Percentage growth inhibition of HT-29 cell line after 48 hour exposure to cyclo(Phe-4Cl-Pro) and cyclo(D-Phe-4Cl-Pro) and melphalan(n =4) (vehicle without PEG)

Agent	Concentration	% Inhibition	P-value
Melphalan	100 μ M	44.45 ± 3.370	< 0.0001
Cyclo(Phe-4Cl-Pro)	2000 μ M	25.66 ± 1.525	0.0007

	1000 μ M	17.83 \pm 0.992	< 0.0001
Cyclo(D-Phe-4Cl-Pro)	2000 μ M	24.60 \pm 2.4200	0.0002
	1000 μ M	21.61 \pm 2.3300	< 0.0001

Results are reported as percentage inhibition relative to the negative control cell lines

6.6 Conclusion

Natural and synthetic peptides have been shown to exhibit therapeutic anticancer activity against human tumours (Lee *et al.*, 2005).

Table 6.10 and Table 6.11 summarises the percentage inhibition of the negative control, positive control, Cyclo(Phe-4Cl-Pro) and Cyclo(D-Phe-4Cl-Pro) on HeLa, HT-29 and MCF-7 cell lines (vehicle with and without 0.05% PEG 300), respectively.

Table 6.10 the percentage inhibition of the negative control, positive control, Cyclo(Phe-4Cl-Pro) and Cyclo(D-Phe-4Cl-Pro) on HeLa, HT-29 and MCF-7 cell lines (vehicle with 0.05% PEG 300)

Cell line	Negative 0.25%	Negative 0.5%	Positive	Cyclo(Phe- 4Cl-Pro) 1mM	Cyclo(Phe- 4Cl-Pro) 2 mM	Cyclo(D- Phe-4Cl- Pro) 1 mM	Cyclo(D- Phe-4Cl- Pro) 2 mM
HeLa	-4.533%	10.86%	86.88%	-1.74%	55.28%	11.75%	32.86%
HT-29	7.90%	3.74%	71.30%	35.73%	56.65%	32.54%	47.63%
MCF-7	-11.27%	-14.91%	82.38%	31.65%	71.62%	31.65%	50.84%

Table 6.11 the percentage inhibition of the negative control, positive control, Cyclo(Phe-4Cl-Pro) and Cyclo(D-Phe-4Cl-Pro) on HeLa, HT-29 and MCF-7 cell lines (vehicle without 0.05% PEG 300)

Cell line	Negative 0.25%	Negative 0.5%	Positive	Cyclo(Phe- 4Cl-Pro) 1 mM	Cyclo(Phe- 4Cl-Pro) 2 mM	Cyclo(D- Phe-4Cl- Pro) 1 mM	Cyclo(D- Phe-4Cl- Pro) 2 mM
HeLa	-16.05%	-10.76%	14.47%	26.28%	34.61%	32.12%	45.86%
HT-29	-25.18%	-14.13%	44.45%	17.82%	25.66%	21.60%	24.59%
MCF-7	5.8635%	4.16%	86.05%	-5.49%	18.56%	19.76%	21.98%

The results with 0.05 %PEG 300 showed more inhibition than the results without 0.05% PEG 300. Cyclo(Phe-4Cl-Pro) at a concentration of 2000 μ M, showed the greatest inhibition for the HeLa, MCF-7 and HT-29 cell lines, with a inhibitions of $55.28\% \pm 0.4332$, $71.62\% \pm 0.1252$ and $56.65\% \pm 0.3647$, respectively. Cyclo(Phe-4Cl-Pro) at a concentration of 1000 μ M produced unexpected results for the HeLa (vehicle with 0.05% PEG 300) cell line of $-1.747\% \pm 2.355$ inhibition and at a concentration of 100 μ M for MCF-7 (Vehicle without 0.05% PEG 300) of $-5.499\% \pm 0.5015$ inhibition. This requires further investigation.

A study conducted by (Brauns, 2004) on the effects of cyclo(Phe-Pro) on HT-29, HeLa and MCF-7 cell lines showed that cyclo(Phe-Pro) exhibited more than 50% growth inhibition ($p < 0.01$) in the three cell lines. Cyclo(Phe-Pro) exhibited significant growth inhibition at concentrations of 5 mM ($p < 0.01$) and 10 mM ($p < 0.01$) in all three cell lines. The IC_{50} values for cyclo(Phe-Pro) were 5.24 ± 1.25 mM in HT-29, 3.85 ± 1.26 mM in HeLa and 5.07 ± 1.32 mM in MCF-7 cells.

Cyclo(Phe-4Cl-Pro) and cyclo(D-Phe-4Cl-Pro) exhibited limited potential as anticancer agents against HeLa, HT-29, MCF-7 cell lines when compared to melphalan. They are only effective at very high concentration (1mM and 2 mM), yielding better results at 2 mM. It has been suggested that the hydrophobicity of peptides, rather than the number of hydrophobic amino acids, may play an important role in anticancer activity or membrane transport (Lee *et al.*, 2005). The limited anticancer activity demonstrated by both cyclic dipeptides may therefore be as a result of poor solubility, which hinders their ability to cross the cell membranes and steric hindrance. Future studies could possibly include, investigating the toxicity with normal cells and ways of optimising the delivery or uptake of the cyclic dipeptides into the cells.

CHAPTER 7

ANTIMICROBIAL STUDIES

7.1 Introduction

The continuous use of antibiotics has resulted in the emergence of multi-resistant bacterial strains all over the world and as expected, hospitals have become breeding grounds for human associated microorganisms. It's widely accepted among clinicians, medical researchers, microbiologist and pharmacologists, that antibiotic resistance will, in the very near future, leave healthcare professionals without effective therapies for bacterial infections. Antibiotics rank the most important medical advancements of the 20th century (Lipsitch 2001). It is now estimated that about half of all *S. aureus* strains found in many medical institutions are resistant to antibiotics such as methicillin. The emerging resistance of enterococci to another useful and widely effective antibiotic, vancomycin might accelerate the spread of vancomycin-resistant genes, eventually limiting the efficacy of this drug. Consequently, the priority for the next decades should be focused on the development of alternative drugs and/or the recovery of natural molecules that will allow the consistent and proper control of pathogen-caused diseases. Ideally, these molecules should be as natural as possible, with a wide range of action over several pathogens, easy to produce, and not prone to introduce resistance (Marshall and Arenas, 2003).

It is important to differentiate between those bacteria that are pathogenic, non-pathogenic and opportunistically pathogenic. The choice of antimicrobial agent is essential to ensure that only the pathogenic organism is eliminated, and not colonising flora, which are crucial for normal body function (Dipiro *et al.*, 2011).

Microorganisms are said to be opportunistically pathogenic, when the growth of colonising flora are unopposed by normal other bacterial flora. Commonly an opportunistic infection can occur as a result of yeast overgrowth, when bacterial flora is eradicated by antibacterial therapy intended to eradicate pathogenic organisms. The

ideal antimicrobial agent would be specific for pathogenic bacteria, without disrupting the normal colonising bacteria (Dipiro *et al.*, 2011). Table 7.1 lists those bacteria that are naturally occurring flora, while Table 7.2 list commonly occurring pathogenic bacteria.

Table 7.1 Normal colonising flora (Dipiro *et al.*, 2011).

<p>Skin</p> <p>Staphylococci (coagulase-negative)</p> <p>Streptococci</p> <p>Diphtheroids (<i>corynebacterium sp.</i>)</p> <p><i>Propionibacteria</i></p>	<p>Upper respiratory tract</p> <p><i>Bacteroides sp.</i></p> <p><i>Haemophilus sp.</i></p> <p><i>Streptococci</i></p> <p><i>Neisseria sp.</i></p>
<p>Gastrointestinal tract</p> <p><i>Bacteroides sp.</i></p> <p>Anaerobic streptococci</p> <p><i>Fusobacterium sp.</i></p> <p><i>Enterobacteriaceae</i></p> <p>Diphtheroids</p> <p><i>Clostridium sp.</i></p>	<p>Genital tract</p> <p>Staphylococci</p> <p>Streptococci</p> <p><i>Enterobacteriaceae</i></p> <p><i>Corynebacterium sp.</i></p> <p><i>Mycoplasma sp.</i></p> <p><i>Lactobacillus sp.</i></p>

Table 7.2 Commonly occurring pathogenic bacteria (Dipiro *et al.*, 2011).

Gram-positive cocci	Gram-negative bacilli
Staphylococci	Anaerobes
Coagulase positive	<i>Bacteroides fragilis</i>
<i>S. aureus</i>	<i>Enterobacteriaceae</i>
Coagulase negative	<i>Citrobacter sp.</i>
<i>S. Epidermidis</i>	<i>Enterobacter sp.</i>
Streptococci	<i>Escherichia coli</i>
Anaerobes	<i>Klebsiella sp.</i>
<i>Peptostreptococcus</i>	<i>Serratia sp.</i>
<i>Streptococcus pneumoniae</i>	<i>Proteus sp.</i>
Group A, β -haemolytic	<i>Salmonella sp.</i>
<i>Streptococcus pyogenes</i>	<i>Pseudomonas sp.</i>
Group B	<i>P. aeruginosa</i>
<i>Streptococcus agalactiae</i>	<i>P. cepacia</i>
Group D	
Enterococcal species	

<p><i>E. raffinosus</i></p> <p><i>E. faecalis</i></p> <p>Non-enterococcal species</p> <p><i>Streptococcus bovis</i></p> <p>Viridans group</p> <p><i>Streptococcus mutans</i></p>	
<p>Gram-positive bacilli</p> <p><i>Bacillus sp.</i></p> <p><i>Bacillus cereus</i></p> <p><i>Clostridium sp.</i></p> <p><i>Clostridium difficile</i></p> <p><i>Clostridium perfringens</i></p> <p><i>Clostridium tetani</i></p> <p><i>Diphtheroids</i></p> <p><i>Corynebacterium diphtheriae</i></p>	<p>Xanthomonas maltophilia</p> <hr/> <p>Gram-negative cocci</p> <p><i>Moraxella catarrhalis</i></p> <p><i>Neisseria gonorrhoeae</i></p> <p><i>Neisseria meningitidis</i></p> <hr/> <p>Mycobacteria (acid-fast bacilli)</p> <p><i>Mycobacterium tuberculosis</i></p> <p><i>Mycobacterium bovis</i></p>

	<p>Fungi</p> <p>Yeasts</p> <p><i>Candida sp.</i></p> <p><i>Cryptococcus neoformans</i></p> <p><i>Aspergillus sp.</i></p> <p><i>Aspergillus fumigatus</i></p>
--	---

7.1.1 Current modes of antimicrobial therapy

Figure 7.1 summarises the classes of antimicrobial agents by their mechanism of action. There are five major processes, namely, inhibition of cell wall synthesis, folate metabolism, DNA and RNA synthesis, protein synthesis and interfering with the bacterial cell membrane, through which currently available antimicrobial agents exhibit their mechanism of action (Katzung, 2009).

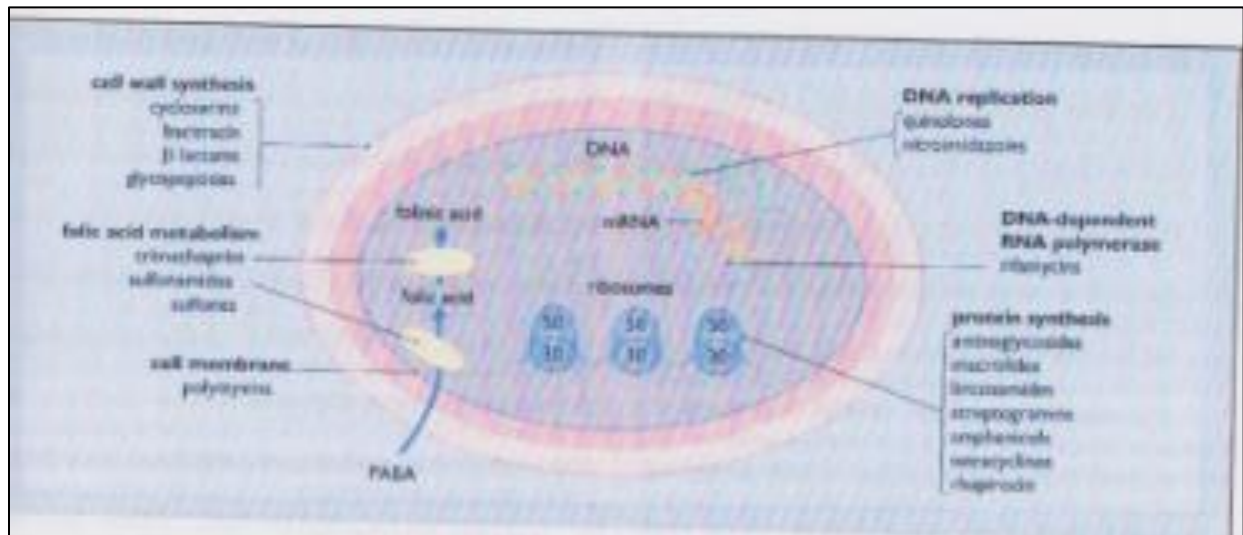


Figure 7.1 Sites of action of antimicrobial agents (Page *et al.*, 1997).

7.1.2 Inhibitors of bacterial cell wall synthesis

Sub-classes within this class include the β -lactams (penicillins, cephalosporins, monobactams, β -lactamase inhibitors and carbapenems), vancomycin, teicoplanin, fosfomycin, bacitracin and cycloserine. Inhibitors of cell wall synthesis exhibit their action through interfering with the synthesis of peptidoglycan, a major component of the bacterial cell wall, which is exclusive to bacteria. This enables the antibacterial agent to destroy the bacterial cell with little or no effect on normal human cells. Initiation of peptidoglycan synthesis (Figure 7.2) begins with the conversion of glucose-6-phosphate (Glc-6-p) to N-acetylglucosamine (NACGlc or G) which complexes with uridine diphosphate (UDP). The N-acetylglucosamine portion of the UDP-G molecule is then converted by enolpyruvate transferase with the addition of phosphoenolpyruvate to UDP-N-acetylmuramic acid (UDP-M). Fosfomycin inhibits enolpyruvate transferase and thus inhibits the formation of peptidoglycan at a very early stage of its synthesis. Once UDP-M is formed, five amino acids are incorporated into the molecule namely L-Ala-D-Glu-L-Lys-D-Ala-D-Ala. Cycloserine is a structural analogue of alanine and blocks the enzyme alanine racemase, which converts L-Ala into D-ala to be incorporated into the pentapeptide unit. The M-pentapeptide unit is then transferred from its UDP carrier to a lipid membrane carrier, bactrophenol (BP). BP requires dephosphorylation in order to bind to the pentapeptide sub-unit. Bacitracin interferes with the dephosphorylation of BP

and therefore prevents the transmembrane transport of peptidoglycan sub-units. A molecule of N-acetylglucosamine is then bonded to the N-acetylmuramic acid portion of the peptidoglycan sub-unit, after which a [Gly]₅ pentapeptide is bonded to the lysine residue. BP then transports this molecule to the extracellular surface, where it binds, with the aid of the enzyme transglycosylase, to a growing peptidoglycan chain. Vancomycin inhibits the actions of transglycosylase by firmly binding to the D-Ala-D-Ala portion of the peptidoglycan sub-unit. Chains are then cross-linked by the removal of the terminal D-Ala and binding to an adjacent peptide. Penicillin-binding proteins (PBP) catalyse this transpeptidase reaction. PBP also bind β -lactams, which then inhibit the cross-linking of peptidoglycan strands and reduces the rigidity, resulting in breakdown of the bacterial cell wall (Dipiro *et al.*, 2011; Katzung, 2009).

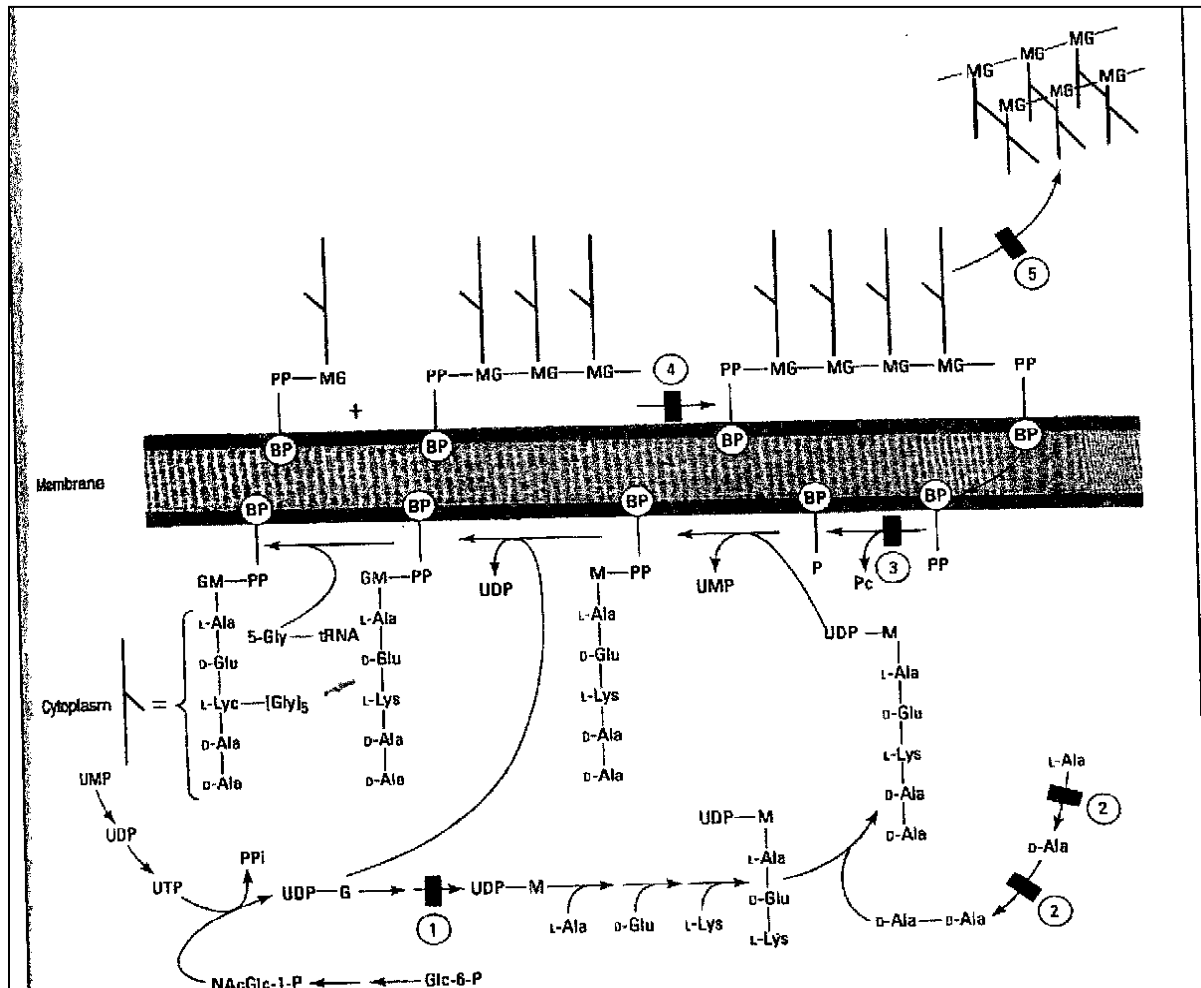


Figure 7.2 Peptidoglycan synthesis (Katzung, 2009).

The biosynthesis of a Peptidoglycan cell wall showing sites of action of fosfomycin (1), cycloserine (2), bacitracins (3), vancomycin (4), β -lactam antibiotics (5).

β -lactams are the most favourable agents to use of the cell wall synthesis inhibitors and consists of five main groups, the penicillin, cephalosporins, monobactams, β -lactamase inhibitors and carbapenems. Penicillins, (see general structure of penicillins Figure 7.3), consist of the β -lactamase sensitive (benzylpenicillin, phenoxymethylpenicillin), β -lactamase resistant (cloxacillin, flucloxacillin) and the extended spectrum penicillins (amoxillin, ampicillin) (Katzung, 2009). Incorporation of clavulanic acid into preparations containing broad-spectrum penicillins decreases the inactivation of the penicillin by β -lactamase. Clavulanic acid is a structural analogue to penicillin with low antibacterial activity, but which has a far greater affinity for the β -lactamase binding site than other active penicillins. Clavulanic acid is thus preferentially broken down, while the penicillins are capable of producing their effect unharmed (Katzung, 2009).

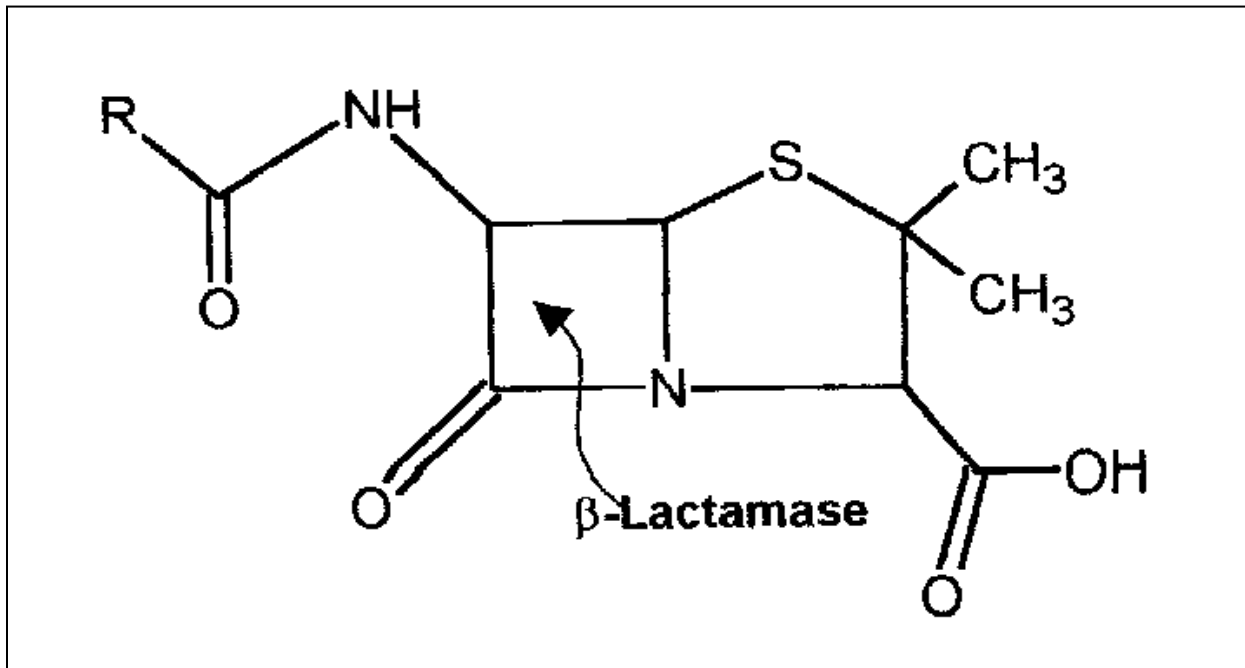


Figure 7.3 General structure of the penicillins (Katzung, 2009).

Cephalosporins:

Cephalosporins, (see general structure of cephalosporins Figure 7.4), are similar to penicillins, with respect to chemistry, mechanism of action and toxicity. Cross sensitivity between cephalosporins and penicillins are common. Cephalosporins are classed as first, second, third and fourth generations. First generations cephalosporins include cephalalexin and cefazolin. This class are more effective against Gram-positive cocci. Second generation cephalosporins include cefamandole, cefaclor and cefoxitin. These agents are active against the same bacteria as the first generation agents, but have an added spectrum covering some Gram-negative bacteria. Cefoxitin are also active against anaerobic bacteria. The third generation encompasses cefotaxime, ceftriaxone and cefpodoxime. They have a greater activity against Gram-negative bacteria. They also have the ability to cross the blood brain barrier (BBB), which is beneficial in the treatment of bacterial meningitidis and other central nervous system infections. The fourth generation cephalosporins (cefepime) are very similar to the third generation with respect to antibacterial activity, but are more resistant to hydrolysis from β -lactamase (Katzung, 2009).

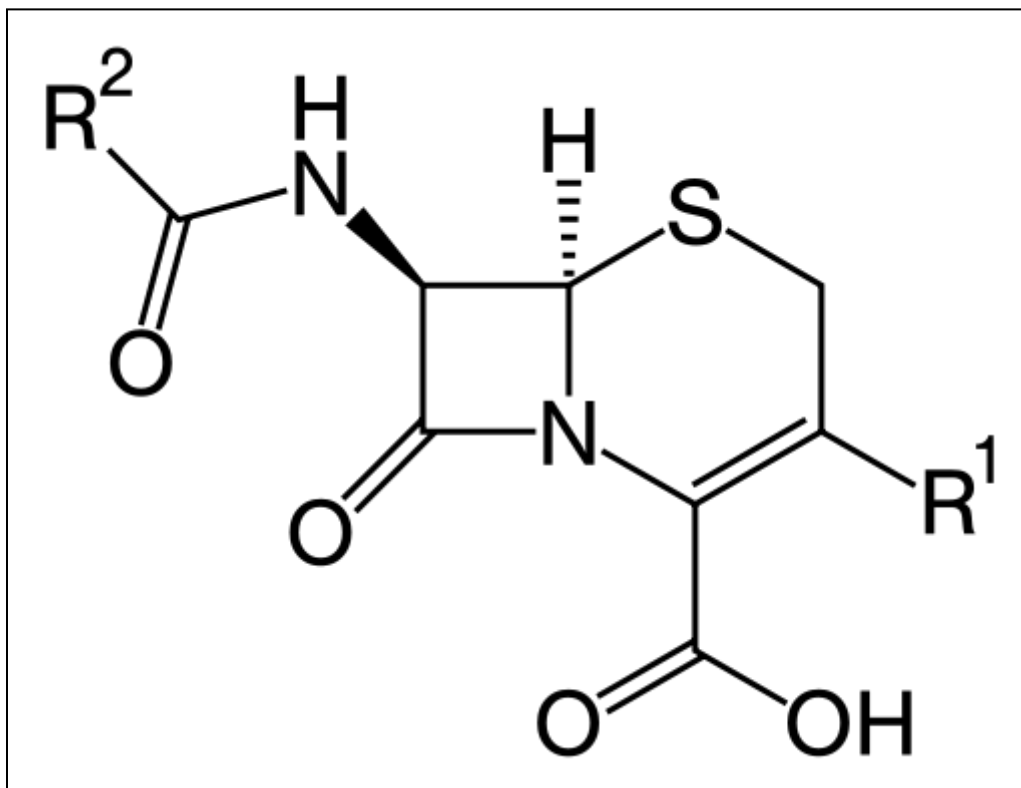


Figure 7.4 General structure of cephalosporins (Katzung, 2009).

Other β -lactam agents:

Other β -lactam agents include the monobactams, β -lactamase inhibitors and carbapenems. Aztreonam is an example of the monobactams and are most active against Gram-negative rods. β -Lactamase inhibitors include clavulanic acid, sulbactam and tazobactam, and while these agents have very little antibacterial activity themselves, they are structurally related to the β -lactams and inhibit β -lactamase by being preferentially broken down by the enzyme instead of the active β -lactam agent. For this reason they are co-administered with other β -lactams such as amoxicillin. Carbapenems are structurally related to β -lactams and have a wide spectrum of activity. Meropenem and imipenem are some examples of this class (Katzung, 2009).

Vancomycin:

Vancomycin is a glycopeptide molecule, which inhibits bacterial cell wall synthesis by binding to the D-Ala-D-Ala portion of the peptidoglycan sub-unit and inhibiting elongation of the structure (Figure 7.2) (Katzung, 2009).

Fosfomycin:

Fosfomycin inhibits the early stages of peptidoglycan synthesis (Figure 7.2). It is structurally unrelated to any other antimicrobial agent and appears to be related in structure to phosphoenolpyruvate, a precursor of N-acetylmuramic acid. Fosfomycin is active against both Gram-positive and Gram-negative bacteria and is used frequently for urinary tract infections (Katzung, 2009).

Bacitracin:

Bacitracin originates from the bacterium *Bacillus subtilis* and is a cyclic peptide “mixture” which inhibits the dephosphorylation of the peptidoglycan transporter bactoprenol. It thus inhibits the transfer of the peptidoglycan sub-units across the bacterial cell membrane (Figure 7.2). Bacitracin is active against Gram-positive organisms, but with limited systemic use, due to it being extremely nephrotoxic. It is however still used topically, limiting its systemic absorption and systemic side-effects (Katzung, 2009).

7.1.3 Inhibitors of cell membrane functioning

The polymyxins are a group of peptides displaying good inhibition of Gram-negative bacteria. Their mechanism is similar to cationic detergents, as they attach to the bacterial lipid membrane, disrupting it, leading to cell death. They are more active against Gram-negative bacteria as they have thinner peptidoglycan cell walls, which enable access of the polymyxins to the cell membrane (Katzung, 2009).

7.1.4 Inhibitors of protein synthesis

Ribosomes, the intracellular organelles responsible for protein synthesis, are found in two sub-units, a smaller and a larger sub-unit, both of which must be associated in order to 'translate' messenger RNA (mRNA) into proteins. In eukaryotic cells such as those found in humans, ribosomes consist of a 40S and a 60S sub-unit. In prokaryotic cells, such as bacteria, the ribosomes comprise a 30S and a 50S sub-unit. Due to the difference in ribosomal sub-units between human and bacterial cells, it is possible to selectively inhibit bacterial protein synthesis by inhibiting the functions of the 30S and 50S bacterial ribosomal sub-units (Dipiro *et al.*, 2011).

Agents that inhibit bacterial ribosomal function, and ultimately protein synthesis, include the aminoglycosides, macrolides, lincosamides, streptogramins, amphenicols, and tetracyclines. These agents require entry into the bacterial cell in order to elicit a response, which often results in the formation of mutant resistant bacteria, which alter their permeability to the antibacterial agents. This is often a problem, but inclusion of cell wall synthesis inhibitors into the regime, results in breakdown of the cell wall and easy access of the inhibitors of protein synthesis. This synergistic effect is frequently exploited by prescribing of agents such as penicillin G and gentamycin together (Dipiro *et al.*, 2011).

Figure 7.5 represents a brief summary of the mechanisms of the individual classes of bacterial protein synthesis inhibitors. Aminoglycosides such as gentamycin, tobramycin and amikacin bind to the 30S ribosomal sub-unit, changing its shape, resulting in incorrect coding of mRNA to transfer RNA (tRNA), which carry the amino acids for peptide bond formation (Dipiro *et al.*, 2011).

Macrolides which include the prototype erythromycin as well as azithromycin and clarithromycin, bind to the 50S sub-unit, preventing movement of the ribosome along the mRNA strand (Katzung, 2009). Tetracycline, including doxycycline, minocycline and

tetracycline, bind to the 30S ribosomal sub-unit, interfering with the attachment of tRNA to the mRNA-ribosome complex, inhibiting protein synthesis (Dipiro *et al.*, 2011).

The amphenicols, chloramphenicol and thiamphenicol, are primarily bacteriostatic. They bind to the 50S ribosomal sub-unit, preventing the amino acid bound portion of the tRNA from binding to the growing peptide chain (Dipiro *et al.*, 2011).

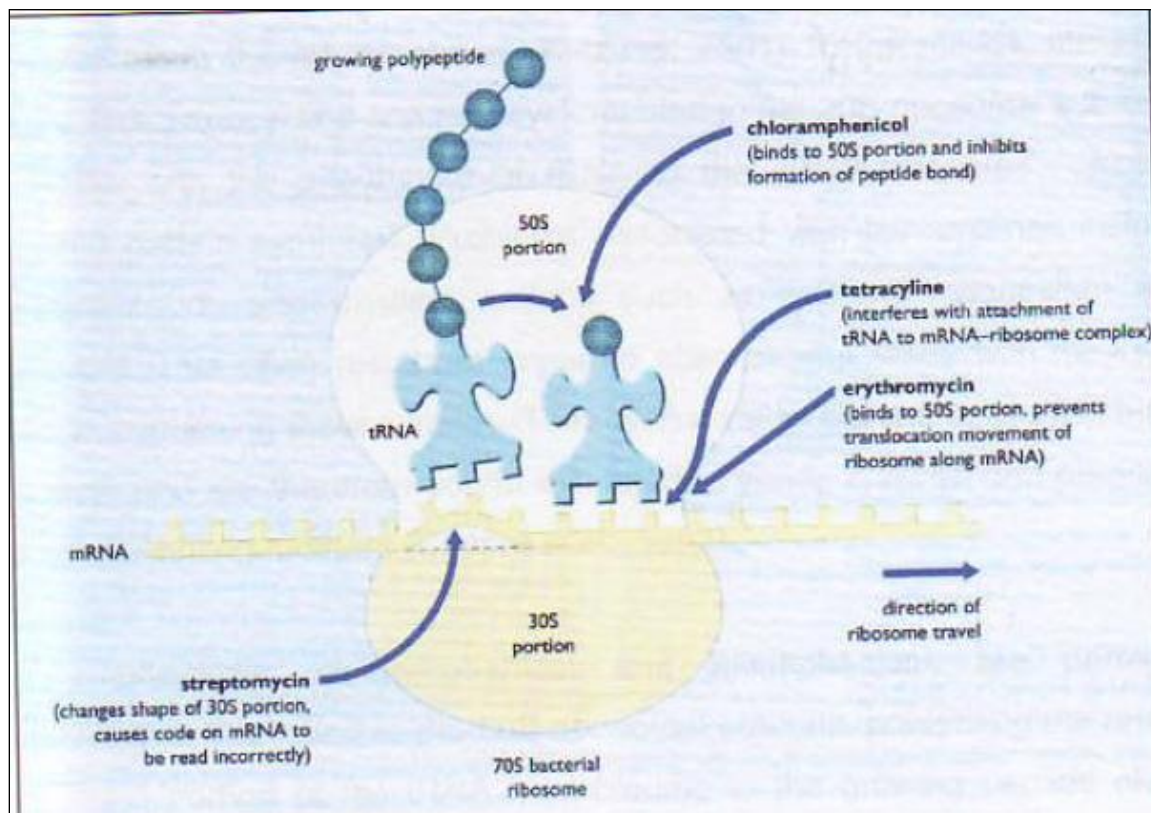


Figure 7.5 Inhibitors of protein synthesis (Page *et al.*, 1997).

7.1.5 Inhibitors of folate metabolism

Folates are precursors to the formation of purine basis in DNA, and although human cells have uptake mechanisms which enable the cell to utilise pre-formed folate for dietary intake, bacterial cells must synthesise their own from p-aminobenzoic acid (PABA). Thus, if the enzymes involved in folate synthesis are inhibited, the production of DNA will also be inhibited. Sulphonamides, (including sulphanilamide,

sulphamethoxazole and sulfadiazine), are structurally related to PABA (Figure 7.6), and compete with PABA binding preferentially to the enzyme, dihydropteroate synthase, which converts PABA into dihydrofolic acid (Figure 7.7). Trimethoprim also inhibits folate synthetase, by inhibiting the enzyme dehydrofolate reductase (Figure 7.7) in bacteria, with about 50000 times greater selectivity than the mammalian enzyme. This ultimately results in the inhibition of tetrahydrofolic acid synthesis, which is the precursor to purines (Katzung, 2009).

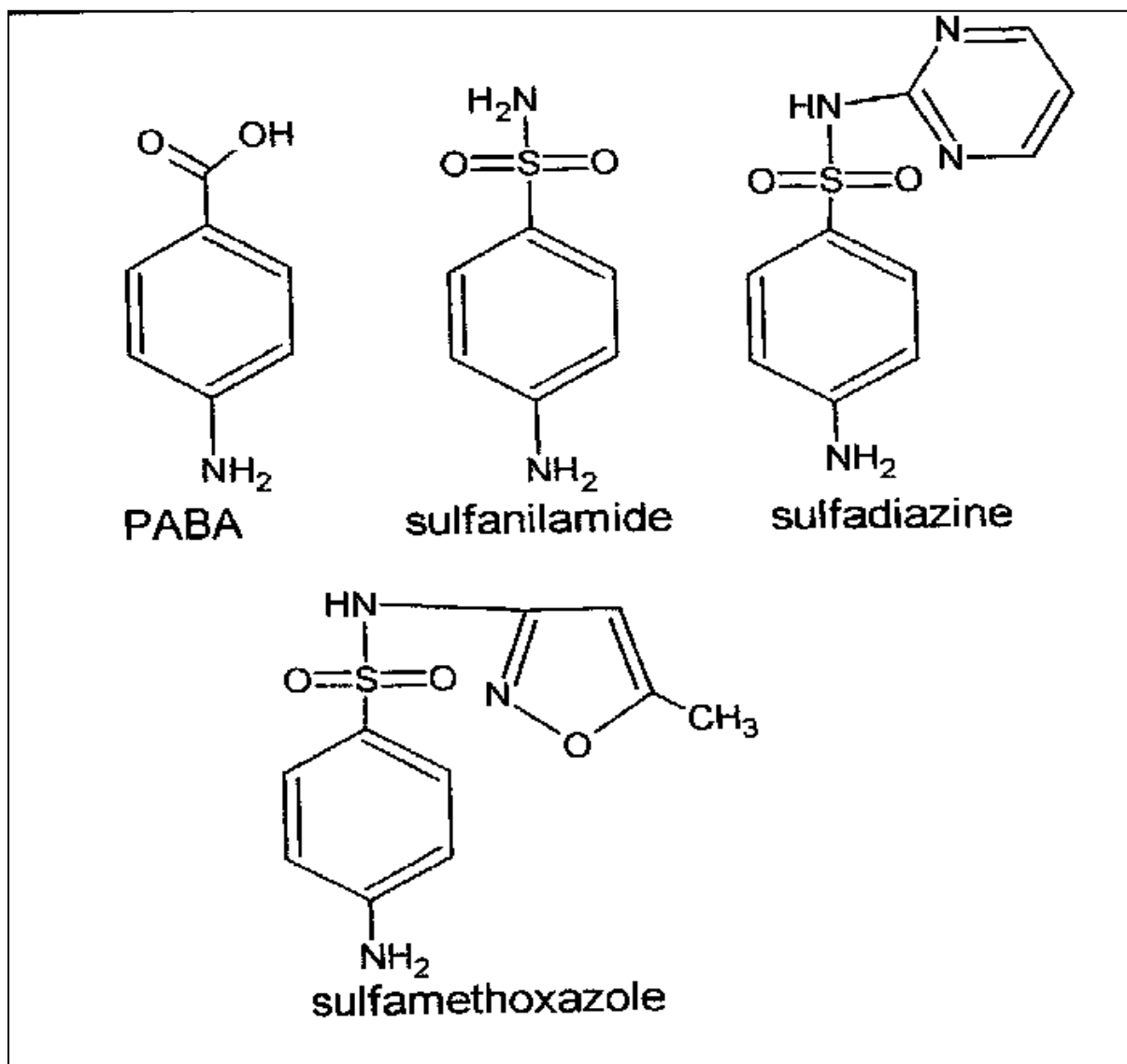


Figure 7.6 Structure of sulphonamides in comparison to p-aminobenzoic acid (PABA) (Katzung, 2009).

Although these agents result in impaired DNA synthesis, resistance develops rapidly, enabling bacteria to utilise other pathways to produce folates. This justifies the clinical use of a sulphonamide with trimethoprim in order to effectively inhibit folate synthesis. This results in the effects of these agents to move from being bacteriostatic individually to being bactericidal in combination (Katzung, 2009). Together these agents are effective against most Gram-negative and Gram-positive bacteria as well as *Chlamydia trachomatis* and some protozoa (Dipiro *et al.*, 2011).

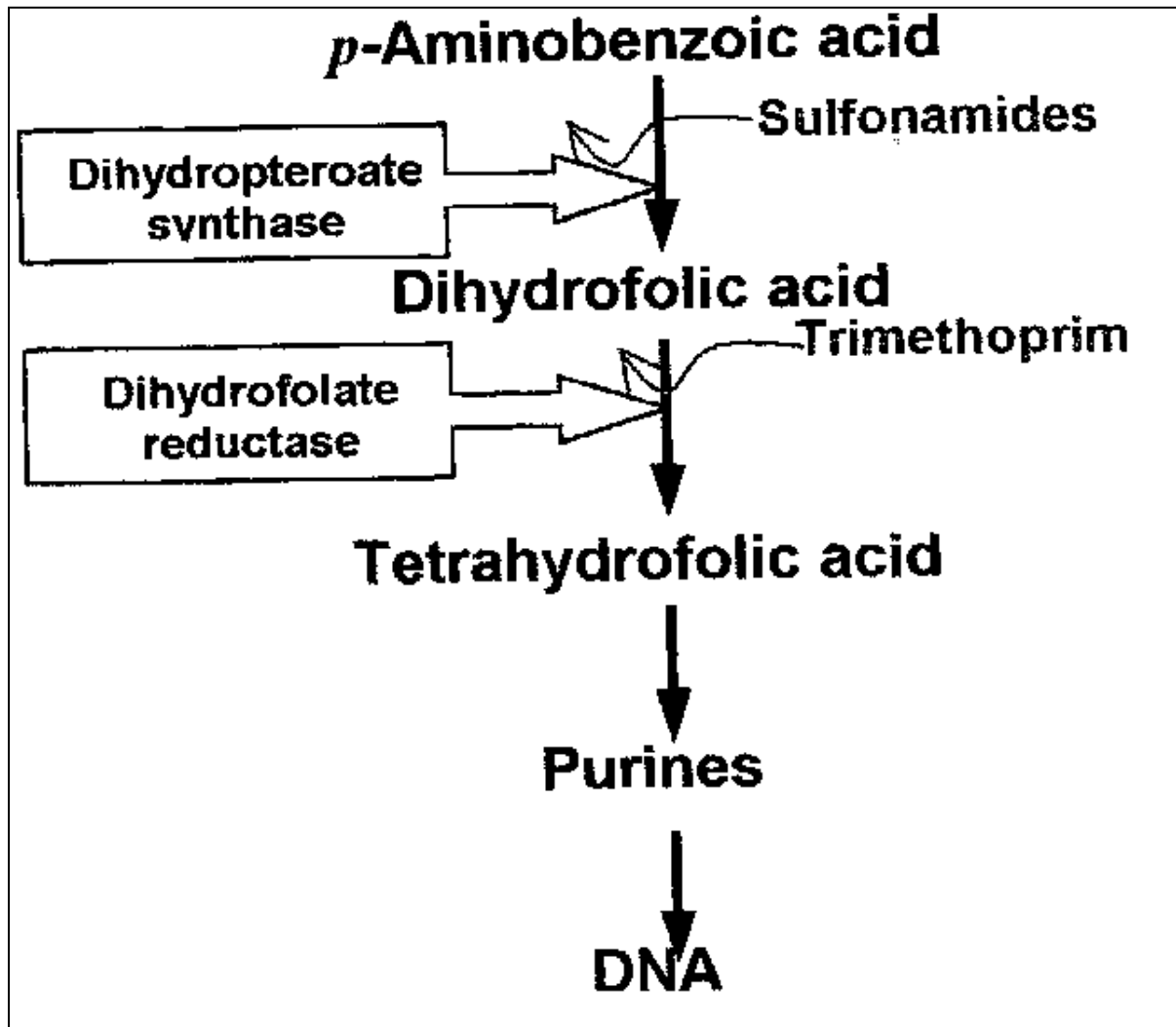


Figure 7.7 Folate metabolism (Katzung, 2009).

7.1.6 Inhibitors of DNA and RNA synthesis

DNA Gyrase inhibitors:

DNA gyrase inhibitors inhibit bacterial topoisomerase II (DNA gyrase). These agents include the quinolones, nalidixic acid, and the fluoroquinolones, (norfloxacin, ciprofloxacin, ofloxacin, levofloxacin and enoxacin) (Katzung, 2009).

RNA synthesis inhibitors:

Inhibitors of RNA synthesis block DNA-dependant RNA polymerase and include the rifamycins that result in the inhibition of RNA production and ultimately cell division and protein synthesis. Two agents fall within this class, Rifampicin and rifabutin. These agents are active against some conventional bacteria such as streptococci, *N. meningitidis*, *H. Influenzae* type B and *S. aureus*, but their primary indication is for the treatment of tuberculosis as well as other non-tubercular mycobacteria (Katzung, 2009).

7.1.7 Bacterial resistance

An increasingly alarming problem in clinical practice today, is bacterial resistance, where bacteria become or are inherently resistant to the effects of antibacterial agents resulting in severe uncontrollable infection.

7.1.8 Mechanisms of bacterial resistance

Two classifications of bacterial resistance can be identified, namely, innate and acquired. Innate refers to the intrinsic resistance a bacterium has based on the mechanisms of the drug, for example, if entry of the antibiotic into the cell required the presence of a specific transport mechanism which a certain bacteria does not possess, the resistance which the bacterium has for the drug is said to be innate. If however, the bacterium was susceptible, it acquires a gene that alters the pathways utilised by the drug in order to elicit its response, the resistance referred to be acquired. All antibiotics known have at least one strain of bacteria that is able to acquire resistance. Acquired resistance genes result in resistance by three main mechanisms, firstly, reduction in

permeability of the cell membrane, secondly preventing the entry of the antibiotic; and the production of bacterial enzymes which break down the drug and thirdly, mutations resulting in alteration of the drug's target site. Reduced permeability of bacterial membranes usually occurs in Gram-negative bacteria and alters the effects of antibiotics whose target site is inside the bacterial cell (Dipiro *et al.*, 2011).

7.1.9 Implications

The production of enzymes which breakdown or alter drug molecules into an inactive form, has become a significant problem with β -lactam antibiotics. Some strains of staphylococci have developed genes for the production of β -lactamase, which breakdown the β -lactam ring of penicillins and cephalosporins, resulting in resistance. This problem is of growing concern, as resistance to these agents due to β -lactamase production is becoming an enormous problem (Livermore, 2000).

The need for newer antibiotics acting by alternative mechanisms is of utmost importance in order to solve the problem of multi-drug resistant bacterial infection. The use of these agents must be prescribed under complete control and monitored carefully to ensure patients are effectively completing courses and eradicating all pathogenic bacteria, so that none survive to develop resistance.

Antimicrobial peptides have a great potential to be the next breakthrough class of antimicrobials (Hancock and Lehrer, 1998). Hundreds of peptide antibiotics have been described in the past half-century. They fall into two major classes: non-ribosomally synthesised peptides, such as the gramicidins, polymyxins, bacitracins, glycopeptides and ribosomally synthesised peptides. Non-ribosomally synthesised peptides are often drastically modified and are largely produced by bacteria, whereas the ribosomally synthesised peptides are produced by all species of life, including bacteria, as a major component of the natural host defence molecules of these species (Hancock and Chapple, 1999).

Many different types of organisms use antimicrobial peptides typically 20 to 40 amino acids in length, for defence against infection. Most are capable of rapidly killing a wide range of microbial cells. Epan and Vogel (1999) have classified antimicrobial peptides according to their structure into six extensive groups. The groups are classified as: amphipathic and hydrophobic helices; β -sheet peptides and small proteins; peptides with irregular amino acid composition; peptides with thioether rings; peptaibols; and macrocyclic cysteine knot peptides (Bradshaw, 2003; Epan and Vogel, 1999). Table 7.3 illustrates some features and examples of the different classified structural groups of antimicrobial peptides.

Table 7.3 Classification of antimicrobial peptides according to Epan and Vogel (1999)

Group	Features	Examples
Amphipathic and hydrophobic helices	Form membrane pores by end-to-end association (gramicidin A) or toroidal pores (alamethicin, magainin)	Gramicidin A Magainin Alamethicin
β -sheet peptides and small proteins	Often cyclical, ring structure formed by disulphide bonds or by cyclization of the peptide backbone	Tachyplesin Protegrin Gramicidin S Polymixin B Tyrocidin Defensins Thionins

Peptides with irregular amino acid composition	Frequently found to contain high levels of a single amino acid	Histatin PR-39 Prophenin Triitripticin Indolicidin
Peptides with thioether rings (lantibiotics)	Contain the unusual amino acids lanthionine and β -methyl lanthionine, as well as dehydrated residues	Nisin Z Cinnamycin
Peptaibols	Conformationally restricted, frequently as α - or 3_{10} -helix. Have a high proportion of α -amino-isobutyric acid residues. Derive their name from the 1,2-amino alcohol at the C-terminus	Trichogin Alamethicin
Macrocyclic cysteine knot peptides	Contain a cysteine knot motif in which a disulphide bond is threaded through two others	Circulin A Circulin B Cyclopsychotride Kalata

There are a number of reasons that make antimicrobial peptides particularly attractive as candidates for clinical development. Firstly, their selectivity. Many antimicrobial

peptides combine selective activity against prokaryotic cells with broad-spectrum activity. Secondly, their speed of action, by targeting the membranes on the outside of bacterial cells, antimicrobial peptides can be effective immediately, without the time-lag imposed by the need to be internalised to reach a receptor molecule. Thirdly, and probably the most attractive reason is that peptides have received so much attention in recent years because of the perturbation they cause to fundamental structural components of the bacterial cell. It is hoped that bacteria will not easily develop resistance against this mechanism of bacterial cell destruction (Bradshaw, 2003).

The concentration of antimicrobial peptide required to inhibit bacterial growth is typically in the micromolar range. This concentration drops to around 1 μM for the best synthetic analogues. These actions of antimicrobial peptides that act against bacterial cell membranes can be attributed to certain gross morphological features. These features includes: the helicity or negative charge of the peptides, their overall hydrophobicity, their hydrophobic moment and domain size, and their degree of amphipathicity (Bradshaw, 2003; Epan and Vogel, 1999).

A study conducted by Milne *et al.* (1998) indicated that the cyclic dipeptides cyclo(Trp-Pro), cyclo(Trp-Trp) and cyclo(Phe-Pro) were active against Gram-positive bacteria. Cyclo(Trp-Pro) was also effective against Gram-negative bacteria. This finding was followed by a study done by Graz *et al.* (1999), which further confirmed the potential of these cyclic dipeptides as antimicrobial agents. Since then, the antimicrobial potential of numerous other cyclic dipeptides has been investigated with some showing promising potential. Screening of cyclo(Phe-4Cl-Pro) and cyclo(D-Phe-4Cl-Pro) as potential antimicrobial agents was therefore warranted.

7.2 Experimental bacterial and fungal cultures

Cyclo(Phe-4Cl-Pro) and cyclo(D-Phe-4Cl-Pro) were tested against a broad spectrum of Gram-positive and Gram-negative bacteria, as well as a fungal microorganism to determine their potential antimicrobial activity.

7.2.1 Gram-positive Bacteria

7.2.1.1 Bacillus subtilis

Bacillus subtilis are gram-positive rods and is usually large with square ends. It is aerobic, sometimes facultative, and catalase positive, a spore forming chemoheterothroph that is mostly motile and peritrichously flagellated (Bauman *et al.*, 2004)

7.2.1.2 Staphylococcus aureus

Staphylococcus aureus is a Gram-positive coccus that is non-motile and non-spore forming and can grow either aerobically or anaerobically. Some strains have notable capsules, it is a spherical-shaped bacterium and is the causative agent of a wide variety of human infections (Bauman *et al.*, 2004; Prescott *et al.*, 2005). *Staphylococcus aureus* cells are characteristically clustered in grapelike arrangements with the cell size ranging from 0.5 – 1.0 µm in diameter, they are usually salt tolerant (Bauman *et al.*, 2004). The diagnosis of a staphylococcal infection involves the identification of Gram-positive bacteria in grapelike arrangements isolated from pus, blood or other body fluids (Bauman *et al.*, 2004). *S. aureus* can then be distinguished from other staphylococci by its ability to clot plasma, since *S. aureus* secretes an enzyme called coagulase which activates the clotting mechanism of normal plasma (Bauman *et al.*, 2004).

7.2.2 Gram-negative Bacteria

7.2.2.1 Escherichia coli

Coliforms are defined as aerobic or facultatively anaerobic, Gram-negative, rod-shaped bacteria that ferment lactose to form gas within 48 hours of being placed in lactose broth at 35 °C. They are commonly found in the intestinal tracts of animals and humans, in soil, and on plants and decaying vegetation (Prescott *et al.*, 2005). *Escherichia coli* is used as an indicator organism in determining the amount of faecal contamination in food and water, since it is one of the predominant facultative anaerobic bacteria of the intestinal tract (Bauman *et al.*, 2004).

7.2.2.2 *Pseudomonas aeruginosa*

Pseudomonas aeruginosa consists of straight or slightly curved Gram-negative rods. Their length varies from 0.5 – 1.0 µm by 1.5 – 5.0 µm, they are motile by one or several polar flagella and lack prosthecae or sheaths. *Aeruginosa* is a chemoheterotroph and is capable of carrying out respiratory metabolism with oxygen (and sometimes nitrate) as the electron acceptor (Prescott *et al.*, 2005). *Aeruginosa* is a motile non-fermentative bacillus, and an obligate aerobe which grows well in most culture media (Bauman *et al.*, 2004).

7.2.3 Fungi

7.2.3 .1 *Candida albicans*

Candida albicans is unicellular and usually appear as oval to round, yeast-like cells that reproduce sexually by budding (Bauman *et al.*, 2004). They are not dimorphic, although chains of cells, each measuring 4 – 6 µm in diameter, sometimes link together, forming structures known as pseudohyphae. *C. albicans* often forms part of the normal microbionta of the skin and the mucous membranes of the mouth, vagina, and intestinal tract (Prescott *et al.*, 2005). Disease can only result when a major change in normal flora or a disturbance of the normal immune response occurs. Under such conditions candida species may multiply rapidly and produce candidiasis (Prescott *et al.*, 2005). Most infections involves the skin or mucous membranes, but can on occasion produce more serious diseases, such as endocarditis, septicaemia, protracted urinary tract infection and oesophagitis (Prescott *et al.*, 2005). Immunocompromised individuals are more prone to such systemic diseases (Bauman *et al.*, 2004).

7.3 Control agents used to compare the antimicrobial activity of the cyclic dipeptides

7.3.1 Amoxicillin

Penicillins are bactericidal, and act by the inhibition of bacterial cell wall synthesis in susceptible organisms. Amoxicillin is a hydroxylated derivative of ampicillin, with improved oral bioavailability and similar spectrum of activity. It is the drug of choice for

otitis media and bacterial sinusitis, and is widely used in the treatment of lower respiratory tract infections. Penicillin remains the agent of choice for numerous infections caused by Gram-positive, Gram-negative bacteria and anaerobes. These include *Streptococcus pyogenes*, *S. pneumoniae*, viridans and non-enterococcal group D streptococci, anaerobic streptococci, *Neisseria meningitidis*, Actinomyces, most clostridia, *Corynebacterium diphtheriae*, *Treponema pallidum* and leptospira (Katzung, 2009).

7.3.2 Chloramphenicol

Chloramphenicol is a broad-spectrum, mainly bacteriostatic antibiotic. Chloramphenicol is a potent inhibitor of microbial protein synthesis. It binds reversibly to the 50S subunit of the bacterial ribosome, and inhibits the peptidyl transferase step of protein synthesis. It is active against staphylococci, streptococci, *Haemophilus* species, anaerobes, rickettsiae, *chlamydia* and *Mycoplasma*. It is however, only reserved for serious infections, or cases in which tetracyclines are contra-indicated (Katzung, 2009).

7.4 Methodology

Methods employed by Stevens and Olsen (1993), Freimoser *et al.* (1999), Kilian (2002) and Janse van Rensburg (2006) were adapted to develop a method to test the antimicrobial activity of cyclo(Phe-4Cl-Pro) and cyclo(D-Phe-4Cl-Pro).

7.4.1 Laboratory conditions

The following precautions were taken, in order to maintain a clean and sterile working environment. Powder-free latex gloves were used when working with any chemicals or equipment. The gloves were sprayed with 70% ethanol at regular intervals in order to keep them dry and sterile. All other equipment was washed with analytical grade water (AGW), and sterilised by moist heat in an autoclave (Model HA-3D, Hirayama Manufacturing Corp., Japan) at 121 °C for 15 minutes. All laboratory benches were swabbed with 70% ethanol prior to use, and at regular intervals during, and after working. Single-strength nutrient broth (Biolab, Merck, Germany) and phosphate-

buffered saline (PBS) was autoclaved at 121 °C for 15 minutes and filtered through 0.22 µm Millipore™ cameo 25AS acetate filters (Millipore™, USA) prior to use, in order to render them pyrogen-free and sterile.

7.4.2 Preparations of solutions

7.4.2.1 Negative controls

The negative controls, consisting of cultures of the relevant test organism in sterile single-strength nutrient broth and 2% dimethyl sulphoxide (DMSO) (final concentration) were utilized to present 100% viability of the test cultures. DMSO was included to assist the solubilisation of the relevant cyclic dipeptides to be tested.

7.4.2.2 Positive controls

Aseptic preparation of the positive control, chloramphenicol (Sigma chemicals Co., USA) at concentrations of 200 µm and 100 µm (final concentrations of 0.25 mg/ml and 0.5 mg/ml, respectively) in single-strength nutrient broth were utilized to test the viability of Gram-negative bacteria. 5% DMSO (final concentration) was added, and together with vortex agitation (Vortex mixer BM300, Laboratory supplies (Pty) Ltd, SA) aided in the solubilisation of chloramphenicol. For Gram-positive organisms, amoxicillin was used as the positive control at a concentration of 1mg/ml and 0.5mg/ml. The positive controls were made up to volume using sterile single-strength nutrient broth, filter-sterilized through 0.22 µm acetate filters into sterile 2000 µl Eppendorf tubes (Eppendorf AG, Germany), and stored at 4 °C until needed.

7.4.2.3 Cyclic dipeptide solutions

Cyclo(Phe-4Cl-Pro) and cyclo(D-Phe-4Cl-Pro) were aseptically prepared prior to use. 5% DMSO (final concentration) was added and together with vortex agitation aided in the solubilisation of the cyclic dipeptides. The solution was made up with reverse osmosis water to give a stock concentration of 2 mM for each cyclic dipeptide. The 2mM stock solutions were then diluted accordingly. Following this, the cyclic dipeptide

solutions were filtered through 0.22 µm acetate filters into sterile Schott bottles and stored at 4 °C until needed.

7.4.2 .4 MTT dye solution

3-(4,5 dimethylthiazol-2-yl)-2,5-diphenyltetrazolium bromide (MTT) is a monotetrazolium, water soluble salt, yielding a yellowish solution when prepared in media or salt solutions lacking phenol red. Dissolved MTT is converted to an insoluble purple formazan by cleavage of the tetrazolium ring by dehydrogenase enzymes. This conversion is only caused by active mitochondrial dehydrogenase of living cells, and not dead cells. The water insoluble formazan can then be dissolved using DMSO or other relevant solvents and the dissolved material is then measured spectrophotometrically yielding absorbance as a function of the converted dye. Absorbance of the converted dye is measured at a wavelength of 540 nm with background subtraction at 630-690 nm.

MTT (Sigma chemicals Co., USA) was dissolved in 0.1 M PBS (pH 7.4) to give a stock concentration of 0.5 mg/ml. The solution was filter-sterilized through a 0.22 µm acetate filter and stored, for not more than two weeks, in a sterile Schott bottle at 4 °C and away from light until needed.

7.5 Test organism cultures

The test organism cultures consisted of Gram-positive *B. subtilis* and *S. aureus*; Gram-negative *E. coli* and *P. aeruginosa*; and the fungus *C. albicans*. The test cultures were obtained from the department of Medical Technology, at the Nelson Mandela Metropolitan University. Each test organism culture was scraped off its relevant agar plate using a flame sterilized platinum loop, and inoculated into 5 ml of single strength nutrient broth (for bacteria) or potato dextrose agar (Merck, Germany) (for *C. albicans*). The cultures were then incubated overnight at 37 °C (for bacteria) or 28 °C (for *C. albicans*) in a Labcon[®] orbital shaker (Labcon[®], SA) at 100 rpm.

The overnight cultures were subcultured by transferring 100 µl of the relevant test organism into 10 ml of sterile Mueller-Hinton broth (Merck, Germany). The sub-cultured cultures were then incubated for a further 2 hours at 37 °C (for bacteria) or 28 °C (for *C. albicans*) in the orbital shaker at 100 rpm.

7.6 Standardisation of the inoculum

In order to improve the reproducibility of the assays, the starting concentrations of all cultures were kept constant by standardising the inoculums. The standardisation procedure was followed for all cultures, prior to each assay performed on separate days. The minimum inhibitory concentration (MIC) is defined as the lowest concentration of an antimicrobial agent that inhibits growth of a micro-organism. MIC is an important research tool that is used to determine the *in vitro* antimicrobial activity of newly synthesised agents (Andrews, 2001). One of the methods used to determine MIC is microdilution testing which uses liquid growth medium, serial dilutions of the antimicrobial agents and standard inoculums of bacteria (Dipiro *et al.*, 2011). A flame sterilised platinum loop was used to scrape the test organisms off from the relevant agar plates. The organisms were then inoculated into 15 ml sterile Mueller-Hinton broth and incubated at 37 °C (for bacteria) or 28 °C (for *C. albicans*) in an orbital shaker (Labcon Incubator Labtec (PTY) Ltd, SA) at 100 rpm for 24 hours. The cultures were sub-cultured by transferring 100 µl of test organism into 15 ml sterile Mueller-Hinton broth and incubated for 16 hours at 37 °C (for bacteria) or 28 °C (for *C. albicans*) in an orbital shaker (Labcon Incubator Labtec (PTY) Ltd, SA) at 100 rpm. The turbidity of the test cultures was thereafter measured at 540 nm for bacteria and 600 nm for *C. albicans* using sterile Mueller-Hinton broth as a blank.

7.7 MTT linearity assay

A volume of 500 µl of each of the standardised inoculums and their respective serial dilutions were placed in separate Eppendorf tubes and 40 µl of MTT tetrazolium dye at a concentration of 0.5 mg/ml was added. To obtain a zero time reading, absorbance was immediately measured on a microplate reader at 540 nm for bacteria and 600 nm for *C. albicans*. The Eppendorf tubes were then incubated at 37 °C (for bacteria) or 28

°C (for *C. albicans*) in an orbital shaker for four hours. Tubes were subsequently removed from the orbital shaker and centrifuged using an Eppendorf® centrifuge 5804R (Eppendorf®, Germany) at 14350 x g for 7 minutes to pellet the microorganisms. The supernatant liquid in each Eppendorf tube was removed and discarded. The formazan product present was dissolved in 500 µl DMSO. Rupture of microorganisms was facilitated by vortexing of suspensions. Tubes were centrifuged again at 14350 x g for 5 minutes to pellet the resultant debris. 40 µl of each dye solution was transferred in triplicate to the wells of 96-well flat bottom microtitre plates (Castor, Corning). The microtitre plates were then read at 540 nm, with a background subtraction at 690 nm to account for cellular debris, utilising a Multiscan MS® (version 4.0) Labsystem® type 352 microtitre plate spectrophotometer (Multiscan MS®, England). Experiments were conducted in triplicate.

Following the initial adjustments of the test cultures to an absorbance reading of 0.22 AU, further serial dilutions of each test culture was made as follows:

0.1 ml standardised culture (0.22 AU) into 9.9 ml sterile water → A

0.1 ml A into 9.9 ml sterile water → B

0.1 ml of B into 9.9 ml of sterile water →C

0.1 ml of C into 9.9 ml of sterile water →D

0.1 ml of each of the dilutions was subsequently plated onto sterile nutrient agar plates for bacteria, and potato dextrose agar plates for the yeast. Plating and counting were performed in triplicate and the numbers of micro-organisms per millilitre in the standardised culture were subsequently calculated.

7.8 Antimicrobial assay

From the counts performed (Section 7.7), the test cultures were diluted to obtain 1×10^6 colony forming units CFU/ml (Freimoser *et al.*, 1999). The calculated volumes were made up to 10 ml using Mueller-Hinton broth.

A volume of 50 μ l of each test organism was pipette into a 96-well microplate and thereafter, 50 μ l of either of the stock solutions of the two cyclic dipeptides at concentrations of 1 mM and 2 mM were added to the wells, which resulted in a final concentration of 0.5 mM and 1 mM in each well. 50 μ l of each of the positive controls, were pipette into the respective cells according to the test organism cultures, giving final concentration of 0.25 mg/ml and 0.5 mg/ml in the respective wells. 50 μ l of the negative control (7.4.2.1) was pipette to separate wells to indicate 100% viability of the test organism growth.

The 96-well microplates were then incubated for 24 hours at 37 °C for bacteria and 28 °C for *C. albicans* in an orbital shaker at 100 rpm. 40 μ l of MTT at a concentration of 0.5 mg/ml was added to each of the cells after incubation. In order to obtain a zero reading time, absorbance was immediately measured on a microplatereader at 540 nm for bacteria and 600 nm for *C. albicans*. Following this the 96-well microplates were incubated for four hours, in an orbital shaker at 100 rpm to allow for the metabolic reduction of MTT. This was followed by centrifugation in an Eppendorf centrifuge at 3000 rpm for seven minutes to pellet the insoluble formazan product (Freimoser *et al.*, 1999; Stevens and Olsen, 1993). The supernatant was aspirated from each of the wells and discarded. 90 μ l of DMSO was subsequently added to each well to solubilise the formazan product and placed on a plate shaker for four minutes. The absorbance was read immediately at 540 nm for bacteria, and 600 nm for *C. Albicans*.

7.9 Statistical analysis

Results were obtained as triplicate values and represented as a mean \pm standard deviation (SD). Percentage growth inhibition, after 24 hours of exposure to the cyclic

dipeptides, was calculated with reference to the negative control cultures and compared to the positive controls.

Percentage growth inhibition was calculated as follows:

$$\% \text{ inhibition} = \frac{NEG_{GROWTH} - DRUG_{GROWTH}}{NEG_{GROWTH}} \times 100$$

WHERE $NEG_{GROWTH} = NEG_{T=24} - NEG_{T=0}$

$$DRUG_{GROWTH} = DRUG_{T=24} - DRUG_{T=0}$$

AND $NEG_{T=24}$ = Absorbance at 540 nm after incubation for control

$DRUG_T$ = Absorbance at 540 nm for drug after incubation

$DRUG_0$ = Absorbance at 540 nm for drug prior to incubation.

Data were represented graphically with the aid of statistical software packages, Microsoft Excel[®] (Version 2007) and GraphPad Prism[®] (version 5). In order to determine whether the cyclic dipeptides under investigation caused statistically significant reduction in cell viability relative to the negative control, Student's *t*-tests were performed on each concentration of the cyclic dipeptides. Calculated P-values of less than 0.05 were defined as statistical significant. MTT linearity was determined by performing a linear regression analysis, where linearity was defined as a Spearman's correlation coefficient (R^2) of between 0.9 and 1.

7.10 Results and discussion

7.10.1 MTT linearity assay

A linear relationship between the number of viable organisms and the intensity of MTT–formazan produced was observed with all organisms tested (Figure 7.8 to 7.12). For all the organisms, the correlation values exceeded 0.95.

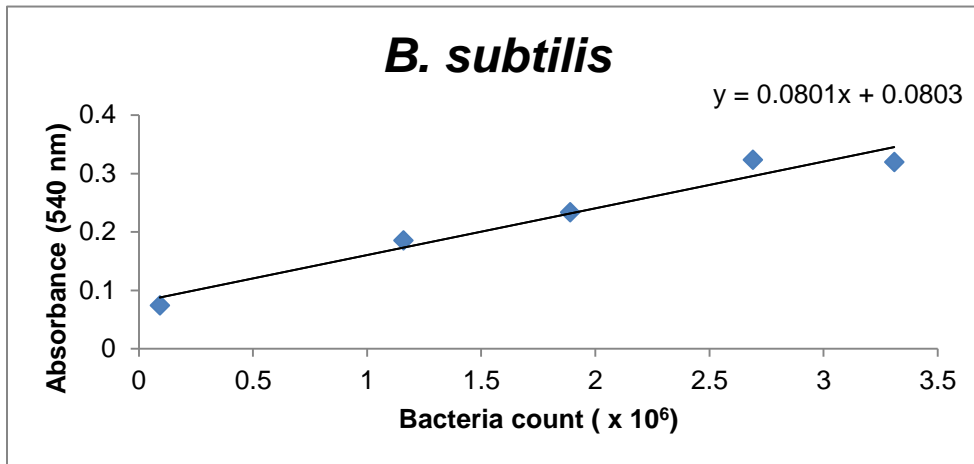


Figure 7.8 *B. subtilis* linearity of MTT against bacteria count ($R^2 = 0.958$)

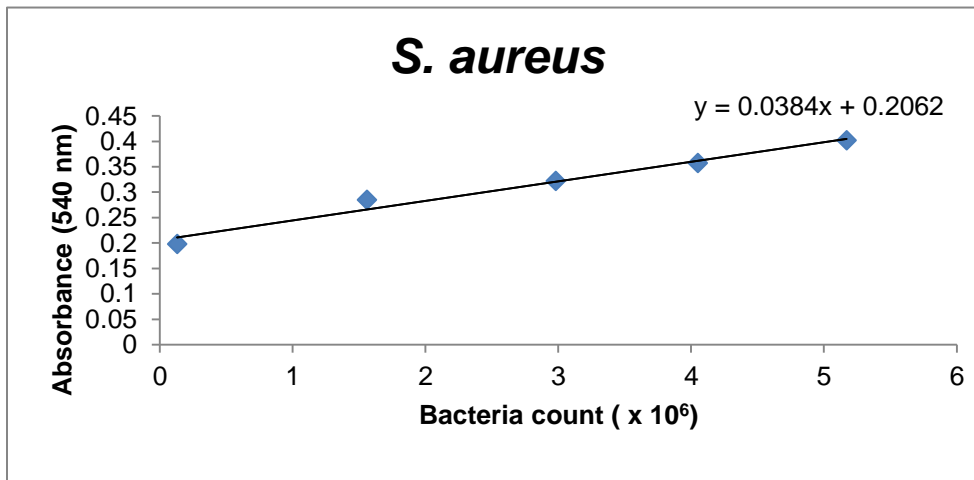


Figure 7.9 *S. aureus* linearity of MTT against bacteria count ($R^2 = 0.976$)

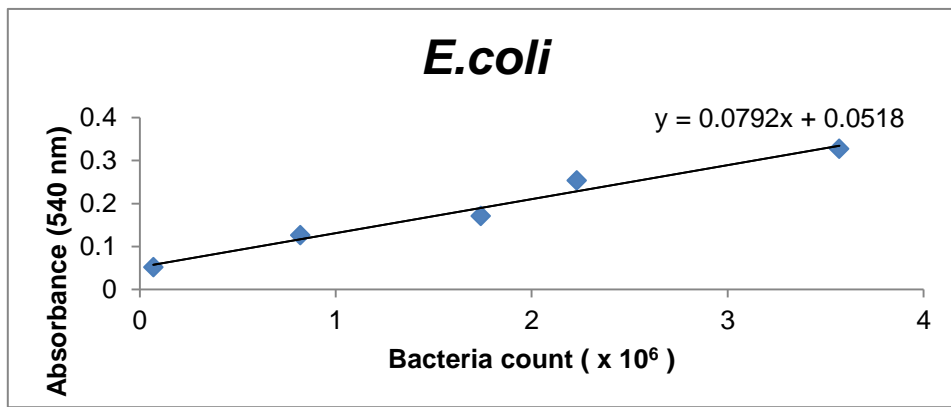


Figure 7.10 *E. coli* linearity of MTT against bacteria count ($R^2 = 0.974$)

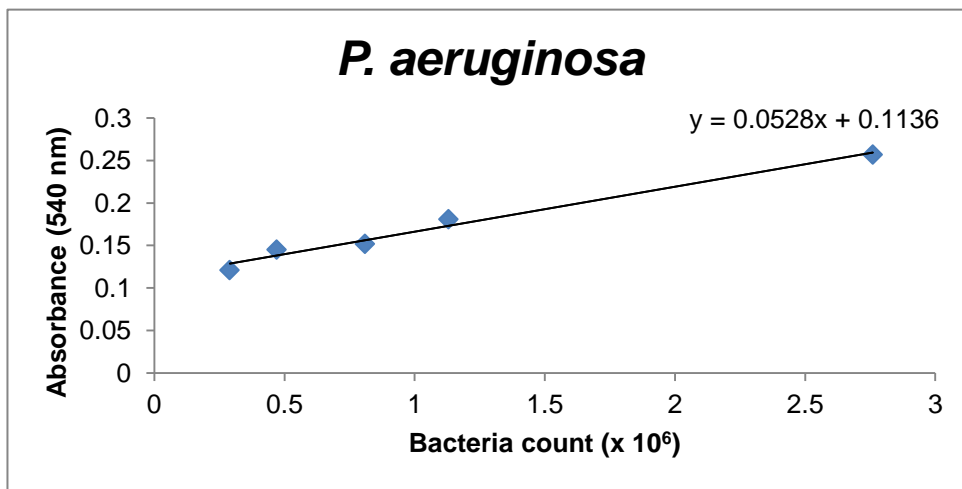


Figure 7.11 *P. aeruginosa* linearity of MTT against bacteria count ($R^2 = 0.982$)

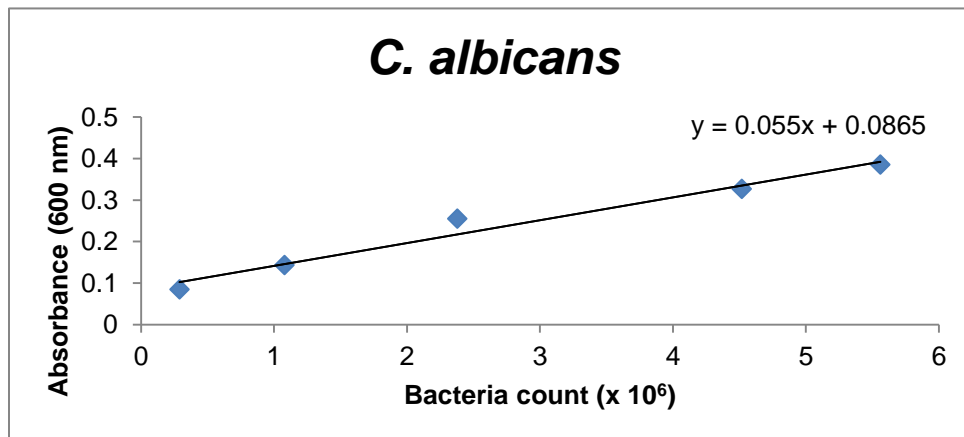


Figure 7.12 *C. albicans* linearity of MTT against bacteria count ($R^2 = 0.969$)

7.10.2 Cyclic dipeptide antimicrobial assay

The antimicrobial effects produced by the different screening concentrations of cyclo(D-Phe-4Cl-Pro), cyclo(Phe-4Cl-Pro), chloramphenicol and amoxicillin on *B. subtilis* growth after 24 hours of exposure to the compounds are illustrated in Figure 7.13. To determine if the growth inhibiting effects produced by chloramphenicol, amoxicillin and the cyclic dipeptides were statistically different compared to the normal growth seen in the negative controls, Student's t-tests were performed on all concentrations of the cyclic dipeptide, chloramphenicol and amoxicillin. P-values of less than 0.05 were defined as an indication of a statistical significant difference between the means of the compounds and the negative controls. Percentage growth inhibition produced by all concentrations of the cyclic dipeptides was also compared to that of chloramphenicol and amoxicillin. Percentage growth inhibition produced by all screening concentrations of cyclo(D-Phe-4Cl-Pro) and cyclo(Phe-4Cl-Pro), was found to be notably less than that produced at both concentrations for chloramphenicol and amoxicillin. Chloramphenicol, at concentrations of 0.5 mg/ml and 0.25 mg/ml exhibited growth inhibition of $83.61 \pm 4.410\%$ ($P < 0.0085$) and $68.28 \pm 2.945\%$ ($P < 0.0103$), respectively. Amoxicillin at concentrations of 1 mg/ml and 0.5 mg/ml exhibited growth inhibition of $50.61 \pm 4.410\%$ ($P < 0.0316$) and $57.55 \pm 2.350\%$ ($P < 0.0144$), respectively while cyclo(D-Phe-4Cl-Pro) at concentrations of 1 mM, 0.5 mM, display growth inhibition of $17.83 \pm 5.500\%$ ($P = 0.8570$), $15.00 \pm 1.335\%$ ($P = 0.7907$). Cyclo(Phe-4Cl-Pro) at concentrations of 1 mM, 0.5 mM, exhibited growth inhibition of $18.27 \pm 2.390\%$ ($P = 0.7438$), $12.33 \pm 2.000\%$ ($P = 0.4900$). Although cyclo(D-Phe-4Cl-Pro) and cyclo(Phe-4Cl-Pro) produced statistically significant inhibition of growth, at all concentrations, relative to the negative control, the effects were very limited compared to the effects produced by chloramphenicol and amoxicillin. The effects produced by cyclo(D-Phe-4Cl-Pro), cyclo(Phe-4Cl-Pro), chloramphenicol and amoxicillin, are represented in Table 7.4

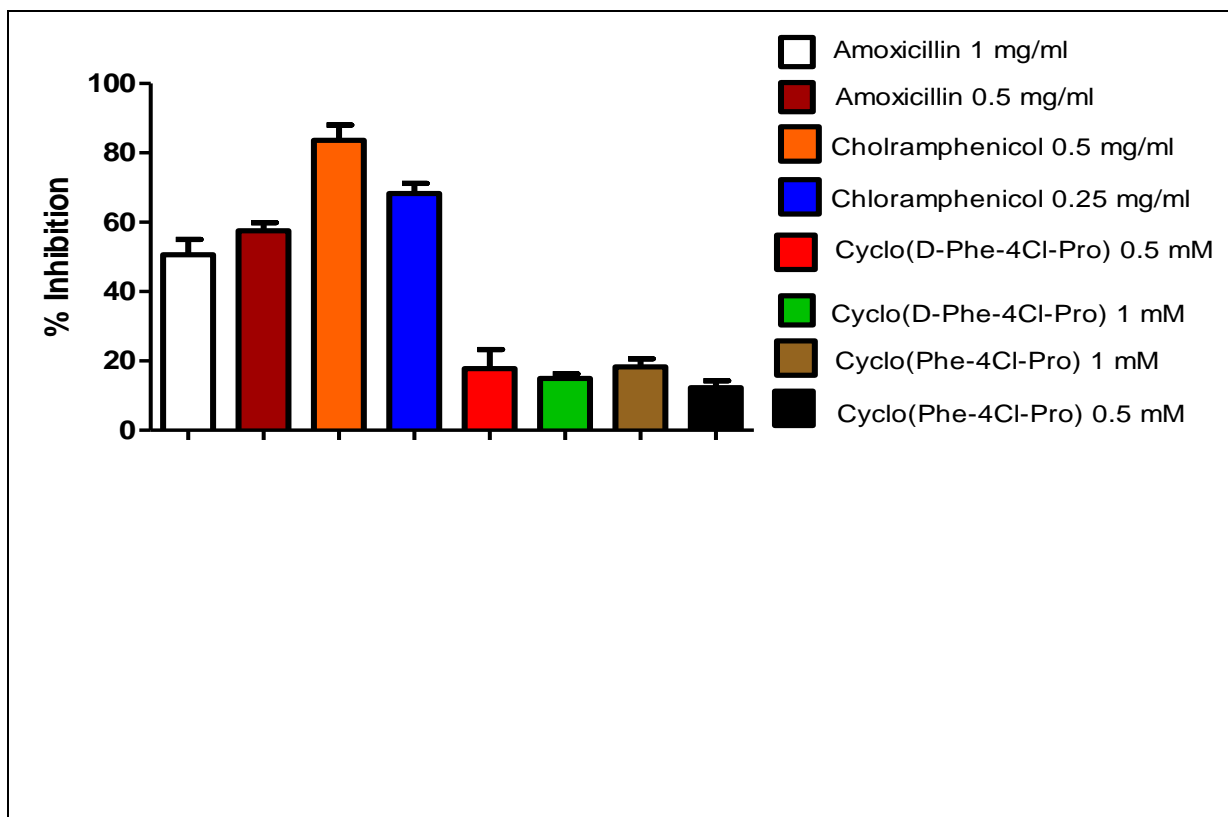


Figure 7.13 Percentage growth inhibition of *B. subtilis* after 24 hour exposure to cyclo(D-Phe-4Cl-Pro), cyclo(Phe-4Cl-Pro), chloramphenicol and amoxicillin

Table 7.4 Percentage growth inhibition of *B. subtilis* after 24 hour exposure to cyclo(D-Phe-4Cl-Pro), cyclo(Phe-4Cl-Pro), chloramphenicol and amoxicillin

Agent	Concentration	Percentage inhibition (%)	P-value
Amoxicillin	1 mg/ml	50.61 ± 4.410	0.0316
	0.5 mg/ml	57.55 ± 2.350	0.0144

Chloramphenicol	0.5 mg/ml	83.61 ± 4.410	0.0085
	0.25 mg/ml	68.28 ± 2.945	0.0103
Cyclo(D-Phe-4Cl-Pro)	1 mM	17.83 ± 5.500	0.8570
	0.5 mM	15.00 ± 1.335	0.7907
cyclo(Phe-4Cl-Pro)	1 mM	18.27 ± 2.390	0.7438
	0.5 mM	12.33 ± 2.000	0.4900

The antimicrobial effects produced by the different screening concentrations of cyclo(D-Phe-4Cl-Pro), cyclo(Phe-4Cl-Pro), chloramphenicol and amoxicillin on *S. aureus* growth after 24 hours of exposure to the compounds are illustrated in Figure 7.14. To determine if the growth inhibiting effects produced by chloramphenicol, amoxicillin and the cyclic dipeptides were statistically different compared to the normal growth seen in the negative controls, Student's t-tests were performed on all concentrations of the cyclic dipeptides, chloramphenicol and amoxicillin. P-values of less than 0.05 were defined as an indication of a statistical significant difference between the means of the compounds and the negative controls. Percentage growth inhibition produced by all concentrations of the cyclic dipeptides was also compared to that of chloramphenicol and amoxicillin. Percentage growth inhibition produced by all screening concentrations of cyclo(D-Phe-4Cl-Pro) and cyclo(Phe-4Cl-Pro) was found to be notably less than that produced at both concentrations for chloramphenicol and amoxicillin. Chloramphenicol, at concentrations of 0.5 mg/ml and 0.25 mg/ml caused growth inhibition of $72.60 \pm 6.600\%$ ($P = 0.00344$) and $69.61 \pm 1.610\%$ ($P = 0.0177$), respectively. Amoxicillin at concentrations of 1 mg/ml and 0.5 mg/ml exhibited growth inhibition of $26.40 \pm 5.600\%$ ($P = 0.0501$) and $58.60 \pm 1.300\%$ ($P = 0.0304$) respectively while cyclo(D-Phe-4Cl-Pro)

at concentrations of 1 mM and 0.5 mM, exhibited growth inhibition of $68.00 \pm 2.665\%$ ($P = 0.0106$), $22.17 \pm 1.165\%$ ($P = 0.05362$). Cyclo(Phe-4Cl-Pro) at concentrations of 1 mM and 0.5 mM, exhibited growth inhibition of $12.22 \pm 2.110\%$ ($P = 0.0062$) and $11.33 \pm 9.00\%$ ($P = 0.0340$). Although cyclo(D-Phe-4Cl-Pro) and cyclo(Phe-4Cl-Pro), produced statistically significant inhibition of growth, at all concentrations, relative to the negative control, the effects were very limited compared to the effects produced by chloramphenicol and amoxicillin. The effects produced by cyclo(D-Phe-4Cl-Pro), cyclo(Phe-4Cl-Pro), chloramphenicol and amoxicillin, are represented in Table 7.5

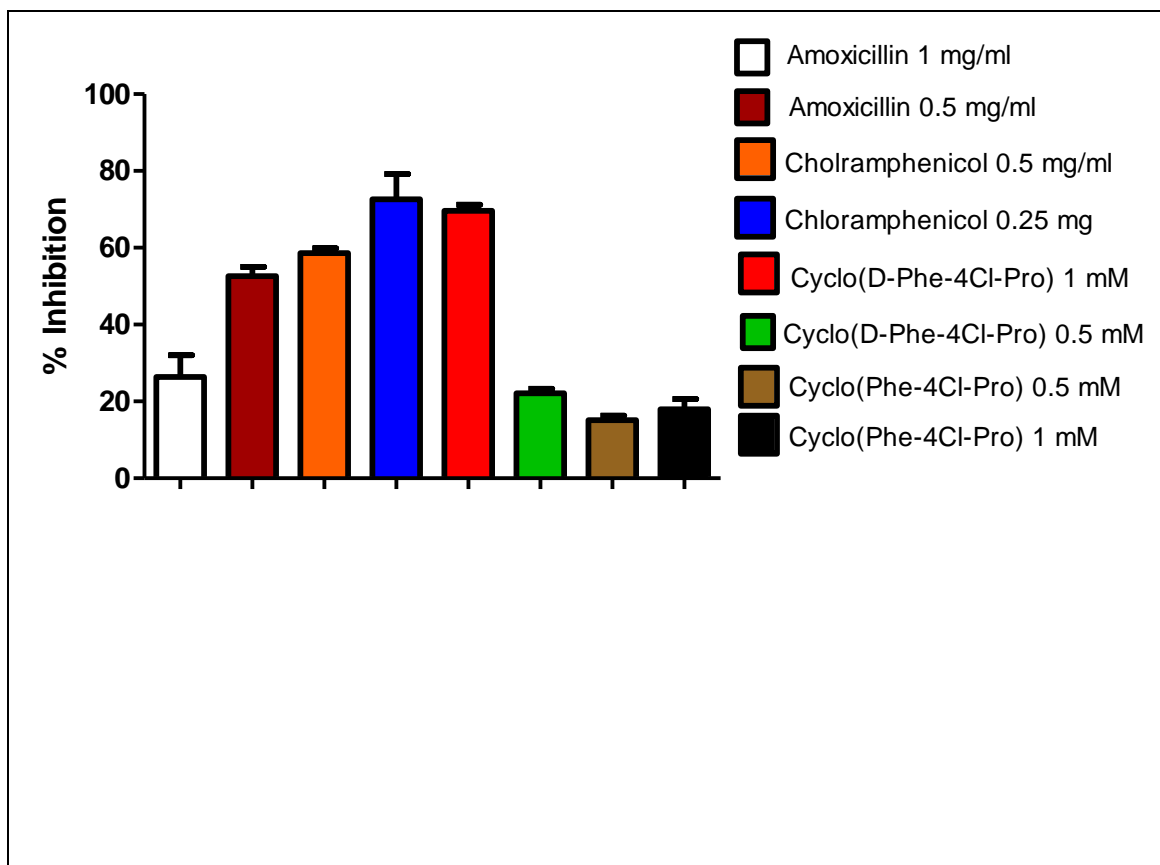


Figure 7.14 Percentage growth inhibition of *S. aureus* after 24 hour exposure to cyclo(D-Phe-4Cl-Pro), cyclo(Phe-4Cl-Pro), chloramphenicol and amoxicillin

Table 7.5 Percentage growth inhibition of *S. aureus* after 24 hour exposure to cyclo(D-Phe-4Cl-Pro), cyclo(Phe-4Cl-Pro), chloramphenicol and amoxicillin

Agent	Concentration	Percentage inhibition (%)	P-value
Amoxicillin	1 mg/ml	26.40 ± 1.5.600	0.0501
	0.5 mg/ml	58.60 ± 1.300	0.0304
Chloramphenicol	0.5 mg/ml	72.60 ± 6.600	0.00344
	0.25 mg/ml	69.61 ± 1.610	0.0177
Cyclo(D-Phe-4Cl-Pro)	1 mM	68.00 ± 2.665	0.0106
	0.5 mM	22.17 ± 1.165	0.05362
Cyclo(Phe-4Cl-Pro)	1 mM	12.22 ± 2.110	0.0062
	0.5 mM	11.33 ± 9.000	0.0340

The antimicrobial effects produced by the different screening concentrations of cyclo(D-Phe-4Cl-Pro), cyclo(Phe-4Cl-Pro), chloramphenicol and amoxicillin on *E. coli* growth after 24 hours of exposure to the compounds are illustrated in Figure 7.15. To determine if the growth inhibiting effects produced by chloramphenicol, amoxicillin and

the cyclic dipeptides were statistically different compared to the normal growth seen in the negative controls, Student's t-tests were performed on all concentrations of the cyclic dipeptide, chloramphenicol and amoxicillin. P-values of less than 0.05 were defined as an indication of a statistical significant difference between the means of the compounds and the negative controls. Percentage growth inhibition produced by all concentrations of the cyclic dipeptides was also compared to that of chloramphenicol and amoxicillin. Percentage growth inhibition produced by all screening concentrations of cyclo(D-Phe-4Cl-Pro) and cyclo(Phe-4Cl-Pro), was found to be notably less than that produced at both concentrations for chloramphenicol and amoxicillin. Chloramphenicol, at concentrations of 0.5 mg/ml and 0.25 mg/ml exhibited growth inhibition of $78.50 \pm 6.165\%$ ($P < 0.0312$) and $69.66 \pm 0.4350\%$ ($P < 0.0277$), respectively. Amoxicillin at concentrations of 1 mg/ml and 0.5 mg/ml exhibited growth inhibition of $73.25 \pm 4.350\%$ ($P < 0.0309$) and $68.89 \pm 1.335\%$ ($P < 0.0293$), respectively while cyclo(D-Phe-4Cl-Pro) at concentrations of 1 mM, 0.5 mM, exhibited growth inhibition of $25.83 \pm 0.500\%$ ($P = 0.7724$) and $11.50 \pm 0.8350\%$ ($P = 0.2771$). Cyclo(Phe-4Cl-Pro) at concentrations of 1 mM, 0.5 mM exhibited growth inhibition of $18.66 \pm 1.000\%$ ($P = 0.6239$), $15.66 \pm 0.6700\%$ ($P = 0.4400$). Although cyclo(D-Phe-4Cl-Pro) and cyclo(Phe-4Cl-Pro), produced statistically significant inhibition of growth, at all concentrations, relative to the negative control, the effects were very limited compared to the effects produced by chloramphenicol and amoxicillin. The effects produced by cyclo(D-Phe-4Cl-Pro), cyclo(Phe-4Cl-Pro), chloramphenicol and amoxicillin, are represented in Table 7.6

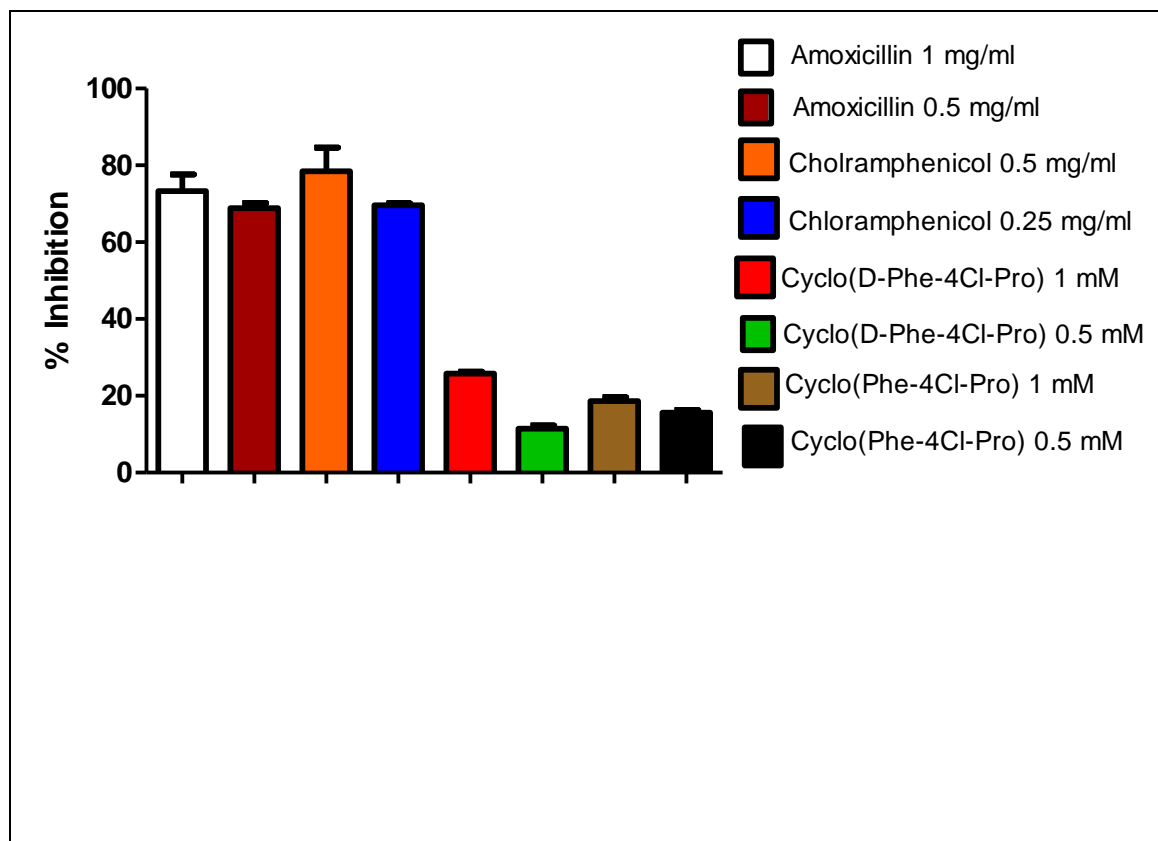


Figure 7.15 Percentage growth inhibition of *E. coli* after 24 hour exposure to cyclo(D-Phe-4Cl-Pro), cyclo(Phe-4Cl-Pro), chloramphenicol and amoxicillin

Table 7.6 Percentage growth inhibition of *E. coli* after 24 hour exposure to cyclo(Phe-4Cl-Pro), cyclo(D-Phe-4Cl-Pro), chloramphenicol and amoxicillin

Agent	Concentration	Percentage inhibition (%)	P-value
Amoxicillin	1 mg/ml	73.25 ± 4.350	0.0309
	0.5 mg/ml	68.89 ± 1.335	0.0293

Chloramphenicol	0.5 mg/ml	78.50 ± 6.165	0.0312
	0.25 mg/ml	69.66 ± 0.4350	0.0277
cyclo(D-Phe-4Cl-Pro)	1 mM	25.83 ± 0.500	0.7724
	0.5 mM	11.50 ± 0.8350	0.2771
cyclo(Phe-4Cl-Pro)	1 mM	18.66 ± 1.000	0.6239
	0.5 mM	15.66 ± 0.6700	0.4400

The antimicrobial effects produced by the different screening concentrations of cyclo(D-Phe-4Cl-Pro), cyclo(Phe-4Cl-Pro), chloramphenicol and amoxicillin on *P. aeruginosa* growth after 24 hours of exposure to the compounds are illustrated in Figure 7.16. To determine if the growth inhibiting effects produced by chloramphenicol, amoxicillin and the cyclic dipeptides were statistically different compared to the normal growth seen in the negative controls, Student's t-tests were performed on all concentrations of the cyclic dipeptides, chloramphenicol and amoxicillin. P-values of less than 0.05 were defined as an indication of a statistical significant difference between the means of the compounds and the negative controls. Percentage growth inhibition produced by all concentrations of the cyclic dipeptides was also compared to that of chloramphenicol and amoxicillin. Percentage growth inhibition produced by all screening concentrations of cyclo(D-Phe-4Cl-Pro) and cyclo(Phe-4Cl-Pro), was found to be notably less than that produced at both concentrations for chloramphenicol and amoxicillin. Chloramphenicol, at concentrations of 0.5 mg/ml and 0.25 mg/ml exhibited growth inhibition of $68.91 \pm 5.690\%$ ($P < 0.0102$) and $54.11 \pm 1.775\%$ ($P < 0.0036$), respectively. Amoxicillin at

concentrations of 1 mg/ml and 0.5 mg/ml exhibited growth inhibition of $90.34 \pm 2.010\%$ ($P < 0.0012$) and $76.23 \pm 1.675\%$ ($P < 0.0015$) respectively while cyclo(D-Phe-4Cl-Pro) at concentrations of 1 mM, 0.5 mM, exhibited growth inhibition of $39.55 \pm 3.00\%$ ($P = 0.0143$) and $15.61 \pm 3.275\%$ ($P = 0.2619$). Cyclo(Phe-4Cl-Pro) at concentrations of 1 mM, 0.5 mM, exhibited growth inhibition of $21.50 \pm 1.835\%$ ($P = 0.0490$), $15.99 \pm 1.00\%$ ($P = 0.1061$). Although cyclo(D-Phe-4Cl-Pro) and cyclo(Phe-4Cl-Pro), produced statistically significant inhibition of growth, at all concentrations, relative to the negative control, the effects were very limited compared to the effects produced by chloramphenicol and amoxicillin. The effects produced by cyclo(D-Phe-4Cl-Pro), cyclo(Phe-4Cl-Pro), chloramphenicol and amoxicillin, are represented in Table 7.7

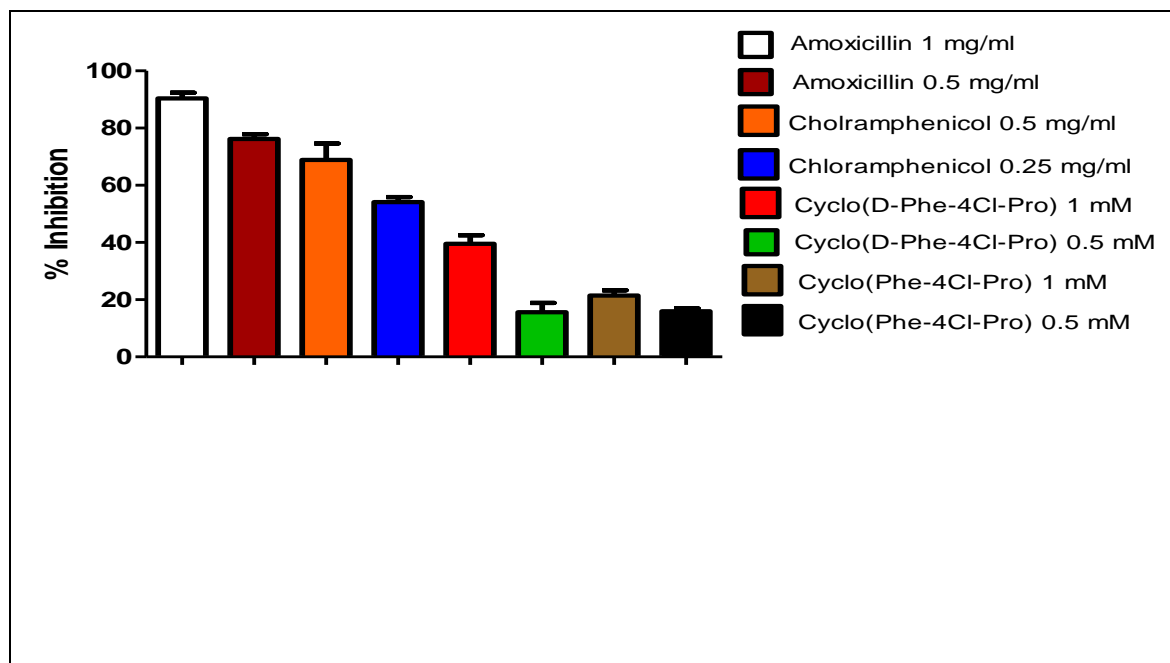


Figure 7.16 Percentage growth inhibition of *P. aeruginosa* after 24 hour exposure to cyclo(D-Phe-4Cl-Pro), cyclo(Phe-4Cl-Pro), chloramphenicol and amoxicillin

Table 7.7 Percentage growth inhibition of *P. aeruginosa* after 24 hour exposure to cyclo(D-Phe-4Cl-Pro), cyclo(Phe-4Cl-Pro), chloramphenicol and amoxicillin

Agent	Concentration	Percentage inhibition (%)	P-value
Amoxicillin	1 mg/ml	90.34 ± 2.010	0.0012
	0.5 mg/ml	76.23 ± 1.675	0.0015
Chloramphenicol	0.5 mg/ml	68.91 ± 5.690	0.0102
	0.25 mg/ml	54.11 ± 1.775	0.0036
Cyclo(D-Phe-4Cl-Pro)	1 mM	39.55 ± 3.000	0.0143
	0.5 mM	15.61 ± 3.275	0.2619
Cyclo(Phe-4Cl-Pro)	1 mM	21.50 ± 1.835	0.0490
	0.5 mM	15.99 ± 1.000	0.1061

The antimicrobial effects produced by the different screening concentrations of cyclo(D-Phe-4Cl-Pro), cyclo(Phe-4Cl-Pro), chloramphenicol and amoxicillin on *C. albicans* growth after 24 hours of exposure to the compounds are illustrated in Figure 7.17. To determine if the growth inhibiting effects produced by chloramphenicol, amoxicillin and the cyclic dipeptides were statistically different compared to the normal growth seen in the negative controls, Student's t-tests were performed on all concentrations of the

cyclic dipeptide, chloramphenicol and amoxicillin. P-values of less than 0.05 were defined as an indication of a statistical significant difference between the means of the compounds and the negative controls. Percentage growth inhibition produced by all concentrations of the cyclic dipeptides was also compared to that of chloramphenicol and amoxicillin. Percentage growth inhibition produced by all screening concentrations of cyclo(D-Phe-4Cl-Pro) and cyclo(Phe-4Cl-Pro), was found to be notably less than that produced at both concentrations for chloramphenicol and amoxicillin. Chloramphenicol, at concentrations of 0.5 mg/ml and 0.25 mg/ml exhibited growth inhibition of $57.61 \pm 2.390\%$ ($P < 0.0030$) and $82.68 \pm 5.345\%$ ($P < 0.0054$), respectively. Amoxicillin at concentrations of 1 mg/ml and 0.5 mg/ml caused growth inhibition of $91.19 \pm 1.165\%$ ($P < 0.0004$) and $63.83 \pm 2.500\%$ ($P < 0.0025$) respectively while cyclo(D-Phe-4Cl-Pro) at concentrations of 1 mM, 0.5 mM, exhibited growth inhibition of $54.28 \pm 5.055\%$ ($P = 0.0128$) and $31.83 \pm 9.500\%$ ($P = 0.1380$). Cyclo(Phe-4Cl-Pro) at concentrations of 1 mM, 0.5 mM, exhibited growth inhibition of $47.84 \pm 7.820\%$ ($P = 0.0387$), $46.18 \pm 3.854\%$ ($P = 0.0114$). Although cyclo(D-Phe-4Cl-Pro) and cyclo(Phe-4Cl-Pro) produced statistically significant inhibition of growth at all concentrations, relative to the negative control, the effects were very limited compared to the effects produced by chloramphenicol and amoxicillin. The effects produced by cyclo(D-Phe-4Cl-Pro), cyclo(Phe-4Cl-Pro), chloramphenicol and amoxicillin, are represented in Table 7.8

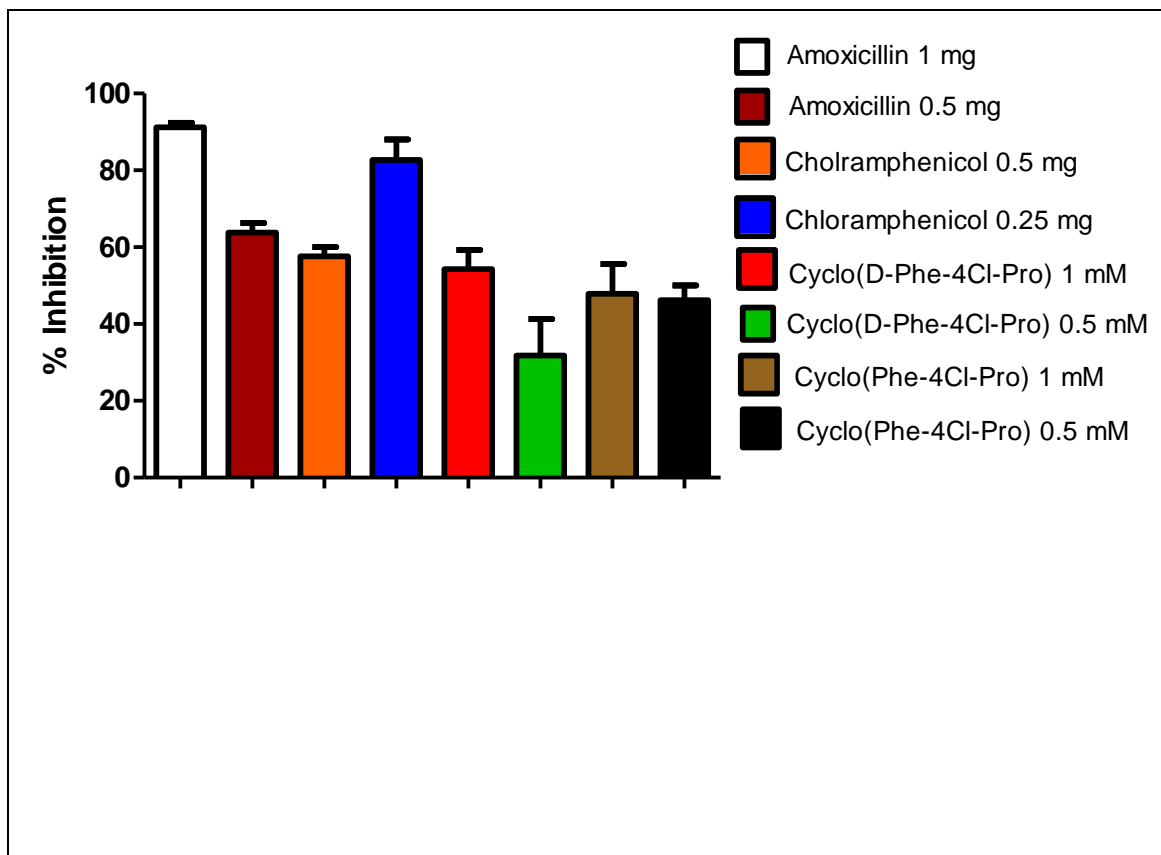


Figure 7.17 Percentage growth inhibition of *C. albicans* after 24 hour exposure to cyclo(D-Phe-4Cl-Pro), cyclo(Phe-4Cl-Pro), chloramphenicol and amoxicillin

Table 7.8 Percentage growth inhibition of *C. albicans* after 24 hour exposure to cyclo(D-Phe-4Cl-Pro), cyclo(Phe-4Cl-Pro), chloramphenicol and amoxicillin

Agent	Concentration	Percentage inhibition (%)	P-value
Amoxicillin	1 mg/ml	91.19 ± 1.165	0.0004
	0.5 mg/ml	63.83 ± 2.500	0.0025
Chloramphenicol	0.5 mg/ml	57.61 ± 2.390	0.0030

	0.25 mg/ml	82.68 ± 5.345	0.0054
Cyclo(D-Phe-4Cl-Pro)	1 mM	54.28 ± 5.055	0.0128
	0.5 mM	31.83 ± 9.500	0.1380
Cyclo(Phe-4Cl-Pro)	1 mM	47.84 ± 7.820	0.0387
	0.5 mM	46.18 ± 3.845	0.0114

7.11 Conclusion

The Antimicrobial effects of cyclo(D-Phe-4Cl-Pro) and cyclo(Phe-4Cl-Pro) on the different microorganisms remain questionable as the inhibiting effects produced by the cyclic dipeptides relative to the positive controls, in each case were minimal.

CHAPTER 8

HEAMATOLOGICAL STUDIES

8.1 INTRODUCTION

Blood is a connective tissue composed of a liquid portion called plasma and a cellular portion consisting of erythrocytes, leukocytes, platelets and various cell fragments. Having a slightly alkaline pH of between 7.35 and 7.45 in healthy individuals with a temperature of 38 °C (Tortora and Grabowski, 2009). Blood, the only liquid connective tissue in the human body, has three general functions: transportation, regulation and protection (Tortora and Grabowski, 2009). Blood transports (1) oxygen and nutrients to cells, (2) carbon dioxide and wastes from the tissues to the lungs and the kidneys where waste can be removed from the body and (3) carries hormones from the endocrine glands to the target tissues. Blood helps to regulate body temperature by removing heat from active areas, such as skeletal muscles and transporting it to other areas of the skin, so that the heat can be dissipated. It plays a significant role in fluid and electrolyte balance because salt and plasma proteins contribute to the osmotic pressure by providing weight and bulk to the blood and functions in pH regulation through the reaction of buffers in the blood. Blood protects the body by initiating clotting mechanisms to prevent fluid loss through haemorrhage when blood vessels become damaged; certain cells in the blood namely, phagocytic leukocytes, help to protect the body against diseases by engulfing and destroying the causative agent (a biological agent that causes a disease, toxins or toxic chemicals causing illness); antibodies in the plasma for example IgG, IgM, IgE and IgA, help protect against diseases by their reactions with offending agents (Hoffbrand and Moss, 2011).

Blood is denser and more viscous than water and constitutes about 8% of the total body weight. The blood volume is 5 to 6 liters in an averaged-sized healthy adult female. Blood is composed of two portions: (1) blood plasma, a watery liquid that contains dissolved substances such as water, amino acids, proteins, carbohydrates, lipids, hormones, vitamins, electrolytes, dissolved gases and cellular wastes and (2) formed

elements, including plasma, erythrocytes, leukocytes and lymphocytes making up the remainder (Tortora and Grabowski, 2009).

8.1.1 Haemostasis

To maintain blood fluidity within the vascular system is an important human physiological process. The term “haemostasis” refers to the normal physiological response of the vessel to injury by forming a clot that serves to limit haemorrhage (Gentry, 2004). Thrombosis is a pathological clot formation that results when haemostasis is excessively activated in the absence of bleeding. Under normal physiological conditions there is a delicate equilibrium between the pathological states of hypercoagulability and hypocoagulability in the circulating blood. Hypercoagulable states and thrombosis are induced by altered blood flow (e.g., stasis, turbulences), defects in the endothelium, and changes in the blood constituents (e.g., reduced inhibitor capacity of the coagulation system and reduced activity of the fibrinolytic system). Hypercoagulable states and bleeding are caused primarily by reduced activity of procoagulant factors (e.g., haemophilia), thrombocytopenia, genetic deficiencies, autoimmune disorders and antithrombotic drugs (Rasche, 2001).

In response to damage, blood vessels rapidly activate the haemostatic apparatus: (1) vascular constriction, (2) platelet plug formation, (3) blood clotting *via* activation of the coagulation cascade, (4) fibrinolysis and (5) repair and regeneration of damaged blood vessels (Tortora and Grabowski, 2009).

8.1.2 Vascular constriction

An immediate vasoconstriction of the injured vessel and reflex constriction of adjacent small arteries and arterioles is responsible for an initial slowing of blood flow to the area of injury. The reduced blood flow allows contact activation of platelets and the release of coagulation factors. The vasoactive amines and thromboxane A₂ from platelets, and the fibrinopeptides liberated during fibrin formation, may also have vasoconstrictive activity (Tortora and Grabowski, 2009).

8.1.3 Platelet plug formation

Following a break in the endothelial lining, there is an initial adherence of platelets to the exposed connective tissue. The platelet adhesion is potentiated by von Willebrand factor (VWF). Collagen exposure and thrombin produced at the site of injury causes the adherent platelets to release their granule contents which include adenosine diphosphate (ADP), serotonin, fibrinogen, lysosomal enzymes and heparin-neutralising factor (PF-4). Collagen and thrombin activate platelet prostaglandin synthesis leading to the formation of thromboxane A_2 which potentiates platelet release reactions, platelet aggregation and also powerful vasoconstriction. Released ADP causes platelets to swell and aggregate. Additional platelets from the circulating blood are drawn to the area of injury. This continuing platelet aggregation promotes the growth of the haemostatic plug which soon covers the exposed connective tissue. Released platelet granule enzymes, ADP and thrombosthenin may all contribute to the consolidation of the accumulated plug (Tortora and Grabowski, 2009).

8.1.4 Blood clotting via activation of the coagulation cascade

After primary haemostasis, i.e., instant vasoconstriction and formation of an initial platelet plug, activation of the coagulation system is needed to stabilise the loose accumulated platelets by cross-linking fibrin. Figure 8.1 illustrates the stages of the coagulation cascade (Vogler and Siedlecki, 2009).

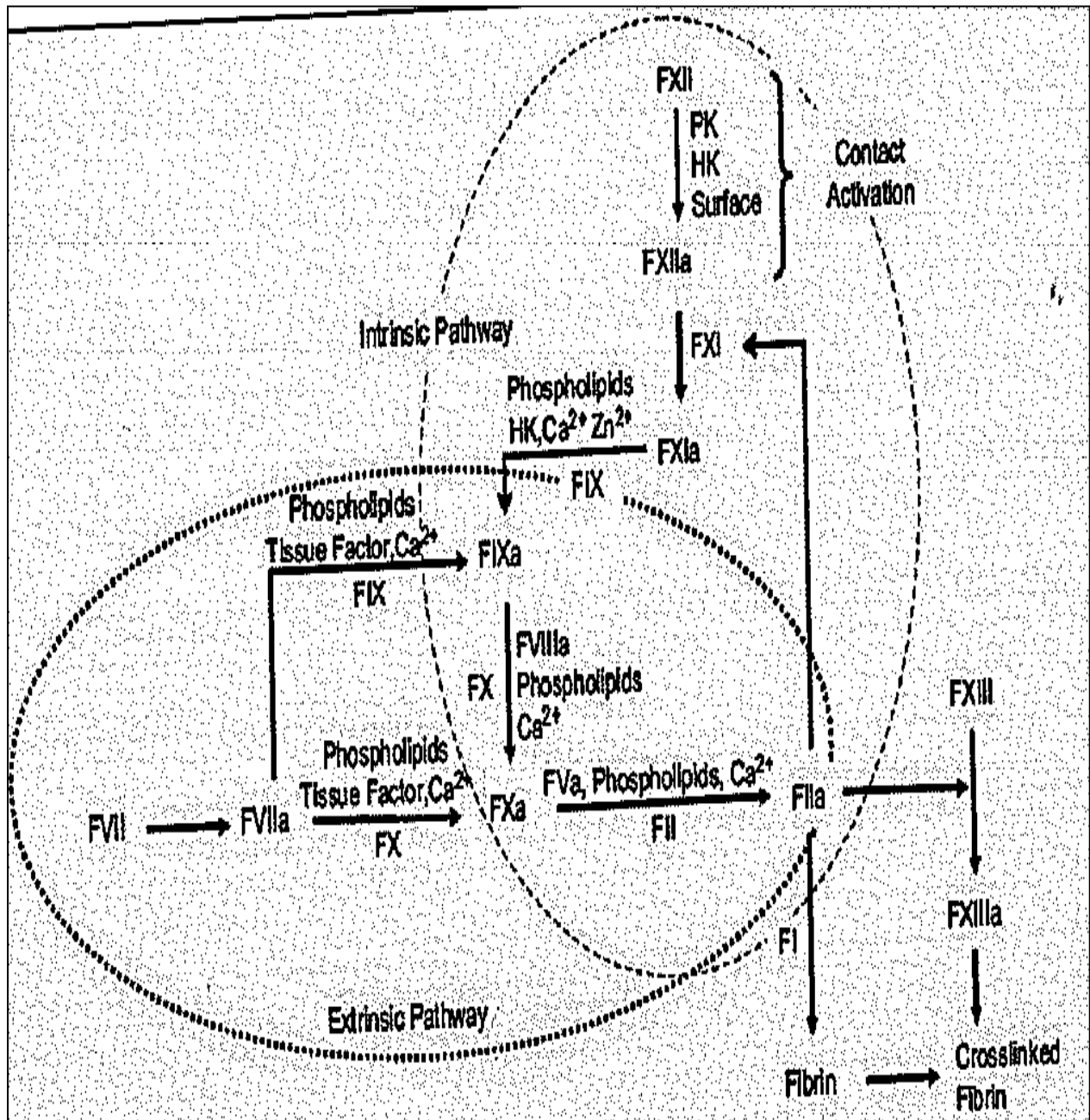


Figure 8.1 A simplified line diagram of the plasma-coagulation cascade showing intersection of the intrinsic and extrinsic pathways (Vogler and Siedlecki, 2009).

The blood coagulation cascade is composed of two inactive pathways, namely the intrinsic and the extrinsic pathway. The two pathways merge and form factor X and V which forms part of the prothrombinase complex that leads to factor IIa (thrombin) formation. The extrinsic pathway which is responsible for haemostatic regulation and

response to vascular injury involves factor VII which is activated by tissue factor (TF). The intrinsic pathway involves factor XII, factor XI, factor IX, and factor VIII (Vogler and Siedlecki, 2009; Ajjan and Ariëns, 2009; Ajjan and Grant, 2006). The blood coagulation cascade consists of a series of interconnected reactions with the resulting pathway of one enzyme activating the next enzyme. The cascade is a self-amplifier with zymogens being activated to enzymes that lead to the formation of thrombin. The final step of the blood coagulation cascade is the conversion of fibrinogen to fibrin by thrombin. The fibrin clot is formed after polymerisation (Figure 8.1). The fibrin clot formation involves both the platelets and interaction between the coagulation proteins, and is thus a complex process. When damage occurs in a vessel wall, TF is brought into contact with the plasma. In this initiation phase, TF binds and activates factor VII. The TF/factor VII complex activates factor IX and factor X, with factor X activating factor V. Prothrombin is cleaved to activate thrombin by factor X and factor V. The thrombin that is released is not enough to sustain the thrombus but enough to maintain platelet activation (Vogler and Siedlecki, 2009; Ajjan and Ariëns, 2009; Ajjan and Grant, 2006). The adhesion of platelets to the site of injury is mediated by the interaction of Von Willebrand Factor (VWF) with collagen. The activation of platelets by exposed collagen and thrombin brings about full platelet activation and degranulation leading to the release of factor V. The coagulation cascade is enhanced, because factor V is activated by factor Xa and thrombin, which activates factor VIII that forms an active complex with factor IXa. The generation of sufficient thrombin from the platelet surface factor Xa/Va complex leads to the conversion of fibrinogen to fibrin. A stable haemostatic plug is generated after factor XIII, a trans-glutaminase that is activated by thrombin, forms cross links in the fibrin clot (Vogler and Siedlecki, 2009; Ajjan and Ariëns, 2009; Ajjan and Grant, 2006).

8.1.5 Fibrinolysis

Fibrinolysis is a physiological process that involves the dissolution of blood clots by the action of a proteolytic enzyme, such as plasmin (fibrinolysin), that dissolves fibrin threads and inactivates fibrinogen and other blood-clotting factors (Tortora and Grabowski, 2009). Plasmin the main enzyme involved in fibrinolysis, is formed by the action of two plasminogen activators, namely tissue plasminogen activator (t-PA) and

urinary plasminogen activator (u-PA) (Castãnon *et al.*, 2007 ; Vadseth *et al.*, 2004). t-PA is mainly active in the vascular system. It is the main agent for the dissolution of thrombi via the activation of plasminogen to plasmin (Castãnon *et al.*, 2007). u-PA is found in connective tissue, and plays a role in tissue remodeling and cell migration (Castãnon *et al.*, 2007). The presence of fibrin enhances the activation of plasminogen to plasmin by t-PA, whereas no influence is observed in the case of u-PA (Castãnon *et al.*, 2007; Bachmann, 2001).

8.1.6 Repair and regeneration of damaged blood vessels

Ultimately the haemostatic plug needs to be replaced by a new layer of endothelial cells and underlying extracellular matrix. The fibrin clot not only serves to close a damaged blood vessel wall, but also acts as a scaffold for invading inflammatory, endothelial, and other tissue cells during tissue repair. The formation of a new endothelium proceeds through a process referred to as angiogenesis. Furthermore, angiogenesis plays an important role in pathological conditions such as cancer (the formation of new blood vessels is essential to supply a tumor with oxygen and nutrients) (Tortora and Grabowski, 2009).

8.1.7 Drugs affecting coagulation

Drugs are used to modify the cascade either when there is a defect in coagulation or when there is an unwanted coagulation.

In genetically determined deficiencies of clotting factors, *i.e.*, classical haemophillia, caused by a lack of factor VIII, and haemophillia B, or Christmas disease, caused by a lack of factor IX, are treated by giving fresh plasma concentrations or concentrated preparations of factor VIII or factor IX. Acquired human defects include liver disease, vitamin K deficiency and excessive oral anticoagulant therapy. The above mentioned conditions are generally treated with vitamin K (Rang *et al.*, 2011).

8.1.8 Drugs used in the treatment of thrombotic and thromboembolic diseases

Injectable anticoagulants include heparin and the low molecular weight heparins. Heparin inhibits coagulation by potentiating the inhibitory effect of antithrombin III on the activated forms of clotting factors XII, XI, IX, X and thrombin. Examples of the low molecular weight heparins currently in use include enoxaparin, dalteparin and nadroparin. The low molecular weight heparins have a longer duration of action than unfractionated heparin and are administered once or twice daily (Rang *et al.*, 2011).

Antithrombin III-independent anticoagulants include hirudin and argatroban and these direct inhibitors of thrombin are still under investigation (Rang *et al.*, 2011).

Oral anticoagulants include warfarin. Warfarin interferes with the post-translational γ -carboxylation of glutamic acid residues in clotting factors II, IX and X. This is achieved by competitively inhibiting the enzymatic reduction of vitamin K to its active hydroquinone form (Rang *et al.*, 2011).

8.1.9 Antiplatelet drugs

Aspirin alters the balance between thromboxane (TXA₂), which promotes aggregation and prostaglandin I₂(PGI₂), which inhibits it. Aspirin inactivates cyclooxygenase (COX)-acting mainly on COX₁ by irreversibly acetylating a serine residue in its active site. This causes the reduction of both TXA₂ synthesis in platelets and PGI₂ synthesis in endothelium (Rang *et al.*, 2011).

Glycoprotein IIB/IIIa receptor antagonists includes abciximab, eptifibatid and tirofiban. The platelet receptor glycoprotein IIB/IIIa is the final common pathway to platelet aggregation. Inhibition at this point thus prevents platelet aggregation regardless of the agonist responsible for platelet activation (Rang *et al.*, 2011).

8.1.10 Fibrinolytic drugs

Antithrombotic enzymes convert plasminogen to plasmin, which in return degrades fibrin thrombi and fibrinogen. Examples of these agents include streptokinase, alteplase and tenecteplase (Rang *et al.*, 2011).

8.2 Methodology

A coagulation assay, thrombin assay, platelet aggregation assay and fibrinolysis assay were utilised to investigate the effects of cyclo(Phe-4Cl-Pro) and cyclo(D-Phe-4Cl-Pro) on haemostasis. All water containing solutions required for experimentation were prepared by utilizing analytical grade water (AGW) obtained from an ultra clear TWF UF TM reverse osmotic water purification system SG[®]. To ensure reproducibility all assays were performed in quadruplicate.

8.2.1 Collection and ethical approval of blood used in experiments

Human blood plasma was used to screen cyclo(Phe-4Cl-Pro) and cyclo(D-Phe-4Cl-Pro) for activity against the various haematological processes. The human ethics committee of the Nelson Mandela Metropolitan University (NMMU) approved the use of human blood samples in the haematological studies (reference number) (HO6SB-003) (September 2006). Human blood used in the platelet aggregation assay was drawn at the NMMU clinic on the day of use. Particular criteria with regards to the use of blood were as follows (Cunningham, 2006):

- Blood was to be drawn in the morning, to allow for an overnight fast. A fatty meal should have been ingested 6 to 8 hours prior to blood been drawn. Severe lipaemia, resulting from a fatty meal, may have decreased the apparent response to aggregating agents in the platelet-rich plasma, such that the plasma would remain turbid even if all of the platelets had aggregated (Mustard *et al.*, 1989; Zucker, 1989).
- Ingestion of non-steroidal anti-inflammatory drugs (NSAIDs), one week prior to blood donation was not permitted. NSAIDs would inhibit the enzyme

cyclooxygenase, therefore preventing secretion *via* the arachidonic pathway (Mustard *et al.*, 1989; Zucker, 1989).

- Collection of blood was to be from the forearm vein. After which, blood had to be mixed with an anticoagulant agent, namely trisodium citrate, and frothing avoided during the mixing procedure (Mustard *et al.*, 1989; Zucker, 1989).
- Smoking of cigarettes for a number of hours prior to the collection was prohibited, since the smoke from a single cigarette would have increased the response of platelets to low adenosine diphosphate (ADP) levels (Zucker, 1989).
- Donors had to be under minimum stress. Excessive anxiety may have caused an abnormally large increase in the primary aggregation response to ADP and norepinephrine (Zucker, 1989).

8.2.2 Coagulation assay

The activation of the extrinsic and intrinsic pathways of the coagulation cascade results in the generation of thrombin, the activation of fibrinogen, the release of fibrinopeptides, the formation of soluble fibrin, and finally the formation of F XIII-mediated cross linked insoluble fibrin (Figure 8.1). Prothrombin time (PT) and activated partial thromboplastin time (APTT) assays were completed to evaluate the effects of the cyclic dipeptides on the extrinsic and intrinsic pathways respectively. The fibrinogen-C test was done to investigate if the cyclic dipeptides would possibly limit or inhibit the formation of fibrin from fibrinogen. The prolongation of clot formation time and the inhibition of fibrin formation would result in less clot formation. Calibration plasma (Beckman) was used to conduct the coagulation studies (PT, APTT, D-Dimer and Fibrinogen-C assays). Healthy donors were used to prepare calibrated plasma.

A quantity of 2.78 mg of the cyclic dipeptides were initially dissolved in 1% dimethylsulphoxide (DMSO) (Associated Chemical Enterprises (Pty) Ltd, SA) and made up to volume with a 0.9 % NaCl solution. The cyclic dipeptides were then made up to final concentrations of 100 mM, 50 mM, 25 mM, and 12.5 mM.

8.2.2.1 Prothrombin time test

The PT test which measures the extrinsic pathway is altered when there are changes in vitamin K-dependant coagulation factors (Azevedo *et al.*, 2007). These factors include: Factor II, VII, V, X. A recomboplastin kit (Beckman, England) was used to determine the clotting time. The recomboplastin reagent which is included in the recomboplastin kit is a liposomal preparation which contains recombinant human tissue factor in a synthetic phospholipid mixture that contains calcium chloride, a buffer, and a preservative (Tripodi *et al.*, 1992). Thromboplastin reagent is very sensitive and the recombinant human tissue factor contains no contaminating coagulation factors. This makes the PT reagent sensitive to deficiencies of factors X, VII, V and II (Quick, 1966). In the PT test, the extrinsic pathway is activated by the calcium ions, resulting in the conversion of fibrinogen into an insoluble fibrin clot (Quick, 1966). The PT test was performed according to the manufacturer's instructions. Recomboplastin (200 µl) was incubated at 37 °C for 180 seconds on the CL Analyser (IVD, Beckman Coulter), while a premix of 100 µl of plasma was incubated for 180 seconds at 37 °C with either the untreated control (C), cyclo(Phe-4Cl-Pro) (1: 4), cyclo(D-Phe-4Cl-Pro) (1: 4) or heparin (0.1 U/ml, positive control {PC}) (Bodene). To evaluate the PT, 150 µl of the plasma premix solutions were added to the recomboplastin (200 µl) and the clotting time was measured.

8.2.2.2 Activated partial thromboplastin time (APTT)

Alteration in the level of factors VIII, IX, X, XI and XII has an impact on APTT, which measures the integrity of the intrinsic pathways (Azevedo *et al.*, 2007). The SynthASil kit (Beckman), which is used to measure APTT contains the APTT buffered reagent. The APTT reagent contains synthetic phospholipids (which are required for optimal platelet-like activity) and highly defined non-settling colloidal silica. SynthASil is sensitive to reduced levels of contact factors (which are involved in the intrinsic and common pathways), the anticoagulant effect of heparin and presence of inhibitors. The presence of conditions such as: a deficiency of factor XII, X, IX, VIII, or fibrinogen, liver

diseases, vitamin K deficiency and the presence of heparin, lupus anticoagulant or other inhibitors will prolong the clotting time (Dipiro *et al.*, 2011).

To evaluate the effect of the cyclic dipeptides on APTT, 100 µl of the APTT reagent was added to tubes containing 100 µl of plasma and either the (C), cyclo(Phe-4Cl-Pro) (1: 3) and cyclo(D-Phe-4Cl-Pro) (1: 3) or heparin (0.1 U/ml, PC). The mixtures were incubated at 37 °C for 180 seconds on the CL Analyser, after which 100 µl of 0.025 M CaCl₂ solution was added to initiate the activation of the intrinsic pathway. The clotting time was measured, and the anticoagulatory activity of test samples evaluated relative to the untreated control (C).

8.2.2.3 Fibrinogen-C assay

Thrombin converts fibrinogen into fibrin in plasma. Under these conditions *i.e.*, high thrombin and low fibrinogen levels, the rate of the reaction is a direct function of the fibrinogen concentration.

A Fibrinogen-C kit (Beckman) was used to determine the effect of the cyclic dipeptides on the conversion of fibrinogen to fibrin by comparing the protein levels of the treated plasma with that of untreated plasma control (C). Impairment in the conversion of fibrinogen to fibrin occurs during the coagulation process when there are abnormalities in fibrinogen (Dipiro *et al.*, 2011). Fibrinogen levels are used as a diagnostic marker to determine disease states that include disseminated intravascular coagulation (DIC), liver disease, inflammatory diseases and malignancies. There is a direct correlation between high levels of fibrinogen and an increased risk in cardiovascular disease. Thrombolytic therapy reduces the fibrinogen levels (Dipiro *et al.*, 2011).

The Fibrinogen-C assay was performed according to the manufacturer's instructions. A ten times dilution of diluted plasma (200 µl) was incubated with 50 µl of either the (C), cyclo(Phe-4Cl-Pro) (1: 4), cyclo(D-Phe-4Cl-Pro) (1: 4) or heparin (0.1 U/ml, PC) at 37 °C on the CL Analyser for 180 seconds. After the incubation period, a thrombin (Beckman) solution (35 U/ml); 100 µl) was added and the effect of the conversion of

fibrinogen to fibrin was evaluated by comparing the fibrin levels of the treated plasma with that of the untreated plasma control (C).

8.2.2.4 D-Dimer

When plasmin digests the insoluble fibrin, it yields a variety of soluble derivatives. These derivatives contain a D-Dimer domain which was not present on the original fibrinogen molecule, its degradation products, or on the insoluble fibrin (Palareti, 1993). The D-Dimer test is used widely as a diagnostic tool for thrombosis and monitoring thrombolytic therapy (Bounameaux *et al.*, 1994). High levels of D-Dimer are present in conditions such as deep vein thrombosis (DVT), pulmonary embolism (PE) and disseminated intravascular coagulation (DIC) (Gaffney *et al.*, 1988).

The D-Dimer latex reagent (Beckman) has a suspension of polystyrene latex particles that are coated with a monoclonal antibody that is highly specific for the D-Dimer domain. The coated latex particles (Latex reagent) agglutinate when plasma contains the D-Dimer domain. The degree of agglutination is directly proportional to the D-Dimer concentration, which is determined by a turbidimetric immunoassay that measures the amount of transmitted light at 405 nm. The reduction of the amount of transmitted light is caused by the formation of the aggregates (Newman *et al.*, 1992).

The D-Dimer assay was performed according to the manufacturer's instructions. The buffer (150 μ l) was added to 42 μ l of the plasma containing 8 μ l of either the (C),cyclo(Phe-4Cl-Pro) (1: 3) or cyclo(D-Phe-4Cl-Pro) (1: 3). The mixture was then incubated at 37 °C in the CL Analyser for 15 minutes. After the incubation period the latex D-Dimer was subsequently added, the effect of the cyclic dipeptides on the rate of fibrinolysis via D-Dimer formation was evaluated by comparing the protein levels of the treated plasma with that of the untreated plasma control. Heparin (0.1 U/ml) was used as the positive control for this assay.

8.3 Platelet aggregation/adhesion studies

Platelets prevent blood loss by constantly “guarding” the inner surface of blood vessels searching for “leaks” to be sealed. Platelets respond to injury in three phases:

(1) Adhesion

During this phase platelets adhere to the injured vessel *via* their receptors GPIb and GPIIb/IIIa mediated by the ligand vWF.

(2) Aggregation

Platelets adhere to each other *via* fibrinogen binding GPIIb/IIIa

(3) Secretion

Granules are released by exocytosis when the platelets are activated, forming a haemostatic plug. Flow cytometry allows researchers to mimic one or several aspects of these three phases to obtain relevant data (Reininger, 2006).

Platelet aggregation and adhesion studies were done to investigate the effects of the cyclic dipeptides on platelet activity.

8.3.1 Isolation of platelets

Blood was drawn by venepuncture from healthy human subjects into sterile 4.5 ml tubes containing 0.5 ml of 0.105 M trisodium citrate (BD Vacutainer Systems, UK). Healthy individuals were defined as people who have not been sick for three months prior to the experiment and were not using any medication. Platelet rich plasma (PRP) was obtained by centrifuging at 300 x g for 10 minutes. The platelets were gently suspended in a buffer composed of 145 mmol/L NaCl, 5 mmol/L KCl, 10 mmol/L HEPES, 0.5

mmol/L Na_2HPO_4 , 6 mmol/L glucose, and 0.2% bovine serum albumin (BSA), pH 7.4 (buffer A). The platelet suspension was kept at room temperature and utilised within one hour. Ten minutes prior to use the platelets were warmed at 37 °C (Bellavite *et al.*, 1994).

8.3.2 Platelet count

A rapid spectrophotometric method for determining the number of platelets in a platelet suspension and in blood plasma developed by Walkowiak *et al.* (1997) was used. Platelet suspensions (200 μl) were placed in a 96-well microtiter plate for measurement of turbidity (Bio Tek Power Wave XS) (600 nm). Each sample was also used to perform triplicate platelet counts using a haemocytometer chamber. A standard curve was constructed correlating to the number of platelets at an absorbance of $A_{600\text{ nm}}$ (Figure 8.2)

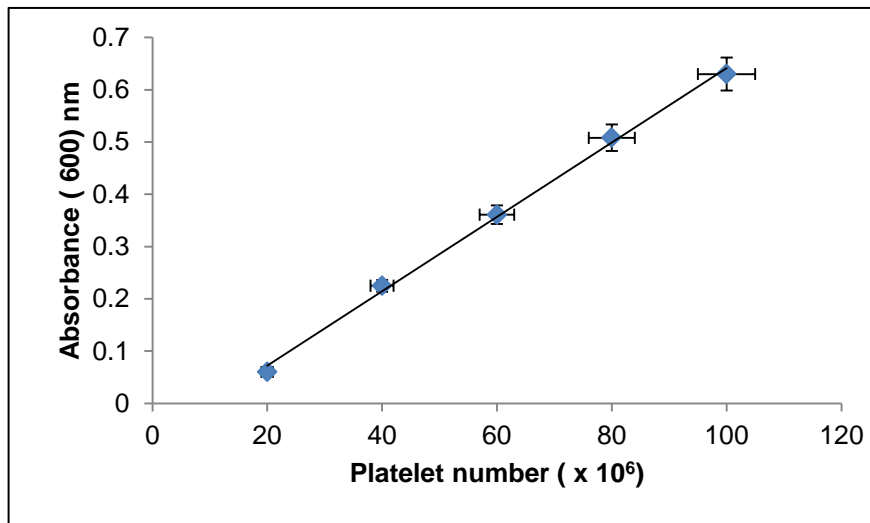


Figure 8.2 Standard curve illustrating the correlation between platelet count numbers and absorbance ($R^2 = 0.9976$)

8.3.3 Platelet aggregation (flow-cytometry method)

One unique feature of flow-cytometry is that it measures fluorescence per cell or particle. Spectrophotometry, in contrast, measures the percent absorption and transmission of a specific wavelength of light for a given sample. Flow-cytometry uses the principles of

light scattering, light excitation, and emission of fluorochrome molecules to generate specific multi-parameter data from particles and cells in the size range of 0.5-40 μm in diameter. Recent developments in flow-cytometric analysis have made it possible to detect specific markers of platelet activation. The most studied markers are P-selectin, a marker for platelet degranulation, and PAC-1, a marker for GPIIb/IIIa activation (Michelson *et al.*, 2000). Flow-cytometry can be used to determine both the activation state of circulating platelets and the reactivity of circulating platelets (Kasuya *et al.*, 2006). The monoclonal antibody used was anti-PAC-1. Anti-PAC-1 (BD-Biosciences) is an antibody that binds to the fibrinogen-binding site exposed by the conformational change that occurs in the GPIIb-IIIa complex when it is activated (Michelson *et al.*, 2000).

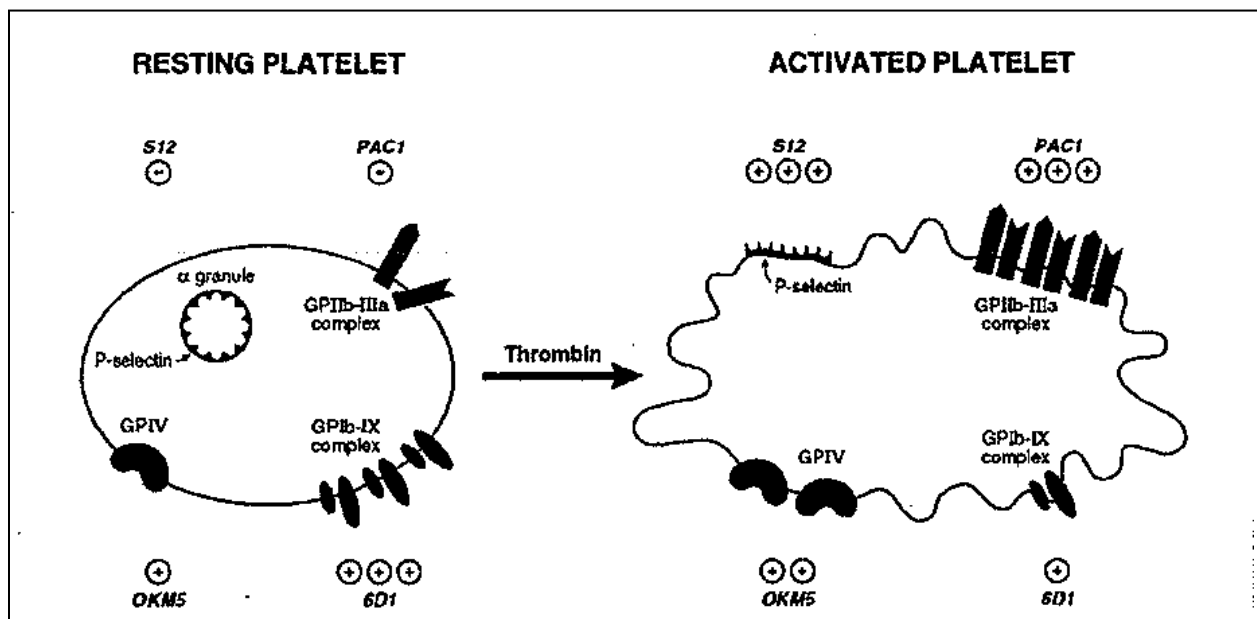


Figure 8.3 The effect of platelet activation on monoclonal antibody binding (Michelson *et al.*, 2000)

A method adapted from Michelson *et al.*, (2000), was used for the experiment. A platelet rich plasma (PRP) sample containing a platelet count of 3×10^7 platelets/ml was used for all cytometry experiments. A volume of 40 μl of PRP was placed into tubes containing 10 μl of a 200 $\mu\text{g/ml}$ saturated concentration of fluorescein isothiocyanate (FITC)-PAC1 (BD Biosciences). The binding of fibrinogen to the gpIIb/IIIa receptor is required for platelet aggregation. PAC-1 binds only to activated platelets and appears to

be specific for this recognition site within gpIIb/IIIa. PAC-1 inhibits fibrinogen-mediated platelet aggregation (Michelson *et al.*, 2000).

To inhibit fibrin polymerization, 2 μ l of 2.5 mmol/L (final concentration) of peptide glycol-L-prolyl-L-arginyl-L-proline (GPRP) (Sigma) was added. For a positive control (PC), 100 μ l of thrombin stock (50 U/ml) was added to give final concentration of 10 U/ml, the same volume of buffer was added for an untreated control (C), cyclo(Phe-4Cl-Pro) (1: 3) or cyclo(D-Phe-4Cl-Pro) (1: 3) were added. Unstained cells were used to determine background staining. The tubes were then incubated at room temperature for fifteen minutes. Following the incubation period the platelets were fixed with 2: 1 ratio of 1% formaldehyde for thirty minutes at room temperature. A threefold volume of Tyrode's buffer was added and the cells were immediately analysed with a Beckman flow cytometer (Coulter, Cytomics FC 500). All parameters were collected in list mode files and then analysed.

8.4 Statistical analysis

Results were obtained as quadruplicate values and represented as a mean \pm standard deviation (SD). Data was represented graphically with the aid of statistical software packages, Microsoft Excel[®] (Version 2007) and Graph Pad Prism[®] (Version 5). Statistical analysis was then carried out on the resultant graph slopes, which represent either inhibition or acceleration of the relevant coagulation pathways. Student's *t*-tests performed in order to determine if the mean response to each cyclic dipeptide concentration indicated significant inhibition or acceleration of a particular coagulation pathway. Calculated *p*-values of less than 0.05 were defined as an indication of statistical significance. The *p*-values were compared to the relevant positive controls.

8.5 Results and discussion

8.5.1 Activated partial thromboplastin time assay (APTT)

The effects of heparin (positive control), cyclo(Phe-4Cl-Pro) and cyclo(D-Phe-4Cl-Pro) on the intrinsic pathway are illustrated in Figure 8.4 and summarised in Table 8.1. APTT

represents the time in seconds it takes for plasma to clot after the addition of an intrinsic pathway activator and calcium. The normal APTT range in human plasma is 24 to 39 seconds. Heparin at a screening concentration of 0.1 U/ml significantly prolonged the clotting time to 106.0 ± 1.350 seconds. Cyclo(Phe-4Cl-Pro) at a screening concentration of 50 mM produced a clotting time of 27.95 ± 0.4000 seconds ($P = 0.0003$). The screening concentrations of 25 mM and 12.5 mM, however produced a shorter clotting time of 20.28 ± 1.055 seconds ($P = 0.0004$) and 10.78 ± 0.4450 seconds ($P = 0.0002$), respectively. Cyclo(D-Phe-4Cl-Pro) at screening concentrations of 50 mM, 25 mM and 12.5mM, produced clotting times of 26.15 ± 0.7050 seconds ($P = 0.0004$), 14.61 ± 0.6150 seconds ($P = 0.0003$) and 8.110 ± 0.5500 seconds ($P = 0.0002$).

Table 8.1 Effects of heparin, cyclo(Phe-4Cl-Pro) and cyclo(D-Phe-4Cl-Pro) on APTT clotting times

Compound	Concentration	Clotting time (seconds)	<i>P</i> -value
Heparin	0.1 U\ml	106 ± 1.350	0.0003
Cyclo(Phe-4Cl-Pro)	50 mM	27.95 ± 0.4000	0.0003
	25 mM	20.28 ± 1.055	0.0004
	12.5 mM	10.78 ± 0.4450	0.0002

Cyclo(D-Phe-4Cl-Pro)	50 mM	26.15 ± 0.7050	0.0004
	25 mM	14.61 ± 0.6150	0.0003
	12.5 mM	8.110 ± 0.5500	0.0002

(P-values are calculated relative to the positive control)

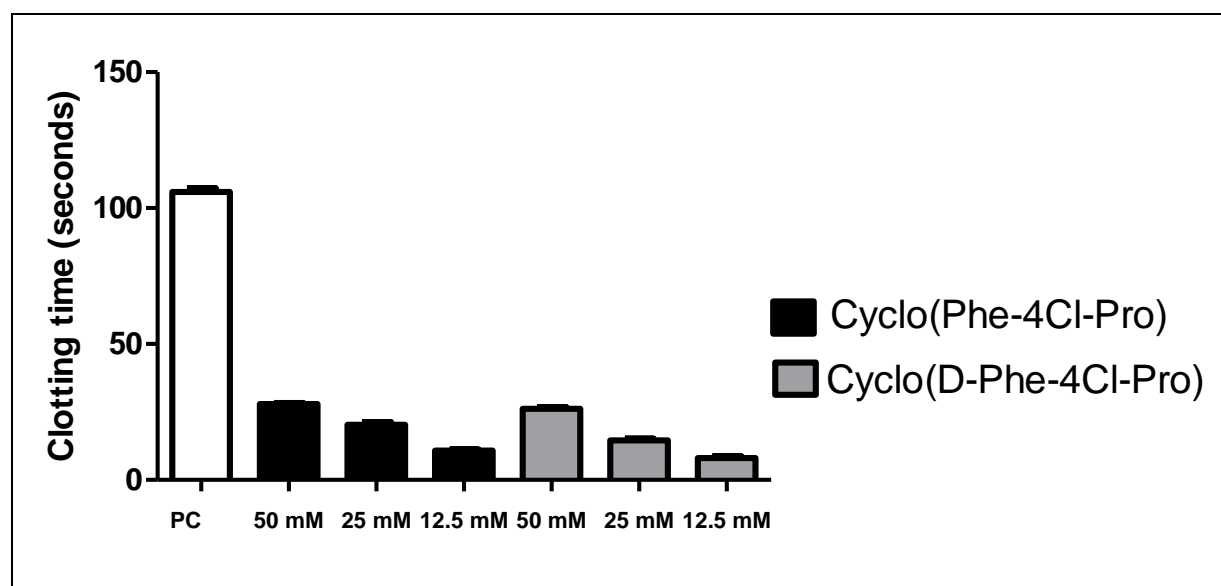


Figure 8.4 Effects of heparin (positive control), cyclo(Phe-4Cl-Pro) and cyclo(D-Phe-4Cl-Pro) on APTT clotting time

8.5.2 Prothrombin time assay (PT)

Prothrombin time represents the time in seconds it takes for plasma to clot after the addition of calcium and thromboplastin. The normal PT range is 11 to 13.5 seconds. The effects of heparin, cyclo(Phe-4Cl-Pro) and cyclo(D-Phe-4Cl-Pro) on PT clotting time

are illustrated in Figure 8.5 and summarised in Table 8.2. Heparin at a screening concentration of 0.1 U/ml, significantly prolonged PT clotting time to 88.80 ± 1.805 seconds. Cyclo(Phe-4Cl-Pro) at screening concentrations of 50 mM, 25 mM produced longer PT clotting times of 20.53 ± 0.9250 seconds ($P = 0.2374$), 17.13 ± 0.1700 seconds ($P = 0.0055$). Cyclo(Phe-4Cl-Pro) at a screening concentration of 12.5 mM, however produced a PT clotting time of 14.41 ± 0.810014 seconds ($P = 0.0125$). Cyclo(D-Phe-4Cl-Pro) at screening concentrations of 50 mM, 25 mM and 12.5 mM, produced PT clotting times of 17.66 ± 0.6700 seconds ($P = 0.0266$), 11.85 ± 0.8550 seconds ($P = 0.0078$) and 10.75 ± 0.4500 seconds ($P = 0.0024$), respectively.

Table 8.2 Effects of heparin, cyclo(Phe-4Cl-Pro) and cyclo(D-Phe-4Cl-Pro) on PT clotting times

Compound	Concentration	Clotting time (seconds)	<i>P</i> -value
Heparin	0.1 U/ml	88.80 ± 1.805	0.0009
Cyclo(Phe-4Cl-Pro)	50 mM	20.53 ± 0.9250	0.2374
	25 mM	17.13 ± 0.1700	0.0055
	12.5 mM	14.41 ± 0.8100	0.0125
Cyclo(D-Phe-4Cl-Pro)	50 mM	17.66 ± 0.6700	0.0266

Pro)	25 mM	11.85 ± 0.8550	0.0078
	12.5 mM	10.75 ± 0.4500	0.0024

(P-values are calculated relative to the positive control)

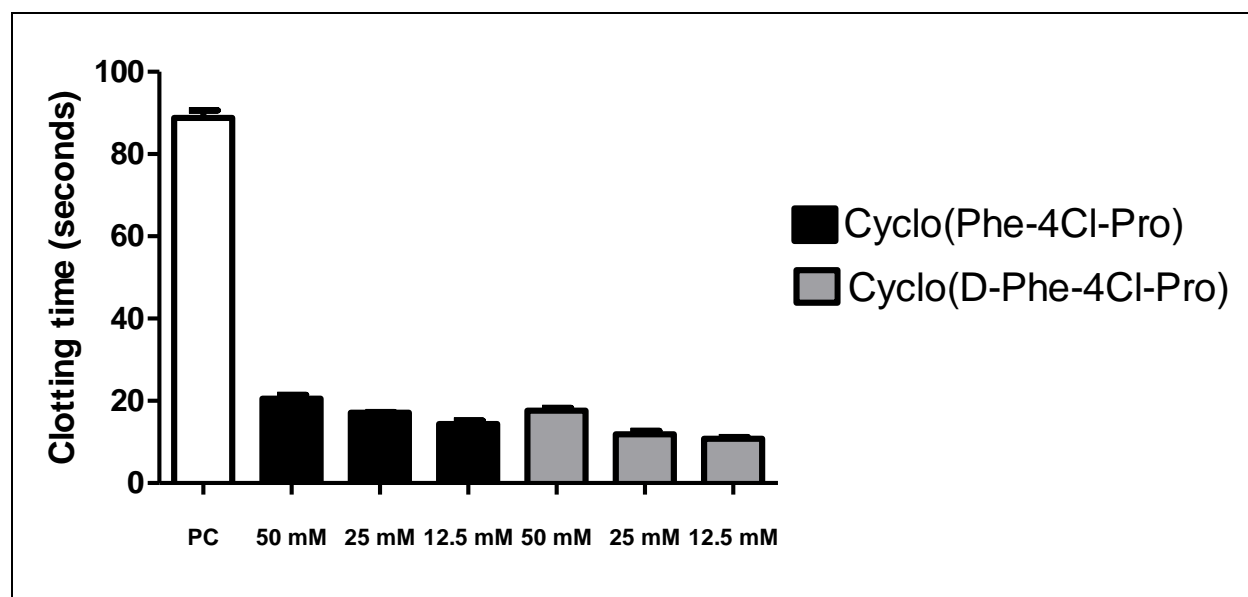


Figure 8.5 Effects of heparin (positive control), cyclo(Phe-4Cl-Pro) and cyclo(D-Phe-4Cl-Pro) on PT clotting time

8.5.3 Fibrinogen-C assay (Fib-C)

The activity of heparin, cyclo(Phe-4Cl-Pro) and cyclo(D-Phe-4Cl-Pro) on fibrin formation is illustrated in Figure 8.6 and summarised in Table 8.3. The conversion of fibrinogen to fibrin elicit a series of reactions that cross-link adjacent fibrin monomers which then stabilises the formed clot (Dipiro *et al.*, 2011). The addition of 100 µl of thrombin to the negative control (untreated plasma) resulted in the formation of 470.29 ± 0.510 mg/dL fibrin. Heparin (positive control) at a screening concentration of 0.1 U/ml decreased the formation of fibrin to 73.66 ± 3.670 mg/dL (P = 0.0144). Cyclo(Phe-4Cl-Pro) formed 116.7 ± 3.725 mg/dL (P = 0.0144) at 50mM, 273.2 ± 3.830 mg/dL (P = 0.0007) at 25 mM, 292.5 ± 2.500 mg/dL (P = 0.0004) at 12.5 mM. Cyclo(D-Phe-4Cl-Pro) formed 172.0

± 2.000 mg/dL ($P = 0.0018$) at 50 mM, 313.4 ± 2.545 mg /dL ($P = 0.0003$) at 25 mM and 369.8 ± 0.8350 mg/dL ($P = 0.0002$) at 12.5 mM.

Table 8.3 Effects of heparin, cyclo(Phe-4Cl-Pro) and cyclo(D-Phe-4Cl-Pro) on the formation of fibrin

Compound	Concentration	Fibrin formation (mg/dL)	<i>P</i> -value
Heparin	0.1 U/ml	73.66 ± 3.670	0.0144
Cyclo(Phe-4Cl-Pro)	50 mM	116.7 ± 3.725	0.0144
	25 mM	273.2 ± 3.830	0.0007
	12.5 mM	292.5 ± 2.500	0.0004
Cyclo(D-Phe-4Cl-Pro)	50 mM		0.0018

Pro)		172.0 ± 2.000	
	25 mM	313.4 ± 2.545	0.0003
	12.5 mM	369.8 ± 0.8350	0.0002

(*P*-values are calculated relative to the positive control)

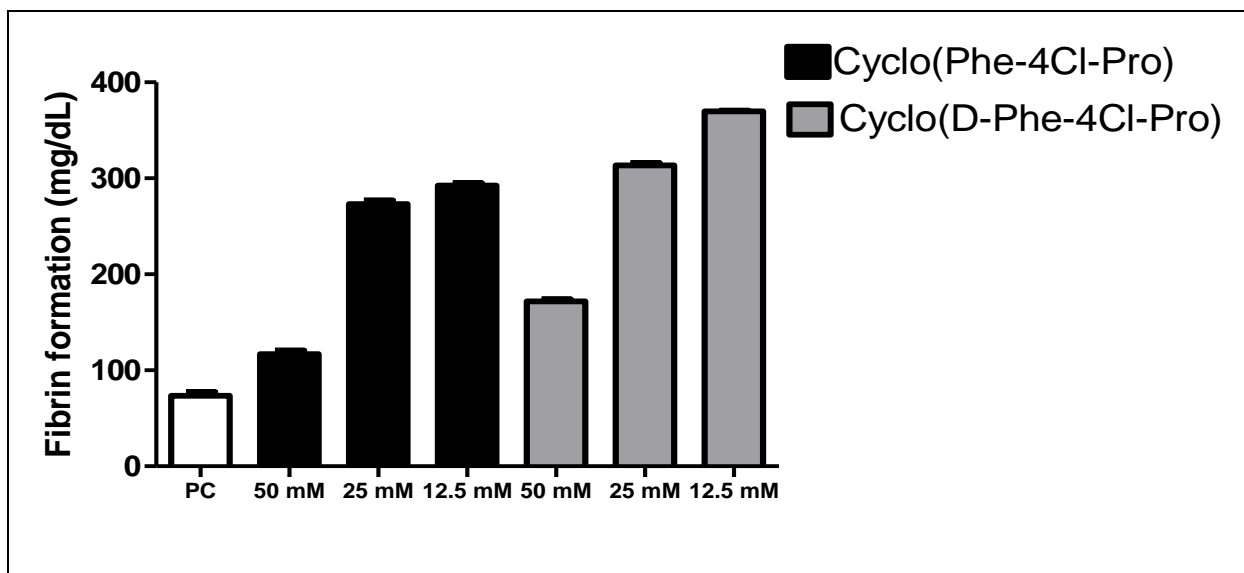


Figure 8.6 Effects of heparin (positive control), cyclo(Phe-4CI-Pro) and cyclo(D-Phe-4CI-Pro) on decreasing the formation of fibrin

8.5.4 D-Dimer assay

The effects of heparin, cyclo(Phe-4CI-Pro) and cyclo(D-Phe-4CI-Pro) on D-Dimer levels are illustrated in Figure 8.7 and summarised in Table 8.4. Heparin at a screening concentration of 0.1 U/ml significantly decreased the levels of D-Dimer (36.99 ± 1.000 ng/ml). Cyclo(Phe-4CI-Pro) at screening concentrations of 50 mM, 25 mM and 12.5 mM, produced results of 69.39 ± 1.055 ng/ml ($P = 0.0020$), 65.43 ± 2.875 ng/ml ($P = 0.0113$) and 53.10 ± 2.105 ng/ml ($P = 0.0203$). Cyclo(D-Phe-4CI-Pro) at screening concentrations of 50 mM, 25 mM and 12.5 mM, produced results of 53.91 ± 0.3100 ng/ml ($P = 0.0038$), 49.16 ± 0.1700 ng/ml ($P = 0.0069$) and 43.95 ± 0.9550 ng/ml ($P = 0.0373$), respectively. D-Dimer levels should under normal physiological conditions not be detectable in blood plasma, except when the coagulation cascade has been activated. High D-Dimer levels in plasma indicate elevated levels of fibrin formation and reflect a state of hypercoagulability (Moresco *et al.*, 2006). The cyclic dipeptides caused elevation of D-Dimer formation.

Table 8.4 Effects of heparin, cyclo(Phe-4Cl-Pro) and cyclo(D-Phe-4Cl-Pro) on D-Dimer formation

Compound	Concentration	D-Dimer formation (ng/ml)	<i>P</i> -value
Heparin	0.1 U/ml	36.99 ± 1.000	0.0020
Cyclo(Phe-4Cl-Pro)	50 mM	69.39 ± 1.055	0.0020
	25 mM	65.43 ± 2.875	0.0113
	12.5 mM	53.10 ± 2.105	0.0203
Cyclo(D-Phe-4Cl-Pro)	50 mM	53.91 ± 0.3100	0.0038
	25 mM	49.16 ± 0.1700	0.0069
	12.5 mM	43.95 ± 0.9550	0.0373

(*P*-values are calculated relative to the positive control)

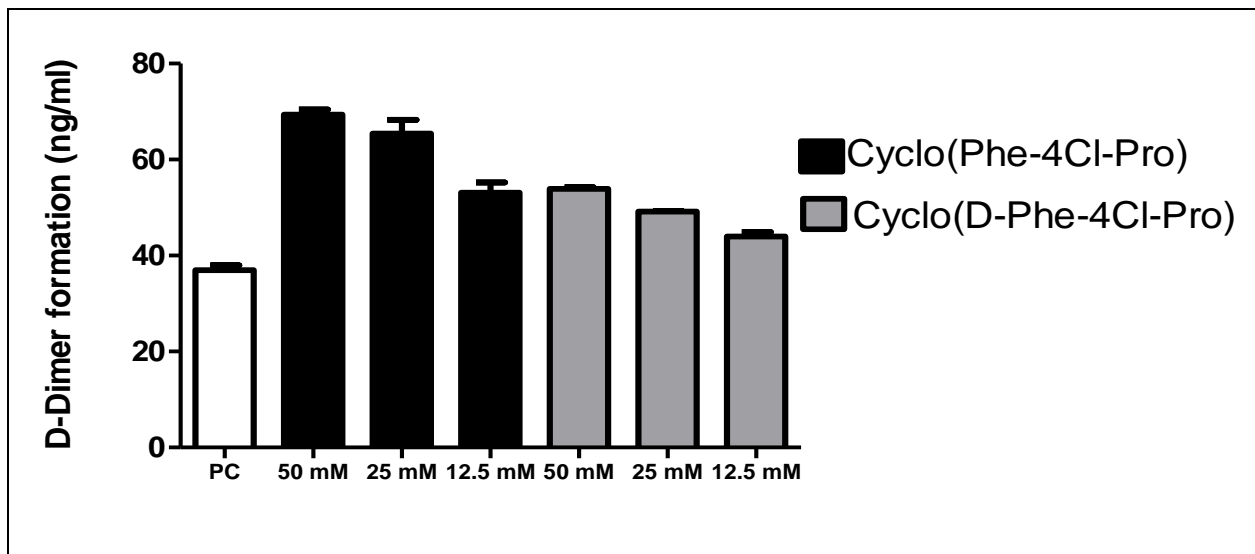


Figure 8.7 Effects of heparin (positive control), cyclo(Phe-4CI-Pro) and cyclo(D-Phe-4CI-Pro) on D-Dimer formation

8.5.5 Platelet aggregation studies

Figures 8.8 to 8.17 illustrate the flow-cytometry diagrams and cell density plots for the untreated control (PRP), treated control (PRP with 50U/ml thrombin), cyclo(Phe-4CI-Pro) and cyclo(D-Phe-4CI-Pro), at screening concentrations of 50 mM, 25 mM and 12.5 mM and 3.125 mM. In order to obtain the percentage of cells that stained positive, a region gate was drawn around a population of intact cells to exclude cell debris and clumped cells. The platelet particles that exhibited aggregation were excluded by the defined gate.

For the untreated control 1.3% of the cells exhibited aggregation. The positive control (thrombin 50 U/ml) indicated an 7.6% increase in aggregation. Cyclo(Phe-4CI-Pro) increased the aggregation to 95.2%, 94.4%, 92.6 and 90.5% at screening concentrations of 50 mM, 25 mM, 12.5 mM and 3.125 mM respectively. Cyclo(D-Phe-

4Cl-Pro) produced percentage aggregations of 93.5%, 32.4%, 0.2% and 0.3% at screening concentrations of 50 mM, 25 mM, 12.5 mM and 3.125 mM respectively.

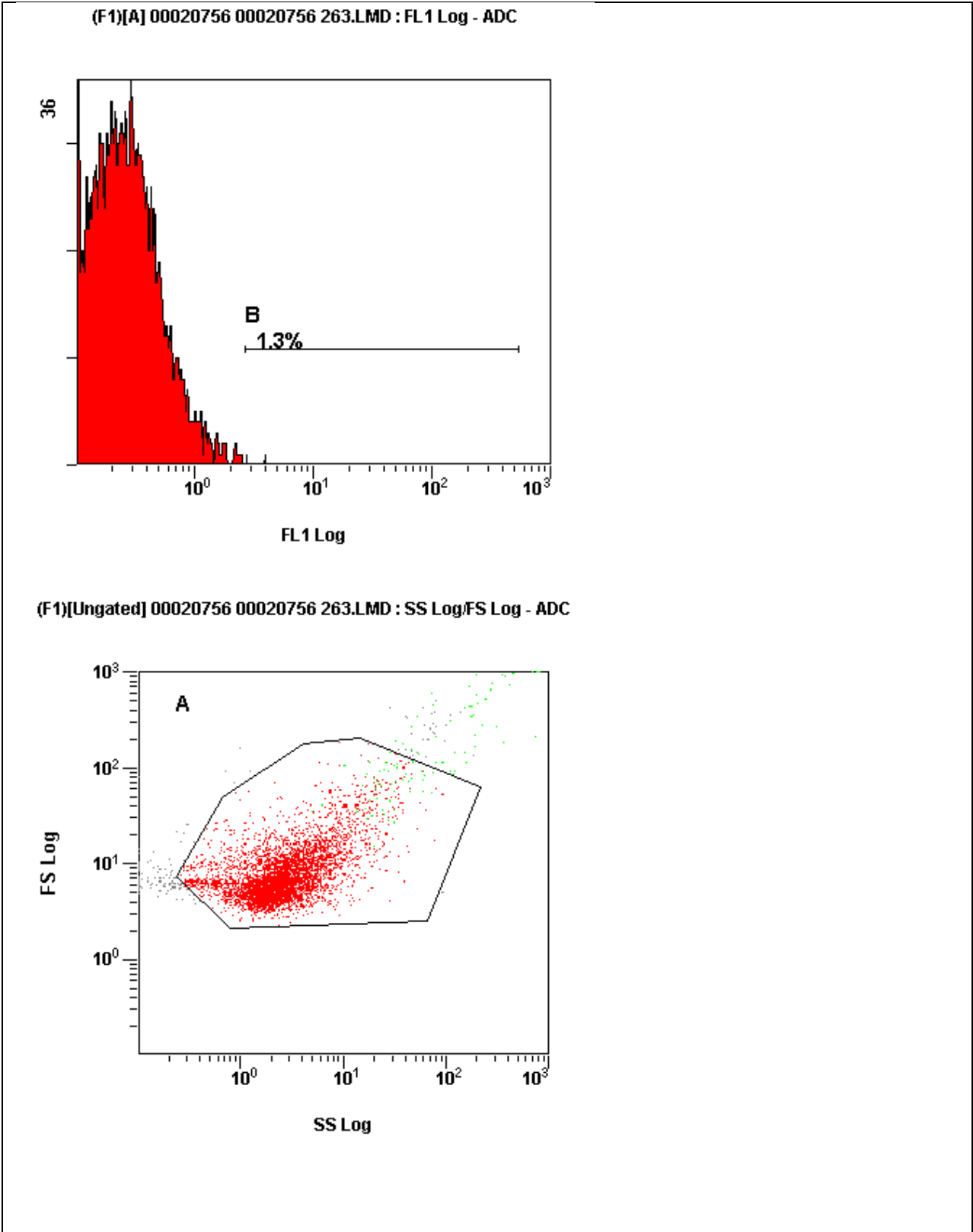


Figure 8.8 Fluorescence intensity and cell density plot representation of platelet aggregation caused by the untreated control (PRP)

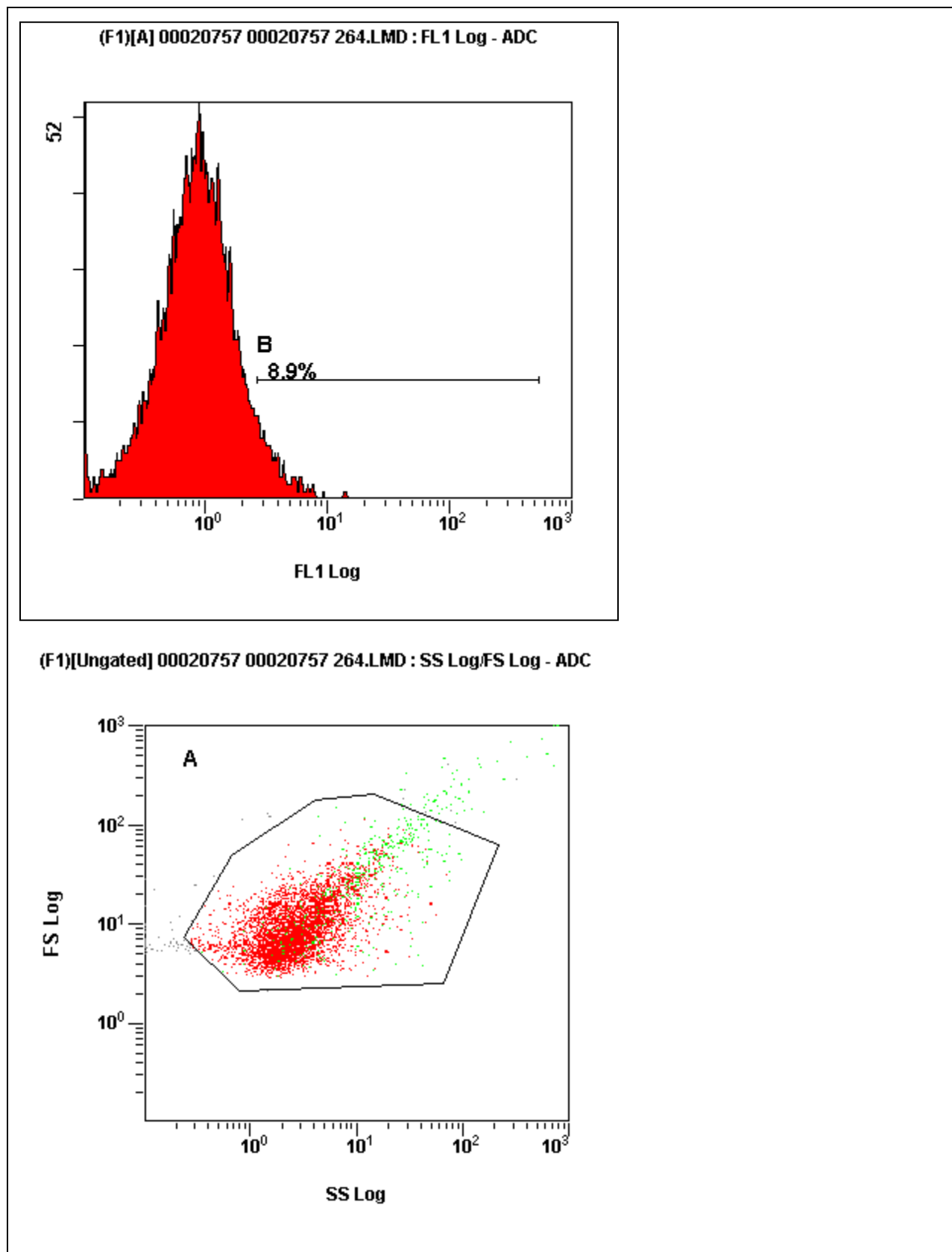


Figure 8.9 Fluorescence intensity and cell density plot representation of platelet aggregation caused by the positive control (PRP with thrombin 50 U/ml)

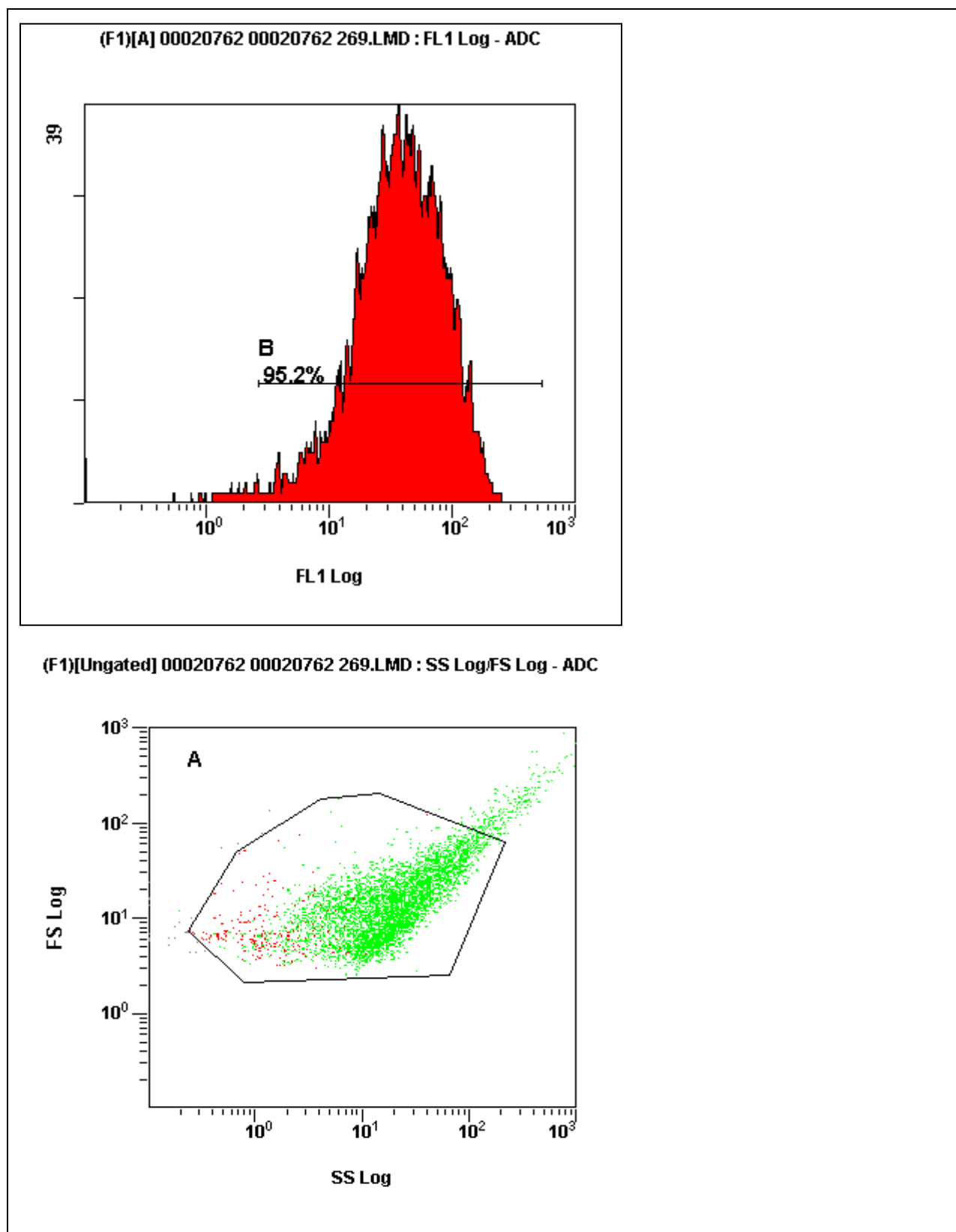


Figure 8.10 Fluorescence intensity and cell density plot representation of platelet aggregation caused by 50 mM cyclo(Phe-4Cl-Pro)

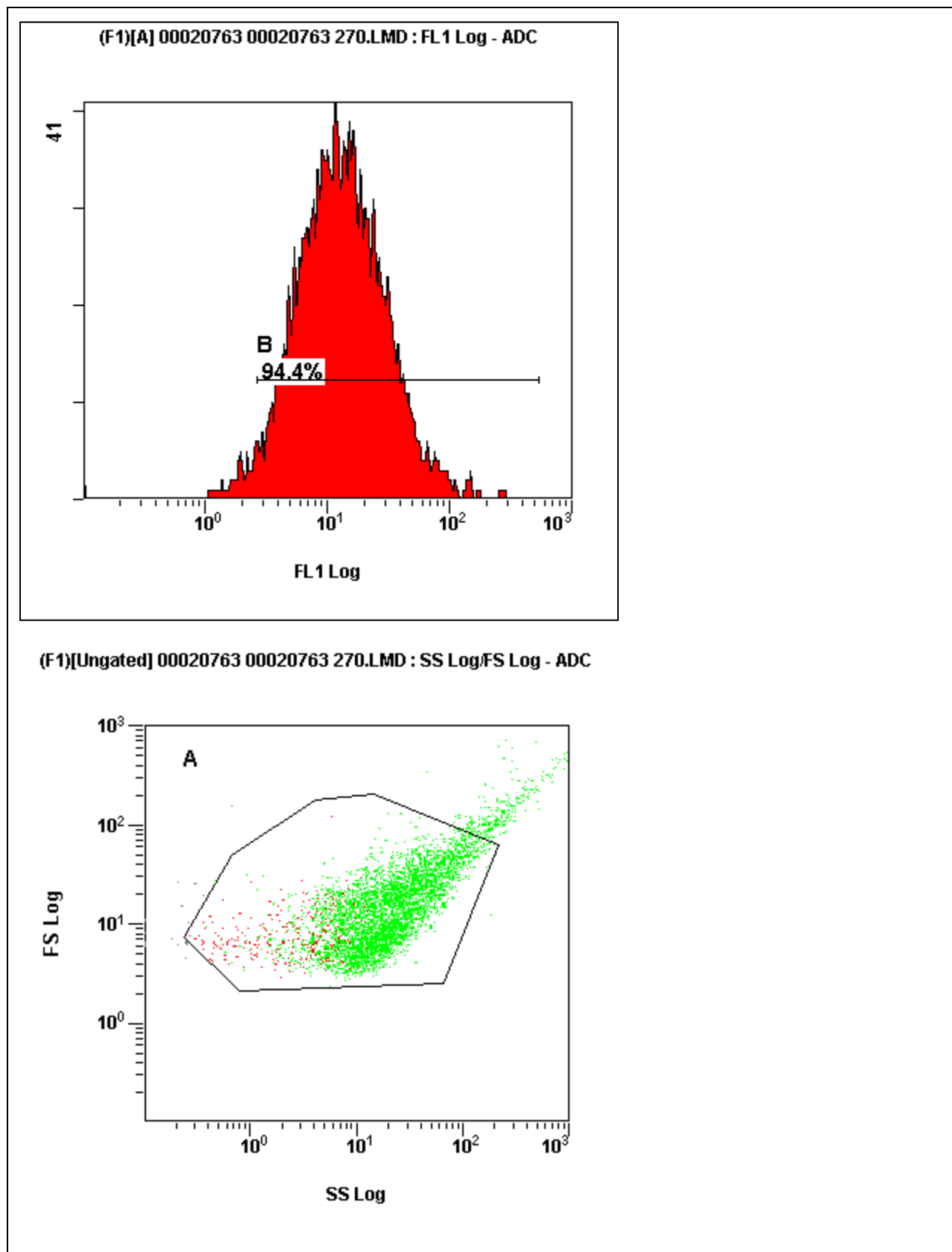


Figure 8.11 Fluorescence intensity and cell density plot representation of platelet aggregation caused by 25 mM cyclo(Phe-4Cl-Pro)

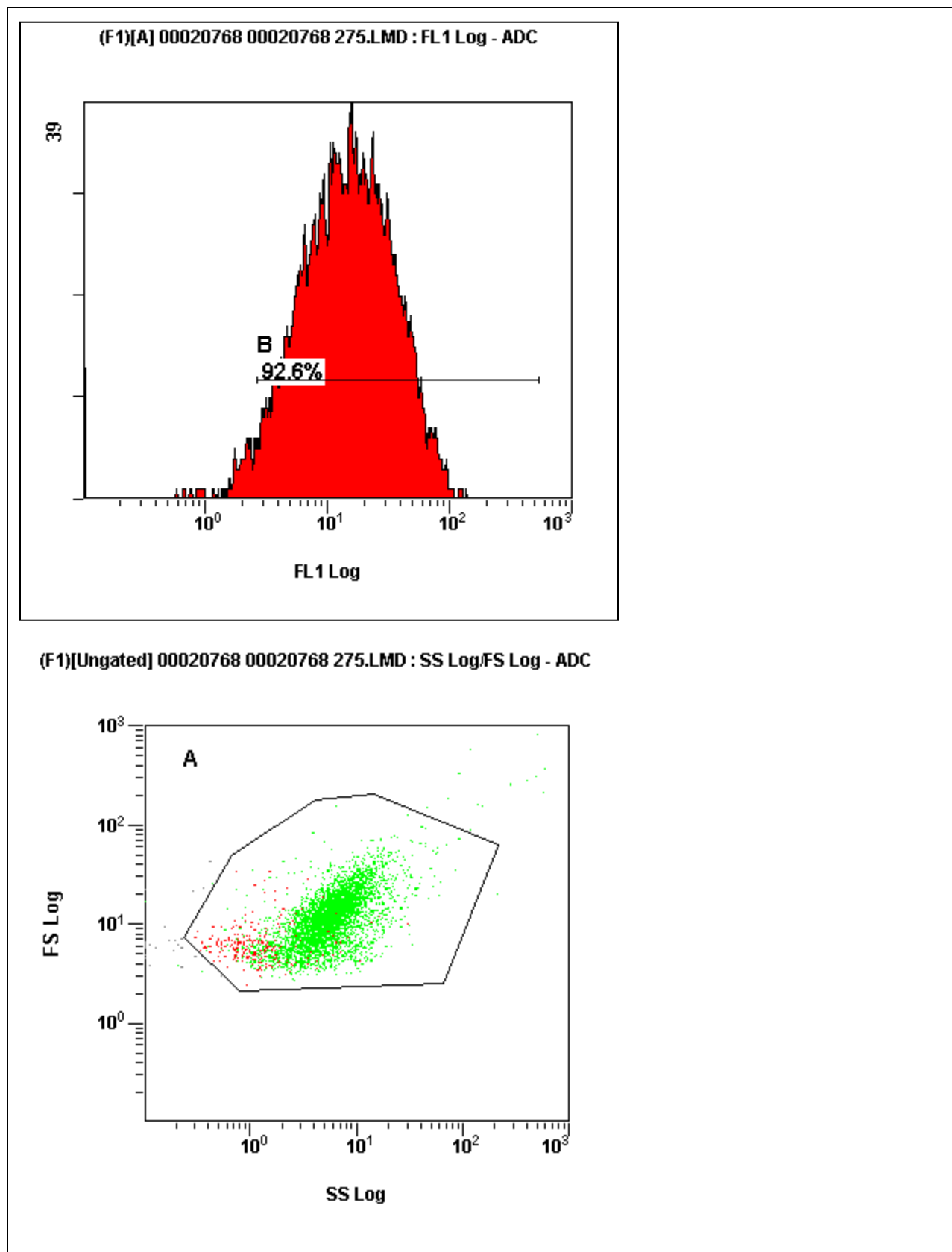


Figure 8.12 Fluorescence intensity and cell density plot representation of platelet aggregation caused by 12.5 mM cyclo(Phe-4Cl-Pro)

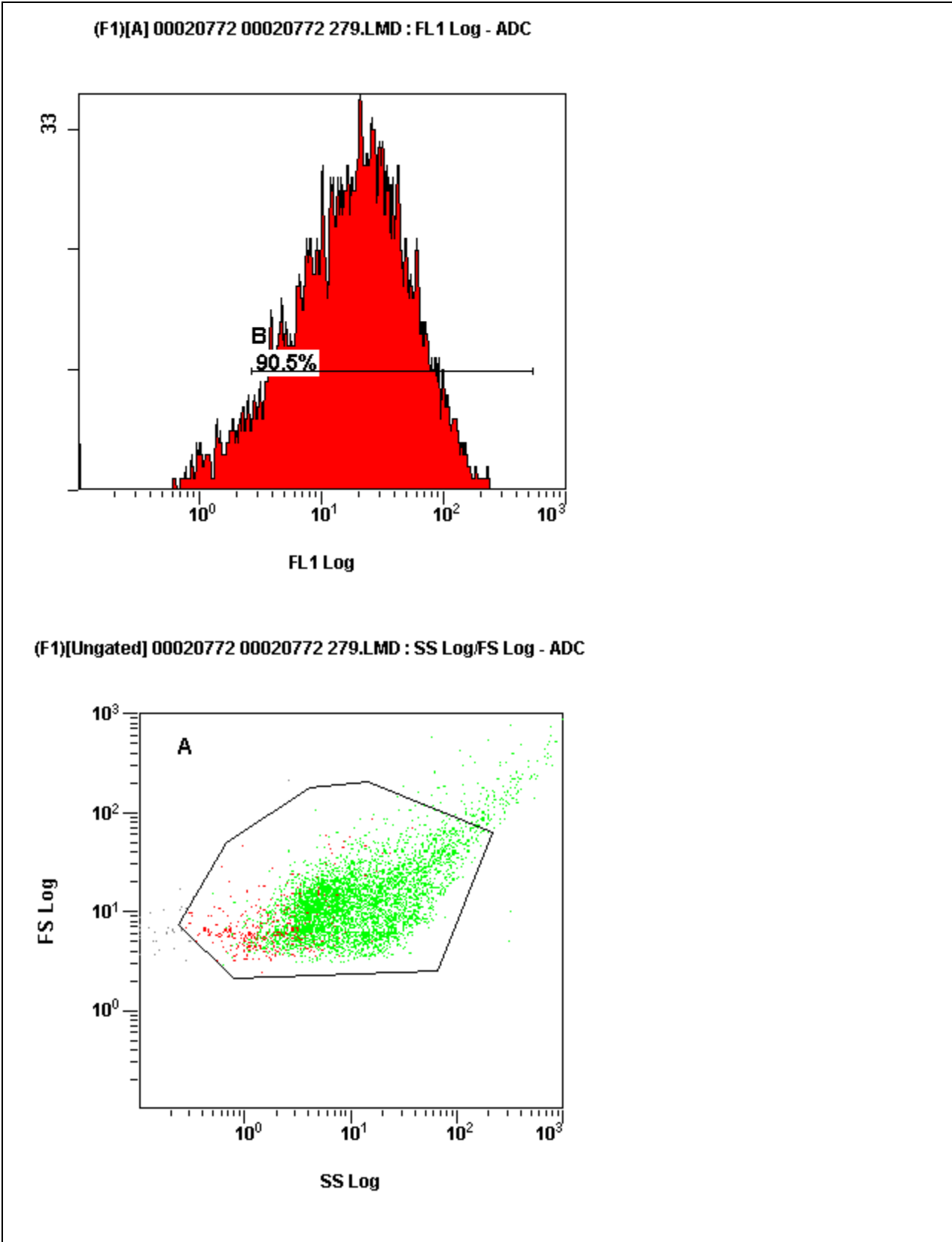


Figure 8.13 Fluorescence intensity and cell density plot representation of platelet aggregation caused by 3.125 mM cyclo(Phe-4Cl-Pro)

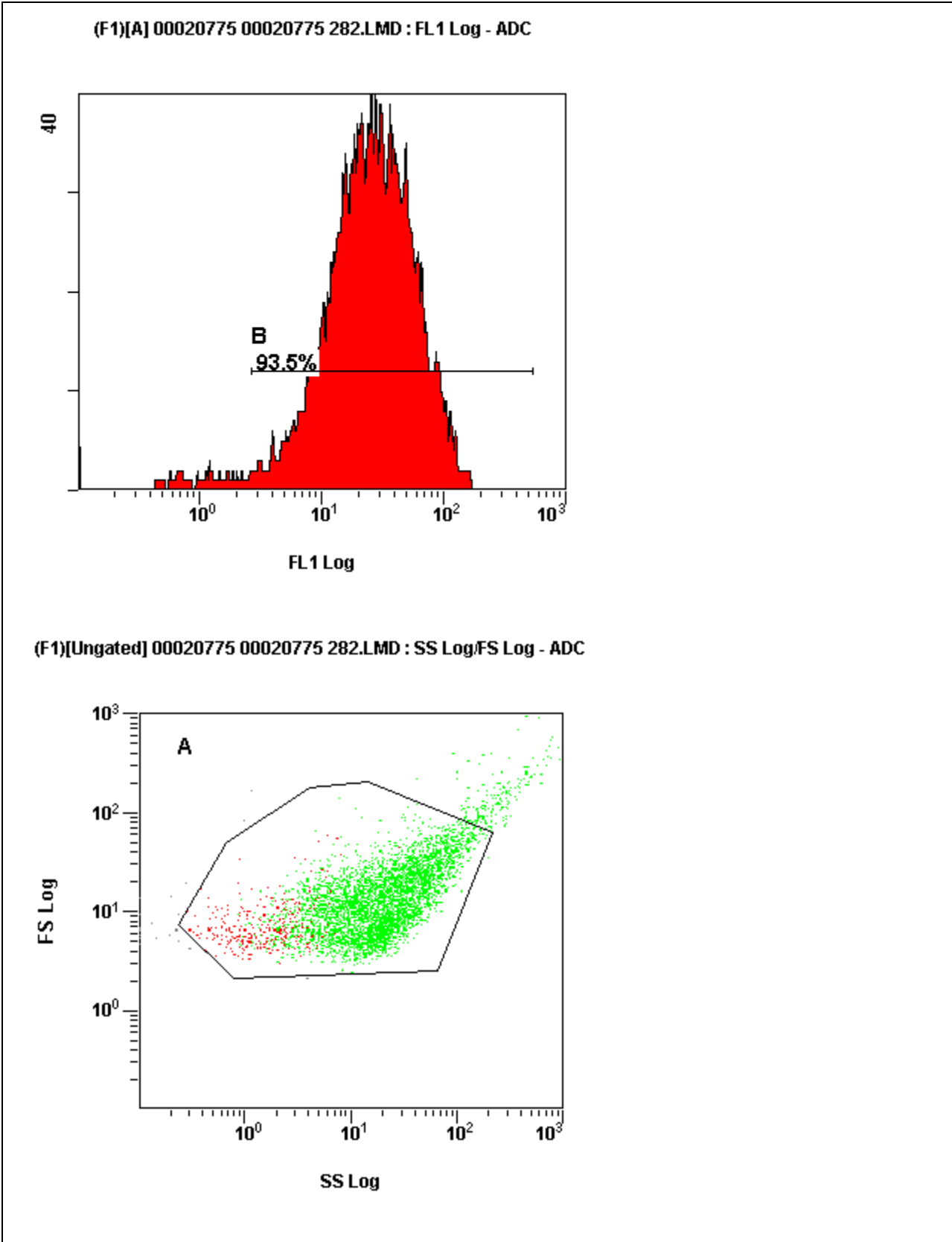


Figure 8.14 Fluorescence intensity and cell density plot representation of platelet aggregation caused by 50 mM cyclo(D-Phe-4Cl-Pro)

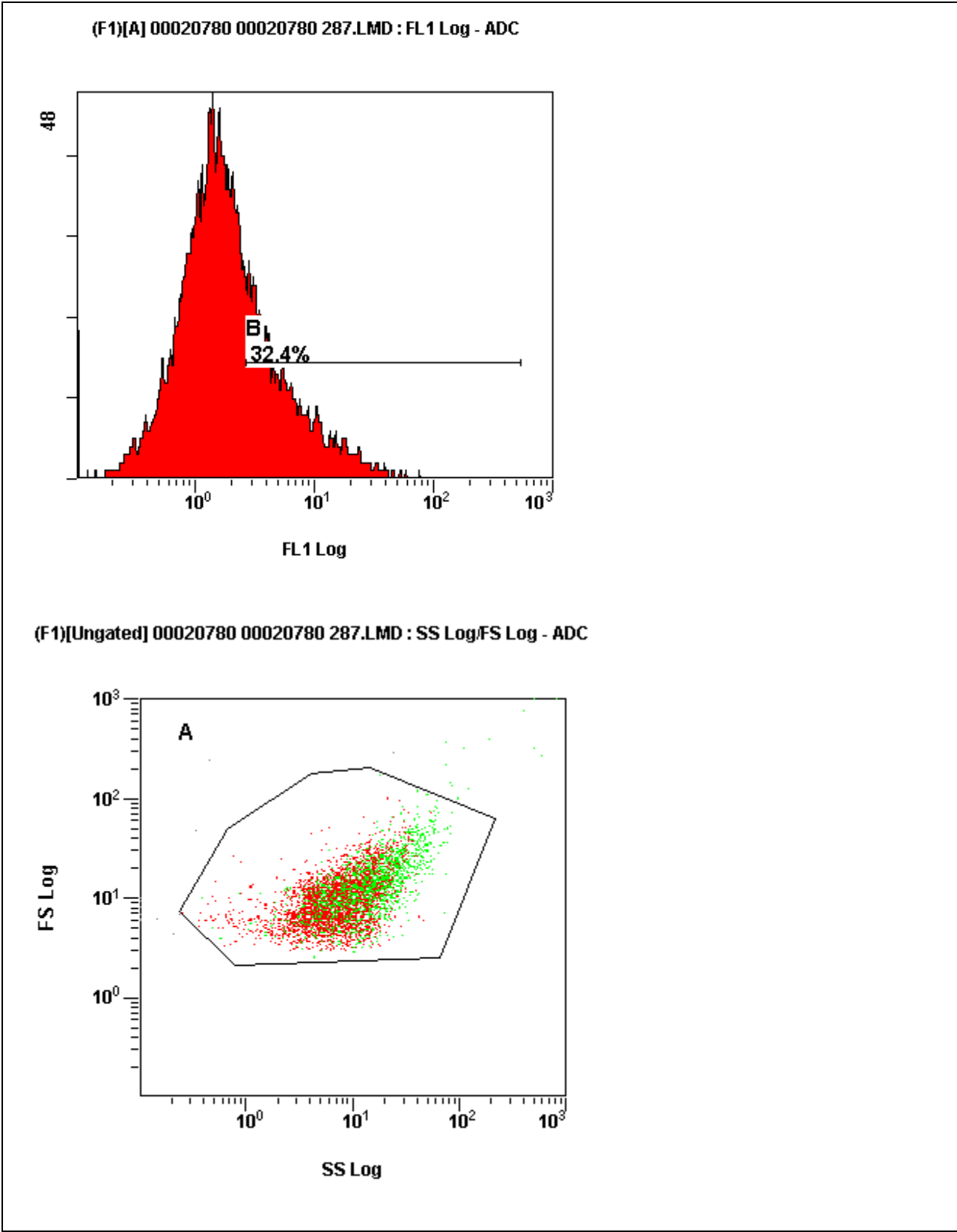


Figure 8.15 Fluorescence intensity and cell density plot representation of platelet aggregation caused by 25 mM cyclo(D-Phe-4Cl-Pro)

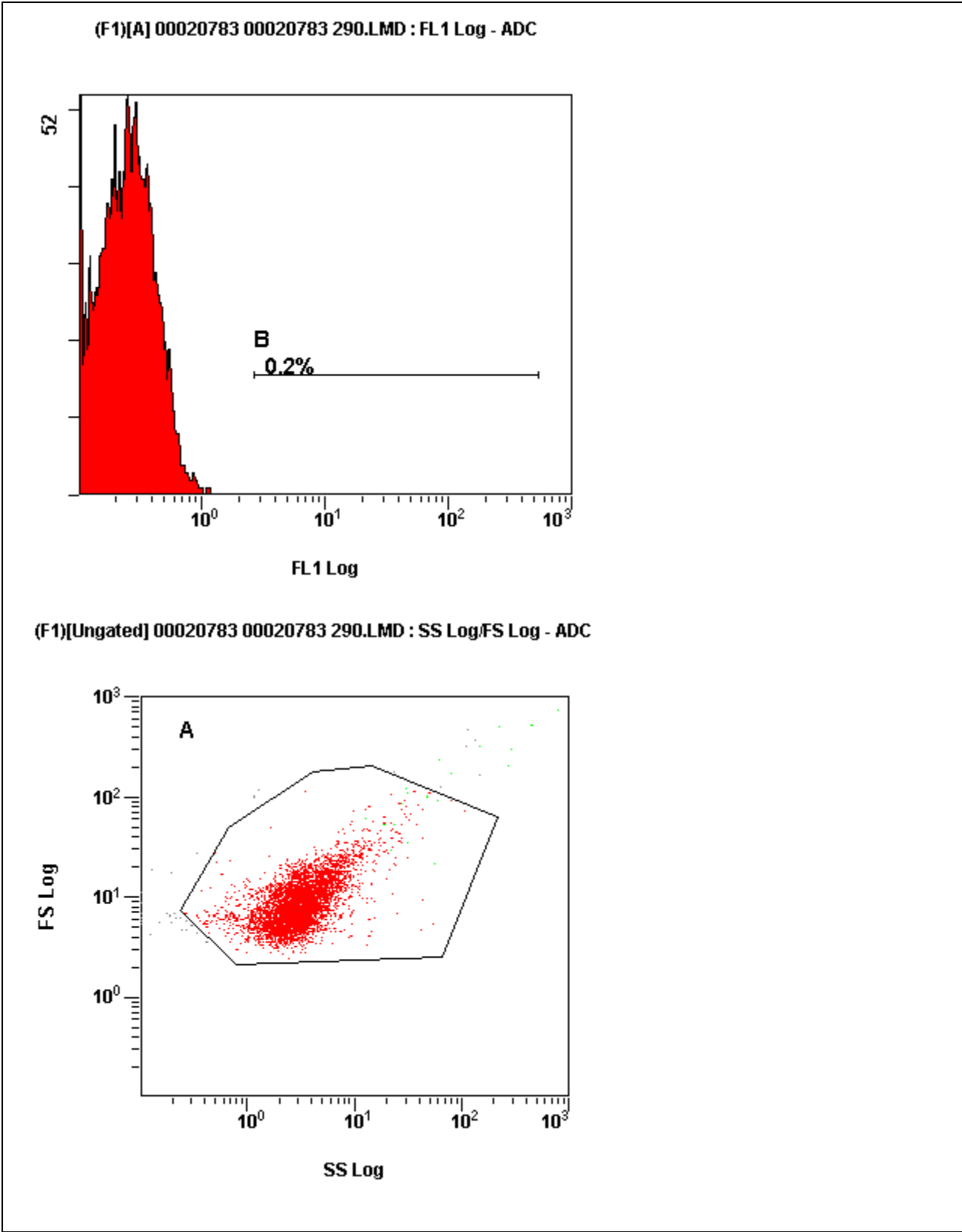


Figure 8.16 Fluorescence intensity and cell density plot representation of platelet aggregation caused by 12.5 mM cyclo(D-Phe-4Cl-Pro)

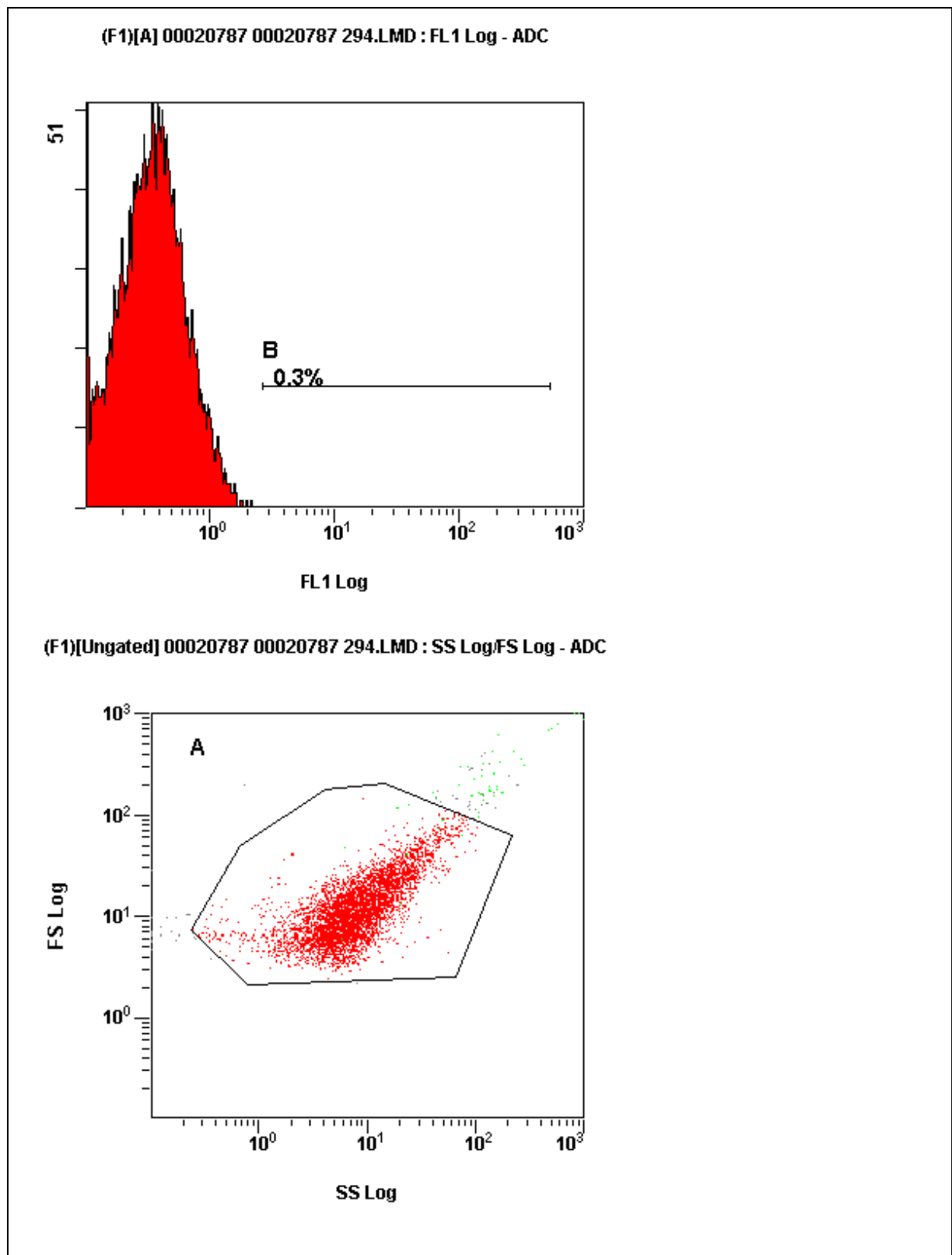


Figure 8.17 Fluorescence intensity and cell density plot representation of platelet aggregation caused by 3.125 mM cyclo(D-Phe-4Cl-Pro)

8.6 Summary

Variables such as blood collection methods, the collection container characteristics, sample storage prior to use and contact activation time could have affected the results obtained from the coagulation and flow-cytometry assay.

The activity of both cyclic dipeptides on the extrinsic and intrinsic pathways was evaluated by conducting APTT and PT assays. The effect of both cyclic dipeptides on prolonging clotting time in both assays was found to be insignificant. It can be concluded therefore that the compounds yielded no anticoagulant activity.

The cyclic dipeptides showed significant reduction of fibrin formation and D-Dimer levels when compared with the relevant controls. The results were however not significant enough to indicate a strong potential for the compounds to be used clinically.

The results of the platelet aggregation assay showed that both cyclic dipeptides enhanced aggregation. The compounds can for this reason not be used as anti-platelet agents. Cyclo (D-Phe-4Cl-Pro) at 12.5 mM and 3.125 mM exhibited the most anti-platelet activity. Future studies could possibly involve conducting further serial dilutions of cyclo(D-Phe-4Cl-Pro), and looking at dose response curves.

CHAPTER 9

ANTI-DIABETES

9.1 Introduction

Diabetes mellitus (DM) is a metabolic disorder which has reached epidemic status (Stunvoll *et al.*, 2005; Bakker *et al.*, 2009). By 2030 366 million people are predicted to be diagnosed with DM (Stunvoll *et al.*, 2005; Bakker *et al.*, 2009). Type 1 DM (T1DM) is characterised by the loss of insulin production due to β -cell failure, while type 2 DM (T2DM) is characterised by the development of insulin resistance in responsive tissues, particularly muscle line and adipose. This impaired insulin production in conjunction with decreased response to insulin results in hyperglycemia. T2DM is the most common form of DM, since it accounts for more than 90% of DM cases (Bakker *et al.*, 2009).

9.2 Physiology of the Islet of Langerhans

The Islet of Langerhans within the pancreas are the primary regulators of blood glucose and contain four main cell types: β -cells secrete insulin and islet amyloid in response to elevated blood glucose levels, A-cells secrete glucagon when blood glucose levels are depressed, D-cells secrete somatostatin and PP cells secrete pancreatic polypeptide. The core of each islet mainly consists of β -cells. Islet amyloid delays gastric emptying and opposes insulin by stimulating glycogen breakdown in striated muscle. Glucagon also opposes insulin, increasing blood glucose and stimulating protein breakdown in muscle. Somatostatin inhibits insulin and glucagon secretion. Somatostatin is also released from the hypothalamus, inhibiting the release of growth hormone from the pituitary (Rang *et al.*, 2011).

9.3. Regulation of glucagon and insulin secretion

The principal action of glucagon is to increase blood glucose levels when it falls below normal. In contrast, insulin helps lower the blood glucose levels when it is too high (enables cellular uptake of glucose to provide energy for the cell). Low blood glucose levels (hypoglycaemia) stimulate the secretion of glucagon from A-cells of the

pancreatic islets. Glucagon then acts on the hepatocytes to accelerate the conversion of glycogen into glucose (glycogenolysis) and to promote the formation of glucose from lactic acid and certain amino acids (gluconeogenesis). Consequently hepatocytes release glucose into the blood more rapidly, and the blood glucose levels rise. If blood glucose levels continue to rise, high blood glucose level (hyperglycaemia) inhibits the release of glucagon and stimulates the release of insulin by the β -cells of the pancreatic islets. Insulin acts on various cells in the body to accelerate facilitated diffusion of glucose into cells, especially skeletal muscle fibers, in order to (I) speed the conversion of glucose into glycogen (glycogenesis), (II) to increase the uptake of amino acids by cells and (III) to increase protein synthesis, to speed up the synthesis of fatty acids (lipogenesis) and (IV) to slow glycogenolysis, and gluconeogenesis. Consequently the blood glucose levels fall. If the blood glucose levels drop below normal, low blood glucose inhibits the release of insulin. Table 9.1 summarises the metabolic effects of insulin and glucagon

Table 9.1 The metabolic effects of insulin and glucagon (Dipiro *et al.*, 2011)

cellular activity	Insulin	glucagon
Glycogenesis	↑	↓
Glycogenolysis	↓	↑
Gluconeogenesis	↓	↑
Ketogenesis	↓	↑
Lipolysis	↓	↑
Lipogenesis	↑	↓

9.4. Diabetes Mellitus

Diabetes Mellitus is a chronic metabolic disorder characterised by a high blood glucose concentration (fasting plasma glucose > 7.0 mmol/L, or plasma glucose >11.1 mmol/L), caused by insulin deficiency, often combined with insulin resistance. Hallmarks of DM are excessive urine production, due to an inability of the kidneys to reabsorb water (polyuria), excessive thirst (polydipsia) and excessive eating (polyphagia) (Rang *et al.*, 2011).

9.4.1 Type 1 DM (T1DM)

Type 1 DM is an autoimmune disease in which the person's immune system destroys the pancreatic β -cells, causing low insulin levels in the body. Here insulin injections are required to prevent death, and it is for this reason that the disease is also called insulin-dependent diabetes mellitus (IDDM). Since insulin is not present to aid entry of glucose into body cells, most cells use fatty acids to produce adenosine triphosphate (ATP). Stores of triglycerides in adipose tissues are catabolised to yield fatty acids and glycerol. The by-products of fatty acid breakdown, ketones, accumulate and cause the blood pH to fall (ketoacidosis). The breakdown of stored triglycerides also results in weight loss. Lipid particles are deposited on the walls of the blood vessels, leading to atherosclerosis and a multitude of cardiovascular problems. A major complication of diabetes is (I) loss of vision, when excessive glucose attaches to the lens proteins causing cloudiness or (II) when damaged is caused to the blood vessels of the retina (Dipiro *et al.*, 2011).

9.4.2 Type 2 DM (T2DM)

In Type 2 DM, β -cells slowly lose their capacity to produce insulin due to damage caused by increased demand on these cells; and target tissues receptors show reduced sensitivity to insulin. The result is reduced glucose uptake and hyperglycaemia (Dipiro *et al.*, 2011).

9.4.3 Diagnosis of DM

Diagnosis of insulin dependent diabetes mellitus (IDDM) is based on the presence of elevated blood glucose levels (hyperglycaemia), the presence of glucose in the urine (glucosuria) and excessive production of urine (polyuria), all resulting from a lack of insulin secretion. For non insulin dependent diabetes mellitus (NIDDM) the glucose tolerance test (GTT) is used. The GTT evaluates the ability of an individual's cells to take up and metabolise glucose. After an oral dose of glucose is given, its level in the blood and urine is monitored. If the blood glucose level goes up and remains elevated, it is a sign that insulin secretion is inadequate to cope with the absorbed glucose (Dipiro *et al.*, 2011).

9.4.4 Treatment of DM

The main aim of DM treatment is the restoration of glucose metabolism. Treatment of IDDM is predominantly by subcutaneous injection of insulin. Meals, consisting of high percentage carbohydrates and low percentage fats, must be taken at regular time intervals, with frequent snacks between meals. Foods rich in sugars are strictly limited as they release glucose from the gastric intestinal lumen into the blood more rapidly than the amount injected insulin can cope with. Battery-powered insulin infusion pumps provide a continuous insulin supply through a subcutaneous needle or intravenously. Transplantation of the pancreas is also being explored (Dipiro *et al.*, 2011).

In the early stages of NIDDM the disease can be controlled with diet and exercise, because both contribute to weight loss. As weight is reduced the insulin receptor numbers on normally insulin responsive cells increase and insulin resistance is diminished (Dipiro *et al.*, 2011).

9.5 Anti-diabetic drugs

9.5.1 Thiazolidinediones

The thiazolidinediones (TZDs) enhance insulin sensitivity, thereby, reducing glucose levels. The TZDs also improve endothelial and inflammatory function, dislipidemia, and

dissolution of blood clots (fibrinolysis). The TZDs have a high affinity for a specific peroxisome proliferator-activated receptor (PPAR) subtype (Nathason and Nyström, 2009; Jellinger and Mace, 2007; Stunvoll *et al.*, 2005). There are three PPAR subtypes. Firstly, PPAR_α which is expressed abundantly in the liver, heart muscle and vascular wall. Secondly, PPAR_{α/β} which is abundantly expressed in skin, brain and adipose tissue and thirdly, PPAR_γ which is predominantly expressed in adipose tissue but also in pancreatic β-cells, the endothelium and macrophages (Nathason and Nyström, 2009). TZDs bind to PPAR_γ and are for this reason thought to act primarily in adipose tissue. TZDs improve insulin sensitivity by causing the redistribution of tissue triglycerides or fats from visceral stores to subcutaneous adipose tissue. The action of TZDs not only reduces 'non-esterified fatty acids' circulating levels but also reduces the plasma levels of free fatty acids, while increasing the levels of adiponectin. TZDs also improve renal function by improving albumin excretion (Jellinger and Mace, 2007; Stunvoll *et al.*, 2005). Currently available TZDs include pioglitazone and rosiglitazone (Dipiro *et al.*, 2011).

9.5.2 Biguanides

Metformin is the drug of choice for T2DM in combination with diet and exercise. It improves insulin sensitivity in tissues by decreasing hepatic glucose production and increasing glucose uptake in skeletal muscle and adipose tissues with minimum risk of hypoglycaemia. It also reduces appetite and consequently calorie intake and may improve insulin secretion by pancreatic β-cells (Dipiro *et al.*, 2011). Metformin reduces the level of circulating triglycerides, free fatty acids and low density lipoprotein cholesterol, while increasing the levels of high density lipoprotein cholesterol. Metformin also improves endothelial function (Nathason and Nyström, 2009; Jellinger and Mace, 2007; Stunvoll *et al.*, 2005). The mechanism of action of metformin is thought to be *via* the activation of 5' adenosine monophosphate-activated protein kinase (AMPK). Metformin indirectly activates AMPK by activating complex-1 in the respiration chain. The activation of AMPK down-regulates gluconeogenesis, cholesterol biosynthesis, and the fatty acid synthesis pathway. AMPK activation in the endothelium and myocardial tissue is also associated with angiogenesis regulation (Nathason and Nyström, 2009).

Metformin also possesses anti-thrombotic effects by lowering the *in vivo* levels of factor (f) VII and fibrinogen and increases fibrinolysis by lowering the levels of PAI-1 (Nathason and Nyström, 2009).

9.5.3 α -Glucosidase inhibitors

Acarbose reduces the blood glucose levels. It mediates this action by inhibiting α -glucosidase found in the small intestine. α -Glucosidase converts oligosaccharides to monosaccharides (Nathason and Nyström, 2009).

9.5.4 Sulphonylurea derivatives

Sulphonylureas (SUs), increase insulin secretion by closing ATP-dependent K^+ -channels that are found in a variety of cells, including pancreatic β -cells, skeletal muscle tissues, vascular smooth muscle cells, the endothelium, kidney and central nervous system. The ATP-dependent K^+ -channels are made up of two sulphonylurea proteins, sulphonylurea receptor 1 (SUR1) and sulphonylurea receptor 2 (SUR2) and Kir 6.2. SUR1 is expressed in β -cells, while SUR2 is expressed in myocardial cells. Kir 6.2 is a pore-forming unit K^+ -inward rectifier channel. The SUs close the K^+ -channels by binding to the pancreatic β -cell SUR1/Kir 6.2 protein. The influx of Ca^{2+} , because of membrane depolarisation, leads to the exocytosis of insulin vesicles. They also improve endothelial function (Dipiro *et al.*, 2011).

Examples of the SUs currently in use are glibenclamide, gliclazide, glimepiride and glipizide. Gliclazide and glipizide have a short duration of action, while glibenclamide and glimepiride have a longer duration of action that can last up to 24 hours. The risk of hypoglycaemia is lower in SUs that have a short duration of action, and gliclazide can be used in patients with reduced renal function. The SUs also decrease the levels of glycosylated haemoglobin (Nathason and Nyström, 2009).

9.5.5 Meglitinides

Nateglinide, like SUs, also binds to SUR1. Repaglinide stimulates insulin secretion by binding to a different site on the receptor. The advantage of using meglitinides is that they do not cause hypoglycaemia, but compared with the SUs, have a shorter duration of action. Meglitinides can also be used in patients with reduced renal function (Dipiro *et al.*, 2011).

9.5.6 Glucagon-like peptide 1

Glucagon-like peptide 1 (GLP-1) is formed from the partial proteolysis of proglucagon that is produced in the small and large intestine by the enteroendocrine L-cells. GLP-1 causes high insulin responses that are glucose dependent, increases the mass of β -cells, and inhibits intestinal motility. GLP-1 is rapidly degraded by dipeptidyl peptidase IV (DPP-IV), and consequently has a very short half-life of between 1 and 2 minutes. It is for this reason that GLP analogues with a longer half-life, such as exenatide and liraglutide and inhibitors of DPP-IV have been developed. GLP-1 has also been reported to improve vascular integrity and protects against endothelial dysfunction (Nathanson and Nyström, 2009).

9.6 Methodology

The anti-diabetic effects of the cyclic dipeptides were determined by conducting α -glucosidase and α -amylase assays. The α -glucosidase enzyme is responsible for the conversion or breakdown of carbohydrates into monosaccharides. Monosaccharides are absorbed in the small intestine resulting in elevated blood glucose levels. α -Amylase assays hydrolysis α -bonds of large α -linked polysaccharides, yielding glucose and maltose (Dipiro *et al.*, 2011).

9.6.1 Preparation of test solutions

100 mg of rat intestinal acetone powder was suspended in 3 ml of 0.01 M phosphate buffer (pH 7.0) and sonicated for 30 seconds, 12 times in an ice bath. The solution was centrifuged at 3000 rpm at 4 °C for 20 minutes. The crude enzyme solution was

removed and the pellets were also discarded. The supernatant solution was kept on ice prior to use.

9.6.1.1 Positive control

A 500 mM stock solution of acarbose was prepared by dissolving 0.321 g/ml in reverse osmosis water. The stock solution was diluted with reverse osmosis water to give a final screening concentration of 50 mM, then filter-sterilised through 0.22 µm acetate filters prior to use.

9.6.1.2 4-Nitrophenyl- α -D-glucopyranoside

A stock concentration of 0.5 mM 4-nitrophenyl- α -D-glucopyranoside was prepared by dissolving 1.5065 mg in 10 ml of 0.1 M phosphate buffer (pH 7.0). The solution was filter-sterilised through 0.22 µm acetate filters prior to use.

9.6.1.3 Sodium carbonate

A stock concentration of 0.2 M sodium carbonate solution was prepared by dissolving 1.06 g sodium carbonate in 50 ml reverse osmosis water. The solution was filter-sterilised through 0.22 µm acetate filters prior to use.

9.6.2 α -glucosidase assay

Methods employed by Sancheti *et al.* (2009) were adapted to determine the effects of cyclo(Phe-4Cl-Pro) and cyclo(D-Phe-4Cl-Pro) on the activity of the α -glucosidase enzyme.

Mixtures consisting of 50 µl of the 0.1 M phosphate buffer, 25 µl of the 0.5 mM 4-nitrophenyl- α -D-glucopyranoside solution, 10 µl of either the acarbose solution, cyclo(Phe-4Cl-Pro) solution or cyclo(D-Phe-4Cl-Pro) solution were incubated at 37 °C for 30 minutes. After incubation 100 µl of 0.2 M sodium carbonate solution was added to terminate the enzymatic reaction. The amount of *p*-nitrophenol released in the reaction was determined spectrophotometrically at 410 nm using a microplate reader (BioTek

Power Wave XS). The amount of *p*-nitrophenol released was proportional to the enzymatic hydrolysis of the substrate. Experiments were conducted in triplicate.

α -Glucosidase inhibition was calculated as a percentage of the control using the formula:

$$\text{Percentage inhibition} = \frac{A_c - A_s}{A_c} \times 100$$

Where A_c is the change in absorbance of the blank control and A_s is the change in absorbance that occurs between the time the substrate is added to the mixture and 30 minutes after incubation.

9.6.3 α -Amylase assay

Methods developed by Fuwa (1954) and modified by Xiao *et al.* (2006) were adapted to determine the effects of cyclo(Phe-4Cl-Pro) and cyclo(D-Phe-4Cl-Pro) on α -amylase activity. The microplate-based starch-iodine assay was utilised. This assay is based on the development of color that results when iodine binds to starch polymers. The amount of starch degraded determines the activity of α -amylase.

40 μ l of starch (Sigma) solution and 40 μ l of the α -amylase enzyme (in 0.1 M phosphate buffer at pH 7.0) were pipetted into microplate wells and incubated at 50 °C for 30 minutes. After incubation 20 μ l of 1 M HCl was added to terminate the enzymatic reaction. 100 μ l of iodine reagent (5 mM iodine and 5 mM potassium iodide) was then added. When color development was evident, 150 μ l of the iodine-treated sample was transferred into a transparent 96-well flat-bottomed microplate and the absorbance was read at 580 nm, using a microplate reader (BioTek Power Wave XS). The experiment was conducted in triplicate.

α -Amylase activity was determined as relative activity according to the following formula:

$$\text{Dextrinising activity} = \frac{(D_0 - D)}{D_0} \times \frac{100}{10}$$

Where D is the absorbance of the enzyme sample and D₀ is the absorbance of the amylase control without the addition of enzyme.

9.7 Statistical analysis

Data was represented graphically with the aid of statistical software packages, Microsoft Excel[®] (Version 2007) and Graph Pad Prism[®] (Version 5). The results obtained from the α-glucosidase and the α-amylase assays were compared with the controls without inhibitor using the Student's *t*-test and expressed as mean ± SD.

9.8 Results and discussion

9.8.1 α-Glucosidase assay

The effects of acarbose (positive control) at a screening concentration of 50 mM, 1 mM of cyclo(Phe-4Cl-Pro) and 1 mM of cyclo(D-Phe-4Cl-Pro) on the activity of α-glucosidase are shown in Figure 9.1

Acarbose at a screening concentration of 50 mM inhibited the activity of the α-glucosidase enzyme by 51.11% ± 4.498 (P < 0.0001) while cyclo(Phe-4Cl-Pro) and cyclo(D-Phe-4Cl-Pro) inhibited the activity by -4.352% ± 1.477 (P < 0.0001) and -6.953% ± 1.740 (P < 0.0001), respectively. These negative values obtained, indicates a stimulation of the α-glucosidase enzyme and thus an increase in the conversion of carbohydrates to monosaccharides and elevated blood glucose levels.

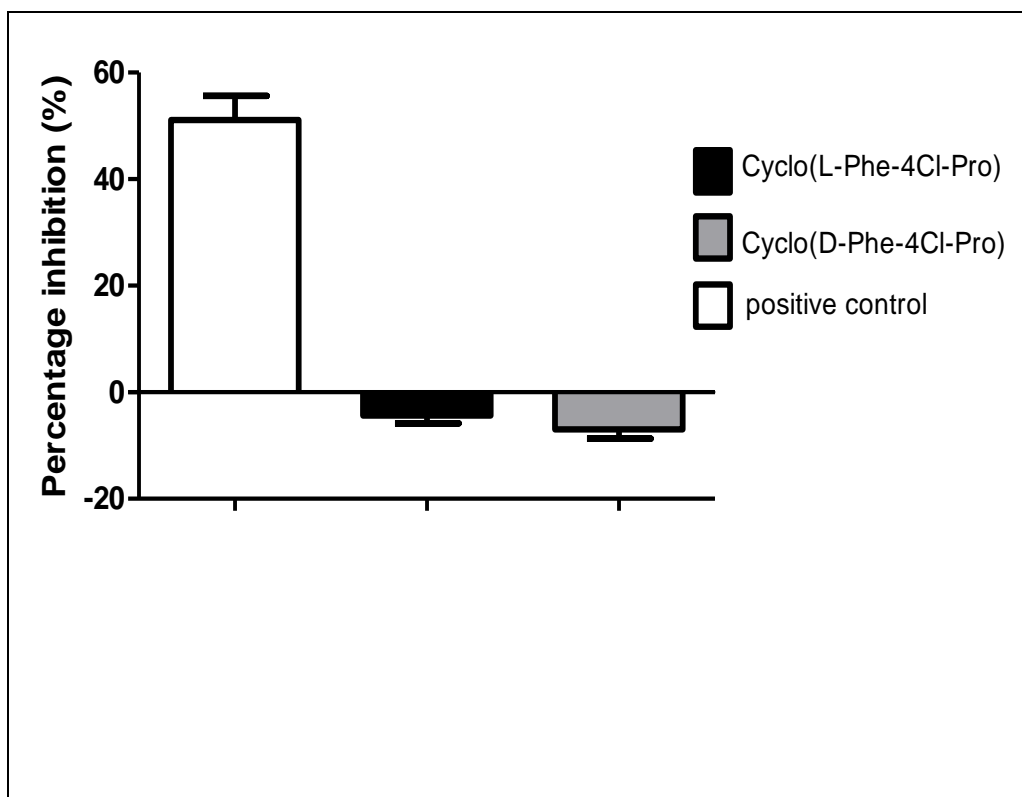


Figure 9.1 α -Glucosidase enzyme inhibition caused by acarbose (positive control), cyclo(Phe-4Cl-Pro) and cyclo(D-Phe-4Cl-Pro)

9.8.2 α -Amylase activity

The effects of acarbose, cyclo(Phe-4Cl-Pro) and cyclo(D-Phe-4Cl-Pro) on the activity of α -amylase are shown in Figure 9.2.

Acarbose inhibited the activity of the α -amylase enzyme by $55.51\% \pm 2.786$ ($P < 0.0001$) at a screening concentration of 50 mM. Cyclo(Phe-4Cl-Pro) and cyclo(D-Phe-4Cl-Pro) inhibited the enzyme's activity by $5.654\% \pm 0.02507$ ($P < 0.0001$) and $5.530\% \pm 0.05743$ ($P < 0.0001$), respectively.

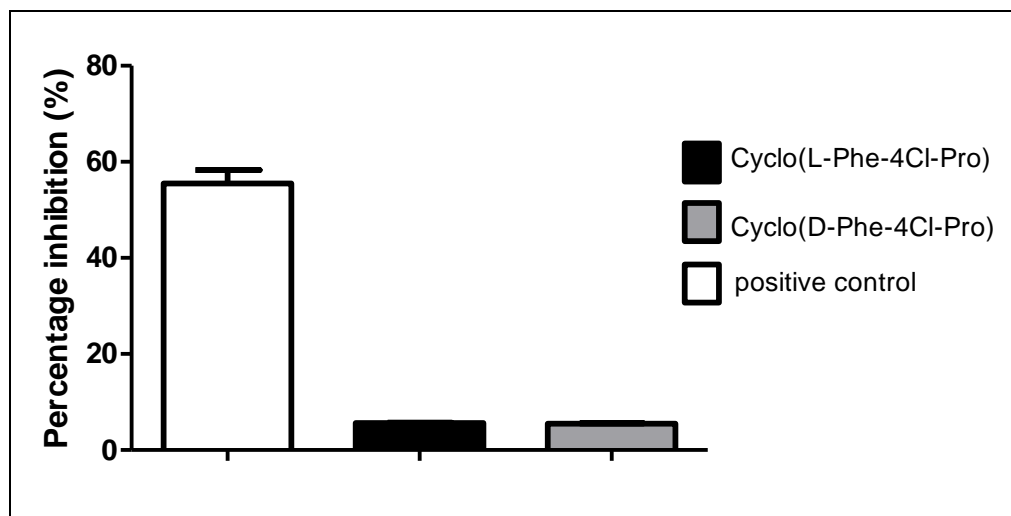


Figure 9.2 α -Amylase enzyme inhibition caused by acarbose, cyclo(Phe-4Cl-Pro) and cyclo(D-Phe-4Cl-Pro)

9.9 Summary

The inhibition of activity of the α -glucosidase and α -amylase enzymes caused by both cyclic dipeptides was revealed to be insignificant as both cyclic dipeptides had an enzyme inhibition of less than 10%. It can also be noted that both cyclic dipeptides slightly increased the activity of the α -glucosidase enzyme. For these reasons it was concluded that cyclo(Phe-4Cl-Pro) and cyclo(D-Phe-4Cl-Pro) have no therapeutic potential in inhibiting α -glucosidase and α -amylase enzymes. Future studies could include conducting cellular assays of the relevant cyclic dipeptides.

CHAPTER 10

CONCLUSIONS AND RECOMMENDATIONS

The cyclic dipeptides cyclo(Phe-4Cl-Pro) and cyclo(D-Phe-4Cl-Pro), were successfully synthesised from their corresponding linear precursors using a modified phenol-induced cyclisation procedure. Yields of 54% and 62% were obtained for cyclo(Phe-4Cl-Pro) and cyclo(D-Phe-4Cl-Pro) respectively. Qualitative analysis, purity determination and evaluation of the physiochemical properties of the cyclic dipeptides were achieved by high-performance liquid chromatography, scanning electron microscopy, thermogravimetric analysis, differential scanning calorimetry and X-ray diffraction. Results confirmed that the synthesised cyclic dipeptides were free from impurities and could therefore be used for further biological studies.

Infrared spectroscopy, mass spectroscopy, nuclear magnetic resonance spectroscopy and molecular modelling were utilised to conduct the structural and conformational analysis of the synthesised compounds. The proposed structures of cyclo(Phe-4Cl-Pro) and cyclo(D-Phe-4Cl-Pro) were confirmed.

Anticancer, antimicrobial, haematological and anti-diabetic studies were conducted to determine the biological activity of cyclo(Phe-4Cl-Pro) and cyclo(D-Phe-4Cl-Pro). The use of dimethyl sulphoxide in the experiments aided in dissolving the respective cyclic dipeptides and other compounds, but was used at minimum concentrations that were not toxic to the cells and would therefore not interfere with the biological studies.

Cyclo(Phe-4Cl-Pro) and cyclo(D-Phe-4Cl-Pro) exhibited limited clinical potential as anticancer agents against HeLa (cervical cancer), HT-29 (colon cancer) and MCF-7 (breast cancer) cell lines, when compared to Melphalan. The limited anticancer activity demonstrated by both cyclic dipeptides may be as a result of their hydrophilic nature, which hinders their ability to cross the respective cell membranes. Of the three cancer cell lines, the growth of MCF-7 cell was inhibited the most by the cyclic dipeptides. The

greatest inhibition of MCF-7 cell growth displayed by the cyclic dipeptides, was produced by cyclo(Phe-4Cl-Pro) at a concentration of 200 μ M. Additional anticancer studies could include the biological testing of both cyclic dipeptides against other cancer cell lines, since cyclic dipeptides have shown to exhibit anticancer effects against a broad spectrum of human cancer cell lines. Studies can also be conducted to determine the effect of both cyclic dipeptides on non cancerous cell lines. Dose response curves should be calculated, where growth inhibitory effects are statistically and clinically significant, in order to determine the minimum inhibitory concentrations (MIC) of the cyclic dipeptides. The cyclic dipeptides could also be tested in combination to determine if they could exert synergistic inhibitory effects on cancer growth. Studies should be performed to determine the selectivity of the cyclic dipeptides for the cancer cells, as antineoplastic therapy is aimed to eliminate cancer cells and inflict minimal damage to normal cells.

Cyclo(Phe-4Cl-Pro) and cyclo(D-Phe-4Cl-Pro) exhibited very limited broad antibacterial and antifungal activity. Both cyclic dipeptides showed limited activity against the Gram-positive bacteria. Cyclo(Phe-4Cl-Pro) at a concentration of 1 mM, exhibited the greatest inhibition for *B. subtilis*, with an inhibition of 18.27%. For *S. aureus* cyclo(D-Phe-4Cl-Pro) at a concentration of 1 mM, displayed the greatest inhibition of 68.00% \pm 2.665. Further studies are required to determine dose response curves to determine the effect of cyclo(D-Phe-4Cl-Pro) on *S. aureus*. For *E. coli*, cyclo(D-Phe-4Cl-Pro) at a concentration of 1 mM displayed the greatest inhibition of 25.83%. For *P. aeruginosa*, cyclo(D-Phe-4Cl-Pro) at a concentration of 1 mM, exhibited the greatest inhibition of 39.55%. For *C. albicans*, Cyclo(D-Phe-4Cl-Pro), at a concentration of 1 mM, exhibited the greatest inhibition of 54.28%. The limited antimicrobial activity demonstrated by both the cyclic dipeptides may be as a result of their hydrophilic nature, which hinders their ability to cross the lipid membranes of the microorganisms. Although the cyclic dipeptides were limited against the selected microorganisms in the antimicrobial study, it is recommended that the respective cyclic dipeptides be tested for activity against other microbial species, including plasmodium, viral and mycobacterium species. MICs should be determined for microorganisms, where statistically and clinically significant

inhibitory effects are observed. Studies should be performed to determine the selectivity of the cyclic dipeptides for the microorganisms. The cyclic dipeptides could also be tested in combination to determine if they could exert synergistic inhibitory effects on microbial growth.

Cyclo(Phe-4Cl-Pro) and cyclo(D-Phe-4Cl-Pro) exhibited very limited effects on the selected haematological studies. Cyclo(Phe-4Cl-Pro) at a concentration of 50 mM, produced the greatest prolongation of the APTT and PT clotting times, with a clotting times of 27.95 seconds and 20.53 seconds, respectively. Cyclo(D-Phe-4Cl-Pro) at a concentration of 12.5 mM produced the highest fibrin formation of 369.8 mg/dL. Cyclo(D-Phe-4Cl-Pro) at a concentration of 12.5 mM, produced the lowest D-Dimer formation of 43.95 ng/dL. Cyclo(D-Phe-4Cl-Pro) at concentrations of 12.5 mM and 3.125 mM, displayed the greatest ant-platelet activity with 0.2% and 0.3%, respectively. Cyclo(Phe-4Cl-Pro) and cyclo(D-Phe-4Cl-Pro) exhibited very limited effects on the selected α -amylase and α -glucosidase assays. Cyclo(D-Phe-4Cl-Pro) at a concentration of 1 mM exhibited the greatest inhibition of α -amylase, with an inhibition of 5.65%. Future studies could include conducting cellular assays.

Some drugs have an optimum concentration range within which maximum therapeutic effects exists, and concentrations above or below this range can be toxic or produce no therapeutic benefit at all. To minimise drug degradation and loss, to prevent harmful side effects and to increase drug bioavailability and the fraction of the drug accumulated in the required region remains the top priority of pharmaceutical scientists. Various drug delivery and drug targeting systems are currently under investigation. Among the drug carriers are soluble polymers, microparticles made of insoluble or biodegradable natural and synthetic polymers, microcapsules, cells, cell ghosts, lipoproteins, liposomes and micelles. Liposomal formulations have been extensively studied to enhance the efficiency of the delivery of drugs *via* several routes of administration (Kaparissides *et al.*, 2006), and have been suggested to improve cyclic dipeptides delivery (Cunningham, 2006; Van der Merwe, 2005; Kilian, 2010). Liposomes are a form of vesicles that consist either of many, few or just one phospholipid bilayers. The polar

character of the liposomal core enables polar drug molecules to be encapsulated (Kaparissides *et al.*, 2006). The limited biological activity of cyclo(Phe-4Cl-Pro) and cyclo(D-Phe-4Cl-Pro) is believed to be due to their hydrophilic nature which would impede their movement across lipophilic cell membranes. Utilising liposomes would therefore aid in encapsulating the cyclic dipeptides and therefore improve their penetration through the cell membranes, resulting in greater bioavailability and subsequent increased activity.

REFERENCES

Abraham RJ, Mobli M. 2004. The Prediction of ^1H NMR Chemical Shifts in Organic Compounds. *Spectroscopy Europe*; 16-22

Adessi C, Soto C. 2002. Converting a Peptide into a Drug: Strategies to Improve Stability and Bioavailability. *Current Medicinal Chemistry*, 9: 963-978

Ahuja S, Dong MW. 2005. Handbook of Pharmaceutical Analysis by HPLC, 2nd edition. United States of America: Elsevier Incorporated; 20, 21, 44, 62, 63, 146

Ajjan R, Ariëns RAS. 2009. Cardiovascular Disease and Heritability of the Prothrombic State. *Blood Reviews*; (23): 67-78

Ajjan R, Grant PJ. 2006. Coagulation and Atherothrombotic Disease; (186): 240-259

Andreeff M, Goodrich DW, Pardee AB. 2000. Cell Proliferation, Differentiation, and Apoptosis; 1-300

Andrews JM. 2001. Determination of Minimum Inhibitory Concentrations. *Journal of Antimicrobial Chemotherapy*; 48: 5-16

Antheunis MJO. 1978. The Cyclic Dipeptides. Proper Model Compounds in Protein Research. *Bulletin des Societes Chimiques Belges*; 87(8): 627-650

Aulton ME. 2002. Pharmaceuticals: The Science of Dosage form and Design, 2nd Edition. Spain:Harcourt Publishers Limited;1-679

Azevedo APS, Farias JC, Costa GC, Ferreira SC, Agragão-Filho WC, Sousa PR, Pinheiro MT, Micheil MC, Silva LA, Lopes AS. 2007. Anti-thrombotic Effect of Chronic

Oral Treatment with *Orbignya Phalerata* Mart. *Journal of Ethnopharmacology*; (11): 155-159

Bachmann F, Colman RW, Hirsh J, Marder VJ, Clowes AW, George JN. 2001. Plasminogen-plasmin Enzyme System. In Haemostasis and Thrombosis. Basic Principles and Clinical Practice. Philadelphia, USA: Lippincott Williams and Wilkins; 275-320

Bakker W, Eringa EC, Sipkema P, Van Hinsbergh VWM. 2009. Endothelial Dysfunction and Diabetes: Roles of Hyperglycaemia, Impaired Insulin Signaling and Obesity. *Cell and Tissue Research*; (335): 165-189

Bauman RW, Machunis-Masuoka E, Tizard IR. 2004. *Microbiology*. San Francisco: Pearson/Benjamin Cummings; 327, 357, 533, 588, 589, 633, 634

Bechmann M, Foerster H, Maisel H and Sebald A. 2004. Double-quantum filtered ^1H MAS NMR spectra. *Solid State Nuclear Magnetic Resonance*; 27 (3):174-9

Beckers D. 2004. The Power of X-ray Powder Diffraction for Pharmaceutical Analysis. *GIT Laboratory Journal*; (4) 21-23

Beers MH, Berkow R. 2004. The Merck Manual, 17th edition. United States of America: Merck and Company, Incorporated; 973-995

Bellavite P, Andrioli G, Guzzo P, Arigliano P, Chirumbolo S, Manzato F, Santonastaso C. 1994. A Calorimetric Method for the Measurement of Platelet Adhesion in Microtiter plates. *Analytical Biochemistry*; (216): 444-450

Bhattyacharyya L, Dabbah R, Hauck W, Sheinin E, Yeoman L, Williams R. 2005. Equivalence Studies for Complex Active Ingredients and Dosage Forms. *The American Association of Pharmaceutical Scientists Journal*; 7 (4): 786-812

Bláha K, Smolíkova J, Vitek A. 1966. Amino acids and Peptides, LXIV. Infrared Spectra of Substituted 2,5 Piperazinediones and the Detection of *cis*-peptide Bonds in Diastereometric Cyclohexapeptides. *Collection of Czechoslovakian Chemical Communications*; 31: 4296-4296

Bodanszky M. 1988. *Peptide Chemistry*. Berlin: Springer-verlag (95): 16, 17, 74-103, 138-143

Bodanszky M. 1993. *Principles of Peptide Synthesis*, 2nd edition. Berlin: Springer-verlag (96): 9-55, 63, 79, 88, 231

Bounameaux H, de Moerloos P, Perrier A, Reber G. 1994. Plasma Measurement of D-Dimer as diagnostic Aid in Suspected Venous Thromboembolism: An Overview. *Thrombosis and Haemostasis*; (71): 1-6

Bradshaw JP. 2003. Cationic Antimicrobial Peptides: Issue for Clinical Use. *Biodrugs*; 17 (4): 233-240

Brauns SCA. 2004. The Effects of Selected Proline-Based Cyclic Dipeptides on Growth and Induction of Apoptosis in Cancer Cells. PhD Thesis. University of Port Elizabeth

Brown ME. 1998. *Introduction to Thermal Analysis: Technique and Applications*. London University Press; 7-12, 17, 19, 25

Bull SD, Davies SG, Parkin RM, Sanchez-Sancho F. 1998. The Biosynthetic Origin of Diketopiperazines Derived from D-Proline. *Journal of the Chemical Society, Perkin Transactions I*; 2313-2320

Campbell MK, Farrell SO. 2003. *Biochemistry*, 3rd edition. Philadelphia: Saunders College; 76-195

Capasso S, Vergara A, Mazzearella I. 1998. Mechanism of 2,5 Dioxopiperazine formation. *Journal of the American Chemical Society*, (120) 1990-1995

Castãnon MM, Gamba C, Kordich LC. 2007. Insight Into the Profibrinolytic Activity of Dermatansulfate: Effects on the Activation of Plasminogen Mediated by Tissue and Urinary Plasminogen Activators. *Thrombosis Research*; (120): 745-752

Castle JE, Zhdan PA. 1997. Characterisation of Surface Topography by SEM and SFM: Problems and solutions. *Journal of physics D-Applied Physics*; 30: 722-740

Cohen CN. 2007. The Molecular Modelling Perspective in Drug Design. London: *Academic Press*; (97): 389-396

Coussens L, Werb Z. 2002. Inflammation and Cancer. *Nature*; 420:860-867

Crescenzi V, Cesaro A, Russo E. 1973. On Some Physico-chemical Properties of Diketopiperazines in Water. *International Journal of Peptide and Protein Research*; 5: 427-434

Cunningham TL. 2006. The Medicinal Chemistry of the Selected Glycine-containing Cyclic Dipeptides: Cyclo(Gly-Thr) and Cyclo(Gly-Ser). MSc Dissertation. Nelson Mandela Metropolitan University

De Rosa S, Mitova M, Tommonaro G. 2003. Marine Bacteria Associated with Sponge as the Source of Cyclic Peptides. *Bimolecular Engineering*; 20: 311-316

Delaforge M, Bouille G, Jaouen M, Jankowski CK, Lamouroux C, Bensoussan C. 2001. Recognition and Oxidative Metabolism of Cyclodipeptides by Hepatic Cytochrome P450. *Peptides*; 22 (4): 557-565

Della Gatta G, Usacheva T, Badea E, Palecz B, Ichim D. 2005. Thermodynamics of Salvation of Some Small Peptides in water at T = 298.15 K. *Journal of Chemical Thermodynamics*; 44: 9691–9702.

Deslauriers R, Grzonka Z, Schaumburg K, Shiba T, Walter R. 1975. Carbon-13 Nuclear Magnetic Resonance Studies of the Conformations of Cyclic Dipeptides. *Journal of the American Chemical Society*; 97 (18): 5093-5100

Dinsmore CJ, Beshore DC. 2002. Recent advances in the Synthesis of Diketopiperazines. *Tetrahedron*; 58: 3297-3312

Dipiro JT, Talbert RL, Yee GC, Matzke GR, Wells BG, Posey LM. 2011. Pharmacotherapy: A Pathological Approach. 8th edition. New York: McGraw-Hill Medical Publishing Division; 2175-2222

Dodd JW, Tonge KH. 1987. Thermal methods. London : John Wiley and Sons; 1-137

Epand RM, Vogel HJ. 1999. Diversity of Antimicrobial Peptides and Their Mechanisms of Action. *Biochimica et Biophysica Acta*; 1462: 11-28

Field LD, Sternhell S, Kalman JR. 2001. Organic Structures from Spectra, 2nd edition. Chichester: John Wiley and Sons; 59-69

Fischer PM. 2002. Diketopiperazine in Peptide and Combinatorial Chemistry. *Journal in Peptide Science*; 9: 9-35

Freimoser FM, Jacob CA, Aebi M, Tuor U. 1999. The MTT [3-(4,5 dimethylthiazol-2-yl)-2,5-diphenyltetrazolium bromide] Assay is a Fast and Reliable Method for Colorimetric Determination of Fungal Cell Densities. *Applied and Environmental Microbiology*; 65 (8):3727-3729

Freshney IR 2006. Culture of Animal Cells – A Manual of Basic Technique, 4th edition. New York: Willey Liss; 1-577

Frokjaer S, Hovgaard L. 2000. Pharmaceutical Formulation Development of Peptides and Proteins. Taylor and Francious Limited; 2, 25, 26, 71-84, 153

Fu X, Ferreira MLG, Schmitz FJ, Kelly-Borges M. 1998. New Diketopiperazines from the Sponge *Disidea Chlorea*. *Journal of Natural Products*; 61: 1226-1231

Funasaki N, Hada S, Neya S. 1993. Conformational effects in Reverse-phase Liquid Chromatographic Separation of Diastereomers of Cyclic Dipeptides. *Analytical Chemistry*; 65: 1861-1867

Fuwa H. 1954. A New Method of Microdetermination of Amylase Activity by the Use of Amylase as the Substrate. *Journal of Biochemistry*; 41: 583-603

Gaffney PL, Creighton LJ, Callus M, Thorpe R. 1988. Monoclonal Antibodies to Crosslinked Fibrin Degradation Products (XL-FDP) II, Evaluation In a Variety of Clinical Conditions. *British Journal of Haematology*; (68): 91-96

Gazes J. 2001. Encyclopedia of Chromatography. Marcel Dekker; 594-597, 719-722

Gentry PA. 2004. Comparative Aspects of Blood Coagulation. *The Veterinary Journal*; 168: 238-251

Gisin BF, Merrifield RB. 1972. Carboxyl-catalysed Intramolecular Aminolysis. A Side Reaction in Solid-phase Peptide Synthesis. *Journal of the American Chemical Society*; 94 (9): 3102-3106

Goolcharran C, Borchardt RT. 1998. Kinetics of Diketopiperazine Formation Using Model Peptides. *Journal of Pharmaceutical Sciences*; 87: 283-288

Grant GD. 2002. The Medicinal Chemistry of Cyclo(Trp-Trp), Cyclo(Gly-Trp) and Cyclo(Gly-Gly). PhD Thesis. University of Port Elizabeth

Graz CJM. 2002. Cyclic Dipeptides as Novel Antimicrobial Agents. PhD Thesis. University of Port Elizabeth

Graz M, Hunt A, Jamie H, Grant G, Milne P. 1999. Antimicrobial Activity of selected Cyclic Dipeptides. *Pharmazie*; 54 (10): 772-775

Gudasheva TA, Boyko SS, Ostrovskaya RU, Voronina TA, Akparov VK, Trofimov SS, Rozantsev GG, Skoldinov AP, Zherdev VP, Seredenin SB. 1996. Identification of a Novel Endogenous Memory facilitating Cyclic Dipeptide Cyclopropylglycine in Rat Brain. *FEBS Letters*; 391 (1-2): 149-152

Gudasheva TA, Boyko SS, Ostrovskaya RU, Voronina TA, Akparov VK, Trofimov SS, Rozantsev GG, Skoldinov AP, Zherdev VP, Seredenin SB. 1997. The Major Metabolite of Dipeptide Piracetam Analogue GVS-111 in Rat Brain and its Similarity to Endogenous Neuropeptide Cyclo-L-Propylglycine. *European Journal of Drug Metabolism and Pharmacokinetics*; 22: 245-252

Han SY, Kim YA. 2004. Recent Development of Peptide Coupling Reagents in Organic Synthesis. *Tetrahedron*; 60: 2447-2467

Hancock REW, Chapple DS. 1999. *Peptide Antibiotics*. Antimicrobial Agents and Chemotherapy; 43 (6): 1317-1323

Hancock REW, Lehrer RI. 1998. Cationic Peptides: a New source of Antibiotics. *Trends in Biotechnology*; 16: 82-87

Harper AE, Yoshimura NN. 1993. Protein Quality, Amino Acid Balance, Utilisation, and Evaluation of Diets Containing amino Acids as Therapeutic Agents. *Nutrition*; 9 (5): 460-469

Haüsler J, Jahn R, Schmidt U. 1978. ÜBer Aminosäuren Und Peptide. XXIV. Radikalisch Und Photochemisch Initiierte Oxidation Von Aminosäurederivaten. *Chemische Berichte*; 111: 361-366

Hayat MA. 1974. Principles and Techniques of Scanning Electron Microscopy. Litton Educational Publishing Inc. 1-9

Haywood A. 2000. The Medicinal Chemistry of the Tryptophan-containing Cyclic Dipeptide: Cyclo(Trp-Pro). PhD Thesis. University of Port Elizabeth

Heath JK. 2001. Principles of Cell Proliferation. Oxford: Blackwell Science; 14:77-120

Hoffbrand AV, Moss P.A.H. 2011. Essential Haematology, 6th edition. Chichester, UK : Wiley-Blackwell; 1-450

Holden MTG , Chhabra SR, de Nys R, Stead P, Bainton NJ, Hill P, Manefield M, Kumar N, Labatte M, England D, Rice S, Givskov M. 1999. Quorum-sensing Cross Talk: Isolation and Chemical Characterisation of Cyclic Dipeptides from *Pseudomonas Aeruginosa* and other Gram-negative Bacteria. *Molecular Microbiology*; 33 (6): 1254-1266

Hruby VJ. 2002. Designing Peptide Receptor agonist and Antagonists. *Nature Reviews Drug Discovery*; 1(11): 847-858

Huang D. 2006. The Medicinal Chemistry of the Selected Glycine-containing Cyclic Dipeptides: Cyclo(Gly-Leu) and Cyclo(Gly-Ile). MSc Dissertation. Nelson Mandela Metropolitan University

Huq F, Daghiri H, Yu JQ, Tayyem H, Beale P, Zhang M. 2004. Synthesis, Characterisation, Activities, Cell Uptake and DNA Binding of [*trans*-PtCl(NH₃)₂] {μ-(H₂N(CH₂)₆NH₂)} [*trans*-PdCl(NH₃)₂] (NO₃)Cl. *European Journal of Medicinal Chemistry*; 39: 947-958

Imanishi Y, Sugihara T, Tanihara M, Hugesimura T. 1975. A Facile Hydrolysis of Hydrophobic Esters by Cyclo(D-Leu-L-His). *Chemical Letters*; 261-264

Jakubke HD, Jeschkeit H. 1997. Amino Acids, Peptides and Proteins. 1st edition. London: The MacMillan Press LTD; 2-7, 92-93, 101-102, 160-161.

Jamie H. 2002. The Medicinal Chemistry of the Isomers of the Cyclic Dipeptide: Cyclo(Trp-Pro). PhD Thesis. University of Port Elizabeth

Jankowska R, Ciarkowski J. 1987. Conformation of Dioxopiperazines. *International Journal of Peptide and Protein Research*; 30: 61-78

Janse van Rensburg H. 2006. The Medicinal Chemistry of Cyclo(Ser-Ser) and Cyclo(Ser-Tyr). MSc Dissertation. Nelson Mandela Metropolitan University

Jellinger PS, Mace MD. 2007. Metabolic Consequences of Hyperglycaemia and Insulin Resistance. *Clinical Cornerstone*; (8): 30-42

Jikihara H, Ikegame H, Koike K, Wada K, Morishige K, Kurachi H, Hirota K, Miyaka A, Tanizawa O. 1993. Intraventricular Administration of Histidyl Proline Diketopiperazine [Cyclo(His-Pro)] Suppresses Prolactin Synthesis and Secretion: Possible role of

Cyclo(His-Pro) as Dopamine Uptake Blocker in Rat Hypothalamus. *Endocrinology*, 132: 953-958

Jones S. 2002. The Medicinal Chemistry of the Cyclic Dipeptides Cyclo(Met-Trp) and Cyclo(Met-Tyr). MSc Dissertation. University of Port Elizabeth

Kanoh K, Kohno S, Asari T, Harada T, Katafa J, Muramatsu M, Kawashima H, Sekiya H, Uno I. 1997. (2) Phenyhistine: a New Mammalian Cell Cycle Inhibitor Produced by *Aspergillus Ustus*. *Bioorganic and Medicinal Chemistry Letters*; 7: 2847-2852

Kaparissides C, Alexandridou S, Kotti K, Chaitidou S. 2006. Recent Advances In Novel Drug Deleviry Systems. *Journal of Nanotechnology Online*; (2): 1-11

Kasuya N, Kishi Y, Isobo M, Yoshida M, Numano F. 2006. P-Selectin Expression, but not GpIIb/IIIa Activation, is Enhanced in the Inflammatory Stage of Takayasu's Arteritis. *Circulation Journal*; (70): 600-604

Katzung BG. 2009. Basic and Clinical Pharmacology, 8th edition. New York: Lange Medical Books/Mcgraw-Hill; 155-240, 754-959

Kilian G. 2002. The Medicinal Chemistry of Aromatic Cyclic Dipeptides: Cyclo(Tyr-Tyr) and Cyclo(Phe-Tyr). MSc Dissertation. University of Port Elizabeth

Kilian G. 2011. Development and Testing of Liposome Encapsulated Cyclic dipeptides. PhD dissertation. Nelson Mandela Metropolitan University

Koda-Kimble MA, Young LY, Wayne A, Kradjan B, Guglielmo J. 2008. Applied Therapeutics: The Clinical Use of Drugs. 9th edition. Philadelphia: Lippincott Williams and Wilkins; 861-8618

Kopple KD, Ghazarian HG. 1968. A Convenient Synthesis of 2,5 Piperazinediones. *Journal of Organic Chemistry*, 33 (2): 862-864

Kopple KD. 1972. Synthesis of Cyclic Dipeptides. *Journal of Pharmaceutical Sciences*; 61 (9): 1345-1356

Koskinen L. 1986. Effect of Low Intravenous Doses of TRH, Acid-TRH, and Cyclo(His-Pro) on Cerebral and Peripheral Blood Flows. *British Journal of Pharmacology*; 87 (3): 509-519

Kourounakis PN, Rekka E. 1994. *Advanced Drug Design and Development: a Medicinal Chemistry Approach*. New York: Ellis Horwood; 1-141

Krejcarek GE, Dominy BH, Lawton RG. 1968. The interaction of Reactive Functional Groups Along Peptide Chains. A Model for Alkaloid Synthesis. *Chemical Communications*; 1450-1452

Kritzinger AL. 2007. *The Medicinal Chemistry of Cyclo(Ser-Ser) and Cyclo(Ser-Tyr)*. MSc Dissertation. Nelson Mandela Metropolitan University

Kukla MJ, Breslin HJ, Bowden CR. 1985. Synthesis, Characterisation and Anorectic Testing of the Four Stereo-Isomers of Cyclo(His-Pro). *Journal of Medicinal Chemistry*; 28: 1745-1747

Laitinen N. 2003. *Opening New Perspectives for Visual Characterisation of Pharmaceutical Solids*. MSc thesis, University of Helsinki

Lambert JN, Mitchell JP, Roberts KD. 2001. Synthesis of Cyclic Dipeptides. *Journal of the Chemical Society, Perkin Transactions I*, 471-484

Lautru S, Gondry M, Genet R, Pernodet J. 2002. The Albonoursin Gene Cluster of *S. Noursei*: Biosynthesis of Diketopiperazine Metabolites Independent of Nonribosomal Peptide Synthetase. *Chemistry and Biology*; 9: 1355-1364

Lee DG, Hahm K, Park Y, Kim H, Lee W, Lim S, Seo Y, Choi C. 2005. Functional and Structural Characteristics of Anticancer Peptide Pep27 Analogues. *Cancer Cell International*; 21: 1-14

Lee T. 1998. A Beginners Guide to Mass Spectral Interpretation. United States of America: John Wiley and Sons; 1-186

Leung SS, Grant DJW. 1997. Solid State Stability Studies of Model Dipeptides: Aspartime and Aspartylphenylalanine. *Journal of Pharmaceutical Sciences*; 86(1); 64-71

Lichtenstein N. 1938. The Behavior of Peptides when Heated in β -naphthol. *Journal of the American Chemical Society*; (60): 560-563

Liotta LA, Kohn EC. 2000. Invasion and Metastasis; 55, 1856–1862

Lipsitch, M. 2001. The Rise and Fall of Antibiotic Resistance. *The Institute of Management Sciences*; 9 (9): 438-444

Litteer B, Beckers D. 2005. Increasing Application of X-ray Powder Diffraction in the Pharmaceutical Industry. *Tetrahedron*; (61): 10827-10852

Livermore DM. 2000. Antibiotic Resistance in Staphylococci. *International Journal of medical sciences. Antimicrobial Agents*; S3-s10

Loughlin WA, Marchall RL, Carreiro A, Elson KE. 2000. Solution-Phase Combinatorial Synthesis and Evaluation of Piperazine-2,5-dione Derivatives. *Bioorganic and Medicinal Chemistry Letters*; 10 (2): 91-94

Lucietto FR. 2004. The Medicinal Chemistry of the Selected 2,5-Diketopiperazines Cyclo(His-Gly) and Cyclo(His-Ala). MSc Dissertation. University of Port Elizabeth

Marshall SH, Arenas G. 2003. Antimicrobial Peptides: A Natural Alternative to Chemical Antibiotics and a Potential for Applied Biotechnology. *Electronic Journal of Biotechnology*; 6 (2): 271-284

McClelland K. 2003. The Medicinal Chemistry of selected Histidine-Containing Cyclic Dipeptides: Cyclo(His-Phe) and Cyclo(His-Tyr). MSc Dissertation. University of Port Elizabeth

McMurry J. 2008. Organic Chemistry, 8th edition. California: Brooks/Cole; 75-79, 440-474, 1073-1117

Meier R. 2005. Aminoacid Deficiency: Clinical Symptoms and Causes. *Schweizerische Zeitschrift für Ganzheits Medizin*; 17 (5): 290-293

Meyer VR. 2004. Practical High Performance Liquid Chromatography 4th edition. Chichester :John Wiley; 5, 7, 14, 159, 160, 167, 170, 173, 174

Meyers RA. 2000. Encyclopedia of Analytical Chemistry. Chichester: John Wiley and Sons Limited,. 13269-13288

Michelson AD, Barnard MR, Kreuger LA, Frelinger AL, Furman MI. 2000. Evaluation of Platelet Function by Flow Cytometry. *Methods*; (21): 259-270

Milne PJ, Hunt AL, Rostoll K, Van der Walt JJ, Graz CJM. 1998. The Biological Activity of Selected Cyclic Dipeptides. *Journal of Pharmacy and Pharmacology*; 50: 1331-1335

Milne PJ, Hunt AL, Rostoll K, Van der Walt JJ, Graz CJM. 1998. The Biological Activity of Selected Cyclic Dipeptides. *Journal of Pharmacy and Pharmacology*; 50: 1331-1335

Milne PJ, Olivier DW, Roos HM. 1992. Cyclodipeptides: Structure and Conformation of Cyclo(Tyrosyl-Prolyl). *Journal of Crystallographic and Spectroscopic Research*; 22 (6): 224-230

Miyazawa T. 1960. Normal Vibrations of Monosubstituted amides in the *cis*-Configuration and infrared spectra of Diketopiperazines. *Journal of Molecular Spectrometry*; 4: 155-167

Mizuma T, Masubuchi S, Awazu S. 1997. Intestinal Absorption of Stable Cyclic Glycylphenylalanine: Comparison with Linear Form. *Journal of Pharmacy and Pharmacology*; 49: 1067-1070

Mizuma T, Masubuchi S, Awazu S. 2003. Concentration-dependent Atypical Absorption of Cyclic Phenylalanylserine: Small Intestine Acts as an Interface between the Body and Ingested Compounds. *Biological and Pharmaceutical Bulletin*; 26 (11): 1625-1628

Mizuma T, Narasaka T, Awazu S. 2002. Uptake of Cyclic Dipeptide by PEPT1 in Caco-2 Cells: Phenolic Hydroxyl Group of Substrate Enhances Affinity for PEPT1. *Journal of Pharmacy and Pharmacology*; 54 (9): 1293-1296

Mohan C. 2001. Proteins, Peptides and Amino acids. 45, 366–372

Montalbetti CAGN, Falque V. 2005. Amide Bond formation and Peptide Coupling

Moresco RN, Vargas LCR, Sila L. 2006. Estimation of the Levels of D-Dimer by use of an Alternative Method Based in the Reaction Time of Fibrinogen/Fibrin Degradation Products Assay. *Journal of Thrombosis and Thrombolysis*; (2): 73-76

Morley JE, Levine AS, Prasad C. 1981. Histidyl-proline Diketopiperazine Decreases Food Intake in Rats. *Brain Research*; 210 (1-2): 475-478

Mustard JF, Kinlough-Rathbone RL, Packham MA. 1989. Isolation of Human Platelets from Plasma by Centrifugation and Washing. *Methods in Enzymology*; 169: 3-11

Nathason D, Nyström T. 2009. Hypoglycaemic Treatment of Type 2 Diabetes: Targeting the Endothelium. *Molecular and Cellular Endocrinology*; (279): 112-126

Nelson DL, Cox MM. 2005. Principles of Biochemistry, 4th edition. New York: Freeman and Company; 75-106

Newman DJ, Henneberry H, Prince CP. 1992. Particle Enhanced Light Scattering Immunoassay. *Analytical Clinical Biochemistry*; (29): 22-42

Nitecki DE, Halpren B, Westley JW. 1968. A Simple Route to Sterically Pure Diketopiperazines. *Journal of Organic Chemistry*; 33 (2): 864-866

Nowak TJ, Handford AG. 2004. Pathophysiology. Concepts and Applications for Health care Professionals. New York: McGraw-Hill; 132-163

Nussberger S, Hediger M. 1995. How Peptides Cross Biological membranes. *Experimental Nephrology*; 3 (4): 211-218

Olivier RE. 2002. The Medicinal Chemistry of the Cyclic Dipeptides Cyclo(Gly-Tyr) and Cyclo(Gly-Phe). MSc Dissertation. University of Port Elizabeth

Ovchinnikov TA, Ivanov VT. 1975. Conformational States and Biological Activity of Cyclic Peptides. *Tetrahedron*; 31: 2177

Ozaki Y, Murayama K and Wang Y. 1999. Application of two-dimensional Near-infrared Correlation Spectroscopy to Protein Research; 127-132

Page CP, Curtis MJ, Sutter MC, Walker MJ, Hoffman BB. 1997. Integrated Pharmacology. London: Mosby; 606

Palacin M, Estevez R, Bertran J, Zorzano A. 1998. Molecular Biology of Mammalian Plasma Membrane Amino acids Transporters. *Physiological Reviews*; 78: 969-1054

Palareti G. 1993. Fibrinogen/fibrin Degradation products: Pathophysiology and Clinical Application. *Fibrinolysis*; (7): 60-61

Park SH, Stroebel GA. 1994. Cellular Protein Receptors of Maculosin, a Host Specific Phytotoxin of Spotted Knapweed (*Centaurea Maculosa* L). *Biochemica Biophysica Acta*; 1199: 13-19

Peng LI, Roller PP. 2002. Cyclisation Strategies in Peptide Derived Drug Design. Current topics in Medicinal Chemistry; (2): 325-341

Percharsky VK, Zavalij PY. 2005. Fundamentals of Powder Diffraction and Structural Characterisation of Materials. New York: Springer; 1-94, 99-256, 261-333

Pervan V, Cohen LH, Jaftha T. 1995. Oncology for Health-care Professionals. Kenwyn: Juta; 197-231

Peterson DC. 2006. The Medicinal Chemistry of the selected Valine-containing Cyclic Dipeptides: Cyclo(Gly-L-Val) and Cyclo(Gly-D-Val). MSc Dissertation. Nelson Mandela Metropolitan University

Phang JM, Pandhare J, Yongmin L. 2008. The Metabolism of Proline as Microenvironmental Stress Substrate. *American Society for Nutrition*; 138 (10): 2008s-2015s

Pieper JA, Rutledge DR. 1989. Current Concepts-Laboratory Techniques for Pharmacists. Michigan: Upjohn Company; 14-34

Pitchen R. 2002. The Medicinal Chemistry of the Cyclic Dipeptides Cyclo(Met-Met) and Cyclo(Met-Gly). MSc Dissertation. University of Port Elizabeth

Pollock RE, Morton DL. 2000. Principles of Surgical Oncology; 1-350

Pope MI, Judd MD. 1977. Differential Thermal Analysis. London: Heyden; 1-85

Prasad C. 1987. Neuropeptide Dopamine Interactions. I. Dopaminergic Mechanisms in Cyclo(His-Pro) Mediated Hypothermia in Rats. *Brain Research*; 437 (2): 345-348

Prasad C. 1995. Bioactive Cyclic Dipeptides Peptides; 16(1): 151-164

Prasad C. 2001. Role of Endogenous Cyclo(His-Pro) in Voluntary Alcohol Consumption by Alcohol-preferring C57BL Mice. *Peptides*; 22: 2113-2117

Prescott LM, Harley JP, Klein DA. 2005. Microbiology 6th edition. Boston: McGraw-Hill; 489, 512, 574, 575, 896, 899, 924-926

Prosser S, Worster B, MacGregor J, Dewar K, Runyard P, Fegan J. 2006. Applied Pharmacology: An Introduction to Pathophysiology and Drug Management for Nurses and Healthcare Professionals. Edinburgh: Mosby; 75-80

Quick AJ. 1966. Hemorrhagic Diseases and Thrombosis; 2nd edition. Philadelphia. Lea and Febiger; 212-219

Ramani R, Sasisekharan V, Venkatesan K. 1977. Conformational studies on Cyclic Dipeptides. *International Journal of Peptide and Protein Research*; 9: 277-292

Rang HP, Dale MM, Ritter JM. 2011. Pharmacology, 8th edition. Edinburg: Churchill Livingstone; 663-684

Rasche H. 2001. Haemostasis and Thrombosis: An Overview. *European Heart Journal Supplements*; 3: Q3-Q7

Reininger AJ. 2006. Primarily Haemostasis and its Assessment by Laboratory tests. *Haemostaseologie*; (1): 42-47

Rozek RP, Tully N. 1999. TRIPS Agreement and Access to Healthcare. *Journal World Intellectual Property*; 2(5): 293-319

Rubio-Aliaga I, Daniel H. 2002. Mammalian Peptide Transporters as Targets for Drug Delivery. *Trends in Pharmacological Sciences*; 23 (9): 434-440

Sammes PG. 1975. Naturally Occuring 2, 5-Diketopiperazines and Related Compounds. *Fortschritte Der Chemie Organischer Naturstoffe*; 32: 51-118

Samuel R, Foston M, Jaing N, Cao S, Allison L, Studer M, Wyman C, Ragauskas AJ. 2011. HSQC (heteronuclear single quantum coherence) ¹³C–¹H Correlation Spectra of Whole Biomass in Perdeuterated Pyridinium Chloride–DMSO System: An Effective Tool for Evaluating Pre-treatment; 90 (9): 2836-28

Sancheti S, Seo S. 2009. Chaenomeles Sinesis: A Potent α - and β -Glucosidase Inhibitor. *American Journal of Pharmacology and Toxicology*; 4 (1): 1-8

Sartoreli AC, Liu MC, Luo MZ, Mozdiesz DE, Lin TS, Dutschman GE, Gullen EA, Cheng YC. 2001. Synthesis of Halogen-substituted 3-deazaadenosine and 3-deazaguanosine Analogues as Potential Antitumor/Antiviral Agents. *Nucleic Acids*; (12): 1037-41

Shen H, Smith D, Yang T, Huang Y, Schnermann J, Brosius F. 1999. Localisation of PEPT1 and PEPT2 Proton-coupled Oligopeptide Transporter mRNA and Protein in Rat Kidney. *American Journal of Physiology: Renal Physiology*; 276: 658

Shlaes, DM, Projan JS, Edwards JE. 2004. Antibiotic Discovery: State of the State; 70 (6): 275-281

Sichina WJ. 2001. Characterisation of Pharmaceuticals using Thermal Analysis. *Thermal Analysis*; 16-25

Siuzdak G. 2005. An Introduction to Mass Spectrometry Ionisation. *The Journal of the Association for Laboratory Atomisation*; 50-63

Siwicka A, Wojtasiewicz K, Zawadzka A, Maurin JK, Czarnocki Z. 2005. The Structure of Some *trans*-Diketopiperazine Derivatives of Isoquinoline and β -Carboline. *Tetrahedron: Asymmetry*; 16: 2071-2073

Skoog DA, West DM, Holler FJ. 2001. Fundamentals of Analytical Chemistry, 8th edition. New York: Saunders College Publishing; 592-597, 703, 705.

Skoog DA, West DM, Holler FJ. 2004. Fundamentals of Analytical Chemistry, 8th edition. New York: Saunders College Publishing; 592-597, 703, 705.

Smith DE, Paclova A, Berger UV, Hediger MA, Yang T, Haung YG, Schnermann JB. 1998. Tubular Localisation and Tissue Distribution of Peptide Transporters in Rat Kidney. *Pharmaceutical Research*; 15: 1244-1249

Stephenson GA. 2005. Application of X-ray Powder Diffraction in the Pharmaceutical Industry. *The Rigaku Journal*; 22 (1) 2-15

Stevens MG, Olsen SC. 1993. Comparative Analysis of Using MTT and XTT in Colorimetric Assays for Quantitative Bovine Neutrophil Bactericidal Activity. *Journal of Immunological Methods*; 157: 225-231

Stuart B. 2004. Infrared Spectroscopy: Fundamentals and Applications. Chichester: John Willey; 1, 2, 18, 23, 24, 45, 137, 138, 168

Stunvoll M, Goldstein BJ, Van Heaften TW. 2005. Type 2 Diabetes: Principles of Pathogenesis and Therapy. *Lancet*; (365): 333-346

Suresh Babu VV. 2001. One Hundred Years of Peptide Chemistry; 640-647

Suzuki K, Sasaki Y, Endo N, Mihara Y. 1998. Acetic Acid-catalysed Diketopiperazines Synthesis. *Chemical Pharmaceutical Bulletin*; 29 (1): 233-237

Svec HJ, Junk GA. 1964. The Mass Spectra of Dipeptides. *Journal of American Chemical Society*; 86: 2278-2282

Szafranek J, Palacz Z, Grzonka Z. 1976. A Comparison of Electron Impact and Field Ionisation Spectra of Some 2,5-diketopiperazines. *Organic Mass Spectrometry*; 11: 920-930

TA211. 2002. Thermal Analysis Review: Modulated DSC Theory. TA Instruments *Thermal Analysis Application Library*; 1-12

Tereda T, Saito H, Mukai M, Inui K. 1997. Recognition of β -Lactam Antibiotics by Rat Peptide Transporters, PEPT1 and PEPT2, in LCC-PK1 Cells. *American Journal of Physiology*; 273 (5): f706-f711

Tortora GJ, Grabowski SR. 2009. Principles of Anatomy and Physiology, 9th edition. New York: John Willey and Sons; 636-737

Tripodi A, Arbin A, Chantarangkul V, Mnnucci, PM. 1992. Recombinant Tissue Factor Substitute for Conventional Thromboplastin in the Prothrombin Time Test. *Journal of Thrombosis and Haemostasis*; (67): 42-45

Vadseth C, Souza JM, Thomson L, Seagraves M, Nagaswami C, Scheiner T, Torbert J, Vilaire G, Benette JS, Murciano J, Muzykantov V, Penn MS, Hazen SL, Weisel JW, Ischiropoulos H. 2004. Prothrombotic-state Induced by Post-translational Modification of Fibrinogen by Reactive Nitrogen Species. *The Journal of Biological Chemistry*; (279): 8820-8826

Van der Merwe E. 2005. The Medicinal Chemistry of Cyclo(Phe-Cys) and Cyclo(Tyr-Cys). MSc Dissertation. Nelson Mandela Metropolitan University

Versluis CW. 2002. The Medicinal Chemistry of Cyclo(L-Trp-L-Tyr) and Cyclo(D-Trp-L-Tyr). MSc Dissertation. University of Port Elizabeth

Vogler EA, Siedlecki CA. 2009. Contact Activation of Blood-plasma Coagulation. *Biomaterials*; (30): 1857-1869

Walkowiak B, Keszy A, Michalec L. 1997. Microplate Reader: A Convenient Tool in Studies of Blood Coagulation. *Thrombosis Research*; (87): 95-103

Walter R, Ritzmann RF, Bhargava HN, Flexner LB. 1978. Prolyl-leucyl Glycinamide, Cyclo(Leucylglycine), and Derivatives Block Development of Physical Dependence on Morphine in Mice. *Proceedings of the National Academy of Sciences of the United States of America*; 76: 518-520

Wang G, Gu P, Kaufman S. 2001. Mutagenesis of the Regulatory Domain of Phenylalanine Hydroxylase. *Biological Sciences*; 98 (4): 1537-1542

Warshawsky D, Landolph JR. 2006. *Molecular Carcinogenesis and the Molecular Biology of Human Cancer*. Florida: *CRC Press*; 1-23, 47-49

Watson DG. 2005. *Pharmaceutical Analysis: a Textbook for Pharmaceutical Students and Pharmaceutical Chemists*. Harcourt Publishers Limited; 195, 239-248, 266, 277-279

Wegerski CJ, France D, Cornell-Kennon S, Crews P. 2004. Using a Kinase Screen to Investigate the Constituents of the Sponge *Stelletta Clavosa* Obtained from Diverse Habitats. *Bioorganic and Medicinal Chemistry*; 12: 5631-5637

Wendlandt WW. 1986. *Thermal analysis*. New York: John Wiley ; 9-82, 137-452

Wermuth CG. 2003. *The Practice of Medicinal Chemistry*, 2nd edition. Amsterdam: Academic; 29

Willard HH, Merritt LL, Dean JA, Settle FA. 1998. *Instrumental Methods of Analysis* 7th Edition. Wadsworth Inc; 287, 310, 340, 349, 378, 422, 473, 761, 763

Wishart DS, Case DA. 2001. Use of Chemical Shifts in Macromolecular Structure Determination. *Methods in Enzymology*, 338: 3-34

Witak DT, Wei Y. 1990. Dioxopiperazines: *Chemistry and Biology*. Progress in Drug Research; 35: 249

Würtz P, Permi P, Nielsen NCHR and Sørensen OW. 2008. Clean HMBC: Suppression of Strong-coupling Induced Artifacts in HMBC Spectra; 194(1):89-98

Wyatt PG, Allen MJ, Borthwick AD, Davies DE, Exall AM, Hatley RJD, Irving WR, Livermore DG, Miller ND, Nerozzi F, Sollis SL and Szardenings AK. 2005. 2,5-Diketopiperazines as Potent and Selective Oxytocin Antagonists 1: Identification, Stereochemistry and Initial SAR. *Bioorganic Medicinal Chemistry Letters* 15 (2005) 2579–2582

Xiao Z, Storms R, Tsang A. 2006. A Quantitative Starch-iodine Method for Measuring alpha-Amylase and Glucosidase activities. *Analytical Biochemistry*; 351 (1): 146-148

Yacobi BG, Holt DB, Kazmerski LL. 1994. Microanalysis of Solids. Plenum Press, New York; 25-60

Young PE, Madison V, Blout ER. 1976. Cyclic peptides. 15. Lanthanide-Assisted ¹³C and ¹H NMR Analysis of Preferred Side-Chain Rotamers in Proline-Containing Cyclic Dipeptides. *Journal of the American Chemical Society*; 98 (17): 5365-5371

Zsoldos Z, Szabo I, Szabo Z, Johnson AP. 2003. Software Tools for Structure Based Rational Drug Design. *Journal of Molecular Structure*; 659-665

Zucker M. 1989. Platelet Aggregation Measured by the Photometric Method. *Method in Enzymology*; 117-122

APPENDIX A

LIST OF CHEMICALS

Acetic acid (glacial)	SAARCHEM (Pty) Ltd., SA
Acetonitrile	BDH Hypersolv™ for HPLC, BDH Laboratory Supplies, England.
Anisole	BDH Laboratory Supplies, England
Bovine serum albumin	Highveld Biological, SA
Thrombin	Sigma Chemical Co., SA
Chloramphenicol	Sigma Chemicals Co., USA
Chloroform	SAARCHEM (Pty) Ltd., SA
Dimethyl sulphoxide (DMSO)	SAARCHEM (Pty) Ltd., SA
Dichloromethane	SAARCHEM (Pty) Ltd., SA
Diethyl ether	SAARCHEM (Pty) Ltd., SA
1,2-Dimethoxyethane	BioChemika Fluka, Germany.
Disodium hydrogen phosphate	Merck, SA.
Ethanol	Associated Chemical Enterprises (Pty) Ltd., SA/BDH Laboratory Supplies, England.
Ethylenediaminetetra-acetic acid	BDH Laboratory Supplies, England.

Formic acid	SAARCHEM (Pty) Ltd., SA.
Foetal Calf Serum	Adcock Ingram, SA
Glucose	SAARCHEM (Pty) Ltd., SA
Heparin sodium (5000 IU/ml)	Fresenius-Kabi, SA.
HEPES	Sigma Chemicals Co., USA
n-Hexane	BDH Laboratory Supplies, England
Hydrochloric acid	Merck, England/SAARCHEM (Pty) Ltd., SA.
Iodine	SAARCHEM (Pty) Ltd., SA
Magnesium chloride	Associated Chemical Enterprises (Pty) SA.
Methanol	BDH Laboratory Supplies, England/ SAARCHEM (Pty) Ltd., SA.
3-(4,5-dimethylthiazole-2yl)-2,5-Diphenyltetrazolium bromide	Sigma Chemicals Co., USA
Mueller hinton	
Nutrient Agar	Biolab, Merck, Germany
Potato dextrose agar	
Pottasium chloride	Merck, Germany

RPMI 1640 growth medium	Highveld Biological, SA.
Sec-butanol	SAARCHEM (Pty)., SA.
Sodium chloride	Labchem (Pty) Ltd., SA.
Sodium hydroxide	BDH Laboratory Supplies, England.
Sodium hydrogen carbonate	Associated Chemical Enterprises (Pty) Ltd., SA.
Sodium hydrogen phosphate	Associated Chemical Enterprises (Pty) Ltd., SA.
Toluene	SAARCHEM (Pty) Ltd., SA.
Triethylamine	BioChemika Fluka, Germany.
Trifluoroacetic acid	SAARCHEM (Pty) Ltd., SA.
Tris	Roche Diagnostics GmbH, Mannheim
Water: Analytical grade, reverse osmosis	Ultra Clear TWF UV TM Reverse Osmotic water purification system SG®
Water: Double-distilled, de-ionised	Buchi Fontavapor 285 Milli-Q™, Millipore.

APPENDIX B

LIST OF SOLUTIONS

Buffer A

NaCl 145 mM

KCl 5 mM

HEPES 10 mM

Na₂HPO₄ 0.5 mM

Bovine serum albumin 0.2%

Glucose 6 mM

Analytical grade water to 100%

Mueller Hinton broth

Mueller hinton 23 g

Analytical grade water to 1000 ml

Nutrient agar

Nutrient agar 31 g

Analytical grade water to 1000 ml

MTT (determination of cell viability)

3-(4,5-dimethylthiazole-2yl)-2,5- 0.5% (0.1 g)

Diphenyltetrazolium bromide

Analytical grade water to 20 ml

Phosphate-buffered saline (PBS)

NaCl 8 g

KH₂PO₄ 0.24 g

Na₂HPO₄·12H₂O 1.44 g

KCl 0.2 g

MgCl₂ 0.047 g

Analytical grade water to 1000 ml (pH 7.4)

Tris buffer

Tris 50 mM

EDTA 7.4 mM

NaCl 175 mM

Analytical grade water to 100% (pH 7.4)

APPENDIX C

LIST OF EQUIPMENT

Autoclave	Model HA-3D, Hirayama Manufacturing Corp., Japan
Centrifuge	Eppendorf Centrifuge® 5804R, Germany.
Computational modeling	Spartan '10 (Version 1.0.0) Wavefunction Inc., USA
Culture flasks	Corningware, Cambridge, USA
Differential Scanning Calorimetry	SDT Q600 V4.2E Simultaneous Differential Scanning Calorimeter and Thermogravimetric Analyser (TA Instruments™, USA.
Electronic Balance	Mettler Toledo®, AB104, Switzerland.
Eppendorfs	Eppendorf AG, Germany
Filter (sterile)	Cameo 25AS acetate filter (Millipore®, Billerica)
High Performance Liquid Chromatography packing column	Shimadzu LC2020 (Shimadzu, Tokyo, Japan)
Wavelength of maximum absorbance	UV-1601 UV Visible Spectrophotometer (Shimadzu®, Japan).
Humidifier	Labotec® ThermoForma, SA

Haemocytometer	Neubauer Improved Bright-line Superior, Germany
Laminar Airflow (anticancer studies)	Labotec, Bioflow II, fitted with a Type A/B3 filter, Labotec, SA.
Incubator	Labcon® orbital shaker.
Infrared Spectroscopy	Shimadzu 1600 spectrophotometer (Shimadzu, Tokyo, Japan)
Orbital shaker	Labchem® orbital shaker
Mass Spectrometry	VG-7070E mass spectrometer (VF, Biotech, Altrincham, UK); VG 2035 data system.
Microscale	Sartorius GMBH, Gottingen.
Micropipette (1000 µl, 200 µl)	Nichiryo, Japan.
Microtitre plates (96-well, flat bottom)	Highveld Biological®, SA.
Microtitre plates (96-well)	
Nuclear Magnetic Resonance Spectroscopy	Bruker Advanced DPX 300 NMR Spectrometer; Bruker Win-NMR® Software
pH meter	744 pH meter, Metrohm®.
Scanning Electron Microscopy	Philips® XL30 Scanning Electron Microscope (Philips, Eindhoven Netherlands); Novotech SEMprep 2®-sputter coater (Novotech, USA).

Spectrophotometer	BioTek Power Wave XS
Statistical software packages	Microsoft Excel® (version 2010), GraphPad Prism® version 5
Thermogravimetric Analysis	SDT Q600 V2.2E Simultaneous Differential Scanning Calorimeter and Thermogravimetric Analyser (TA Instruments™, USA.
Water bath	Labcon®; Labdesign Engineering (Pty) Ltd.
Vortex	Vortex Mixer BM300; Laboratory Supplies (Pty) Ltd
X-Ray Powder Diffraction	Bruker Advanced Solutions XRD Commander Diffractometer (Diffrac ^{Plus} Version 2.3, Germany); Bruker Advanced X-ray Solutions; Eva software (Diffrac ^{Plus} Version 10.0 Rev.1).

APPENDIX D

HUMAN ETHICAL APPROVAL FORM

• PO Box 77000 • Nelson Mandela Metropolitan University
• Post Bag 16 • 6021 • South Africa • www.nmmu.ac.za



**Nelson Mandela
Metropolitan
University**

for tomorrow

Chairperson of the Research Ethics Committee (Human)

NMMU

Tel: +27 (0)41 504-2499 Fax: +27 (0)41 504-2770

Rosa.DuRandt@nmmu.ac.za

Ref: N 01/11/03/07 [H06SB-003/Approval]

Contact person: Mrs U Spies

12 September 2006

Dr C Frost
NMMU
Department of Biochemistry and Microbiology
Faculty of Sciences

Dear Dr Frost

TO INVESTIGATE MULTI-THERAPEUTIC ANTICOAGULANT/ANTI-PLATELET OR ANTI-FIBRINOLYTIC AGENTS WHICH CAN PROVIDE INSIGHT FOR THE PRODUCTION OF DRUGS WHICH WOULD BE USEFUL IN TROMBOSIS

Your above-entitled re-application for ethics approval served at the August 2006 ordinary meeting of the Research Ethics Committee (Human).

The Committee approved the above-mentioned application.

Please inform your co-investigators of the outcome. We wish you well with the project.

Yours sincerely

A handwritten signature in black ink, appearing to read 'Rosa Du Randt'.

Prof R du Randt
Chairperson: Research Ethics Committee (Human)

cc: Department of Research Management;
Faculty Officer, Faculty of Health Sciences

APPENDIX E

ARTICLE TO BE SUBMITTED FOR PUBLICATION

The Medicinal Chemistry of Cyclo(Phe-4Cl-Pro) and Cyclo(D-Phe-4Cl-Pro)

M. Milne, P.J. Milne, M van de Venter, C.L. Frost, G. Dealtry

Cyclic Peptide Research Unit, Department of Pharmacy, Box 77000, Nelson Mandela Metropolitan University, Port Elizabeth 6031, South Africa. Department of Biochemistry, and Microbiology, Box 77000, Nelson Mandela Metropolitan University, Port Elizabeth 6031, South Africa

Email addresses: Pieter.Milne@live.nmmu.ac.za (P. J. Milne), Maryna.van.de.venter@live.nmmu.ac.za (M van de Venter), Carmanita.Frost@live.NMMU.ac.za (C.L. Frost), 205003702@live.nmmu.ac.za (M. Milne).

Correspondence: P.J. Milne, Department of Pharmacy, Box 77000, Nelson Mandela Metropolitan University, Port Elizabeth 6031, Republic of South Africa. Tel: 0415042631.

Fax: 0415042744.

ABSTRACT

Cyclo(Phe-4Cl-Pro) and cyclo(D-Phe-4Cl-Pro), were synthesised from their corresponding linear precursors using the method of Milne *et al.* (1992). The phenol induced cyclisation procedure resulted in good yields and purity of the cyclic dipeptides. Quantitative analysis and evaluation of the physiochemical properties of the cyclic dipeptides was achieved by using high-performance liquid chromatography, scanning electron microscopy, thermal analysis and X-ray powder diffraction. Structural elucidation of the cyclic dipeptides was done by means of infrared spectroscopy, mass spectroscopy, nuclear magnetic resonance spectroscopy and molecular modelling. The study anticipated that by introducing chlorine into the aromatic ring and consequently altering the structure of the diketopiperazines, the biological properties of the compounds would be enhanced (Naumann, 1999). The anticancer results obtained indicated that both cyclo(Phe-4Cl-Pro) and cyclo(D-Phe-4Cl-Pro) produced lower inhibitions than that

obtained by Graz *et al.* (2000), or Brauns *et al.*, (2004). Antimicrobial studies revealed that both cyclo(Phe-4Cl-Pro) and cyclo(D-Phe-4Cl-Pro), demonstrated insignificant effects on Gram-positive and Gram-negative organisms, but illustrated significant effects against *C.albicans*. The haematological studies revealed that cyclo(D-Phe-4Cl-Pro) at a concentration of 12.5 mM significantly shortened the Activated partial thromboplastin time and prothrombin time clotting times. cyclo(D-Phe-4Cl-Pro) at a concentration of 12.5 mM, and 3.125 mM produced significant anti-platelet properties. The anti-diabetic studies demonstrated limited activity of both cyclo(Phe-4Cl-Pro) and cyclo(D-Phe-4Cl-Pro) in inhibiting the activity of α -glucosidase and α -amylase enzymes.

Key words: cyclic dipeptides, chlorine, antimicrobial, anticancer, haemostasis, antidiabetic

INTRODUCTION

The study aimed to determine the biological activity of cyclo(Phe-4Cl-Pro) and cyclo(D-Phe-4Cl-Pro) (Figures 1 and 2 respectively) with respect to their anticancer, antimicrobial, heamatological and anti-diabetic effects.

All living tissues consist of proteins. Proteins play a major role in regulating most signal transductions in eukaryotic cells and as hormones, neurotransmitters and neuromodulators (Nelson and Cox, 2005). Even though the use of peptides as novel drug compounds has been limited by their poor chemical and physical properties, structural similarities of cyclic dipeptides, also known as diketopiperazines (DKPs), cyclo dipeptides, 2,5-diketopiperazines (DKPs), 2,5-dioxopiperazines (DOPs), or dipeptide anhydrides to peptides, the abundance of their ring structure in several natural products coupled with the simplicity of their chemical structure has inspired new research (Witak and Wei, 1990).

2,5-Diketopiperazines (DKPs) are cyclic dipeptide derivatives, which show a multitude of interesting biological activities including efficient interactions with opioid receptors, potent cytotoxic effects and neuroprotective effects. Recently, they have also been associated with blockade of L-type calcium channels, tryptase inhibition, oxytocin receptor antagonism and plasminogen activator inhibition (Wyatt *et al.*, 2005).

MATERIALS AND METHODS

Molecular modeling methods

The energetically favourable conformation distributions of cyclo(Phe-4Cl-Pro) and cyclo(D-Phe-4Cl-Pro) was elucidated by using Spartan'10[®] (Professional Version 1.10) computer molecular modeling software. Local minima conformations were obtained for each cyclic dipeptide by the use of molecular mechanics (AMBER force field) optimisation methods, due to the fact that it does not consider hydrogens explicitly (Wishart and Case, 2001).

The cyclic dipeptides cyclo(Phe-4Cl-Pro) and cyclo(D-Phe-4Cl-Pro) were initially built by using the amino acid database included in the Spartan'10[®] software. A step-wise approach to energy minimisation was then followed. Geometrical optimisation was achieved by an initial steepest-descent run, which was run for at least 200 cycles or until the root mean square (RMS) of $0.1 \text{ kcal.mol}^{-1}\text{Å}^{-1}$ was achieved. Geometrical optimisation of the cyclic dipeptides was then followed by a PolakRibiere (Conjugated gradient) minimisation, which was done in repeated runs of 32560 cycles, until suitable low energy conformations with RMS of less than $0.001 \text{ kcal.mol}^{-1}\text{Å}^{-1}$ was obtained. The conformational search was executed in order to identify the three lowest energy conformations, which could then be analysed to produce conclusions on the conformations of the cyclic dipeptides.

Anticancer methods

Three human cancerous cell lines, namely HeLa (cervical carcinoma), HT-29 (colon carcinoma) and MCF-7 (breast carcinoma), were used in the experiments to determine the potential anticancer activity of cyclo(Phe-4Cl-Pro) and cyclo(D-Phe-4Cl-Pro). Primary cell cultures were obtained from Highveld Biological, South Africa (SA), and were stored in liquid nitrogen until needed. Tetrazolium salt 3-(4,5-dimethylthiazol-2-yl)-2,5-diphenyltetrazolium bromide (MTT) was used in the microculture assay to measure cell growth and viability.

All experiments were conducted in accordance with standard sterile culture techniques and all procedures were carried out under aseptic conditions in laminar flow units. HeLa, HT-29 and MCF-7 cell lines were maintained in RPMI 1640 growth medium (Sigma-Aldrich) in culture flasks (Corningware, USA) supplemented with 10% heat-inactivated bovine foetal calf serum (FCS) (Adcock Ingram, SA) at 37 °C with 5% CO₂ humidification (Labtec[®] ThermoForma[®]). The RPMI 1640 (Sigma-Aldrich) growth medium was replaced every 48 hours by aspirating the old medium off, washing twice with phosphate buffered

saline (PBS) and adding fresh medium. Cell lines were cultured until they achieved approximately 80% confluence and were then sub-cultured by aspirating medium from the confluent flasks, and washed twice with 1 ml of 0.25% trypsin in ethylenediaminetetraacetic acid (EDTA), pre-warmed to 37 °C. Cells were dissociated by adding 1 ml trypsin/EDTA for approximately 5 minutes at 37 °C. The cells were incubated in a Labtec® humidified CO₂ incubator (Labcon, SA) for 10 minutes and suspended in 9 ml growth medium and incubated at 37°C. Portions from each sub-cultured generation were stored in liquid nitrogen for preservation of the cell line.

Prior to use the cells were dissociated from the culture flasks by adding 1 ml of 0.25% trypsin (Highveld Biological, SA). Trypsin was deactivated by adding 10 ml of RPMI 1640 (Sigma-Aldrich) growth medium. The cells were gently agitated to disperse and suspend them into single-cell suspensions. The concentration of the cells was determined with a haemocytometer by utilizing trypan-blue staining. The cell suspensions were then diluted with culture medium to obtain a standard of 6000 cells/ml.

Each cell line was tested in separate 96-well flat-bottom microtitre plates (Costar, Corning). 200 µl of each cell suspension was transferred to the wells of 96-well flat-bottom microtitre, plates leaving a control set of 4 replicate wells that contained the medium alone (blanks for MTT) assay. This was incubated at 37 °C with 5% CO₂ humidification for 24 hours. After incubation the cells had attached to the bottom of the wells, which enabled the growth medium to be aspirated off. The negative controls, positive control and cyclic dipeptide solutions were then added to the wells in aliquots of 200 µl at appropriate final concentration in culture medium, such that each treatment yielded results in quadruplicate. The microtitre plates were subsequently incubated at 37 °C with 5% CO₂ humidification for a further 48 hours. Incubation allowed for the drug compounds to interact with the respective cell lines. After 48 hours of incubation the growth medium was aspirated off and discarded from each well. 200 µl aliquots of MTT solution were then added to each well of the microtitre plates. The MTT containing microtitre plates were then incubated at 37 °C with 5% CO₂ humidification for three hours to allow for the metabolic reduction of the MTT. This resulted in the formation of insoluble formazan precipitates. The MTT supernatant was aspirated off and discarded, and replaced with 200 µl aliquots of DMSO, which were required to dissolve the formazan precipitate. Each microtitre plate was then placed on a plate shaker for 5 minutes and the absorbance read immediately at 540 nm on a multiscan MS® (version 4.0) Labsystem® type 352 microtitre plate spectrophotometer (Multiscan MS®, England) (Huq *et al.*, 2004; Cunningham, 2006). Experiments were conducted in quadruplicate. Results were reported as the percentage inhibition of growth for each cell culture, after 48 hours of exposure to the cyclic dipeptides or the positive control, relative to the appropriate negative vehicle control culture.

Antimicrobial methods

The colony numbers of the bacteria and fungus were standardised by dilution and plating methods. From the counts the test cultures were diluted to obtain 1×10^6 CFU/ml (colony forming units). The calculated volumes were then made up to 10 ml using Mueller-Hinton broth.

50 μ l of each test organism was pipette into a 96-well microplate and thereafter, 50 μ l of either of the stock solutions of the two cyclic dipeptides at concentrations of 1 mM and 2 mM were added to the wells, which resulted in a final concentration of 0.5 mM and 1 mM in each well. 50 μ l of each of the positive controls, were pipette into the respective cells according to the test organism cultures, giving final concentration of 0.25 mg/ml and 0.5 mg/ml in the respective wells. 50 μ l of the negative control was pipette to separate wells to indicate 100% viability of the test organism growth.

The 96-well microplates were then incubated for 24 hours at 37 °C for bacteria and 28 °C for *C. albicans* in an orbital shaker at 100 rpm. 40 μ l of MTT at a concentration of 0.5 mg/ml was added to each of the cells after incubation. In order to obtain a zero reading time, absorbance was immediately measured on a microplatereader at 540 nm for bacteria and 600 nm for *C. albicans*. Following this the 96-well microplates were incubated for four hours, in an orbital shaker at 100 rpm to allow for the metabolic reduction of MTT. This was followed by centrifugation in an Eppendorf centrifuge at 3000 rpm for seven minutes to pellet the insoluble formazan product (Freimoser *et al.*, 1999; Stevens and Olsen, 1993). The supernatant was aspirated from each of the wells and discarded. 90 μ l of DMSO was subsequently added to each well to solubilise the formazan product and placed on a plate shaker for four minutes. The absorbance was read immediately at 540 nm for bacteria, and 600 nm for *C. Albicans*. The 96-well microplates were incubated thereafter for 4 hours at 37°C, in an orbital shaker at 100 rpm to allow for the metabolic reduction of MTT. This was followed by centrifugation in an Eppendorf centrifuge at 3000 rpm for seven minutes to pellet the insoluble formazan product (Freimoser *et al.*, 1999; Stevens and Olsen, 1993). The supernatant was aspirated off from each of the cells and discarded. 90 μ l of DMSO was subsequently added to each well to solubilise the formazan product and placed on a plate shaker for 4 minutes. The absorbance was read immediately at 540 nm for bacteria and 600 nm for *C.albicans*. The results calculated as illustrated below, were reported as percentage inhibition relative to the respective negative control.

$$\% \text{ inhibition} = \frac{NEG_{GROWTH} - DRUG_{GROWTH}}{NEG_{GROWTH}} \times 100$$

WHERE $NEG_{GROWTH} = NEG_{T=24} - NEG_{T=0}$

$$\text{DRUG}_{\text{GROWTH}} = \text{DRUG}_{\text{T}=24} - \text{DRUG}_{\text{T}=0}$$

AND $\text{NEG}_{\text{T}=24}$ = Absorbance at 540 nm after incubation for control

DRUG_{T} = Absorbance at 540 nm for drug after incubation

DRUG_0 = Absorbance at 540 nm for drug prior to incubation.

Haematological methods

Prothrombin time (PT), activated partial thromboplastin time (APTT) and fibrinogen-C assays

A CL Analyser (Instrumental Laboratory Corporation, Beckman) and an ACL-assay reagent kit (Instrumental Laboratory Corporation, Beckman) were used to perform the assays. The in vitro tests were performed according to the Clinical and Laboratory Standards Institute (CLSI) guidelines and the manufacturer's package insert guidelines.

Activated partial thromboplastin time (APTT)

A Synthasil kit (Beckman) was used in the assay and consist of APTT buffered reagent and a contact activator. The reagent contains synthetic phospholipids, which are required for optimal platelet-like activity and highly defined non-settling colloidal silica.

The APTT assay was conducted by adding 100 μl of the APTT reagent to tubes containing 100 μl of plasma and either the (C), cyclo(Phe-4Cl-Pro) (1: 3) and cyclo(D-Phe-4Cl-Pro) (1: 3) or heparin (0.1 U/ml, PC). The mixtures were incubated at 37 °C for 180 seconds on the CL Analyser, after which 100 μl of 0.025 M CaCl_2 solution was added to initiate the activation of the intrinsic pathway. The clotting time was measured, and the anticoagulatory activity of test samples evaluated relative to the untreated control (C).

Prothrombin time assay

A RecombiPlastin kit (Beckman) was used in the assay. The thromboplastin reagent (phospholip/tissue factor preparation), included in the Recomboplastin kit, is a liposomal preparation which constitutes of recombinant human tissue factor in a phospholipid mixture with calcium chloride, buffer and a preservative.

Recomboplastin (200 µl) was incubated at 37 °C for 180 seconds on the CL Analyser (IVD, Beckman Coulter), while a premix of 100 µl of plasma was incubated for 180 seconds at 37 °C with either the untreated control (C), cyclo(Phe-4Cl-Pro) (1: 4), cyclo(D-Phe-4Cl-Pro) (1: 4) or heparin (0.1 U/ml, positive control {PC}) (Bodene). To evaluate the PT, 150 µl of the plasma premix solutions were added to the recomboplastin (200 µl) and the clotting time was measured.

Fibrinogen-C assay

A fibrinogen-C kit (Beckman) was used in evaluating the effect of cyclo(Phe-4Cl-Pro) and cyclo(D-Phe-4Cl-Pro) on conversion of fibrinogen to fibrin by comparing the protein levels of the treated plasma with those of the untreated plasma controls. A ten times dilution of diluted plasma (200 µl) was incubated with 50 µl of either the (C), cyclo(Phe-4Cl-Pro) (1: 4), cyclo(D-Phe-4Cl-Pro) (1: 4) or heparin (0.1 U/ml, PC) at 37 °C on the CL Analyser for 180 seconds. After the incubation period, a thrombin (Beckman) solution (35 U/ml; 100µl) was added and the effect of the conversion of fibrinogen to fibrin was evaluated by comparing the fibrin levels of the treated plasma with that of the untreated plasma control (C).

D-Dimer assay

A D-Dimer kit was used in the assay. The kit consisted of a D-Dimer latex reagent and reaction buffer (Beckman). The latex reagent is a suspension of uniform sized polystyrene latex particles coated with a monoclonal antibody that is highly specific for the D-Dimer domain. When plasma containing D-Dimer is mixed with the latex reagent and reaction buffer the coated latex particles agglutinate. The degree of agglutination is directly proportional to the concentration of D-Dimer in the solution. The buffer (150 µl) was added to 42 µl of the plasma containing 8 µl of either the (C), cyclo(Phe-4Cl-Pro) (1: 3) or cyclo(D-Phe-4Cl-Pro) (1: 3). The mixture was then incubated at 37 °C in the CL Analyser for 15 minutes. After the incubation period the latex D-Dimer was subsequently added, the effect of the cyclic dipeptides on the rate of fibrinolysis via D-Dimer formation was evaluated by comparing the protein levels of the treated

plasma with that of the untreated plasma control. Heparin (0.1 U/ml) was used as the positive control for this assay.

Platelet aggregation/adhesion studies

Human blood plasma was used to screen cyclo(Phe-4Cl-Pro) and cyclo(D-Phe-4Cl-Pro) for activity against the various haematological processes. The human ethics committee of the Nelson Mandela Metropolitan University (NMMU) approved the use of human blood samples in the haematological studies (reference number) (HO6SB-003) (September 2006). Human blood used in the platelet aggregation assay was drawn at the NMMU clinic on the day of use.

A method adapted from Michelson *et al.*, (2000), was used for the experiment. A platelet rich plasma (PRP) sample containing a platelet count of 3×10^7 platelets/ml was used for all cytometry experiments. A volume of 40 μ l of PRP was placed into tubes containing 10 μ l of a 200 μ g/ml saturated concentration of fluorescein isothiocyanate (FITC)-PAC1 (BD Biosciences). The binding of fibrinogen to the gpIIb/IIIa receptor is required for platelet aggregation. PAC-1 binds only to activated platelets and appears to be specific for this recognition site within gpIIb/IIIa. PAC-1 inhibits fibrinogen-mediated platelet aggregation (Michelson *et al.*, 2000).

To inhibit fibrin polymerization, 2 μ l of 2.5 mmol/L (final concentration) of peptide glycol-L-prolyl-L-arginyl-L-proline (GPRP) (Sigma) was added. For a positive control (PC), 100 μ l of thrombin stock (50 U/ml) was added to give final concentration of 10 U/ml, the same volume of buffer was added for an untreated control (C), cyclo(Phe-4Cl-Pro) (1: 3) or cyclo(D-Phe-4Cl-Pro) (1: 3) were added. Unstained cells were used to determine background staining. The tubes were then incubated at room temperature for fifteen minutes. Following the incubation period the platelets were fixed with 2: 1 ratio of 1% formaldehyde for thirty minutes at room temperature. A threefold volume of Tyrode's buffer was added and the cells were immediately analysed with a Beckman flow cytometer (Coulter, Cytomics FC 500). All parameters were collected in list mode files and then analysed.

Anti-diabetic studies

The anti-diabetic effects of the cyclic dipeptides were determined by conducting α -glucosidase and α -amylase assays.

α-glucosidase assay

Methods employed by Sancheti *et al.* (2009) were adapted to determine the effects of cyclo(Phe-4Cl-Pro) and cyclo(D-Phe-4Cl-Pro) on the activity of the α-glucosidase enzyme.

Mixtures consisting of 50 μl of the 0.1 M phosphate buffer, 25 μl of the 0.5 mM 4-nitrophenyl-α-D-glucopyranoside solution, 10 μl of either the acarbose solution, cyclo(Phe-4Cl-Pro) solution or cyclo(D-Phe-4Cl-Pro) solution were incubated at 37 °C for 30 minutes. After incubation 100 μl of 0.2 M sodium carbonate solution was added to terminate the enzymatic reaction. The amount of *p*-nitrophenol released in the reaction was determined spectrophotometrically at 410 nm using a microplate reader (BioTek Power Wave XS). The amount of *p*-nitrophenol released was proportional to the enzymatic hydrolysis of the substrate. Experiments were conducted in triplicate.

α-Glucosidase inhibition was calculated as a percentage of the control using the formula:

$$\text{Percentage inhibition} = \frac{A_c - A_s}{A_c} \times 100$$

Where A_c is the change in absorbance of the blank control and A_s is the change in absorbance that occurs between the time the substrate is added to the mixture and 30 minutes after incubation.

α-Amylase assay

Methods developed by Fuwa (1954) and modified by Xiao *et al.* (2006) were adapted to determine the effects of cyclo(Phe-4Cl-Pro) and cyclo(D-Phe-4Cl-Pro) on α-amylase activity. The microplate-based starch-iodine assay was utilised. This assay is based on the development of color that results when iodine binds to starch polymers. The amount of starch degraded determines the activity of α-amylase.

40 μl of starch (Sigma) solution and 40 μl of the α-amylase enzyme (in 0.1 M phosphate buffer at pH 7.0) were pipetted into microplate wells and incubated at 50 °C for 30 minutes. After incubation 20 μl of 1 M HCl was added to terminate the enzymatic reaction. 100 μl of iodine reagent (5 mM iodine and 5 mM potassium iodide) was then added. When color development was evident, 150 μl of the iodine-treated sample was transferred into a transparent 96-well flat-bottomed microplate and the absorbance was read at 580 nm, using a microplate reader (BioTek Power Wave XS). The experiment was conducted in triplicate.

α -Amylase activity was determined as relative activity according to the following formula:

$$\text{Dextrinising activity} = \frac{(D_0 - D)}{D_0} \times \frac{100}{10}$$

Where D is the absorbance of the enzyme sample and D_0 is the absorbance of the amylase control without the addition of enzyme.

Statistical analysis

All the results obtained were obtained as triplicate values and represented as a mean \pm standard deviation (SD). Data were represented graphically with the aid of statistical software packages, Microsoft Excel[®] (Version 2007) and GraphPad Prism[®] (version 5). In order to determine whether the cyclic dipeptides under investigation caused statistically significant effects relative to the controls, Student's t -tests were performed on each concentration of the cyclic dipeptides. Calculated P-values of less than 0.05 were defined as statistical significant.

RESULTS AND DISCUSSION

Molecular modeling

The Boltzmann distribution obtained from the molecular calculations of the DKPs in the gas phase, water and DMSO indicated conformer one as the most stable conformer for each of the DKPs (Figure 3 and 4). The molecular calculations for each DKP in the gas phase, water and DMSO are illustrated in Tables 1, 2, 3, 4, 5 and 6. These conformers have the lowest relative energies and are most likely to be found under standard conditions. The different conformations of the water phase are not illustrated, due to the fact that the energies and conformations in the water phase were almost similar to that of the gas phase. DMSO was used as the solvent to dissolve the cyclic dipeptides for most of the biological studies and for this reason necessitates the illustration of the different conformations and molecular calculations.

Anticancer studies

cyclo(Phe-4Cl-Pro)

The results obtained from individual t-tests which were performed by comparing the percentage inhibition of growth by Melphalan and the DKPs relative to 100% cell line viability. The percentage inhibition of the HeLa, MCF-7 and HT-29 cancer cell lines caused by cyclo(Phe-4Cl-Pro) and Melphalan, with and without 0.05% PEG 300 are illustrated in figures 5 and 6 respectively. The conjugation of 0.05% PEG 300 with Melphalan enhanced the inhibition of growth against all cell lines with significant percent inhibitions of $86.88\% \pm 5.869$ ($P < 0.0001$) against the HeLa, $82.39\% \pm 2.058$ ($P < 0.0001$) against MCF-7 and $71.30\% \pm 1.035$ ($P = 0.0006$) against HT-29.

Cyclo(Phe-4Cl-Pro) at a screening concentration of 2 mM showed significant percentage inhibitions when compared with the screening concentrations of 1 mM. Cyclo(Phe-4Cl-Pro) showed the highest percentage inhibition against MCF-7 with a percentage inhibition of $71.62\% \pm 0.1252$ ($P < 0.0001$). Percentage inhibitions of $55.28\% \pm 0.4332$ ($P < 0.0001$) and $56.65\% \pm 0.3647$ ($P = 0.0006$) were observed for HeLa and HT-29 cell lines at a screening concentration of 2 mM. It was also apparent that at a screening concentration of 1 mM, cyclo(Phe-4Cl-Pro) showed no significant effect on the HeLa cell line. The lower concentrations of cyclo(Phe-4Cl-Pro) (1 mM) showed percentage growth inhibitions of $31.66\% \pm 1.127$ ($P < 0.0001$) and $35.73\% \pm 2.645$ ($P < 0.0001$) against the MCF-7 and HT-29 cell lines respectively.

The percentage growth inhibitions of HeLa, MCF-7 and HT-29 cell lines by Melphalan and cyclo(Phe-4Cl-Pro), without 0.05% PEG 300 (Figure), yielded interesting results. Melphalan at a screening concentration of 0.5 mM caused greater inhibition of the MCF-7 ($86.06\% \pm 1.632$) cell line compared to HeLa ($14.47\% \pm 6.606$) and HT-29 ($44.45\% \pm 3.370$) cell lines.

Cyclo(Phe-4Cl-Pro) at a screening concentration of 2 mM, without 0.05% PEG 300, inhibited the growth of HeLa and HT-29, but caused marginal stimulation of MCF-7 cell line. With percentage inhibitions of 34.61 ± 1.4519 ($P = 0.0402$) against the HeLa, $18.56\% \pm 1.972$ ($P < 0.0001$) against MCF-7 and $25.66\% \pm 1.525$ ($P = 0.0007$) against HT-29 cell line. At a screening concentration of 1 mM, cyclo(Phe-4Cl-Pro) caused percentage inhibitions of $26.29\% \pm 1.4287$ ($P < 0.0001$), $-5.499\% \pm 0.5015$ ($P < 0.0001$) and $17.83\% \pm 0.992$ ($P = 0.0007$) against HeLa, MCF-7 and HT-29, respectively.

Cyclo(D-Phe-4Cl-Pro)

The percentage growth inhibitions caused by Melphalan 0.5 mM and cyclo(D-Phe-4Cl-Pro) at screening concentrations of 2 mM, and 1 mM, conjugated with 0.05% PEG 300 are illustrated in Figure 7. Melphalan at a screening concentration of 0.5 mM caused inhibitions of $86.88\% \pm 5.869$ ($P < 0.0001$) against the HeLa, $82.39\% \pm 2.058$ ($P < 0.0001$) against MCF-7 and $71.30\% \pm 1.035$ ($P = 0.0006$) against HT-29.

Cyclo(D-Phe-4Cl-Pro) inhibited the growth of the MCF-7 cell line by $50.84\% \pm 0.5489$ ($P < 0.0001$) at a screening concentration of 2 mM compared with HeLa ($32.13\% \pm 19.779$) ($P < 0.0001$) and HT-29 ($47.63\% \pm 1.583$) ($P < 0.0001$). Cyclo(D-Phe-4Cl-Pro) at the lower screening concentration of 1 mM showed inhibitions of $11.75\% \pm 2.697$ ($P < 0.0001$) for HeLa, $29.79\% \pm 0.9773$ ($P < 0.0001$) for MCF-7 and $32.54\% \pm 3.261$ ($P < 0.0001$) for HT-29 cell lines.

The percentage growth inhibitions of HeLa, MCF-7 and HT-29 cell lines by Melphalan and cyclo(Phe-4Cl-Pro), without 0.05% PEG 300 (Figure 8). Melphalan (0.5 mM) inhibited the growth of HeLa cell line by $14.47\% \pm 6.606$ ($P < 0.0001$), the MCF-7 cell line by $86.06\% \pm 1.632$ ($P < 0.0001$) and the HT-29 cell line by $44.45\% \pm 3.370$ ($P < 0.0001$). At a screening concentration of 2 mM, cyclo(D-Phe-4Cl-Pro) caused greater percentage growth inhibitions of the HeLa, MCF-7 and HT-29 cell lines compared with the lower screening concentration of 1 mM. Cyclo(D-Phe-4Cl-Pro) at screening concentrations of 2 mM inhibited the growth of the HeLa cell line by $45.86\% \pm 7.706$ ($P < 0.0001$), the MCF-7 cell line by $21.98091\% \pm 4.750$ ($P = 0.0340$) and HT-29 by $24.60\% \pm 2.4200$ ($P = 0.0002$). At the lower screening concentration of 1 mM, cyclo(D-Phe-4Cl-Pro) produced percentage growth inhibitions of $19.77\% \pm 2.382$ ($P < 0.0001$), $32.13\% \pm 19.779$ ($P < 0.0001$) and $21.61\% \pm 2.3300$ ($P < 0.0001$) for HeLa, MCF-7 and HT-29 respectively.

Antimicrobial studies

Gram-negative bacteria

Pseudomonas aeruginosa

The percentage growth inhibitions caused by amoxicillin, chloramphenicol, cyclo(D-Phe-4Cl-Pro) and cyclo(Phe-4Cl-Pro) against *Pseudomonas aeruginosa* are illustrated in Figure 9 and summarised in Table

8. Chloramphenicol at concentrations of 0.5 mg/ml and 0.25 mg/ml inhibited the growth of *Pseudomonas aeruginosa* by $68.91\% \pm 5.690$ and $54.11\% \pm 1.775$ respectively, when compared with amoxicillin. Amoxicillin at screening concentrations of 1 mg/ml and 0.5 mg/ml showed percentage inhibitions of $90.34\% \pm 2.010$ and $76.23\% \pm 1.675$ respectively. At final screening concentrations of 1 mM and 0.5 mM, cyclo(D-Phe-4Cl-Pro) showed percentage inhibitions of $39.55\% \pm 3.000$ ($P = 0.0143$) and $15.61\% \pm 3.275$ ($P = 0.2619$) respectively. Cyclo(Phe-4Cl-Pro) at final screening concentrations of 1 mM and 0.5 mM, caused percentage inhibitions of $21.50\% \pm 1.835$ ($P = 0.0490$) and $15.99\% \pm 1.000$ ($P = 0.1061$) respectively.

Escherichia coli

The percentage growth inhibitions caused by amoxicillin, chloramphenicol, cyclo(D-Phe-4Cl-Pro) and cyclo(Phe-4Cl-Pro) against *Escherichia coli* are illustrated in Figure 10 and summarised in Table 9. Chloramphenicol at concentrations of 0.5 mg/ml and 0.25 mg/ml inhibited the growth of *Escherichia coli* by $78.50\% \pm 6.165$ and $69.66\% \pm 0.4350$ respectively, when compared with amoxicillin. Amoxicillin at screening concentrations of 1 mg/ml and 0.5 mg/ml showed percentage inhibitions of $73.25\% \pm 4.350$ and $76.23\% \pm 68.89\% \pm 1.335$ respectively. At final screening concentrations of 1 mM and 0.5 mM, cyclo(D-Phe-4Cl-Pro) showed percentage inhibitions of $25.83\% \pm 0.500$ ($P = 0.7724$) and $11.50\% \pm 0.8350$ ($P = 0.2771$) respectively. Cyclo(Phe-4Cl-Pro) at final screening concentrations of 1 mM and 0.5 mM, caused percentage inhibitions of $18.66\% \pm 1.000$ ($P = 0.6239$) and $15.66\% \pm 0.6700$ ($P = 0.4400$) respectively.

Gram-positive bacteria

Bacillus subtilis

The percentage growth inhibitions caused by amoxicillin, chloramphenicol, cyclo(D-Phe-4Cl-Pro) and cyclo(Phe-4Cl-Pro) against *Bacillus subtilis* are illustrated in Figure 11 and summarised in Table 10. Chloramphenicol at concentrations of 0.5 mg/ml and 0.25 mg/ml inhibited the growth of *Bacillus subtilis* by $83.61\% \pm 4.410$ and $68.28\% \pm 2.945$ respectively, when compared with amoxicillin. Amoxicillin at screening concentrations of 1 mg/ml and 0.5 mg/ml showed percentage inhibitions of $50.61\% \pm 4.410$ and $76.23\% \pm 57.55\% \pm 2.350$ respectively. At final screening concentrations of 1 mM and 0.5 mM, cyclo(D-Phe-4Cl-Pro) showed percentage inhibitions of $17.83\% \pm 5.500$ ($P = 0.8570$) and $11.50\% \pm 15.00\% \pm 1.335$ ($P = 0.7907$) respectively. Cyclo(Phe-4Cl-Pro) at final screening concentrations of 1 mM

and 0.5 mM, caused percentage inhibitions of $18.27\% \pm 2.390$ ($P = 0.7438$) and $12.33\% \pm 2.000$ ($P = 0.4900$) respectively.

Staphylococcus aureus

The percentage growth inhibitions caused by amoxicillin, chloramphenicol, cyclo(D-Phe-4Cl-Pro) and cyclo(Phe-4Cl-Pro) against *Staphylococcus aureus* are illustrated in Figure 12 and summarised in Table 11. Chloramphenicol at concentrations of 0.5 mg/ml and 0.25 mg/ml inhibited the growth of *Staphylococcus aureus* by $72.60\% \pm 6.600$ and $69.61\% \pm 1.610$ respectively, when compared with amoxicillin. Amoxicillin at screening concentrations of 1 mg/ml and 0.5 mg/ml showed percentage inhibitions of $26.40\% \pm 1.5600$ and $58.60\% \pm 1.300$ respectively. At final screening concentrations of 1 mM and 0.5 mM, cyclo(D-Phe-4Cl-Pro) showed percentage inhibitions of $68.00\% \pm 2.665$ ($P = 0.0106$) and $11.50\% \pm 22.17 \pm 1.165$ ($P = 0.05362$) respectively. Cyclo(Phe-4Cl-Pro) at final screening concentrations of 1 mM and 0.5 mM, caused percentage inhibitions of $12.22\% \pm 2.110$ ($P = 0.0062$) and $11.33\% \pm 9.000$ ($P = 0.0340$) respectively.

Fungus

Candida albicans

The percentage growth inhibitions caused by amoxicillin, chloramphenicol, cyclo(D-Phe-4Cl-Pro) and cyclo(Phe-4Cl-Pro) against *Candida albicans* are illustrated in Figure 13 and summarised in Table 12. Chloramphenicol at concentrations of 0.5 mg/ml and 0.25 mg/ml inhibited the growth of *Candida albicans* by $57.61\% \pm 2.390$ and $82.68\% \pm 5.345$ respectively, when compared with amoxicillin. Amoxicillin at screening concentrations of 1 mg/ml and 0.5 mg/ml showed percentage inhibitions of $91.19\% \pm 1.165$ and $63.83\% \pm 2.500$ respectively. At final screening concentrations of 1 mM and 0.5 mM, cyclo(D-Phe-4Cl-Pro) showed percentage inhibitions of $54.28\% \pm 5.055$ ($P = 0.0128$) and $31.83\% \pm 9.500$ ($P = 0.1380$) respectively. Cyclo(Phe-4Cl-Pro) at final screening concentrations of 1 mM and 0.5 mM, caused percentage inhibitions of $47.84\% \pm 7.820$ ($P = 0.0387$) and $46.18\% \pm 3.845$ ($P = 0.0114$) respectively.

Haematological studies

Activated partial thromboplastin time assay (APTT)

The effects of heparin (positive control), cyclo(Phe-4Cl-Pro) and cyclo(D-Phe-4Cl-Pro) on the intrinsic pathway are illustrated in Figure 15 and summarised in Table 13. APTT represents the time in seconds it takes for plasma to clot after the addition of an intrinsic pathway activator and calcium. The normal APTT range in human plasma is 24 to 39 seconds. Heparin at a screening concentration of 0.1 U/ml significantly prolonged the clotting time to 106.0 ± 1.350 seconds. Cyclo(Phe-4Cl-Pro) at a screening concentration of 50 mM produced a clotting time of 27.95 ± 0.4000 seconds ($P = 0.0003$). The screening concentrations of 25 mM and 12.5 mM, however produced a shorter clotting time of 20.28 ± 1.055 seconds ($P = 0.0004$) and 10.78 ± 0.4450 seconds ($P = 0.0002$), respectively. Cyclo(D-Phe-4Cl-Pro) at screening concentrations of 50 mM, 25 mM and 12.5mM, produced clotting times of 26.15 ± 0.7050 seconds ($P = 0.0004$), 14.61 ± 0.6150 seconds ($P = 0.0003$) and 8.110 ± 0.5500 seconds ($P = 0.0002$).

Prothrombin time assay (PT)

Prothrombin time represents the time in seconds it takes for plasma to clot after the addition of calcium and thromboplastin. The normal PT range is 11 to 13.5 seconds. The effects of heparin, cyclo(Phe-4Cl-Pro) and cyclo(D-Phe-4Cl-Pro) on PT clotting time are illustrated in Figure 14 and summarised in Table 14. Heparin at a screening concentration of 0.1 U/ml, significantly prolonged PT clotting time to 88.80 ± 1.805 seconds. Cyclo(Phe-4Cl-Pro) at screening concentrations of 50 mM, 25 mM produced longer PT clotting times of 20.53 ± 0.9250 seconds ($P = 0.2374$), 17.13 ± 0.1700 seconds ($P = 0.0055$). Cyclo(Phe-4Cl-Pro) at a screening concentration of 12.5 mM, however produced a PT clotting time of 14.41 ± 0.810014 seconds ($P = 0.0125$). Cyclo(D-Phe-4Cl-Pro) at screening concentrations of 50 mM, 25 mM and 12.5 mM, produced PT clotting times of 17.66 ± 0.6700 seconds ($P = 0.0266$), 11.85 ± 0.8550 seconds ($P = 0.0078$) and 10.75 ± 0.4500 seconds ($P = 0.0024$), respectively.

Fibrinogen-C assay (Fib-C)

The activity of heparin, cyclo(Phe-4Cl-Pro) and cyclo(D-Phe-4Cl-Pro) on fibrin formation is illustrated in Figure 15 and summarised in Table 15. The conversion of fibrinogen to fibrin elicit a series of reactions that cross-link adjacent fibrin monomers which then stabilises the formed clot (Dipiro *et al.*, 2011). The addition of 100 μ l of thrombin to the negative control (untreated plasma) resulted in the formation of 470.29 ± 0.510 mg/dL fibrin. Heparin (positive control) at a screening concentration of 0.1 U/ml decreased the formation of fibrin to 73.66 ± 3.670 mg/dL ($P = 0.0144$). Cyclo(Phe-4Cl-Pro) formed 116.7 ± 3.725 mg/dL ($P = 0.0144$) at 50mM, 273.2 ± 3.830 mg/dL ($P = 0.0007$) at 25 mM, 292.5 ± 2.500 mg/dL ($P = 0.0004$) at 12.5 mM. Cyclo(D-Phe-4Cl-Pro) formed 172.0 ± 2.000 mg/dL ($P = 0.0018$) at 50 mM, 313.4 ± 2.545 mg/dL ($P = 0.0003$) at 25 mM and 369.8 ± 0.8350 mg/dL ($P = 0.0002$) at 12.5 mM.

D-Dimer assay

The effects of heparin, cyclo(Phe-4Cl-Pro) and cyclo(D-Phe-4Cl-Pro) on D-Dimer levels are illustrated in Figure 16 and summarised in Table 16. Heparin at a screening concentration of 0.1 U/ml significantly decreased the levels of D-Dimer (36.99 ± 1.000 ng/ml). Cyclo(Phe-4Cl-Pro) at screening concentrations of 50 mM, 25 mM and 12.5 mM, produced results of 69.39 ± 1.055 ng/ml ($P = 0.0020$), 65.43 ± 2.875 ng/ml ($P = 0.0113$) and 53.10 ± 2.105 ng/ml ($P = 0.0203$). Cyclo(D-Phe-4Cl-Pro) at screening concentrations of 50 mM, 25 mM and 12.5 mM, produced results of 53.91 ± 0.3100 ng/ml ($P = 0.0038$), 49.16 ± 0.1700 ng/ml ($P = 0.0069$) and 43.95 ± 0.9550 ng/ml ($P = 0.0373$), respectively. D-Dimer levels should under normal physiological conditions not be detectable in blood plasma, except when the coagulation cascade has been activated. High D-Dimer levels in plasma indicate elevated levels of fibrin formation and reflect a state of hypercoagulability (Moresco *et al.*, 2006). The cyclic dipeptides caused elevation of D-Dimer formation.

Platelet aggregation studies

Figures 17 to 26 illustrate the flow-cytometry diagrams and cell density plots for the untreated control (PRP), treated control (PRP with 50U/ml thrombin), cyclo(Phe-4Cl-Pro) and cyclo(D-Phe-4Cl-Pro), at screening concentrations of 50 mM, 25 mM and 12.5 mM and 3.125 mM. In order to obtain the percentage of cells that stained positive, a region gate was drawn around a population of intact cells to exclude cell debris and clumped cells. The platelet particles that exhibited aggregation were excluded by the defined gate.

For the untreated control 1.3% of the cells exhibited aggregation. The positive control (thrombin 50 U/ml) indicated an 7.6% increase in aggregation. Cyclo(Phe-4Cl-Pro) increased the aggregation to 95.2%, 94.4%, 92.6 and 90.5% at screening concentrations of 50 mM, 25 mM, 12.5 mM and 3.125 mM respectively. Cyclo(D-Phe-4Cl-Pro) produced percentage aggregations of 93.5%, 32.4%, 0.2% and 0.3% at screening concentrations of 50 mM, 25 mM, 12.5 mM and 3.125 mM respectively.

Anti-diabetes assay

α -Glucosidase assay

The effects of acarbose (positive control) at a screening concentration of 50 mM, 1 mM of cyclo(Phe-4Cl-Pro) and 1 mM of cyclo(D-Phe-4Cl-Pro) on the activity of α -glucosidase are shown in Figure 27

Acarbose at a screening concentration of 50 mM inhibited the activity of the α -glucosidase enzyme by $51.11\% \pm 4.498$ ($P < 0.0001$) while cyclo(Phe-4Cl-Pro) and cyclo(D-Phe-4Cl-Pro) inhibited the activity by $-4.352\% \pm 1.477$ ($P < 0.0001$) and $-6.953\% \pm 1.740$ ($P < 0.0001$), respectively. These negative values obtained, indicate a stimulation of the α -glucosidase enzyme and thus an increase in the conversion of carbohydrates to monosaccharides and elevated blood glucose levels.

α -Amylase activity

The effects of acarbose, cyclo(Phe-4Cl-Pro) and cyclo(D-Phe-4Cl-Pro) on the activity of α -amylase are shown in Figure 28

Acarbose inhibited the activity of the α -amylase enzyme by $55.51\% \pm 2.786$ ($P < 0.0001$) at a screening concentration of 50 mM. Cyclo(Phe-4Cl-Pro) and cyclo(D-Phe-4Cl-Pro) inhibited the enzyme's activity by $5.654\% \pm 0.02507$ ($P < 0.0001$) and $5.530\% \pm 0.05743$ ($P < 0.0001$), respectively.

Conclusions

The anticancer results obtained indicated that the percentage growth inhibitions produced by both cyclic dipeptides were lower than those proposed by Graz *et al.* (2000) for proline-containing cyclic dipeptides, where a greater than 50% inhibition was observed for cyclo(Phe-Pro), and for (Brauns, 2004) on the effects of cyclo(Phe-Pro) on HT-29, HeLa and MCF-7 cell lines showed that cyclo(Phe-Pro) exhibited more than 50% growth inhibition ($p < 0.01$) in the three cell lines. Cyclo(Phe-Pro) exhibited significant growth inhibition at concentrations of 5 mM ($p < 0.01$) and 10 mM ($p < 0.01$) in all three cell lines. The IC_{50} values for cyclo(Phe-Pro) were 5.24 ± 1.25 mM in HT-29, 3.85 ± 1.26 mM in HeLa and 5.07 ± 1.32 mM in MCF-7 cells. Antimicrobial effects revealed that both cyclic dipeptides showed marginal effects on Gram-positive and Gram-negative organisms, but showed significant effects against *C.albicans*. The Haematological studies revealed that cyclo(D-Phe-4Cl-Pro) at screening concentrations of 12.5 mM and 3.125 mM showed significant anti-platelet activities.

ACKNOWLEDGEMENTS

I extend my sincere appreciation and grateful thanks to the following people for their continuous invaluable support, guidance, time and dedication to this research undertaken:

Prof PJ Milne, for his constant encouragement, knowledge and guidance. Dr G. Dealtry, to whom I owe much gratitude for all her assistance, time and knowledge. Prof C Frost for all her assistance with the blood work. Prof C McClelland for his assistance in the molecular modeling studies. Prof M van de Venter, for her assistance in the cell and isotope labs. Ms A Van Jaarsveld for all her assistance in the laboratory.

REFERENCES

Cunningham TL. 2006. The Medicinal Chemistry of the Selected Glycine-containing Cyclic Dipeptides: Cyclo(Gly-Thr) and Cyclo(Gly-Ser). MSc Dissertation. Nelson Mandela Metropolitan University

Freimoser FM, Jacob CA, Aebi M, Tuor U. 1999. The MTT [3-(4,5 dimethylthiazol-2-yl)-2,5-diphenyltetrazolium bromide] Assay is a Fast and Reliable Method for Colorimetric Determination of Fungal Cell Densities. *Applied and Environmental Microbiology*; 65 (8):3727-3729

Fuwa H. 1954. A New Method of Microdetermination of Amylase Activity by the Use of Amylase as the Substrate. *Journal of Biochemistry*; 41: 583-603

Graz CJM, Grant GD, Brauns SC, Hunt A, Jamie H, Milne PJ. 2000. Cyclic Dipeptides in the Induction of Maturation for Cancer Therapy. *Journal of Pharmaceutical Pharmacology*; (52): 75-82

Huq F, Daghiri H, Yu JQ, Tayyem H, Beale P, Zhang M. 2004. Synthesis, Characterization, Activities, Cell Uptake and DNA Binding of $[\{trans\text{-PtCl}(\text{NH}_3)_2\} \{\mu\text{-(H}_2\text{N}(\text{CH}_2)_6\text{NH}_2)\} \{trans\text{-PdCl}(\text{NH}_3)_2\} (\text{NO}_3)\text{CL}$. *European Journal of Medicinal Chemistry*; 39: 947-958

Michelson AD, Barnard MR, Kreuger LA, Frelinger AL, Furman MI. 2000. Evaluation of Platelet Function By Flow Cytometry. *Methods*; (21): 259-270

Milne PJ, Olivier DW, Roos HM. 1992. Cyclodipeptides: Structure and Conformation of Cyclo(Tyrosyl-Prolyl). *Journal of Crystallographic and Spectroscopic Research*, 22(6): 224-230

- Naumann K. 1999. Influence of Chlorine Substituents on Biological Activity of Chemicals. *Journal Für Praktische Chemie*; 341 (5): 417-435
- Nelson DL, Cox MM. 2005. Principles of Biochemistry, 4th edition. New York: Freeman and Company; 75-106
- Sancheti S, Seo S. 2009. Chaenomeles Sinesis: A Potent α -and β -Glucosidase Inhibitor. *American Journal of Pharmacology and Toxicology*; 4 (1): 1-8
- Stevens MG, Olsen SC. 1993. Comparative Analysis of Using MTT and XTT in Colorimetric Assays for Quantitative Bovine Neutrophil Bactericidal Activity. *Journal of Immunological Methods*; 157: 225-231
- Wishart DS, Case DA. 2001. Use of Chemical Shifts in Macromolecular Structure Determination. *Methods in Enzymology*; 338: 3-34
- Witak DT, Wei Y. 1990. Dioxopiperazines: Chemistry and Biology. *Progress in Drug Research*; 35: 249
- Wyatt PG, Allen MJ, Borthwick AD, Davies DE, Exall AM, Hatley RJD, Irving WR, Livermore DG, Miller ND, Nerozzi F, Sollis SL and Szardenings AK. 2005. 2,5-Diketopiperazines as Potent and Selective Oxytocin Antagonists 1: Identification, Stereochemistry and Initial SAR. *Bioorganic Medicinal Chemistry Letters* 15 (2005) 2579–2582
- Xiao Z, Storms R, Tsang A. 2006. A Quantitative Starch-iodine Method for Measuring alpha-Amylase and Glucosidase activities. *Analytical Biochemistry*; 351 (1): 146-148

LIST OF ABBREVIATIONS

%	Percentage
°C	Degrees Celsius

APTT	Activated partial thromboplastin time
CaCl_2	calcium chloride
CFU	Colony forming units
CLSI	Clinical and Laboratory Standards Institute
CO_2	Carbon Dioxide
DKPs	Diketopiperazines
DMSO	Dimethyl sulphoxide
EDTA	Ethylenediaminetetraacetic acid
FITC	Fluorescein isothiocyanate
GPRP	Peptide glycol-L-prolyl-L-arginyl-L-proline
M	Molar concentration
mg	milligrams
ml	milliliter
mM	millimolar
MTT	3-(4,5-dimethylthiazol-2-yl)-2,5-diphenyltetrazolium bromide
PRP	Platelet rich plasma
PT	Prothrombin time

Rel. E Relative energy

U/ml Units per Millilitre

μl Microlitre

VWF Von Willebrand factor

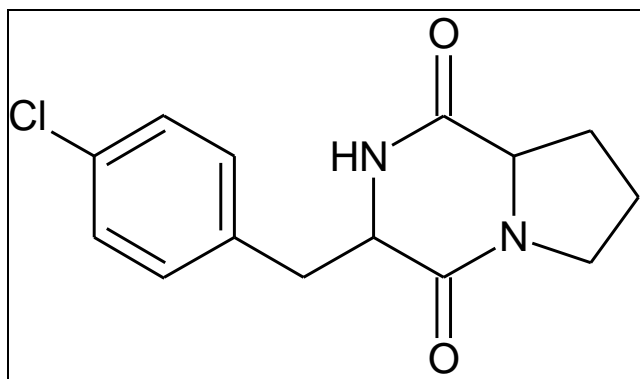


Figure 1 Structure of Cyclo(Phe-4Cl-Pro)

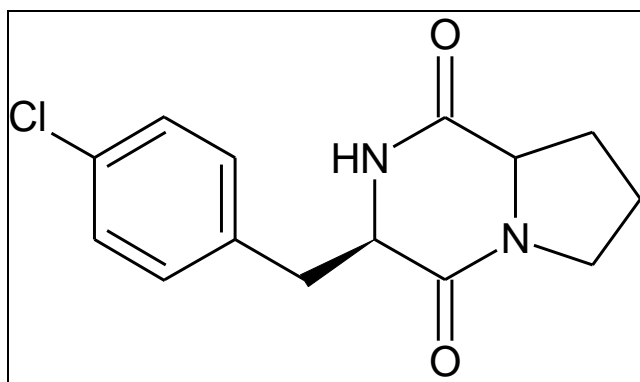


Figure 2 Structure of Cyclo(D-Phe-4Cl-Pro)

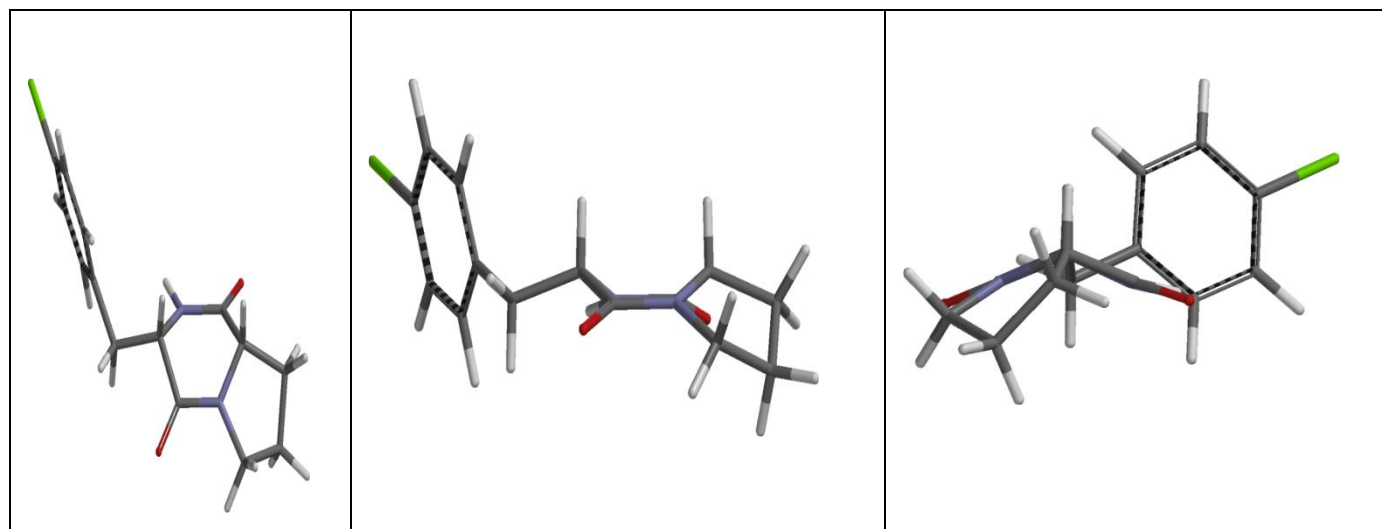


Figure 3 Conformation 1 of cyclo(Phe-4Cl-Pro) in dimethyl sulphoxide (DMSO)

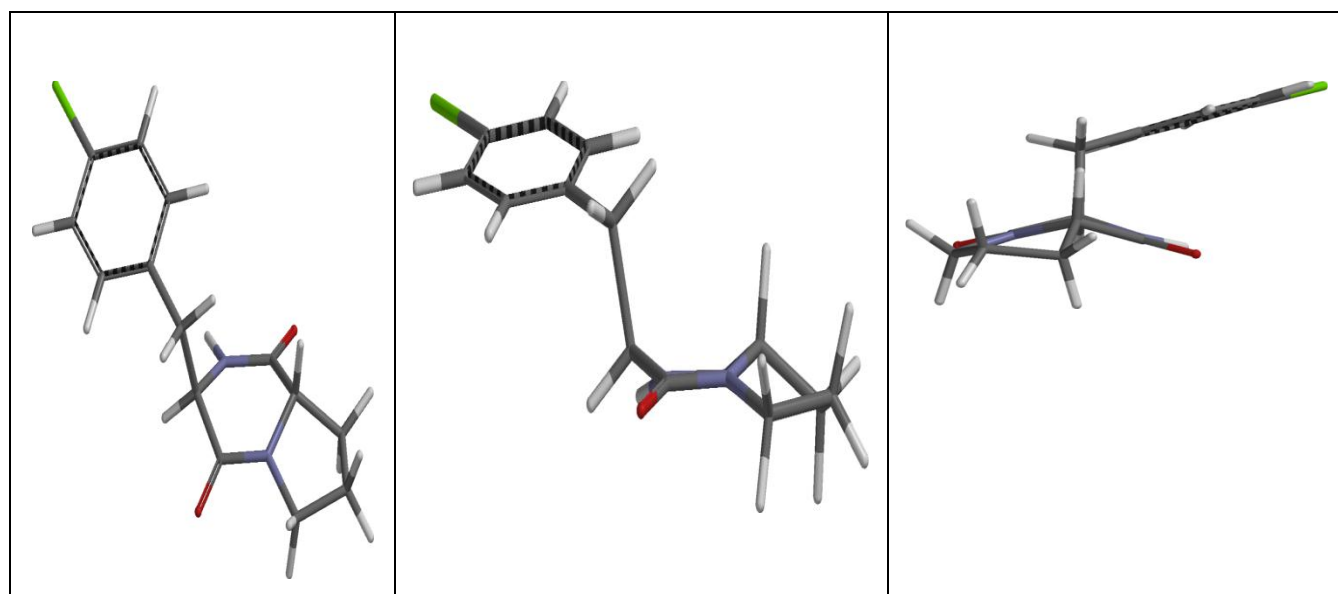


Figure 4 Conformation 1 of cyclo(D-Phe-4Cl-Pro) in dimethyl sulphoxide (DMSO)

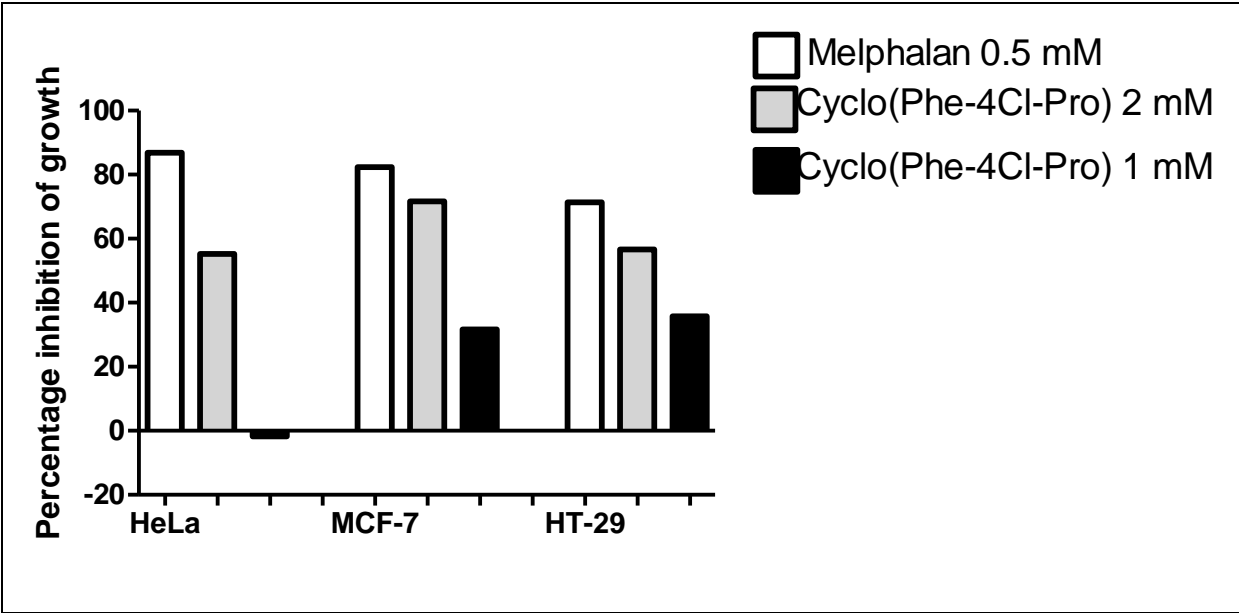


Figure 5 Percentage Inhibition of growth of HeLa, MCF-7 and HT-29 cell lines caused by melphalan (0.5 mM) and cyclo(Phe-4Cl-Pro) at screening concentrations of 1 mM and 2 mM, all conjugated with 0.05% PEG 300

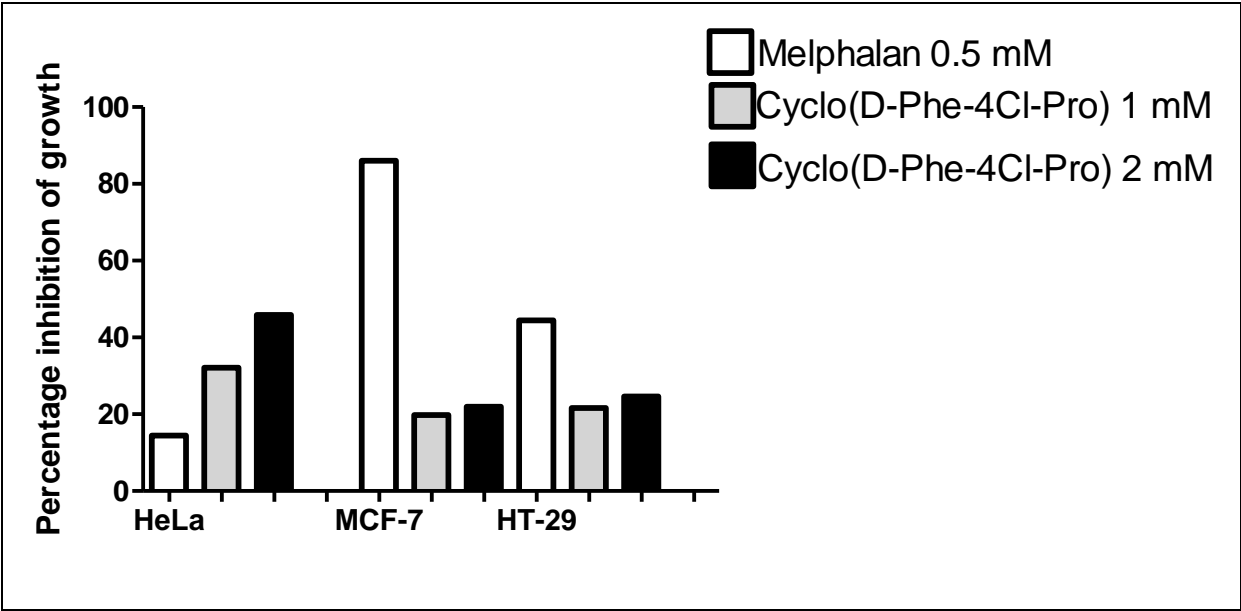


Figure 6 Percentage Inhibition of growth of HeLa, MCF-7 and HT-29 cell lines caused by melphalan (0.5 mM) and cyclo(Phe-4CI-Pro) at screening concentrations of 1 mM and 2 mM, all conjugated without 0.05% PEG 300

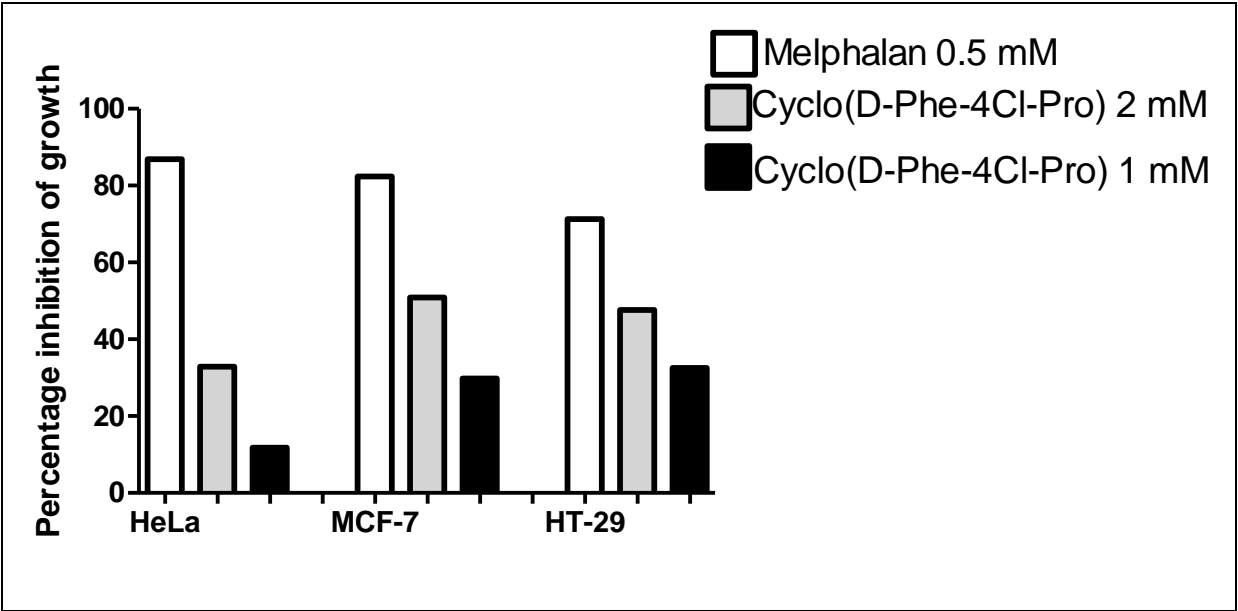


Figure 7 Percentage Inhibition of growth of HeLa, MCF-7 and HT-29 cell lines caused by melphalan (0.5 mM) and cyclo(D-Phe-4Cl-Pro) at screening concentrations of 1 mM and 2 mM, all conjugated with 0.05% PEG 300

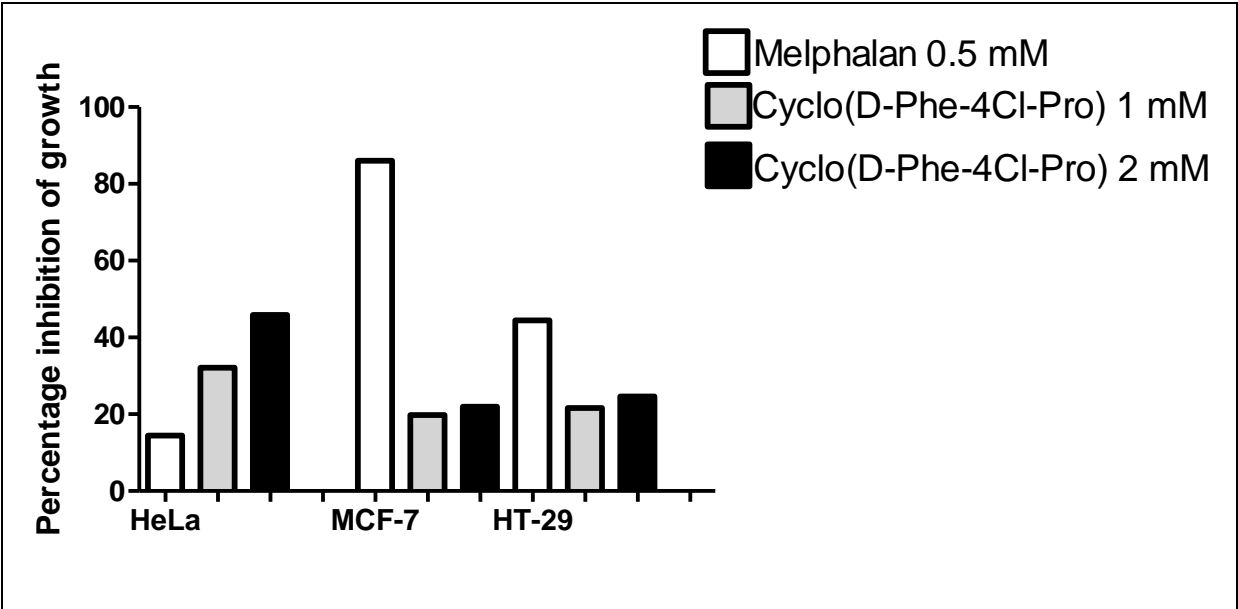


Figure 8 Percentage Inhibition of growth of HeLa, MCF-7 and HT-29 cell lines caused by melphalan (0.5 mM) and cyclo(D-Phe-4CI-Pro) at screening concentrations of 1 mM and 2 mM, all conjugated without 0.05% PEG 300

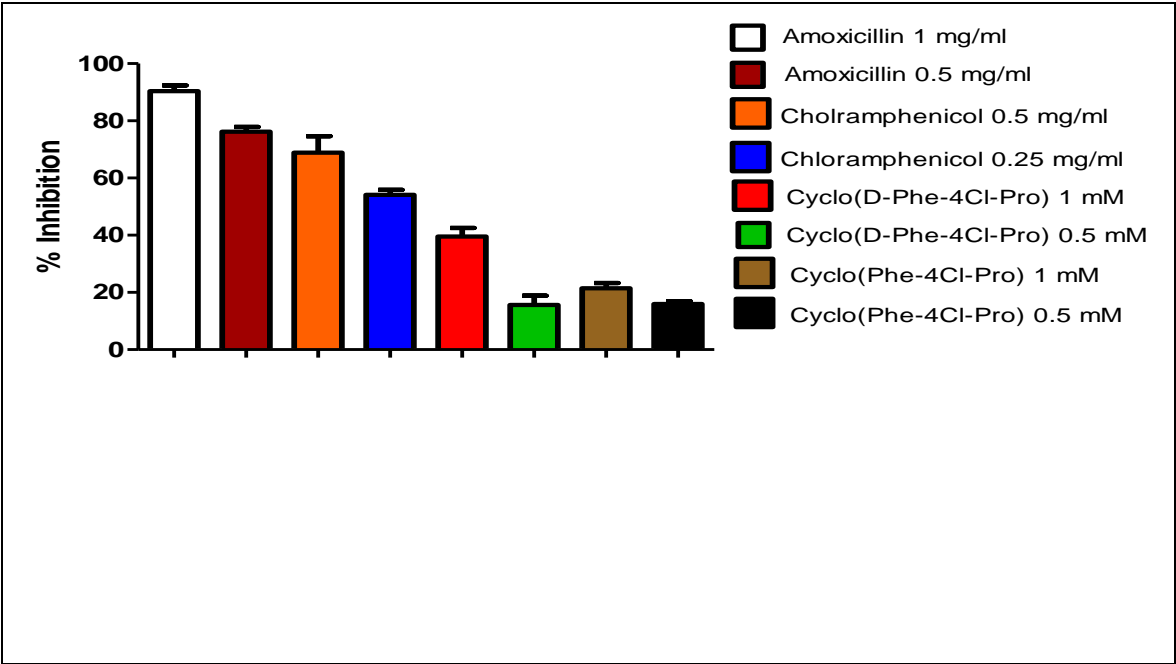


Figure 9 Percentage inhibition of *P. aeruginosa* caused by amoxicillin, chloramphenicol, cyclo(Phe-4Cl-Pro) and cyclo(D-Phe-4Cl-Pro)

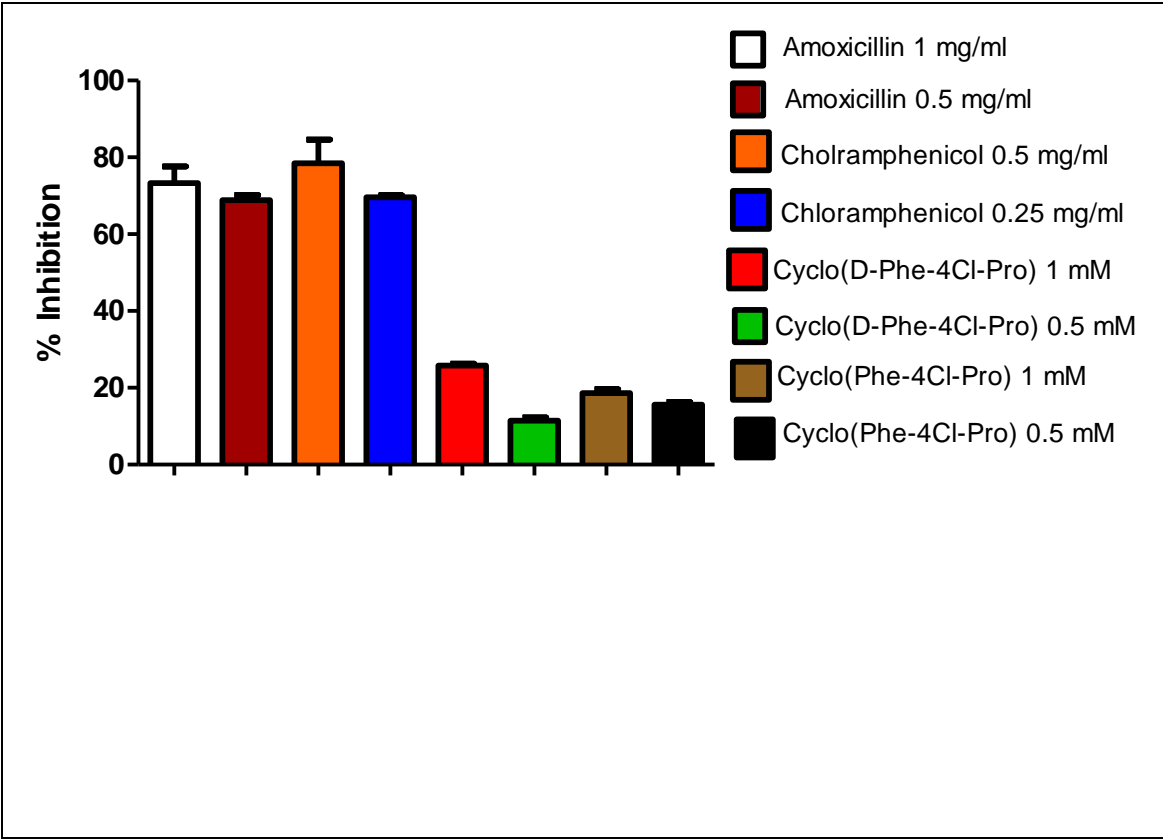


Figure 10 Percentage inhibition of *E. coli* caused by amoxicillin, chloramphenicol, cyclo(Phe-4Cl-Pro) and cyclo(D-Phe-4Cl-Pro)

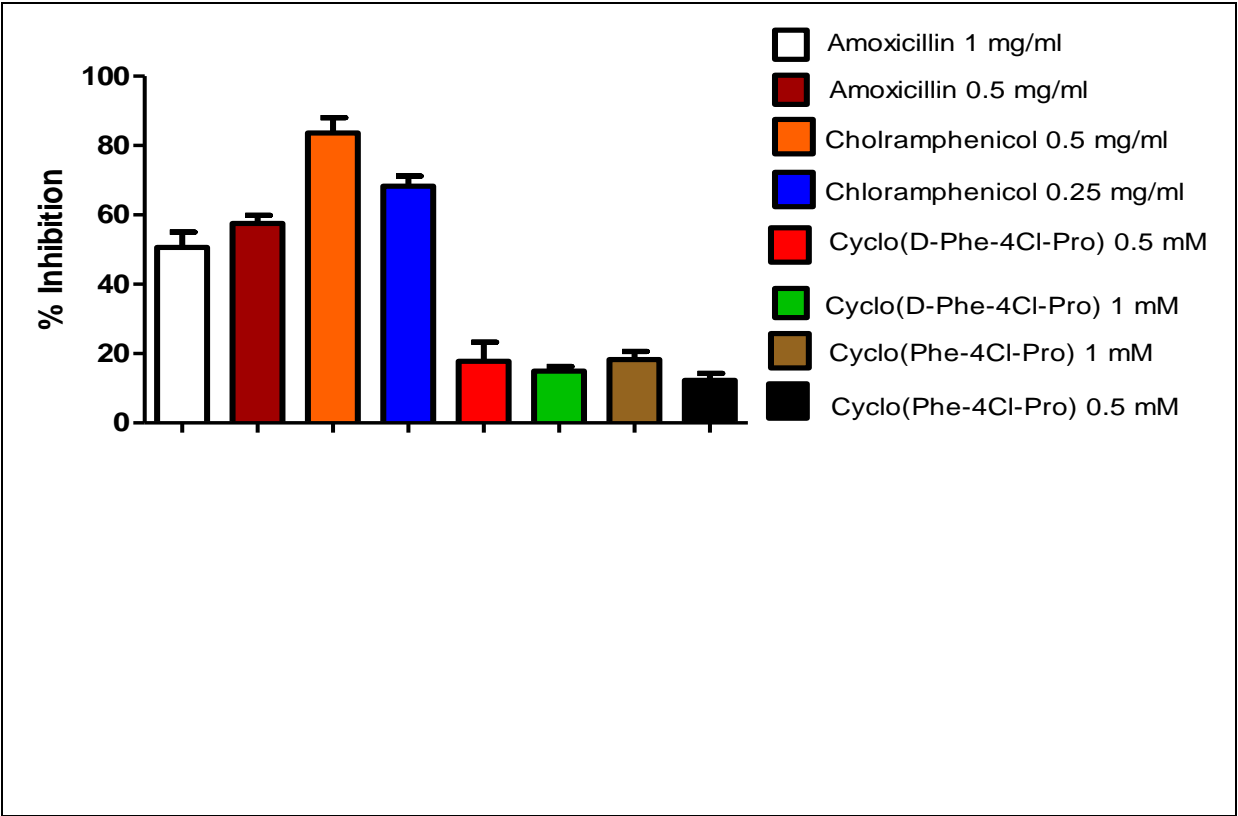


Figure 11 Percentage inhibition of *B. subtilis* caused by amoxicillin, chloramphenicol, cyclo(Phe-4Cl-Pro) and cyclo(D-Phe-4Cl-Pro)

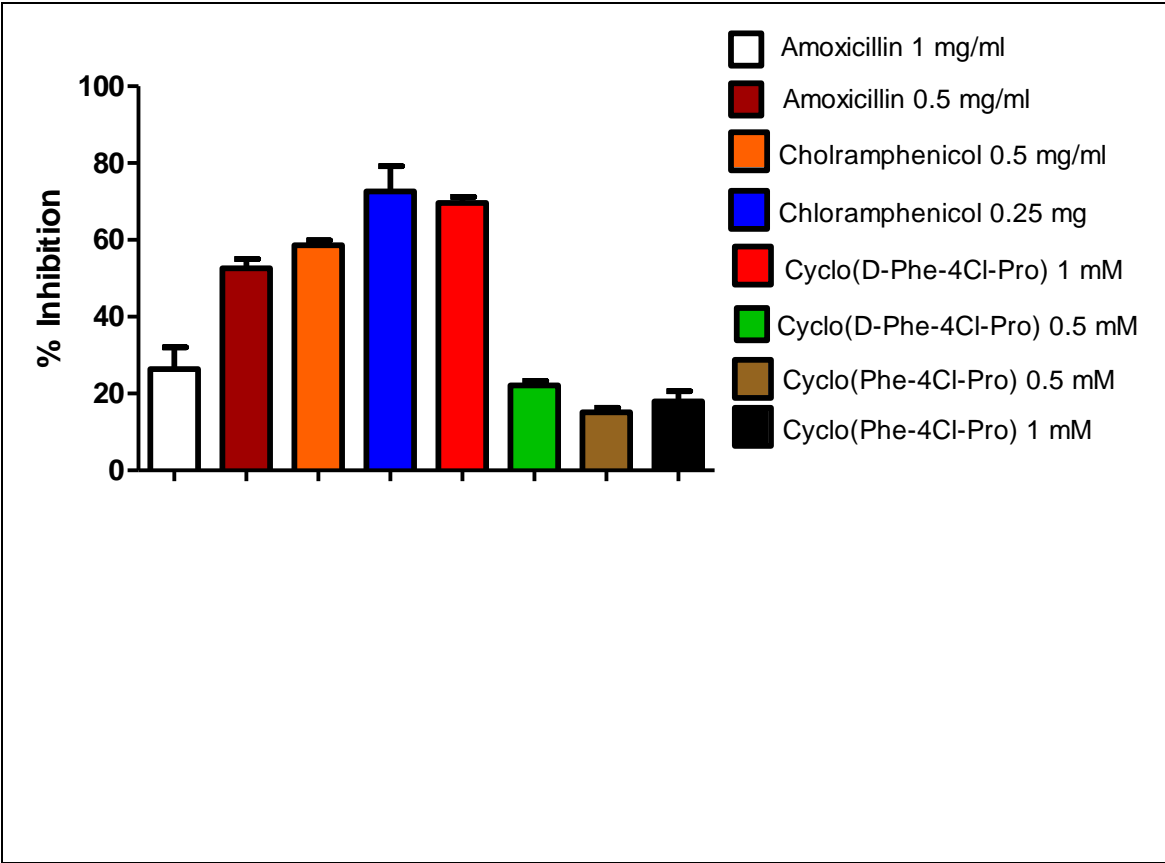


Figure 12 Percentage inhibition of *S. aureus* caused by amoxicillin, chloramphenicol, cyclo(Phe-4Cl-Pro) and cyclo(D-Phe-4Cl-Pro)

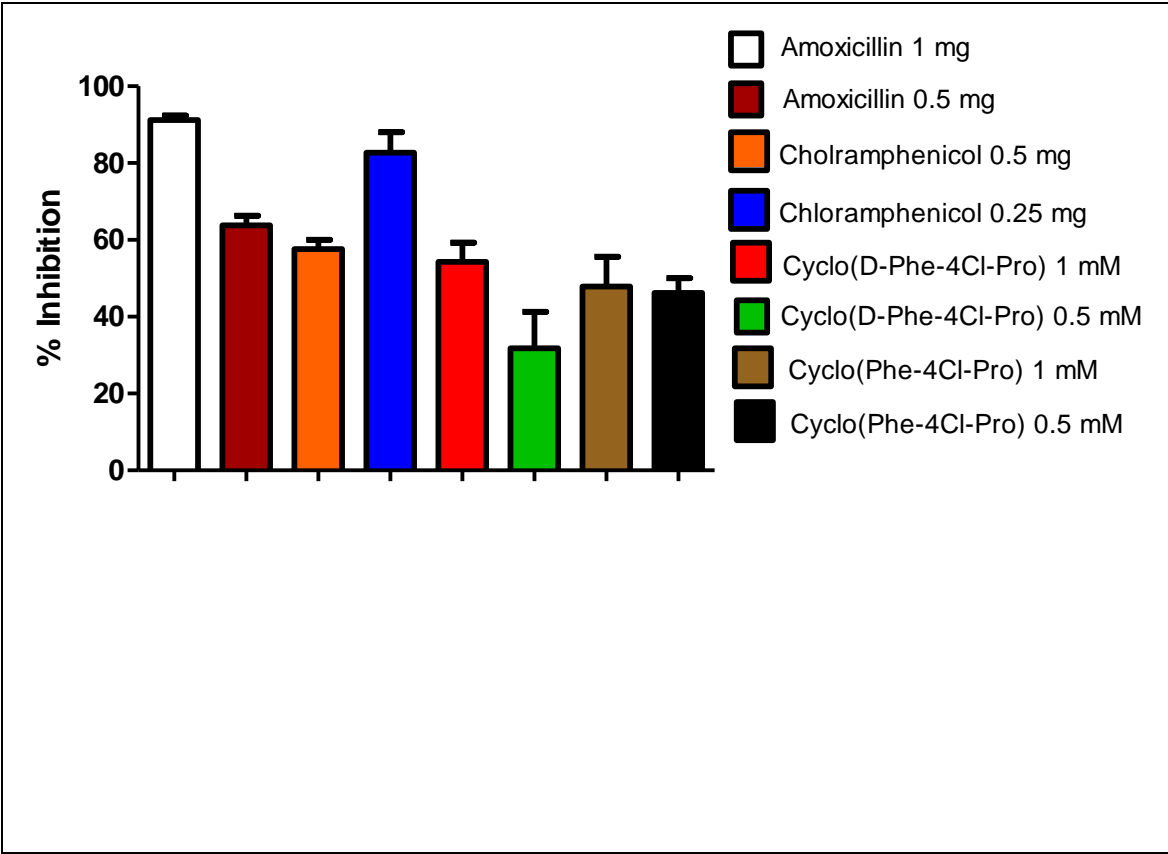


Figure 13 Percentage inhibition of *C. albicans* caused by amoxicillin, chloramphenicol, cyclo(Phe-4Cl-Pro) and cyclo(D-Phe-4Cl-Pro)

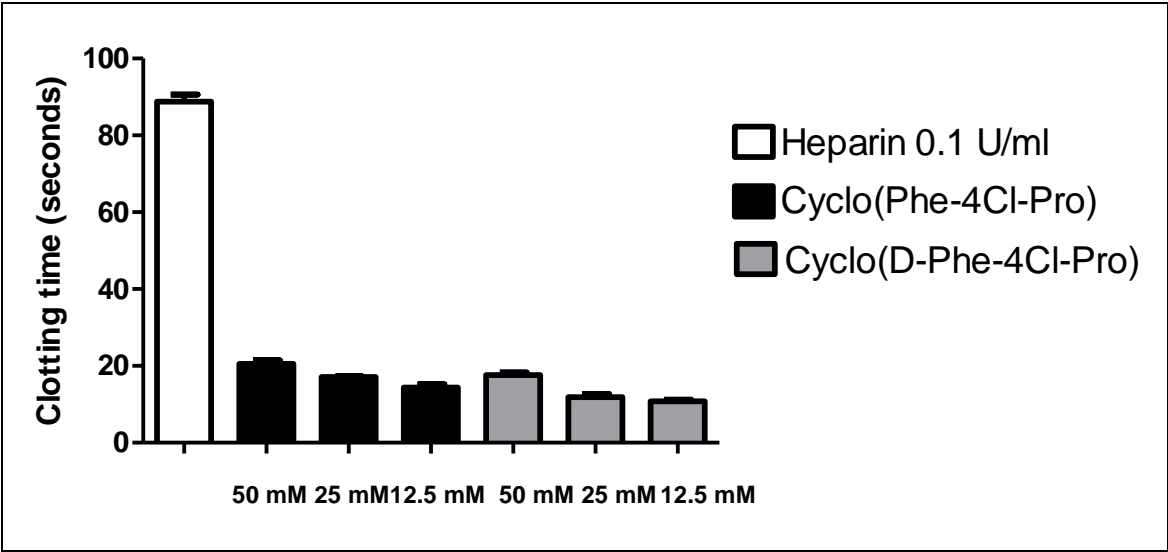


Figure 14 Effects of heparin (positive control), cyclo(Phe-4Cl-Pro) and cyclo(D-Phe-4Cl-Pro) on PT clotting time.

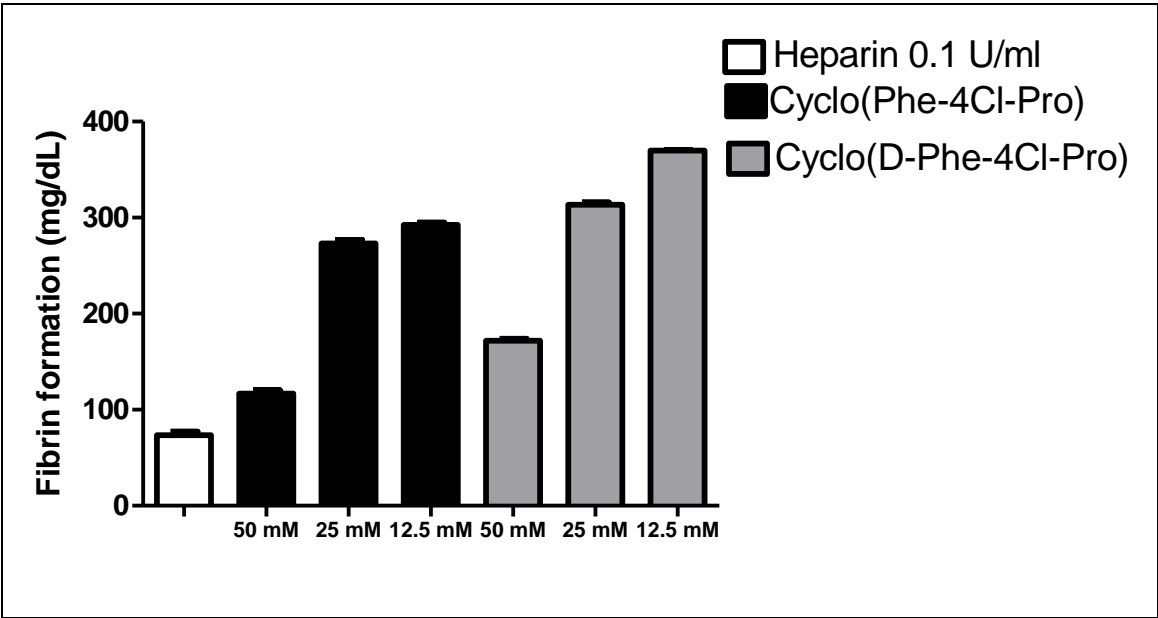


Figure 15 Effects of heparin (positive control), cyclo(Phe-4Cl-Pro) and cyclo(D-Phe-4Cl-Pro) on decreasing the formation of fibrin

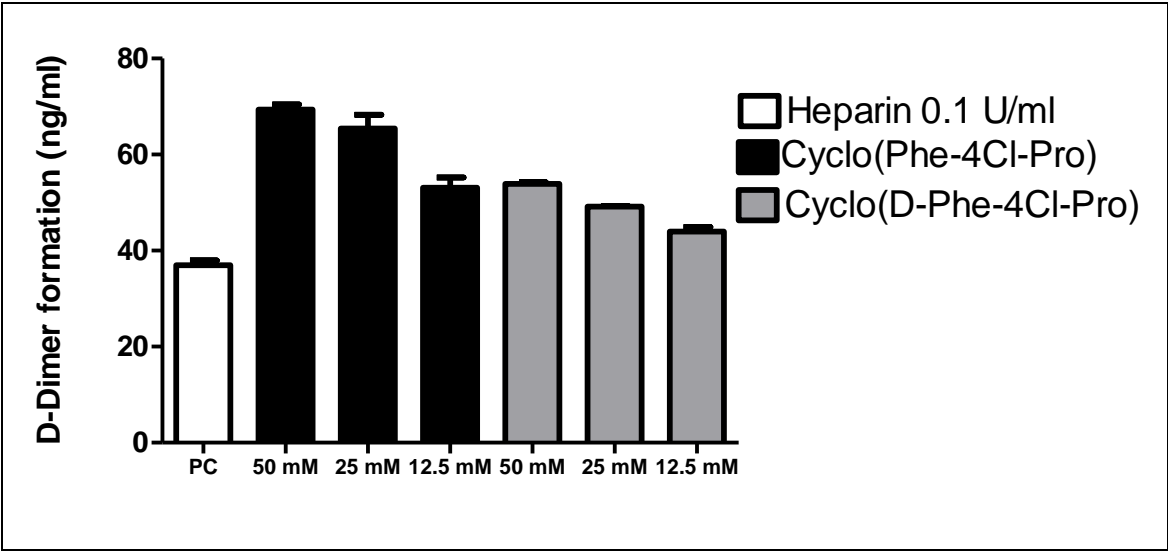


Figure 16 Effects of heparin (positive control), cyclo(Phe-4CI-Pro) and cyclo(D-Phe-4CI-Pro) on D-Dimer formation

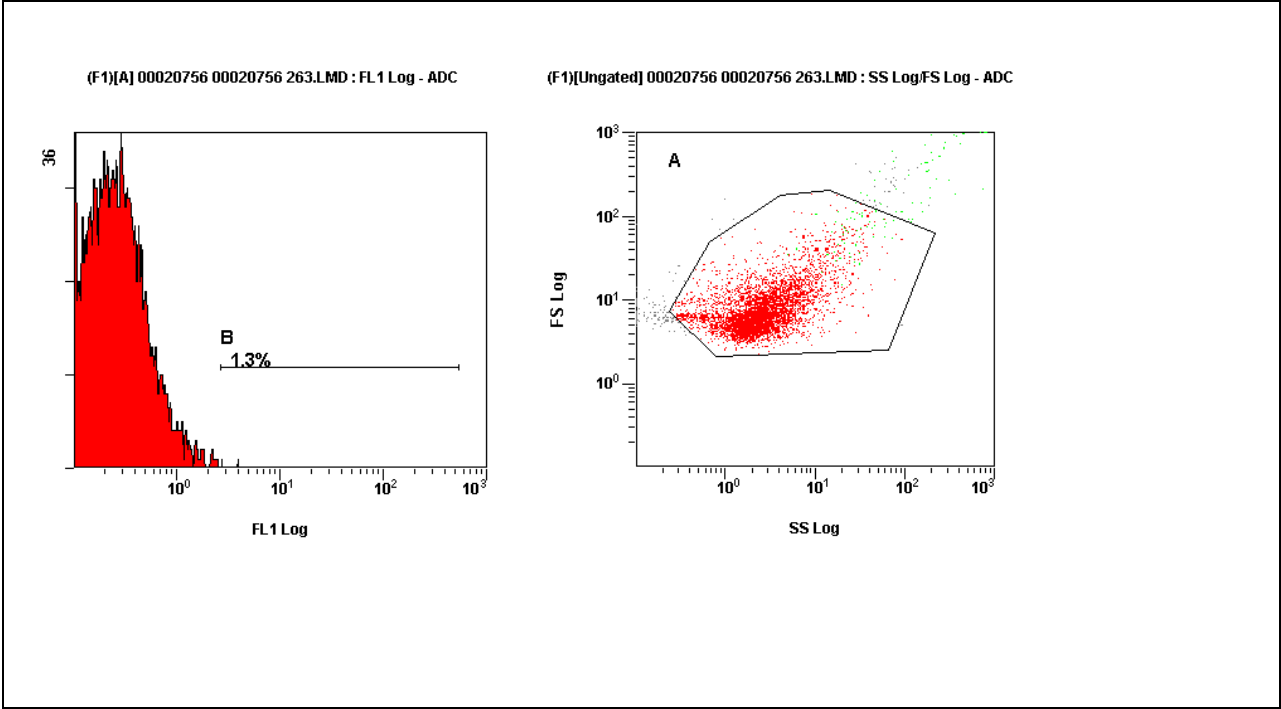


Figure 17 Fluorescence intensity and cell density plot representation of platelet aggregation caused by the untreated control (PRP)

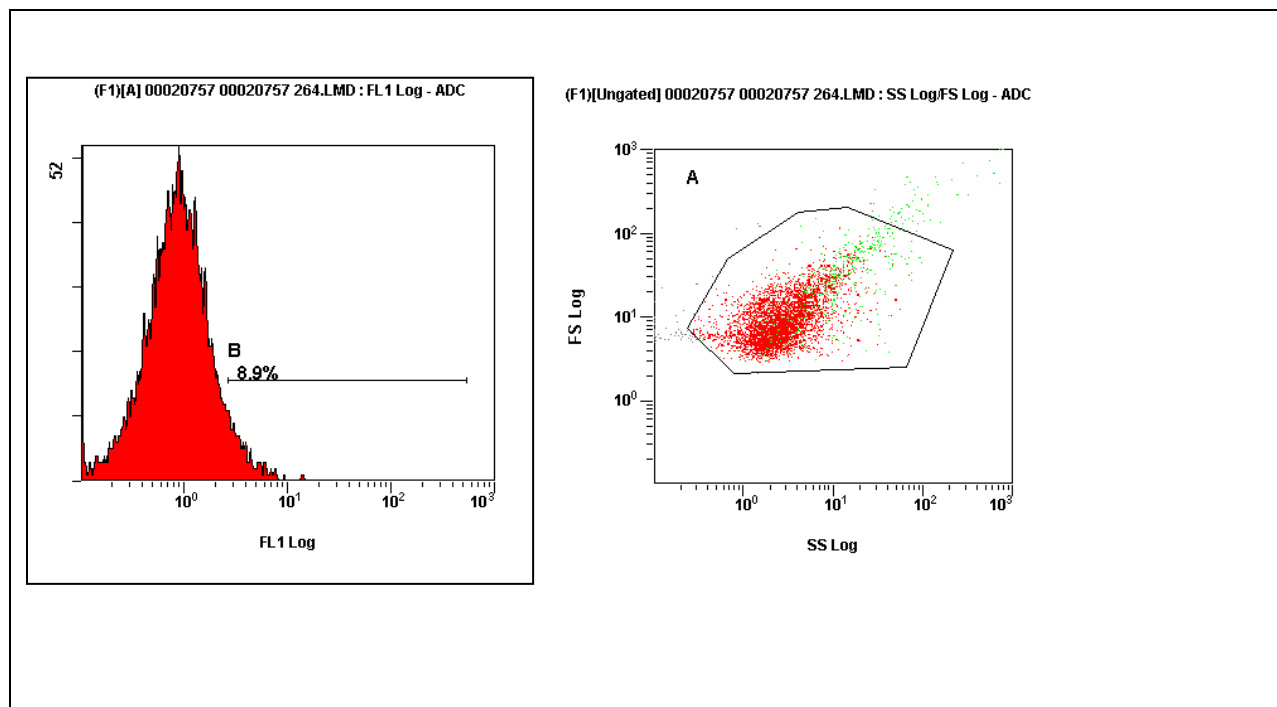


Figure 18 Fluorescence intensity and cell density plot representation of platelet aggregation caused by the positive control (PRP with thrombin 50 U/ml)

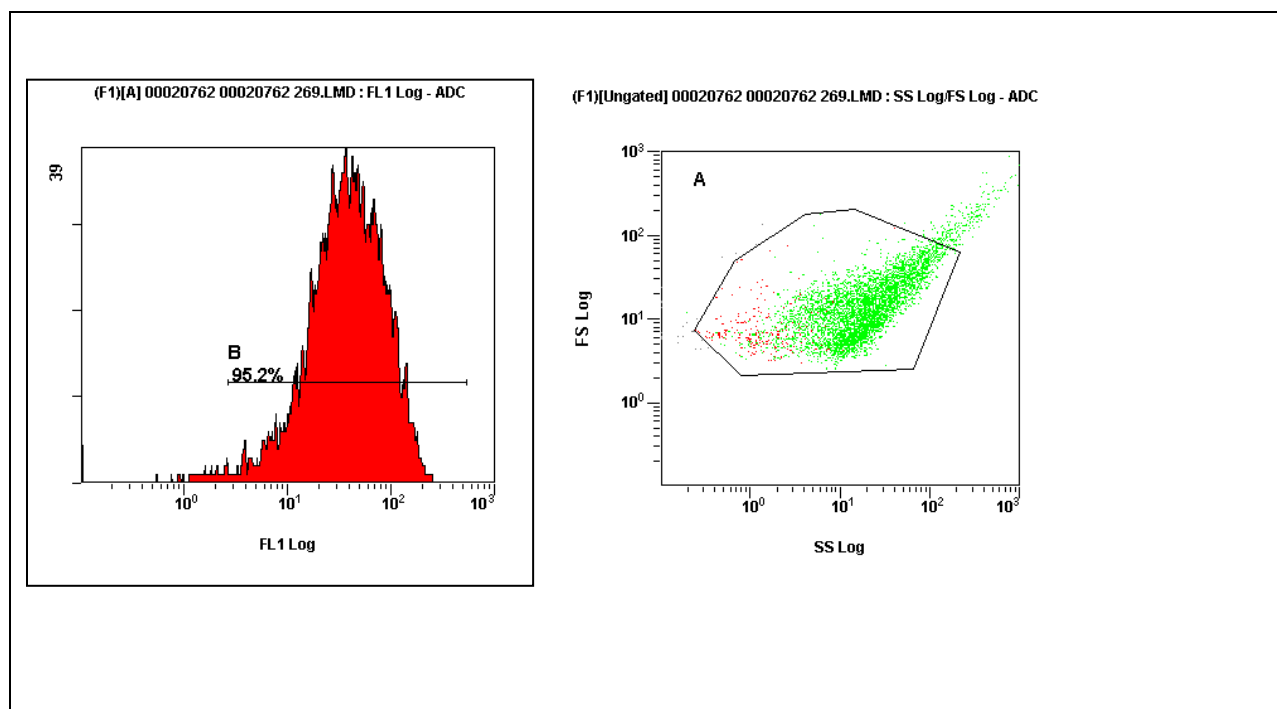


Figure 19 Fluorescence intensity and cell density plot representation of platelet aggregation caused by 50 mM cyclo(Phe-4Cl-Pro)

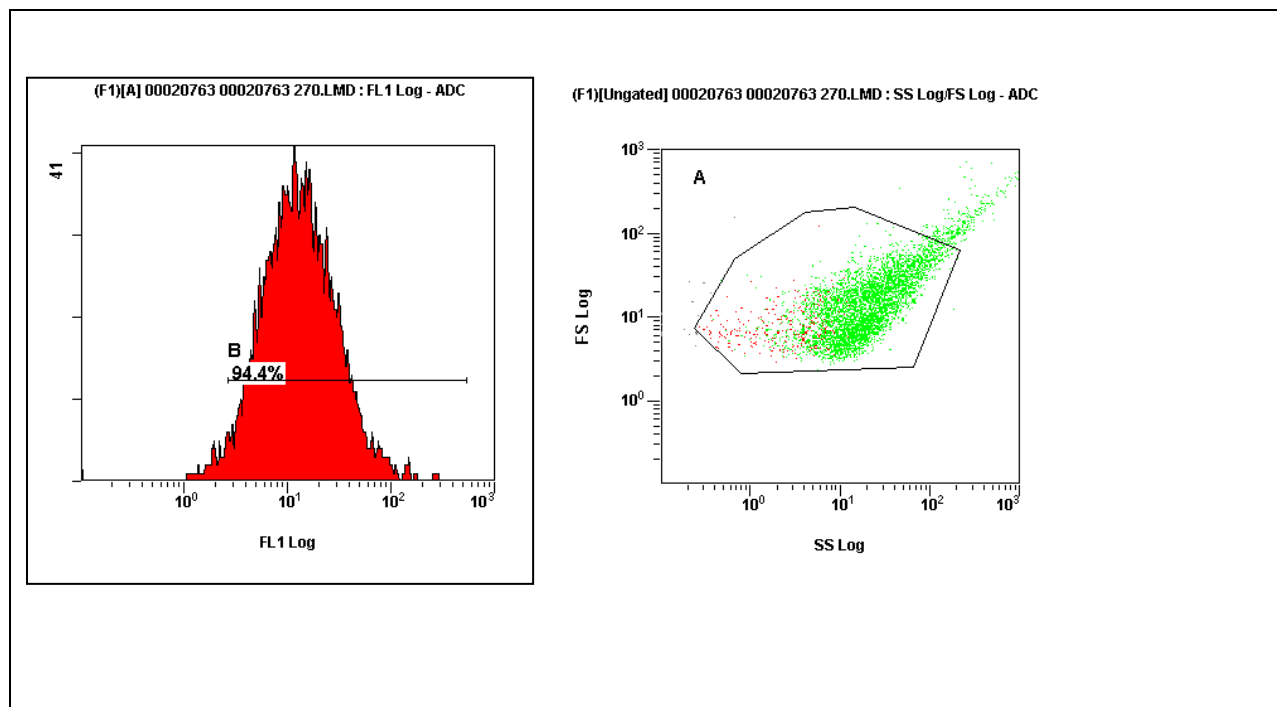


Figure 20 Fluorescence intensity and cell density plot representation of platelet aggregation caused by 25 mM cyclo(Phe-4CI-Pro)

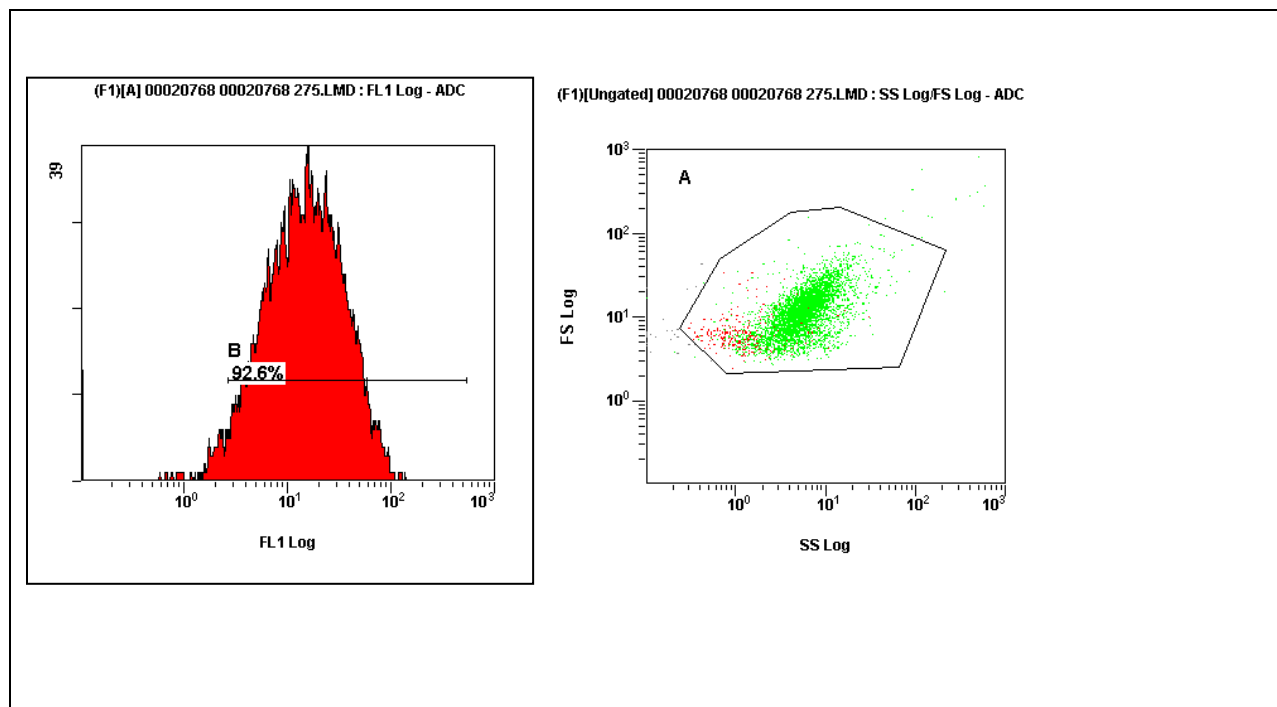


Figure 21 Fluorescence intensity and cell density plot representation of platelet aggregation caused by 12.5 mM cyclo(Phe-4CI-Pro)

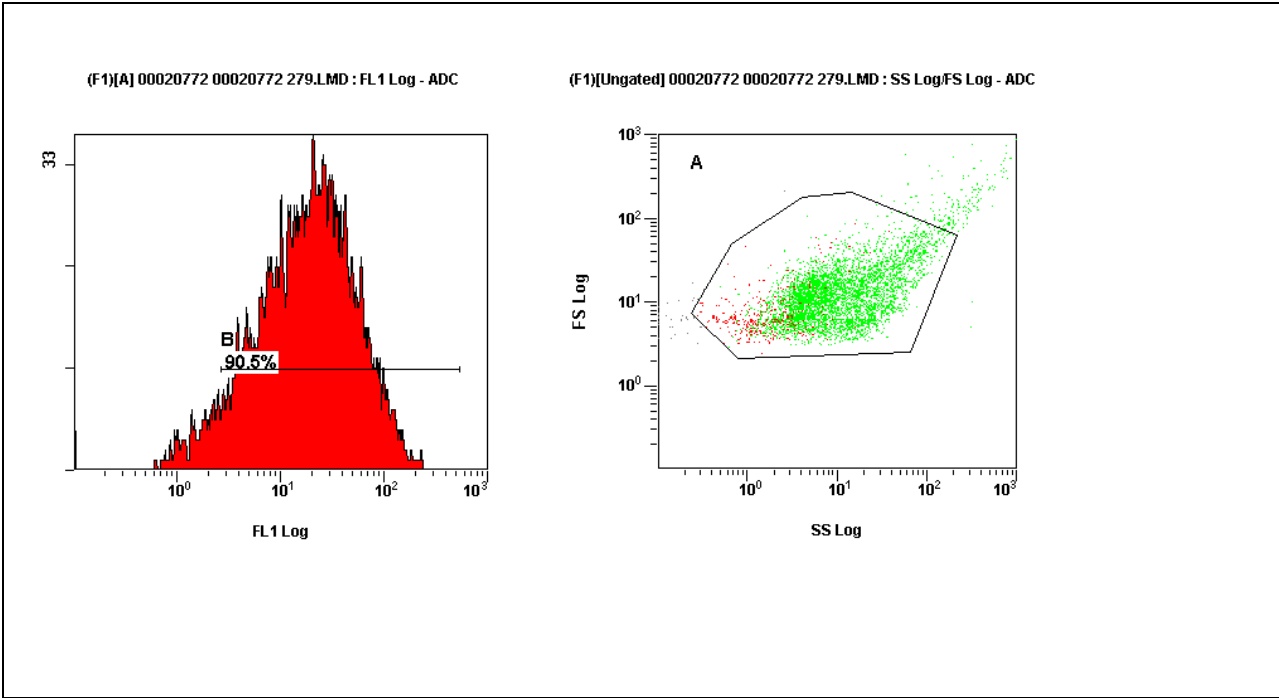


Figure 22 Fluorescence intensity and cell density plot representation of platelet aggregation caused by 3.125 mM cyclo(Phe-4CI-Pro)

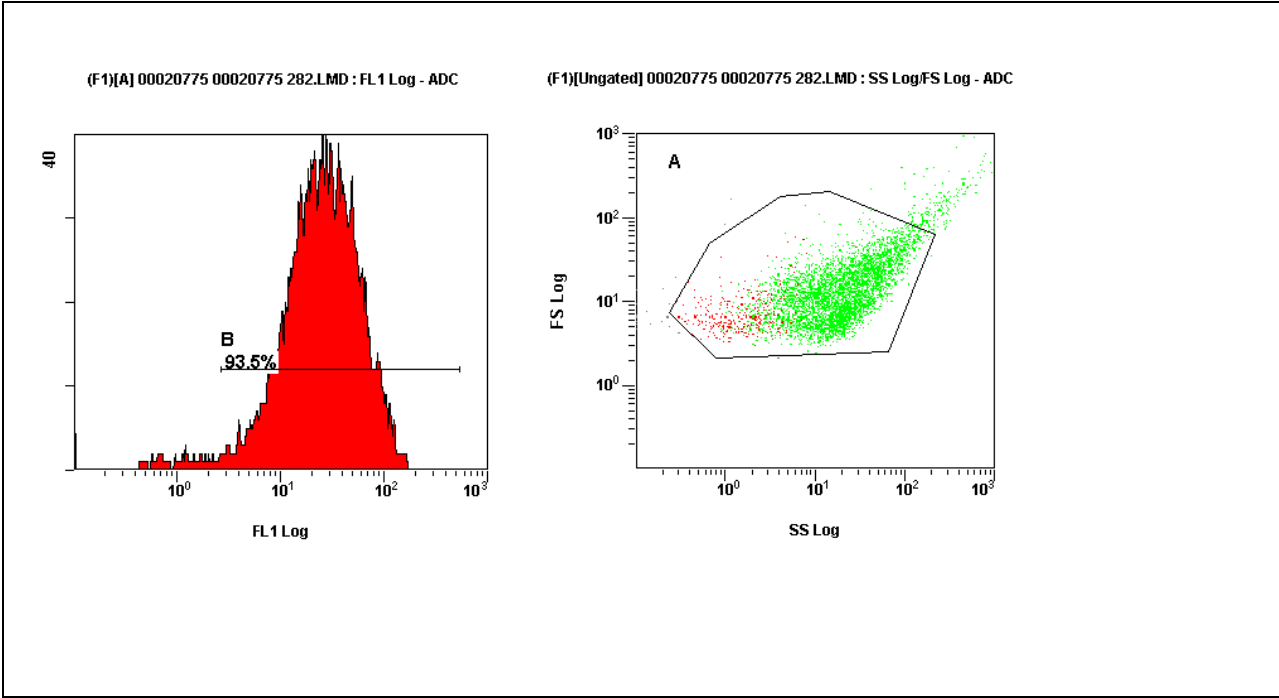


Figure 23 Fluorescence intensity and cell density plot representation of platelet aggregation caused by 50 mM cyclo(D-Phe-4CI-Pro)

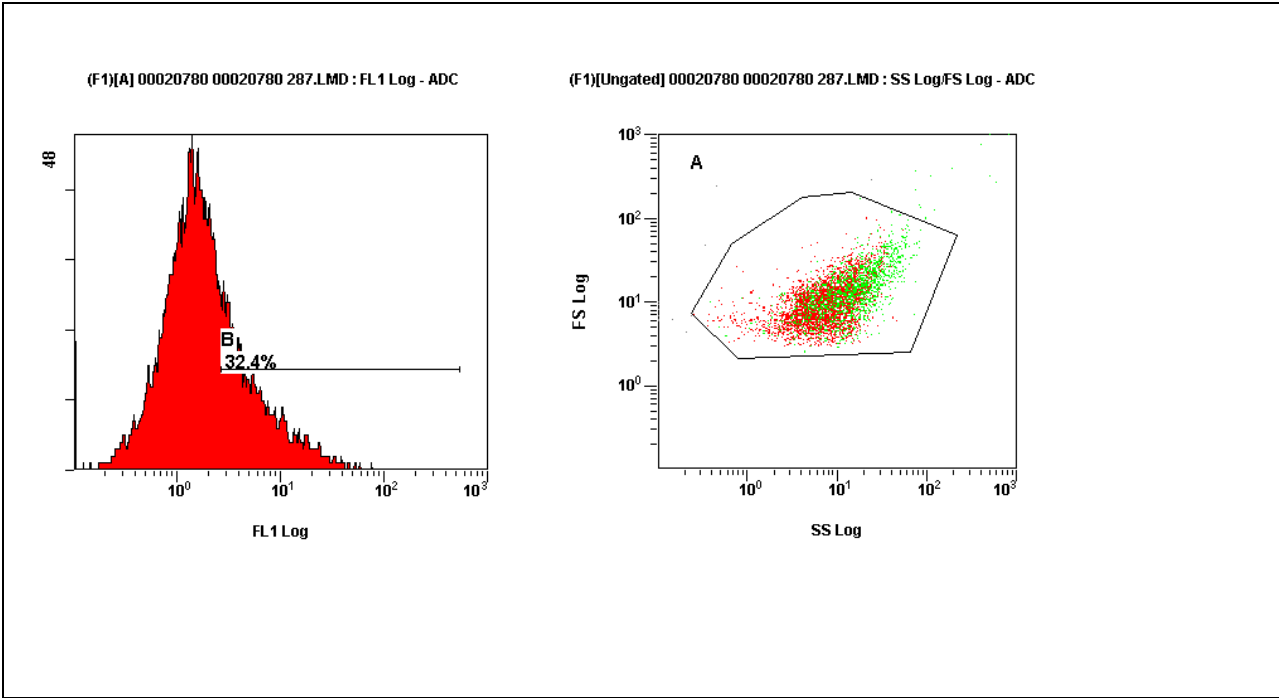


Figure 24 Fluorescence intensity and cell density plot representation of platelet aggregation caused by 25 mM cyclo(D-Phe-4Cl-Pro)

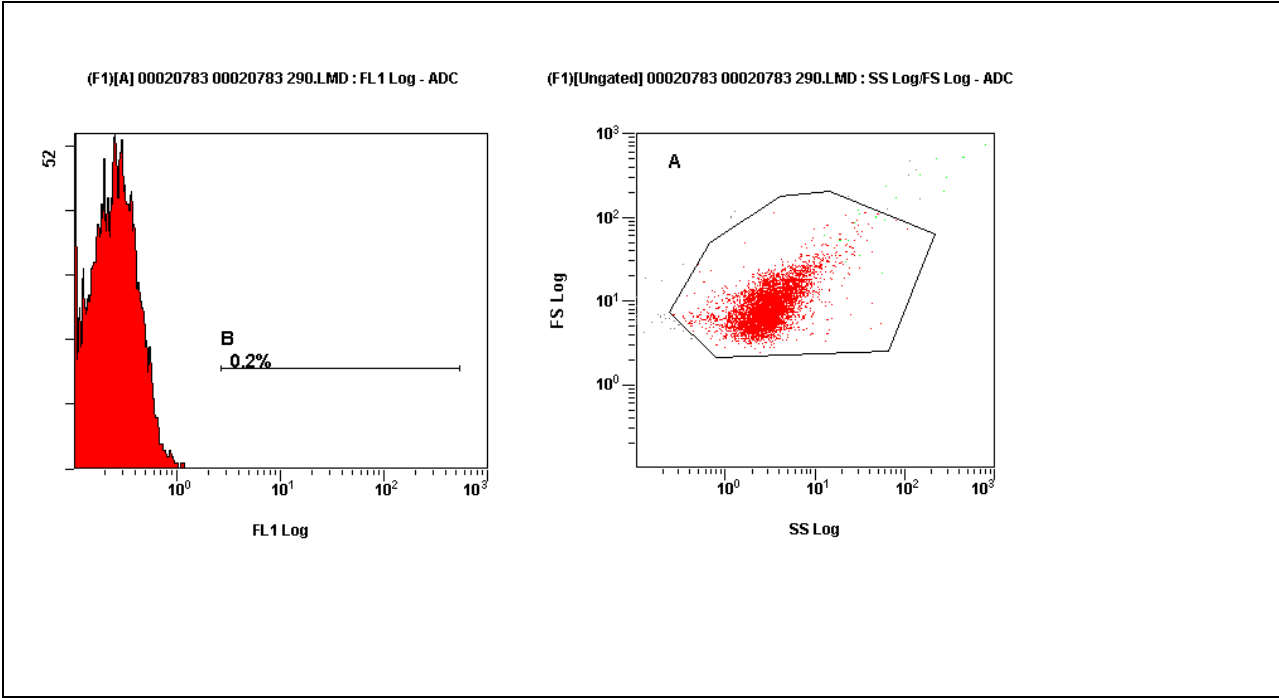


Figure 25 Fluorescence intensity and cell density plot representation of platelet aggregation caused by 12.5 mM cyclo(D-Phe-4Cl-Pro)

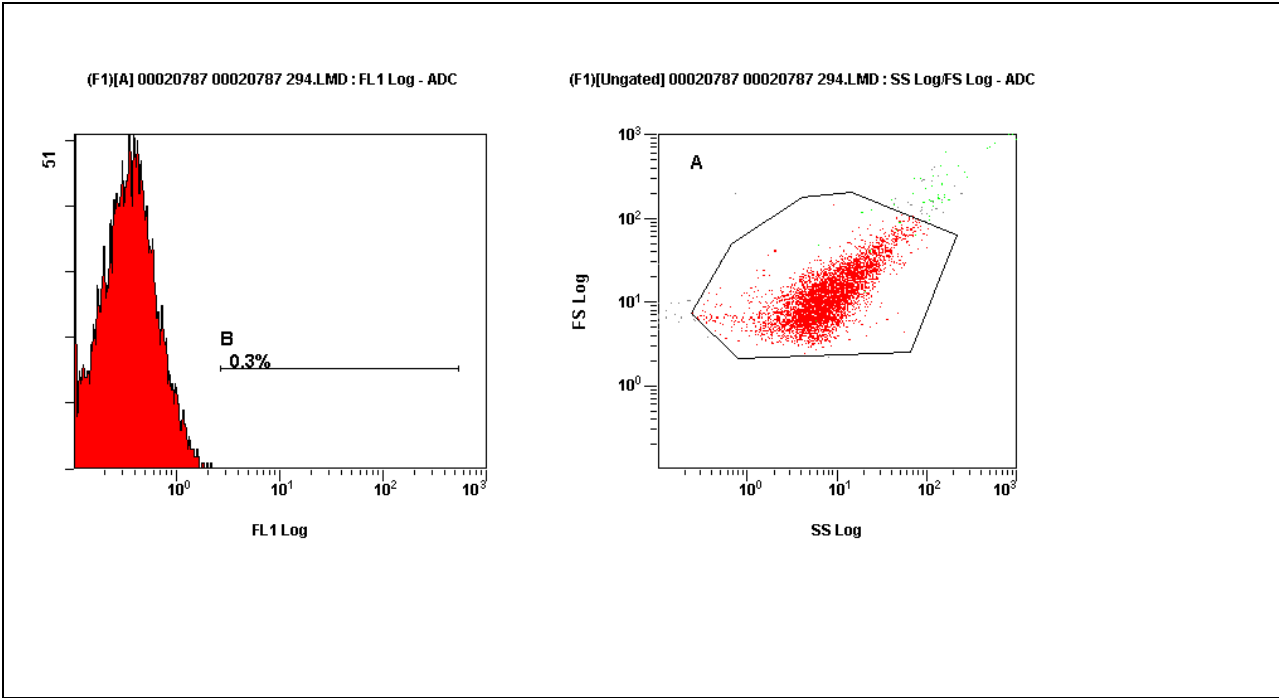


Figure 26 Fluorescence intensity and cell density plot representation of platelet aggregation caused by 3.125mM cyclo(D-Phe-4Cl-Pro)

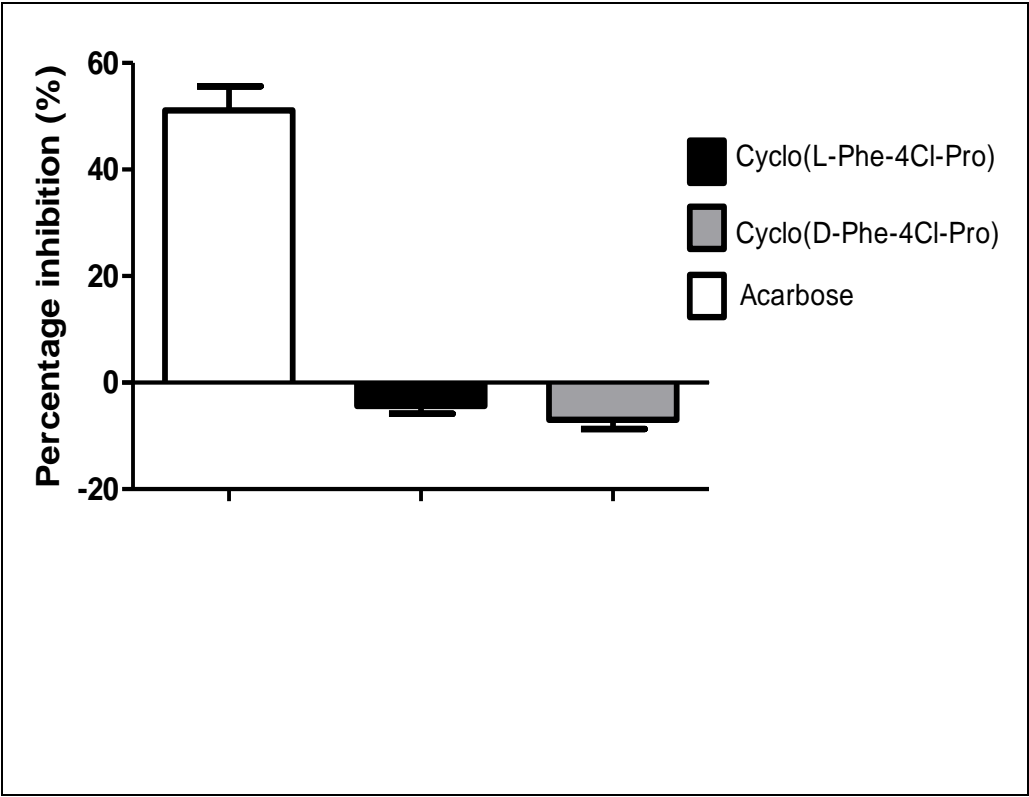


Figure 27 α -Glucosidase enzyme inhibition caused by acarbose (positive control), cyclo(Phe-4Cl-Pro) and cyclo(D-Phe-4Cl-Pro)

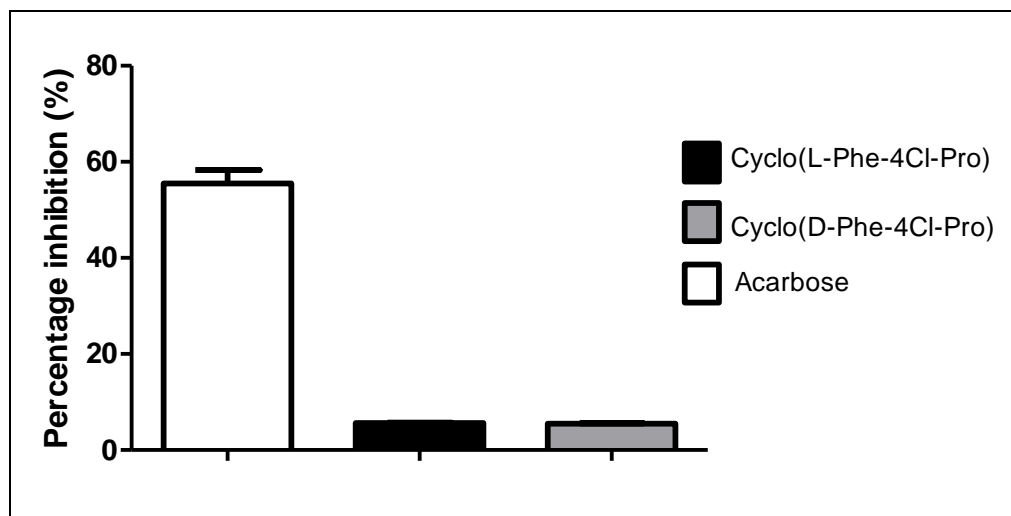


Figure 28 α-Amylase enzyme inhibition caused by acarbose, cyclo(Phe-4Cl-Pro) and cyclo(D-Phe-4Cl-Pro)

Table 1 Conformational search results calculated for cyclo(Phe-4Cl-Pro) in the gas phase

Conformer	Energy (kJ/mol)	Rel. E (kJ/mol)	Boltzmann Distribution
1	360.77	0	0.924
2	368.03	7.26	0.049
3	369.53	8.76	0.027

Table 2 Conformational search results calculated for cyclo(Phe-4Cl-Pro) in the solvated (water) phase

Conformer	Energy (kJ/mol)	Rel. E (kJ/mol)	Boltzmann Distribution
1	287.86	0	0.942
2	296.19	8.33	0.033
3	296.84	8.98	0.025

Table 3 Conformational search results calculated for cyclo(Phe-4Cl-Pro) in dimethyl sulphoxide (DMSO)

Conformer	Energy (kJ/mol)	Rel. E (kJ/mol)	Boltzmann Distribution
1	-3315302.5	0	0.648
2	-3315300.02	2.49	0.238
3	-3315298.2	4.3	0.114

Table 4 Conformational search results calculated for cyclo(D-Phe-4Cl-Pro) in the gas phase

Conformer	Energy (kJ/mol)	Rel. E (kJ/mol)	Boltzmann Distribution
1	0	365.03	0.814
2	3.88	368.91	0.17
3	9.76	374.8	0.016

Table 5 Conformational search results calculated for cyclo(D-Phe-4Cl-Pro) in the solvated (water) phase

Conformer	Energy (kJ/mol)	Rel. E (kJ/mol)	Boltzmann Distribution
1	291.37	0	0.791
2	294.83	3.46	0.916
3	301.54	10.16	0.013

Table 6 Conformational search results calculated for cyclo(D-Phe-4Cl-Pro) in dimethyl sulphoxide (DMSO)

Conformer	Energy (kJ/mol)	Rel. E (kJ/mol)	Boltzmann Distribution
1	-3315307	0	0.673
2	-3315304	2.05	0.295
3	-3315299	7.54	0.032

Table 7 Effects of heparin, cyclo(Phe-4Cl-Pro) and cyclo(D-Phe-4Cl-Pro) on APTT clotting times

Table 8 Percentage growth inhibition of *P. aeruginosa* after 24 hour exposure to cyclo(D-Phe-4Cl-Pro), cyclo(Phe-4Cl-Pro), chloramphenicol and amoxicillin

Agent	Concentration	Percentage inhibition (%)	P-value
Amoxicillin	1 mg/ml	90.34 ± 2.010	0.0012
	0.5 mg/ml	76.23 ± 1.675	0.0015
Chloramphenicol	0.5 mg/ml	68.91 ± 5.690	0.0102
	0.25 mg/ml	54.11 ± 1.775	0.0036
Cyclo(D-Phe-4Cl-Pro)	1 mM	39.55 ± 3.000	0.0143
	0.5 mM	15.61 ± 3.275	0.2619
Cyclo(Phe-4Cl-Pro)	1 mM	21.50 ± 1.835	0.0490
	0.5 mM	15.99 ± 1.000	0.1061

Table 9 Percentage growth inhibition of *E. coli* after 24 hour exposure to cyclo(Phe-4Cl-Pro), cyclo(D-Phe-4Cl-Pro), chloramphenicol and amoxicillin

Agent	Concentration	Percentage inhibition (%)	P-value
Amoxicillin	1 mg/ml	73.25 ± 4.350	0.0309
	0.5 mg/ml	68.89 ± 1.335	0.0293
Chloramphenicol	0.5 mg/ml	78.50 ± 6.165	0.0312
	0.25 mg/ml	69.66 ± 0.4350	0.0277
cyclo(D-Phe-4Cl-Pro)	1 mM	25.83 ± 0.500	0.7724
	0.5 mM	11.50 ± 0.8350	0.2771
cyclo(Phe-4Cl-Pro)	1 mM	18.66 ± 1.000	0.6239
	0.5 mM	15.66 ± 0.6700	0.4400

Table 10 Percentage growth inhibition of *B. subtilis* after 24 hour exposure to cyclo(D-Phe-4Cl-Pro), cyclo(Phe-4Cl-Pro), chloramphenicol and amoxicillin

Agent	Concentration	Percentage inhibition (%)	P-value
Amoxicillin	1 mg/ml	50.61 ± 4.410	0.0316
	0.5 mg/ml	57.55 ± 2.350	0.0144
Chloramphenicol	0.5 mg/ml	83.61 ± 4.410	0.0085
	0.25 mg/ml	68.28 ± 2.945	0.0103
Cyclo(D-Phe-4Cl-Pro)	1 mM	17.83 ± 5.500	0.8570
	0.5 mM	15.00 ± 1.335	0.7907
cyclo(Phe-4Cl-Pro)	1 mM	18.27 ± 2.390	0.7438
	0.5 mM	12.33 ± 2.000	0.4900

Table 11 Percentage growth inhibition of *S. aureus* after 24 hour exposure to cyclo(D-Phe-4Cl-Pro), cyclo(Phe-4Cl-Pro), chloramphenicol and amoxicillin

Agent	Concentration	Percentage inhibition (%)	P-value
Amoxicillin	1 mg/ml	26.40 ± 1.5.600	0.0501
	0.5 mg/ml	58.60 ± 1.300	0.0304
Chloramphenicol	0.5 mg/ml	72.60 ± 6.600	0.00344
	0.25 mg/ml	69.61 ± 1.610	0.0177
Cyclo(D-Phe-4Cl-Pro)	1 mM	68.00 ± 2.665	0.0106
	0.5 mM	22.17 ± 1.165	0.05362
Cyclo(Phe-4Cl-Pro)	1 mM	12.22 ± 2.110	0.0062
	0.5 mM	11.33 ± 9.000	0.0340

Table 12 Percentage growth inhibition of *C. albicans* after 24 hour exposure to cyclo(D-Phe-4Cl-Pro), cyclo(Phe-4Cl-Pro), chloramphenicol and amoxicillin

Agent	Concentration	Percentage inhibition (%)	P-value
Amoxicillin	1 mg/ml	91.19 ± 1.165	0.0004
	0.5 mg/ml	63.83 ± 2.500	0.0025
Chloramphenicol	0.5 mg/ml	57.61 ± 2.390	0.0030
	0.25 mg/ml	82.68 ± 5.345	0.0054
Cyclo(D-Phe-4Cl-Pro)	1 mM	54.28 ± 5.055	0.0128
	0.5 mM	31.83 ± 9.500	0.1380
Cyclo(Phe-4Cl-Pro)	1 mM	47.84 ± 7.820	0.0387
	0.5 mM	46.18 ± 3.845	0.0114

Table 13 Effects of heparin, cyclo(Phe-4Cl-Pro) and cyclo(D-Phe-4Cl-Pro) on APTT clotting times

Compound	Concentration	Clotting time (seconds)	<i>P</i> -value
Heparin	0.1 U/ml	106 ± 1.350	0.0003
Cyclo(Phe-4Cl-Pro)	50 mM	27.95 ± 0.4000	0.0003
	25 mM	20.28 ± 1.055	0.0004
	12.5 mM	10.78 ± 0.4450	0.0002
Cyclo(D-Phe-4Cl-Pro)	50 mM	26.15 ± 0.7050	0.0004
	25 mM	14.61 ± 0.6150	0.0003
	12.5 mM	8.110 ± 0.5500	0.0002

Table 14 Effects of heparin, cyclo(Phe-4Cl-Pro) and cyclo(D-Phe-4Cl-Pro) on PT clotting times

Compound	Concentration	Clotting time (seconds)	<i>P</i> -value
Heparin	0.1 U/ml	88.80 ± 1.805	0.0009
Cyclo(Phe-4Cl-Pro)	50 mM	20.53 ± 0.9250	0.2374
	25 mM	17.13 ± 0.1700	0.0055
	12.5 mM	14.41 ± 0.8100	0.0125
Cyclo(D-Phe-4Cl-Pro)	50 mM	17.66 ± 0.6700	0.0266
	25 mM	11.85 ± 0.8550	0.0078
	12.5 mM	10.75 ± 0.4500	0.0024

Table 15 Effects of heparin, cyclo(Phe-4Cl-Pro) and cyclo(D-Phe-4Cl-Pro) on the formation of fibrin

Compound	Concentration	Fibrin formation (mg/dL)	<i>P</i> -value
Heparin	0.1 U/ml	73.66 ± 3.670	0.0144
Cyclo(Phe-4Cl-Pro)	50 mM	116.7 ± 3.725	0.0144
	25 mM	273.2 ± 3.830	0.0007
	12.5 mM	292.5 ± 2.500	0.0004
Cyclo(D-Phe-4Cl-	50 mM		0.0018

Pro)		172.0 ± 2.000	
	25 mM	313.4 ± 2.545	0.0003
	12.5 mM	369.8 ± 0.8350	0.0002

Table 16 Effects of heparin, cyclo(Phe-4Cl-Pro) and cyclo(D-Phe-4Cl-Pro) on D-Dimer formation

Compound	Concentration	D-Dimer formation (ng/ml)	<i>P</i> -value
Heparin	0.1 U/ml	36.99 ± 1.000	0.0020
Cyclo(Phe-4Cl-Pro)	50 mM	69.39 ± 1.055	0.0020

	25 mM	65.43 ± 2.875	0.0113
	12.5 mM	53.10 ± 2.105	0.0203
Cyclo(D-Phe-4Cl-Pro)	50 mM	53.91 ± 0.3100	0.0038
	25 mM	49.16 ± 0.1700	0.0069
	12.5 mM	43.95 ± 0.9550	0.0373